

**Identification of genes and mutations involved in primary
microcephaly and inherited limb disorders in Pakistani families**



*A dissertation submitted in the partial fulfillment of the requirements
for the degree of*

Doctor of Philosophy

In

Biotechnology

By

Muhammad Farooq

School of Biotechnology
National Institute for Biotechnology and Genetic Engineering
(NIBGE), Faisalabad
&
Quaid-i-Azam University
Islamabad
(2010)

Declaration

I hereby declare that the work presented in the following thesis is my own effort, except where otherwise acknowledged, and that the thesis is my own composition. No part of this thesis has been previously presented for any other degree.

Muhammad Farooq

Certificate

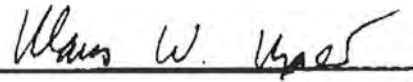
This thesis, submitted by Muhammad Farooq, is accepted in its present form by the School of Biotechnology, National Institute for Biotechnology and Genetic Engineering (NIBGE), Faisalabad, and Quaid-i-Azam University, Islamabad, Pakistan, as satisfying the requirement for the degree of Doctor of Philosophy in Biotechnology.

Supervisor:



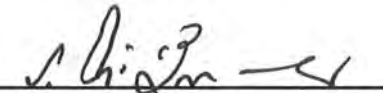
Dr. Shahid M. Baig

Co-Supervisor:



Dr. Klaus Wilbrandt Kjaer

External Examiner:



Dr. Sheikh Riaz ud Din

External Examiner:



Dr. Abdul Rauf Shakoori

Director, NIBGE:



Dr. Zafar M. Khalid

Dated:

29.11.2010.

*Dedicated
To
My
Family*

Table of contents

Acknowledgements	I
List of Figures	III
List of Tables	XI
List of Abbreviations	XIV
Summary	XVI

Part 1 Primary microcephaly

1	INTRODUCTION	I
1.1	Primary microcephaly (MCPH)	2
1.2	Structure of cerebral cortex	5
1.3	Development of cerebral cortex	7
1.4	Clinical features of primary microcephaly	8
1.5	MCPH genes and their function	10
1.5.1	Microcephalin (<i>MCPHI</i>)	10
1.5.2	Abnormal spindle like microcephaly associated (<i>ASPM</i>)	11
1.5.3	Cyclin dependent kinase5 regulatory associated protein (<i>CDK5RAP2</i>)	12
1.5.4	Centrosomal protein J (<i>CENPJ</i>)	13
1.5.5	<i>STIL</i> (SCL/TAL1 interrupting locus)	13
1.6	Objectives of study	16
2	MATERIALS AND METHODS	17
2.1	Families studied	17
2.1.1	MCP3	18
2.1.2	MCP6	19

2.1.3	MCP7	20
2.1.4	MCP9	21
2.1.5	MCP11	22
2.1.6	MCP15	23
2.1.7	MCP17	24
2.1.8	MCP18	25
2.1.9	MCP21	26
2.1.10	MCP22	27
2.1.11	MCP35	28
2.1.12	MCP36	29
2.2	Clinical data	29
2.3	Blood sampling	32
2.4	DNA extraction	33
2.5	Polymerase chain reaction	33
2.6	Agarose gel electrophoresis	33
2.7	Genotyping using fluorescently labeled primers	34
2.8	Preparation of samples for ABI 3130x/ genetic analyzer	35
2.9	Linkage analysis	35
2.10	Mutation screening	36
2.10.1	DNA sequencing	36
2.10.2	Purification of PCR product from agarose gel	37
2.10.3	Purification of PCR product	37

2.10.4	Sequencing PCR reactions	37
2.10.5	Precipitation of sequencing PCR products	38
2.10.6	Sequencing data analysis	38
2.11	Restriction analysis	39
3	RESULTS	51
3.1	Linkage studies	51
3.2	Mutation analysis	52
3.2.1	Sequencing of <i>ASPM</i> in MCPH5 linked families	52
3.2.2	Compound heterozygous <i>ASPM</i> mutations	53
3.2.2.1	Family MCP18	53
3.2.2.2	Family MCP35	53
3.2.3	Sequencing of <i>CENPJ</i>	54
3.2.4	Mutation screening in control population	54
3.2.5	Family MCP15	54
3.2.6	Sequencing of candidate genes in MCPH2 region	55
3.2.7	Sequencing of <i>MCPHI</i>	56
4	DISCUSSION	71
Part 2 Inherited limb disorders		
5	INTRODUCTION	79
5.1	Polydactyly	79
5.2	Types of polydactyly	80

5.2.1	Preaxial polydactyly (PPD)	80
5.2.1.1	Thumb polydactyly (PPD1, OMIM: 174400)	80
5.2.1.2	Polydactyly of triphalangeal thumb (PPD2/TPT; OMIM: 174500)	80
5.2.1.3	Index finger polydactyly (polydactyly, Preaxial III, OMIM: 174600)	81
5.2.1.4	Preaxial polydactyly type IV (PPD IV, OMIM: 174700)	81
5.2.2	Postaxial polydactyly (PAP)	82
5.2.2.1	Postaxial polydactyly type A (PAPA)	82
5.2.2.2	Postaxial polydactyly type B (PAPB, OMIM: 174200)	82
5.3	Brachydactyly	83
5.3.1	Brachydactyly type A	84
5.3.1.1	Brachydactyly type A1 (BDA1; OMIM: 112500)	84
5.3.1.2	Brachydactyly type A2 (BDA2; OMIM: 112600)	84
5.3.1.3	Brachydactyly type A3 (BDA3; OMIM: 112700)	85
5.3.1.4	Brachydactyly type A4 (BDA4; OMIM: 112800)	85
5.3.1.5	Brachydactyly type A5 (BDA5; OMIM: 112900)	85
5.3.2	Brachydactyly type B (BDB; OMIM: 113000)	86
5.3.3	Brachydactyly type C (BDC; OMIM: 113100)	86
5.3.4	Brachydactyly type D (BDD; OMIM: 113200)	87
5.3.5	Brachydactyly type E (BDE; OMIM: 113300)	87
5.3.6	Brachymetatarsus IV (OMIM: 113475)	88
5.3.7	Sugarman brachydactyly (OMIM: 272150)	88

5.3.8	Kirner deformity (OMIM: 128000)	88
5.3.9	Brachydactyly as a part of syndrome	89
5.4	Syndactyly	90
5.4.1	Classification of syndactylies	90
5.4.1.1	Syndactyly Type I (SDI; MIM 185900)	91
5.4.1.2	Syndactyly Type II, Synpolydactyly (SPD; MIM 186000)	91
5.4.1.3	Syndactyly Type III (MIM 186100)	92
5.4.1.4	Syndactyly Type IV, Haas Type Syndactyly (MIM 186200)	93
5.4.1.5	Syndactyly Type V (MIM 186300)	93
5.4.1.6	Syndactyly Type VI, Mitten syndactyly	93
5.4.1.7	Syndactyly Type VII, Cenani-Lenz Syndactyly (MIM 212780)	94
5.4.1.8	Syndactyly Type VIII	94
5.4.1.9	Syndactyly Type IX, Malik-Percin type syndactyly	94
5.5	Syndromic hand anomalies	94
5.5.1	Greig cephalopolysyndactyly syndrome	94
5.6	Limb development	96
6	MATERIALS AND METHODS	97
6.1	Methods	97
6.1.1	Nuclear extract preparation	97
6.1.2	Annealing of probes for EMSA	98
6.1.3	Radioactive labelling of double stranded EMSA probes	98

6.1.4	Electrophoretical mobility shift assay (EMSA) procedure	98
6.1.5	Genome wide linkage analysis	99
6.1.6	Candidate gene search	99
6.1.7	Copy number variation detection	100
6.2	Families studied	101
6.2.1	Family PD1	101
6.2.2	Family PD2	103
6.2.3	Family PD316	107
6.2.4	Family PD7	109
6.2.5	Family PD16	111
6.2.7	Family BD1	113
6.2.7.1	Clinical description	114
6.2.8	Syndactyly families	116
6.2.8.1	Family PD14A	117
7	RESULTS AND DISCUSSION	129
7.1	Family PD1	129
7.1.1	Linkage analysis and Mutation detection	129
7.1.2	Electrophoretic mobility shift assay	129
7.1.3	Discussion	134
7.2	Family PD2	136
7.2.1	Linkage analysis and Mutation detection	136

7.3	Family PD316	139
7.4	Family PD7	141
7.5	Family PD16	143
7.6	Discussion	145
7.3	Family BD1	148
7.3.1	Exclusion of locus on 2q31 (<i>HOXD13</i>) for brachydactyly type E	148
7.3.2	Genome-wide search using 10K SNP array and fine mapping	148
7.3.3	Mutation screening	145
7.3.4	Genome wide SNP array 6.0 analysis to detect copy number variation	150
7.3.5	Discussion	156
7.4	Family PD14A	157
7.4.1	Novel isolated autosomal recessive 2nd and 3rd digit syndactyly	157
7.4.2	Exclusion studies and Genome wide linkage analysis	157
7.4.3	Sequencing of candidate gene	158
7.4.4	Discussion	164
	REFERENCES	166

Appendix

Acknowledgements

In the name of “Allah” The Most Merciful and Beneficent, I am so grateful to Him and bow to Him for His infinite mercy, Who blessed me with such a strength and made me able to explore the field of human genetics. All praises for His “Prophet Muhammad (SAW)”, as he is “The Teacher” of humanity in all kind of knowledge.

I would like to express my deepest gratitude Dr. Zafar M. Khalid, Director, NIBGE, and Dr. Javed Anver Qureshi, Head, Health Biotechnology Division, for their support and providing excellent research facilities to complete this work.

I express my deepest gratitude and sincerest appreciation to my supervisor Dr. Shahid Mahmood Baig for his guidance, kindness, continuous advice and insight throughout the research. It is indeed impossible for me to express my exact feelings of gratefulness. The best advisor and teacher I could have wished for, he has always been a continuous source of inspiration for me. I am also grateful to my co-supervisor Dr. Klaus Wilbrandt Kjaer who has been untiringly helpful, patient to me and guidance during my stay in his lab at Wilhelm Johannsen Centre for Functional Genome Research (WJC), University of Copenhagen, Denmark. I am indebted to him for all his support, care and help.

I would like to express my endless thanks to Prof. Niels Tommerup the Director, WJC, for helping me in many ways. I am also deeply thankful to Dr. Lars Hansen, Dr. Hans Eiberg, Dr. Jesper Troelsen, and Dr. Asli Silahtaroglu for their suggestion, valuable help in data analysis, and nice company during my stay at WJC. I would also like to pay my special thanks to Annemette Frijs Mikelsen, Lillian Rasmussen, Theresa Wass, Maria, Minna Becher, Lene Logstrup and Biyarke for their care, nice company and support in the laboratory.

I would like to thank to all scientists and colleagues in my lab for their invaluable help and cooperation whenever I needed during my study, especially Muhammad Aslam, and Dr. Fazli Rabbi. I would like to pay special thanks to Muhammad Sajid Hussain, Mahmood Rasool, Aysha Azhar, Iram Anjum, Shoaib-ur-Rehman, Muhammad Tariq, Ilyas Ahmad, Amjad Ali, and

Marriam Bakhtiar and Usman Raza for their support and sharing memorable movements. Their sense of humor has been great help to encounter problems.

I have no words to pay sincerest thanks to my friends especially, Muhammad Aamir Mehmood, Dr. Kashif Saleemi, Mr. Muhammad Shafiq, Mr. Muhammad Mubin, Mr. Khadim Hussain, Mr. Muthar Mansoor, Dr. Zahid Iqbal, Dr. Ahsan-ul-Haq for their help, encouragement and great friendship that made easier for me to overcome difficulties.

Finally, I would like to express my heartfelt gratitude to my family, my father Muhammad Yasin, brothers, sisters and extended family members for their understanding, support and sacrifices that helped me to finish my thesis. They will remain my source of inspiration for today and in future.

At the end, I would like to acknowledge Higher Education Commission, Pakistan, for providing me funds for my research in Pakistan, and Wilhelm Johannsen Centre for Functional Genome Research (WJC), University of Copenhagen, for hosting my stay in Denmark. Without, their financial support I might have not been able to focus on my research.

Muhammad Farooq

LIST OF FIGURES

Fig. #	Title of Figure	Page #
1.1	The cerebral neocortex features six layers that are illustrated above by two different staining methods.	6
1.2	A comparison of magnetic resonance images from an individual with primary microcephaly and an unaffected individual of a similar age. (a) Sagittal T1-weighted image from an unaffected 11-year-old female control. (b) Sagittal T1-weighted image from a 13-year-old female with an MCPH5 mutation showing striking reduction in the size of the cerebral cortex, prominent sloping of the forehead and preserved midline structures.	9
1.3	Phenotypic appearance of a typical MCPH patient. (A) Frontal view. (B) Side view, prominent sloping forehead.	9
1.4	MCPH proteins and probable functional domains. (a) The <i>MCPH1</i> protein microcephalin contains three BRCT C-terminal domains, (b) <i>ASPM</i> contains an N-terminal microtubule-associated domain (green). The N-terminal region also contains two putative calponin-homology (CH) domains. The 81 IQ repeats are Ise-Gln calmodulin-binding domains. (c) The MCPH3 gene, <i>CDK5RAP2</i> , encodes a spindle associated domain in the N-terminus. There are also several coiled-coil domains (d) <i>CENPJ</i> , similar to <i>CDK5RAP2</i> , also consists of numerous coiled-coil regions. At the C-terminus is the TCP10 C-terminus domain.	15
2.1	Pedigree of family MCP3 with autosomal recessive primary microcephaly. Solid symbols represent affected subjects, while the open symbols represent normal individuals. Horizontal bars above symbols denote individuals who were physically examined and their blood was sampled for molecular study.	18

2.2	Pedigree of family MCP6 with autosomal recessive primary microcephaly. Solid symbols represent affected subjects, while the open symbols represent normal individuals. Horizontal bars above symbols denote individuals who were physically examined and their blood was sampled for molecular study.	19
2.3	Pedigree of family MCP7 with autosomal recessive primary microcephaly. Solid symbols represent affected subjects, while the open symbols represent normal individuals. Horizontal bars above symbols denote individuals who were physically examined and their blood was sampled for molecular study.	20
2.4	Pedigree of family MCP9 with autosomal recessive primary microcephaly.	21
2.5	Pedigree of family MCP11 with autosomal recessive primary microcephaly.	22
2.6	Pedigree of family MCP15 with autosomal recessive primary microcephaly.	23
2.7	Pedigree of family MCP17 with autosomal recessive primary microcephaly.	24
2.8	Pedigree of family MCP18 with autosomal recessive primary microcephaly.	25
2.9	Pedigree of family MCP21 with autosomal recessive primary microcephaly.	26
2.10	Pedigree of family MCP17 with autosomal recessive primary microcephaly.	27
2.11	Pedigree of family MCP35 with autosomal recessive primary microcephaly.	28
3.1	Representative Chromatogram of (A) homozygous affected individual and (B) a homozygous normal individual of family MCP3. Arrow shows site of mutation c.3477_3481delCGCTA in exon 14 of <i>ASPM</i> . (C) <i>HgaI</i> restriction analysis of all sampled members of family MCP3; mutant allele (599bp) and wild type allele (303,296bp).	57
3.2	Representative Chromatogram of (A) homozygous affected individual, (B) homozygous normal individual of family MCP17. Arrow shows site of mutation c.9492T>G in exon 23 of <i>ASPM</i> . (C) <i>AluI</i> restriction analysis of all sampled members of family MCP3; mutant allele (167bp) and wild type allele	58

(191bp).

- | | | |
|-----|---|----|
| 3.3 | Chromatogram of representative homozygous affected individual (A) and homozygous normal individual (B) of family MCP6. Arrow shows site of mutation c.6732delA in exon 18 of <i>ASPM</i> . | 59 |
| 3.4 | Chromatogram of representative homozygous affected individual (A) and homozygous normal individual (B) of family MCP7. Arrow shows site of mutation c.9697C>T in exon 24 of <i>ASPM</i> . | 59 |
| 3.5 | Chromatogram of representative homozygous affected individual (A) and homozygous normal individual (B) of family MCP9. Arrow shows site of mutation c.9730C>T in exon 24 of <i>ASPM</i> . <i>TaqI</i> restriction analysis of all sampled members (C) of family MCP9; mutant allele (574bp), wild type (310 + 264bp). | 60 |
| 3.6 | Chromatogram of representative homozygous affected individual (A) and homozygous normal individual (B) of family MCP11. Arrow shows site of mutation c.9557C>G in exon 23 of <i>ASPM</i> . | 61 |
| 3.7 | Chromatogram of (A) representative heterozygous affected individual with c.7894C>T mutation, (B) homozygous normal individual (C) heterozygous affected individual with c.3055C>T mutation and (D) homozygous normal for c.3055C>T mutation. | 62 |
| 3.8 | Segregation of compound heterozygous mutations (c.3055C>T and c.7894C>T) in MCP18 family. Affected individuals in right loop are homozygous for c.3055C>T. Whereas, affected subjects in middle and left loop are compound heterozygous. | 63 |
| 3.9 | Chromatogram of representative compound heterozygous affected individual for mutation c.9319GC>T in exon 22 of <i>ASPM</i> (A) and homozygous normal individual (B) of family MCP35. Chromatogram of representative homozygous affected individual for mutation c.3978G>A in exon 17 of <i>ASPM</i> (C) and | 64 |

	homozygous normal individual (D) of family MCP35. Arrow shows site of mutation.	
3.10	(A) Segregation of compound heterozygous mutations (c.3978G>A and c.9319C>T) in MCP35 family. Affected individuals in right loop (loop II) are homozygous for c.3978G>A, affected individuals in the left loop (loop I) are compound heterozygous. (B) Restriction digests using <i>TaqI</i> enzyme for 'c.9319C>T' mutation. (C) restriction digest using <i>AhdI</i> enzyme for 'c.3978G>A' mutation.	65
3.11	Chromatogram of representative homozygous affected individual in exon 2 of <i>CENPJ</i> in families MCP21 and MCP22 demonstrating single bp deletion (c.17_18delC). Site of deletion is indicated by arrow, (A) mutated, (B) wild type.	66
3.12	Haplotypes of the individuals in family MCP15 for nine microsatellite markers from chromosome 19 at MCPH2 locus. The homozygous region in affected subjects segregating with phenotype is shown in box.	67
3.13	Genetic map of chromosome 19 markers. Distances are shown in centimorgan. The blackened bar indicates the minimum homozygous region shared by both affected individuals in family MCP15 at MCPH2 locus. Candidate genes sequenced in both affected individuals are written in red.	68
3.14	Chromatogram of representative homozygous affected individual in exon 4 of <i>MCPHI</i> in MCP36 demonstrating C>G substitution (c.302C>G). Site of mutation is indicated by arrow, (A) mutant, (B) wild type.	70
3.15	Domains of full length (A) and truncated protein (B) predicted by SMART (http://smart.embl-heidelberg.de/). Mutant protein lacks both C-terminal BRCT domains.	70
6.1	Pedigree of family PD1 with preaxial polydactyly with triphalangial thumb phenotype. Phenotypically affected individuals are shown by black filled in	102

symbols. Clinically examined individuals are shown by straight line over the symbol.

- 6.2 Phenotypic appearance of affected subjects in family PD1 with preaxial polydactyly triphalangial thumb. (A & B) hands and feet of III-12; (C) clinical appearance of hands of male subject III-6; (D) radiograph of III-6 demonstrate duplicated thumbs with three phalanges. 102
- 6.3 Pedigree of Family PD2 with PPD. Phenotypically affected individuals are shown by black filled in symbols. Clinically examined individuals are shown by straight line over the symbol. 103
- 6.4 Phenotypic appearance of affected subjects in Family PD2. (A, B & C) Photographs of face, hands and feet of subject III-6. Mild hypertelorism, bilateral postaxial postminimus, short distal phalanx of left thumb and syndactyly of first four toes with preaxial duplication; (D, E & F) face, left foot and hands of subject II-3. Postaxial postminimus, complete bilateral syndactyly of third and fourth digit, and partial syndactyly between thumb and index finger. In foot syndactyly of first four toes with preaxial duplication, (G, H & I) face, hands and feet of subject II-2. Only feet are involved, duplicated great toe with syndactyly of 1st 2nd and 3rd toe in right foot. 105
- 6.5 Photographs and radiographs of hands and feet of IV-5. (A) Present complete syndactyly of last three digits in right hand and 3rd and 4th digit in left hand, (B) radiographs of hands of IV-5 indicated synostosis of distal phalanges of 4th and 5th finger and middle phalanx of 4th digit, (C& D) shows bilateral incomplete syndactyly of 1st and 2nd toe. Duplicated rudimentary distal phalanx of 1st toe is indicated by arrows, (E) photograph of face of individual IV-5. 106
- 6.6 Pedigree of family PD316. Phenotypically affected individuals are shown by black filled in symbols. Clinically examined individuals are shown by straight line over the symbol. 107

6.7	Pedigree of Family PD7 with Greig cephalopolysyndactyly syndrome. Phenotypically affected individuals are shown by black filled in symbols. Clinically examined individuals are shown by straight line over the symbol.	109
6.8	Phenotypic appearance of affected subjects in family PD7. (A, B, C, D & E) present face feet and hands of proband IV-6, facial dismorphism and bilateral PAPA/B, (F, G, H & I) present hands and feet of III-4 with bilateral PAPA.	110
6.9	Pedigree of family PD16 with PAPB. Phenotypically affected individuals are shown by black filled in symbols. Clinically examined individuals are shown by straight line over the symbol.	111
6.10	Phenotypic appearance of affected subject in family PD16 with PAPB. (A) Hands of subject IV-2 and (B) hand of individual V-4, site of PAPB (removed surgically) is indicated by arrow.	112
6.11	Pedigree of family BD1 with brachydactyly type E with autosomal recessive mode of inheritance. Solid symbols represent affected subjects, while the open symbols represent normal individuals. Clinically examined individuals are shown by horizontal bar over the symbol.	113
6.12	Clinical appearance of the proband in BD1 family with brachydactyly type E. (A & B) Hands of proband showing shortening of 3rd and 4th metacarpals in both hands. (C and D) Feet represent bilateral shortening of 3rd and 4th metatarsal. (E) Feet of IV-5 bilateral shortening of 4th metatarsal. (F) Feet of V-5 with mild hypoplasia of right 3rd and 4th metatarsal.	115
6.13	Pedigree of family PD14A with autosomal recessive syndactyly of 3rd and 4th finger	117
6.14	Phenotype appearance of affected subjects in family PD14A. (A, B) hands and feet of proband V-4, (C, D) hands and feet of subject V-3, (E) left hands of V-1.	118
6.15	Sequences of double stranded oligonucleotide probes used for EMSAs.	128

7.1	Pedigree of family PD1 and haplotypes of the individuals at 7q36 using microsatellite markers. The homozygous region in affected subjects segregating with phenotype is shown in box.	130
7.2	Representative chromatogram of mutation (4976 T>G) in ZRF (Shh regulatory element) in the intron 5 of <i>LMBR1</i> identified in family PD1. A. Mutant, B. Wild type, C. Restriction analysis using <i>MseI</i> restriction enzyme in all the sampled family members (normal and affected), 268bp mutant allele is indicated by arrow.	131
7.3	Electrophoretic mobility shift assay of the conserved element demonstrating binding of Caco-2 cell line nuclear extract to both wild type (T-allele) and mutant allele (G-allele). Unlabelled probes were added to demonstrate specific binding to both alleles. Specific binding is indicated by arrow.	132
7.4	Linkage analysis using STRs flanking <i>GLI3</i> in family PD2.	137
7.5	Chromatogram and restriction analysis of family PD2. (A) heterozygous mutant, (B) homozygous normal, (C) restriction analysis after PCR amplifying exon 13 of <i>GLI3</i> of whole PD2 family using <i>BglII</i> enzyme, mutant allele (496 bp), wild type alleles (276 & 220 bp) are indicated by arrow.	138
7.6	Chromatogram of mutation in family PD316. (A) Heterozygous mutant (B) homozygous normal.	140
7.7	Chromatogram of mutation in family PD7. (A) Heterozygous mutant, (B) homozygous normal, and (C) amino acids sequence comparison of <i>GLI3</i> proteins from different species and site of missense mutation (P1525L) in family PD7 is indicated by arrow.	142
7.8	Chromatogram and restriction analysis of family PD16. (A) Heterozygous mutation carrier, (B) wild type, and (C) restriction analysis for the identified mutation in all the sampled family members.	144

7.9	Whole genome parametric (Allegro) linkage result using easyLINKAGE plus v5.08 in family BD1. Maximum multipoint LOD score obtained on chromosome six.	151
7.10	Family BD1 with autosomal recessive brachydactyly type E. Microsatellite markers used to narrow down the homozygous region identified by 10K SNP array. Minimum disease associated haplotype shared by all the affected individuals are shown in red.	152
7.11	Genetic map of novel locus on chromosome 6 mapped in BD1 family	153
7.12	Whole genome parametric (Allegro) linkage result using easyLINKAGE plus v5.08 in family PD14A. Maximum multipoint LOD score obtained on chromosome 2 and 9.	160
7.13	Family PD14A with autosomal recessive 3rd and 4th digit syndactyly. Microsatellite markers used to narrow down the homozygous region on chromosome 9 identified by 10K SNP array. Minimum disease associated haplotype shared by all the affected individuals are shown by box.	161
7.14	Chromatogram and restriction analysis of family PD14A. (A) Homozygous affected mutant, (B) heterozygous carrier, (C) homozygous normal, (D) restriction analysis after PCR amplification of exon 8 of <i>Frem1</i> for all the sampled members in PD14A family using <i>XhoI</i> enzyme, mutant allele (347 bp), wild type alleles (204 & 143 bp).	162
7.15	Amino acid sequence comparison of 2nd CSPG repeat in <i>Frem1</i> , <i>Frem2</i> and <i>Frem3</i> proteins. Site of substitution is indicated by arrow is highly conserved among all family members.	163
7.16	Conservation of <i>Frem1</i> among various vertebrate species. Six consecutive amino acids are highly conserved among all the species. Site of substitution (p.R430Q) indicated by arrow is highly conserved among all family members.	163

LIST OF TABLES

Table #	Title	Page #
1.1	Overview of the MCPH loci mapped to date and the genes identified.	4
2.1	Standard solutions and kits used for experiments.	31
2.2	PCR profile for amplification of genomic fragments.	33
2.3	PCR thermal cycling conditions for fluorescently labeled microsatellite markers.	34
2.4	Sequencing PCR master mix.	37
2.5	Sequencing PCR profile.	38
2.6	List of microsatellite markers used for Genotyping of Primary microcephaly families.	40
2.7	Primers used for PCR amplification and subsequent sequencing of ASPM gene.	41
2.8	Primer pairs used for PCR amplification and subsequent sequencing of <i>CENPJ</i> exons.	42
2.9	Primer pairs used to PCR amplify and subsequent sequencing of <i>MAG</i> exons.	43
2.10	Primer pairs used to PCR amplify and subsequent sequencing of <i>SNX26</i> exons.	44
2.11	Primer pairs used to PCR amplify and subsequent sequencing of <i>CHST8</i> exons.	45
2.12	Primer pairs used to PCR amplify and subsequent sequencing of <i>ZNF302</i> exons.	46

2.13	Primer pairs used to PCR amplify and subsequent sequencing of <i>ZNF599</i> exons.	47
2.14	Primer pairs used to PCR amplify and subsequent sequencing of <i>SIRT2</i> exons.	48
2.15	Primer pairs used to PCR amplify and subsequent sequencing of <i>MCPH1</i> exons.	49
2.16	Primer sequences and restriction enzymes used for the confirmation of identified mutations.	50
3.1	Two point LOD score in family MCP15 at chromosome 19.	69
4.1	Reported MCPH mutations in <i>ASPM</i> .	76-78
6.1	Clinical description of family PD2.	104
6.2	Clinical description of family PD316.	108
6.3	List of microsatellite markers used for linkage studies.	119
6.4	Primer pairs used to PCR amplify and subsequent sequencing of <i>GLI3</i> exons.	120
6.5	Primer pairs used to PCR amplify and subsequent sequencing of <i>HOXD13</i> exons.	121
6.6	Primer pairs used to PCR amplify and subsequent sequencing of <i>TFAP2A</i> exons.	121
6.7	Primer pairs used to PCR amplify and subsequent sequencing of <i>JARID2</i> exons.	122
6.8	Primer pairs used to PCR amplify and subsequent sequencing of <i>DTNBP1</i> exons.	123
6.9	Primer pairs used to PCR amplify and subsequent sequencing of <i>GMPR</i> exons.	124

6.10	Primer pairs used to PCR amplify and subsequent sequencing of <i>MYLIP</i> exons.	125
6.11	Primer pairs used to PCR amplify and subsequent sequencing of <i>ATXN1</i> exons.	126
6.12	Primer pairs used to PCR amplify and subsequent sequencing of <i>FREMI</i> exons.	127
6.13	Primer pairs used to PCR amplify and subsequent sequencing of putative regulatory regions.	128
6.14	Primer pairs used to PCR amplify and sequencing of sonic hedgehog (<i>SHH</i>) regulatory element (ZRS) in intron5 of <i>LMBR1</i> .	128
7.1	Spectrum of ZRS mutations identified in different species.	133
7.2	Two point LOD score for family PD2 on chromosome 7p13.	137
7.3	Two point LOD score for family BD1 on chromosome 6p24.1-p22.3.	153
7.4a	Copy number variations (CNVs) identified by SNP6 analysis.	154
7.4b	Copy number variations (CNVs) identified by SNP6 analysis.	155

LIST OF ABBREVIATIONS

<i>ASPM</i>	Abnormal spindle like microcephaly associated
bp	Base pairs
cM	Centimorgan
<i>CDK5RAP2</i>	Cyclin Dependent Kinase 5 Regulatory Associated protein 2
<i>CENPJ</i>	Centrosomal associated protein J
DNA	Deoxyribonucleic acid
dNTPs	Deoxynucleotide phosphates
EDTA	ethylenediaminetetraacetic acid
<i>Frem</i>	Fras1 related extracellular matrix protein
HC	Head circumference
kb	Kilo bases
LOD	Logarithm of odds ratio
M	Molar
MCPH	Primary microcephaly
<i>MCPHI</i>	Microcephalin
mg	Milligram
ml	Milliliter
mM	Millimolar
MRI	Magnetic resonance imaging
mRNA	Messenger RNA
MTOC	Microtubule organizing centre
ng	Nanogram
NMD	Nonsense mediated decay
NMR	nuclear magnetic resonance
NWFP	North Western Frontier Province
OMIM	Online Mendelian Inheritance in Man
PCC	Premature chromosomal condensation
PCR	Polymerase chain reaction

pH	Potential of hydrogen ions
RNA	Ribonucleic acid
SD	Standard deviation
<i>SHH</i>	Sonic hedgehog
SNP	Single nucleotide polymorphism
<i>STIL</i>	Pericentriolar and centrosomal protein
UTRs	Untranslated regions
°C	Degree celcius
µg	microgram
µl	Microlitre
µM	Micromolar
θ	Theta (recombination fraction)
v/v	Volume by volume

ABSTRACT

Numerous genetic conditions have been described clinically but the molecular etiology for most of them is still unknown. With the advancement in the field of molecular biology powerful techniques have been developed to localize these conditions in the human genome and subsequent identification of causative genes. Functional analysis of causative genes leads to the discovery and understanding of novel genetic processes and pathways underlying disease conditions including normal developmental pathways. Linkage analysis studies in Mendelian disorders to identify the causative genes and mutations are possible using large pedigrees with multiple affected individuals. Analysis of alleles using microsatellite markers and genome wide SNPs lead to the discovery of novel genes and loci for specific disorders.

The main aim of this thesis was to analyze families with autosomal recessive primary microcephaly and families with inherited limb disorders particularly polydactyl, syndactyly and brachydactyly to identify the causative mutations or chromosomal loci.

Autosomal recessive primary microcephaly (MCPH) is a neurogenic disorder characterized by reduced head circumference (≤ 4 SD) and variable degree of mental retardation without any other neurological manifestations. The normal brain architecture is preserved despite the fact that brain size is reduced to three folds. In the first part of this study, genetic analysis of eleven primary microcephaly families was carried out. Linkage analysis using highly polymorphic microsatellite markers confirmed linkage in six families to *ASPM* (MCPH5), two *CENPJ* (MCPH6), one MCPH2 locus and haplotype analysis in two families demonstrated compound heterozygosity for *ASPM*. Sequencing of *ASPM* in six potentially linked families (MCP3, MCP6, MCP7, MCP9, MCP11 and MCP17) revealed six homozygous mutations in the affected subjects (A1160fs1181X, Y2245fs2258X, R3233X, Y3164X, S3186X, and R3244X respectively) and two possible compound heterozygous families (MCP35 and MCP18) demonstrated compound heterozygous mutations (W1326X/R3107X and R1019X/Q2632X, respectively). Compound heterozygous patients (W1326X & R3107X) also have additional clinical symptoms of seizures.

Two families linked to MCPH6 locus (MCP21, MCP22) demonstrate 1bp deletion mutation c.17_18delC (T6fsX3) in exon 2 of *CENPJ* leading to premature termination of protein. This mutation was previously reported in two Northern Pakistani families.

Family MCP15 established linkage to MCPH2 locus on chromosome 19q (19q13.1-q13.2). MCPH2 locus was defined by markers D19S416 and D19S420 which was about 7.6 cM in two consanguineous families from Northern Pakistan. However, the region is significantly reduced in MCP15 which is defined by markers D19S416 and D19S47. This substantially decreases the minimum critical interval from 7.6 cM to about 4.4 cM containing 162 genes.

Family MCP36 has only single affected child. Molecular analysis using microsatellite markers revealed that affected individual is homozygous for the MCPH1 locus. By sequencing I have identified a novel nonsense mutation in exon 4 of *MCPH1*/microcephalin. The mutant protein lacks both of the C-terminal BRCT domains required for the normal functioning of protein during cell cycle progression and DNA repair mechanism.

The second part of thesis comprised of genetic analysis of inherited limb disorders. Inherited limb malformations are genetically heterogeneous group of conditions with wide range of phenotypic manifestations. Inherited limb disorders occur as an isolated entity or syndromic form and are of clinical significance due to their severity and overall frequency. Limb development is a cascade of complex pathways involving patterning, growth and differentiation. Molecular characterization of inherited limb disorders may lead to the identification of novel genes and signalling pathways important for normal limb development during organogenesis. Family PD1 with preaxial polydactyly and triphalangeal thumb revealed autosomal dominant inheritance. Linkage analysis using microsatellite markers D7S550, D7S559 and D7S2423 was performed and maximum multipoint LOD score of 1.93 at recombination frequency $\theta = 0.1$ was obtained. This region spans *SHH* and its cis-acting regulatory element (ZRS), which is well conserved among various species lying in intron 5 of *LMBR1*. Direct Sequencing of ZRS identified a novel point mutation (T>G) in ZRS element at base position 4976 in intron 5 of *LMBR1*. Many point mutations have been identified in ZRS leading to disruption of *SHH* expression during limb development leading to preaxial duplication in upper limbs. Electrophoretic mobility shift assay (EMSA) demonstrated a marked difference between wild and the mutant probe which uniquely bound a specific subset of nuclear transcription factors extracted from Caco-2 cells. It is suggested that altered transcription factor affinity may be important for our understanding of how single nucleotide substitutions in long distance regulatory elements changes cis-regulation of its target gene.

Greig cephalopolysyndactyly syndrome (GCPS) is an autosomal dominant disorder which affects limb and craniofacial development. GCPS was mapped to chromosome 7p13. Mutations in *GLI3* had been described in GCPS patients. In the present study four novel *GLI3* mutations in four distinct families have been identified. In family PD2, a single nucleotide substitution mutation [c.1702A>T (p.R568X)] leading to immediate stop codon in exon 13 is identified. Two base pairs deletion mutation [c.1853_1854delAC (p.Y618fs)] leading to frameshift and premature terminated protein product of 673 amino acids is identified in family PD316 in a family from Denmark. Both the mutations R568X and Y618fs lie in zinc finger domain in the first third of *GLI3* producing truncated protein product which may affect the DNA binding property of zinc finger domain leading to possibly haploinsufficiency of *GLI3*. In family PD7, a novel C to T substitution at coding nucleotide 4574 (p.P1525L) in exon 15 of *GLI3* is identified. The third mutation which is a missense (c.4574C>T (p.P1525L) lies in the last third of *GLI3*. Missense mutation P1525L lies in the C terminal region of *GLI3* protein in the transactivation domain. In family PD16, at coding nucleotide position 3557, C to T substitution leading to missense incorporation of amino acid (p.P1186L) is identified. The variability in phenotype with respect to mutation in the affected family members may help to understand the phenotypic spectrum of *GLI3* mutation.

Brachydactyly is a rare and genetically heterogeneous disorder. In the present study a novel locus in a large consanguineous family with recessive form of brachydactyly type E is localized on chromosome 6p22.3 by homozygosity mapping using 10K SNP analysis. The physical linkage interval lies between 15,837,143 to 16,579,402 bp which is about 742 Kb. Maximum two point LOD score (Z_{max}) of 5.00 at recombination fraction ($\theta=0.0$) was calculated at marker locus D6S18xAG. This region spans only seven genes including four pseudogenes. Sequencing of protein coding genes which include *MYLIP*, *GMPPR* and *ATXN1* did not reveal any mutation. Analysis using SNP6 array also did not identify any homozygous deletion or duplication in the region. However, smaller deletions or duplication (≤ 30 kb) cannot be excluded.

Family PD14A shows cutaneous syndactyly of 3rd and 4th digit in hands. After exclusion using microsatellite markers on chromosome 2q34-q36 (syndactyly type I), 3p21.31 (zygodactyly), 2q31 (SPD1 locus, HOXD13), 6q22.31 (*GJAI*, syndactyly type III), 22q13.31 (SPD2), 14q11.2-q12 (SPD3) and 17p13.3 (syndactyly type IX) genome wide 10K SNP analysis was performed.

After fine mapping using microsatellite markers a single homozygous region on chromosome 9 flanked by markers, SNP_A-1518820 and D9S21AT (marker not available in Marshfield genetic map) was identified. The physical positions of flanking markers are 12018387 bp to 15340449 bp on chromosome 9 with maximum LOD score (Z_{\max}) of 2.35 for given locus ($\theta=0.00$). The region spans only 22 genes. A novel single nucleotide G to A substitution at coding nucleotide position 1289 (c.1289G>A) in exon eight leading to missense incorporation of glutamine instead of arginine at amino acid position 430 of *Frem1* (p.R430Q) is identified. Arginine at 430 amino acid position of *Frem1* is not only conserved among different vertebrate species but also conserved among *Frem* family of genes. However, possibility of missense mutation in *Frem1* producing a defect in digit separation requires more families to study in addition to the functional studies in experimental models to prove the pathogenic nature of this mutation.

Papers from the research work presented in this thesis.

1. **Farooq M**, Mahmood Baig, S., Hansen, L., Sajid Hussain, M., Anjum Inayat, I., Aslam, M., Anver Qureshi, J., Toilat, M., Kirst, E., Wajid, M., Nurnberg, P., Eiberg, H., Tommerup, N., and Kjaer, K. W. (2009). Compound heterozygous ASPM mutations in Pakistani MCPH families. *Am J Med Genet A* 149A(5), 926-30.
2. **Farooq M**, Troelsen JT, Boyd M, Eiberg H, Hansen L, Hussain MS, Rehman SU, Azhar A, Ali A, Bakhtiar SM, Tommerup N, Baig SM, and Kjaer KW. Preaxial polydactyly/triphalangeal thumb is associated with changed transcription factor-binding affinity in a family with a novel point mutation in the long-range cis-regulatory element ZRS. *Eur J Hum Genet.* 18, 733-736 (June 2010) doi:10.1038/ejhg.2009.225. PMID: 20068592.
3. **Farooq M**, Baig S, Tommerup N, Kjaer KW. 2010. Craniosynostosis-microcephaly with chromosomal breakage and other abnormalities is caused by a truncating MCPH1 mutation and is allelic to premature chromosomal condensation syndrome and primary autosomal recessive microcephaly type 1. *Am J Med Genet Part A* 152A:495-497.
4. Identification of novel *GLI3* mutations in families with Greig cephalopolysyndactyly (GCPS) syndrome from Pakistan. (Manuscript in preparation)
5. A novel locus for autosomal recessive brachydactyly type E localized on chromosome 6p22.3. (In progress)

Part 1

Primary microcephaly

1 INTRODUCTION

Pakistan is a unique country in the world with population size of 172 millions according to 2008 estimates. About 70% of its population is living in villages holding small area of land and are engaged in small scale agriculture farming and livestock business, while 30% population living in cities are engaged in services department and small scale business to earn their living. Literacy rate is about 40% which is far low as compared to many other developing countries. There is a strong tradition of marrying within the same caste or tribe. First cousin marriages are most commonly practiced (60%). Due to high percentage of consanguineous marriages there is an increased risk for recessive genetic disorders in Pakistani population. Moreover, social/religious customs allows families to have more number of children. Lack of knowledge about the genetic disorders and unavailability of prenatal diagnostic facilities lead to multiple numbers of affected individuals in affected families. Those large families with multiple affected individuals are providing a best starting point to study the inheritance pattern and could also describe the phenotypic variability. Families with multiple numbers of affected individuals are ideal for linkage studies to find out the chromosomal location of disease gene. Large pedigrees could provide the ideal explanation to the questions about genetic heterogeneity that can otherwise confound linkage studies.

Genetic disorders can be differentiated into single gene disorders (so-called monogenic disorders), genetic disorders with complex etiology, and somatic genetic diseases. Monogenic disorders may be autosomal recessive, autosomal dominant or they may show X-linked inheritance pattern. Numerous genetic conditions have been described clinically but the molecular etiology is still unknown for many of them. Powerful approaches to identify the underlying gene of a monogenetic disorder involve strategies such as linkage analysis, characterization of cytogenetic rearrangements and microdeletions. The most powerful strategy is the linkage analysis of a Mendelian trait in families, especially when sufficient family data are available and the mode of inheritance is known. The identification of a chromosomal region linked to a specific disorder allows the identification of the underlying gene by a candidate gene approach. This approach became feasible with the Human Genome Project: to date, almost all of the 20, 000 to 25, 000 human genes and coding sequences are known and available in public databases. After the identification of the gene subsequent analysis of the gene function will help

to understand the underlying defect of a genetic disorder, which is prerequisite for sophisticated therapeutic approaches for the disease in question.

Prerequisite for the linkage approach are large families in which the segregation of the disorder can be analyzed by following the segregation of polymorphic DNA sequences such as short tandem repeats (STRs) or single nucleotide polymorphisms (SNPs). Initial studies show that consanguinity augments the prevalence of hereditary recessive disorders in Pakistani families, which can be employed for the isolation of the respective disease loci. Large, consanguineous, stable and in some cases overlapping families make Pakistan very suitable for the study of hereditary disorders. These families are an ideal source for linkage studies, as only large individual families contain enough potential to allow the disease gene to be localized. This is of special importance when a disorder displays genetic heterogeneity like primary microcephaly.

Recently, linkage analysis involving Pakistani families with inherited deafness, hereditary skin disorders and microcephaly have resulted in the identification of novel chromosomal loci for these disorders (Malik *et al.*, 2006; Malik *et al.*, 2004; Pattison *et al.*, 2000; Roberts *et al.*, 1999). Efforts are now directed to isolate and functionally characterize the causative genes.

1.1 Primary microcephaly (MCPH)

Microcephaly refers to small head which is greater than three standard deviations below the population age and sex related mean. Microcephalic patients have small cranial capacity resulted from hypoplasia of underlying cerebral cortex rather than abnormal development of skull. Microcephaly is known to have a heterogeneous etiology with number of genetic and environmental factors responsible for the condition. There are number of environmental conditions which leads to secondary microcephaly include intrauterine infections, radiation exposure during prenatal life, maternal phenylketonuria, birth asphyxia and drugs or poison ingestion (fetal alcohol syndrome, fetal hydantion syndrome) during pregnancy. But all these are known to be rare causes of microcephaly except for birth asphyxia. Most of the time microcephaly is caused by genetic factors which include cytogenetic abnormalities like translocations, inversions and large deletions, or it may be caused by abnormality in single gene (Jackson *et al.*, 1998).

Autosomal recessive primary microcephaly (MCPH; MIM 251200) or microcephaly vera is inherited as an autosomal recessive condition. This is a congenital condition in which the head circumference of affected individuals is greatly reduced ($>3SD$) as compared to the population age and sex means and affected individuals have variable degree of mental retardation which persists throughout their life without additional morphological or clinical symptoms (Woods *et al.*, 2005). The degree of mental retardation remains static throughout their life span. The reduction in head circumference is due to hypoplasia of underlying cerebral cortex during fetal development resulting in a disproportionally small cerebral cortex (Figure 1.2) even though it may preserve its normal architecture (Dobyns, 2002; McCreary *et al.*, 1996; Mochida and Walsh, 2001). Prior to the discovery of MCPH genes, autosomal recessive microcephaly was reported to have an incidence of 1/30,000 in Japan, 1/250,000 in Holland, and 1/2,000,000 in Scotland (Komai *et al.*, 1955; Tolmie *et al.*, 1987; Van Den Bosch, 1959). The incidence is higher in populations with a high rate of consanguineous marriages including Pakistan (one in 10,000 in Northern Pakistanis), Turkey, Brazil and Morocco. Clinical surveys from mid 20th century suggested that MCPH was expected to be an autosomal recessive Mendelian disorder. However, molecular studies of this disorder were not started until the late 1990s. Seven loci have been mapped designated as MCPH1-MCPH7 between 1998 and 2009; five genes have been described for MCPH (Table 1.1). Seventh locus and corresponding gene for MCPH has been mapped recently in five Indian families (Kumar *et al.*, 2009). 18/56 northern Pakistani families excluded from previously six known loci may be linked to this newly identified locus (Bond *et al.*, 2002). However, four additional MCPH families from India were excluded from all the seven known loci suggested that more MCPH genes may exist (Kumar *et al.*, 2009).

Table: 1.1 Overview of the MCPH loci mapped to date and the genes identified

Locus	Chromosomal location	Protein	Characteristics of the protein	Reference
MCPH1	8p22-pter	<i>Microcephalin</i>	Microcephalin contains three BRCT domains implicated in cell cycle control and/or DNA repair, mutations lead to aberrant chromosome condensation	(Jackson <i>et al.</i> , 2002; Jackson <i>et al.</i> , 1998; Trimborn <i>et al.</i> , 2004)
MCPH2	19q13.1-13.2	Unknown		(Roberts <i>et al.</i> , 1999)
MCPH3	9q34	<i>CDK5RAP2</i>	Cyclin Dependent Kinase 5 Regulatory Associated protein 2, localized at the centrosomes during mitosis	(Bond <i>et al.</i> , 2005; Moynihan <i>et al.</i> , 2000)
MCPH4	15q15-q21	Unknown		(Jamieson <i>et al.</i> , 2000; Jamieson <i>et al.</i> , 1999)
MCPH5	1q31	<i>ASPM</i>	ASPM protein contains a putative amino terminal microtubule binding domain, organization and bundling of microtubules at the spindle poles	(Bond <i>et al.</i> , 2002; Jamieson <i>et al.</i> , 2000)
MCPH6	13q12.2	<i>CENPJ</i>	Centromere associated Protein J, localized at the centrosomes during mitosis	(Bond <i>et al.</i> , 2005; Leal <i>et al.</i> , 2003)
MCPH7	1p32.3-p33	<i>STIL</i>	Pericentriolar and centrosomal protein	(Kumar <i>et al.</i> , 2009)

1.2 Structure of cerebral cortex

The cerebral cortex is a structure within the human brain that plays a key role in acquiring complex cognitive functions, such as language and memory. During the evolution of *Homo sapiens* the surface of cortex has increased tremendously. The cerebral cortex is a multi layered structure that is highly convoluted in mammals. This folding allows more volume to pack into the limited volume of skull. This disproportionate increase in size of cerebral cortex in humans is thought to lie behind the growth in intellectual capacity and their ability to execute complex cognitive skills (Finlay and Darlington, 1995). The outermost layer of cerebrum is grayish in color which comprises of neurons and unmyelinated nerve fibers whereas the white matter below the gray matter consists mainly of myelinated axons. Human cerebral cortex is about 2 mm thick. In large mammals the outer folded surface of cerebral cortex is called “gyri” while most of the cortical surface in grooves is called “sulci”. Cerebral cortex also called neocortex is divided into 6 horizontal layers. According to Korbinian Brodmann (1909), histologically neurons of the cerebral cortex are grouped into six main layers, from outside (pial surface) to inside (white matter):

1. The molecular layer I, which contains few scattered neurons and consists mainly of extensions of apical dendrites and horizontally-oriented axons.
2. The external granular cell layer II, which contains small pyramidal neurons and numerous stellate neurons.
3. The external pyramidal cell layer III, which contains predominantly small and medium-size pyramidal neurons, as well as non-pyramidal neurons with vertically-oriented intracortical axons.
4. The internal granular cell layer IV, which contains different types of stellate and pyramidal neurons.
5. The internal pyramidal cell layer V, which contains large pyramidal neurons (such as the Betz cells in the primary motor cortex).
6. The multiform layer VI, which contains few large pyramidal neurons and many small spindle-like pyramidal and multiform neurons.

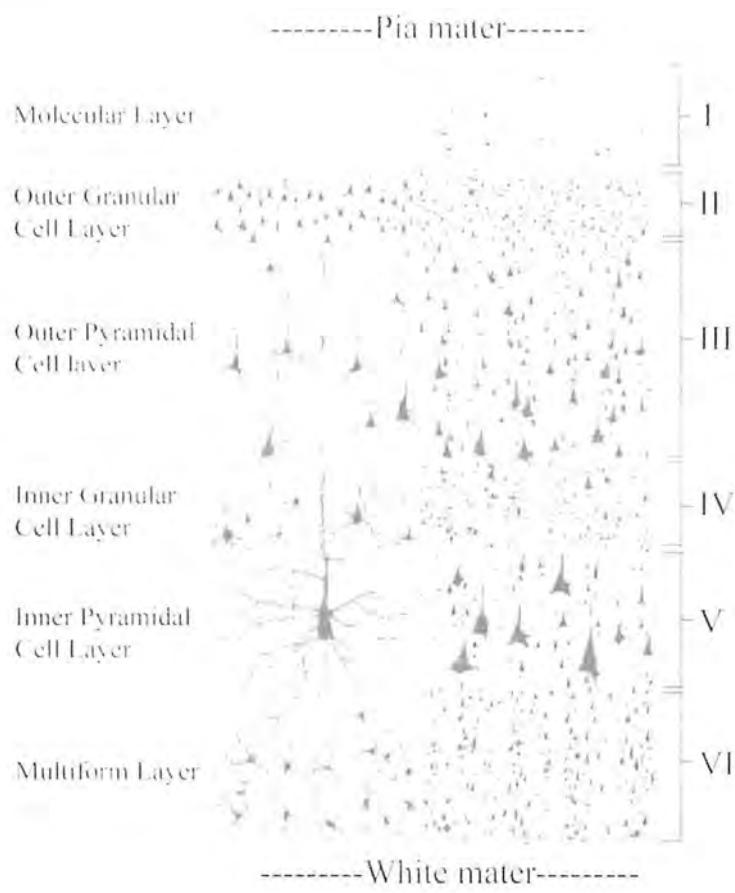


Figure 1.1: The cerebral neocortex features six layers that are illustrated above by two different staining methods. Golgi silver impregnation (left) stains selective individual neurons entirely. Nissl stain (right) stains only the cell bodies of all neurons (Source; <http://www.benbest.com/science/anatmind/anatmd5.html>).

1.3 Development of cerebral cortex

The development of cerebral cortex is complex phenomenon which involves neuronal proliferation, migration and differentiation. The cerebral cortex develops from most anterior part of the neural plate. The neural plate folds and closes to form the neural tube. The cavity inside the neural tube develops the ventricular system. Neurons are derived from the neuronal progenitor cells residing in the neuroepithelium of the ventricular zone, the region surrounding the ventricles of the developing brain (Brand and Rakic, 1979).

Cortical neurons are generated within the ventricular zone, next to the ventricles. At first, this zone contains "progenitor" cells. Before the start of neurogenesis the neuronal progenitor cells undergo multiple rounds of symmetric (proliferative) cell division, which occur when the mitotic spindles are oriented horizontal to the neuroepithelium ventricular surface this symmetric division leads to production of two daughter progenitor cells. The majority of the neurons are produced by asymmetric (neurogenic) division, when mitotic spindles rotate to lie vertical to the neuroepithelium. This asymmetric cell division gives rise two daughter cells with different fates, one neuronal progenitor cell and one neuron (Chenn and McConnell, 1995; Haydar *et al.*, 2003). The glial fibers produced in the first divisions of the progenitor cells are radially oriented, spanning the thickness of the cortex from the ventricular zone to the outer, pial surface, and provide scaffolding for the migration of neurons outwards from the ventricular zone. The first divisions of the progenitor cells are symmetric, which duplicates the total number of progenitor cells at each mitotic cycle. Cortical progenitor cells undergo 11 cycles of cell divisions in mice (Takahashi *et al.*, 1995), and much more times in human during cortical development in pre-natal life. Then, some progenitor cells begin to divide asymmetrically, producing one postmitotic cell that migrates along the radial glial fibers, leaving the ventricular zone, and one progenitor cell, which continues to divide until the end of development, when it differentiates into a glial cell or an ependymal cell. The migrating daughter cells become the pyramidal neurons of the cerebral cortex.

The centrosome plays a key role in regulating cell division, functioning as a microtubule organizing centre. The function of centrosome is to nucleate microtubule polymerization from free tubulin subunits and to organize the microtubules (Badano *et al.*, 2005).

The layered structure of the mature cerebral cortex is formed during development. The first pyramidal neurons generated migrate out of the ventricular zone and form the preplate. Next, a group of neurons migrating into the middle of the preplate divides this transient layer into the superficial marginal zone, which will become layer one of the mature neocortex, and the subplate, forming a middle layer called the cortical plate. These cells will form the deep layers of the mature cortex, layers five and six. Later born neurons migrate radially into the cortical plate past the deep layer neurons, and become the upper layers (two to four). Thus, the layers of the cortex are created in an inside-out order.

1.4 Clinical features of primary microcephaly

The most common clinical finding in primary microcephaly is severe reduction in head circumference with variable degree of mental retardation. The size of human brain is approximately three times larger than its closest primate relatives (Ponting and Jackson, 2005). Brain growth also occurs in postnatal life in first 3 year of human life, the brain becomes four times larger than the size at birth. This brain growth is accommodated by the growth of skull bones and delayed closure to sutures between the skull bones. Measurement of head circumference (HC) as measured by occipito-frontal circumference is an indirect method of calculating brain size. Even though more-accurate techniques are now available like volumetric nuclear magnetic resonance (NMR) scanning. Measurement of HC remains the most common, simple method for evaluating gross brain size (Aicardi, 1998). Charts are available to plot HC against age and sex. The term microcephaly refers to the clinical finding of an HC significantly smaller than expected for a normal individual, taking into consideration age and sex (Aicardi, 1998). Using charts, microcephaly is defined as an HC that is three standard deviations below the mean (-3SD). Reduced cranial size is directly correlated with degree of mental retardation (Dolk, 1991). Microcephaly may not be detectable by ultrasonography until the third trimester of pregnancy which makes it difficult for prenatal diagnosis and genetic counseling (Tolmie *et al.*, 1987). So diagnosis using molecular tools will be most reliable method to provide genetic counseling to families at risk.

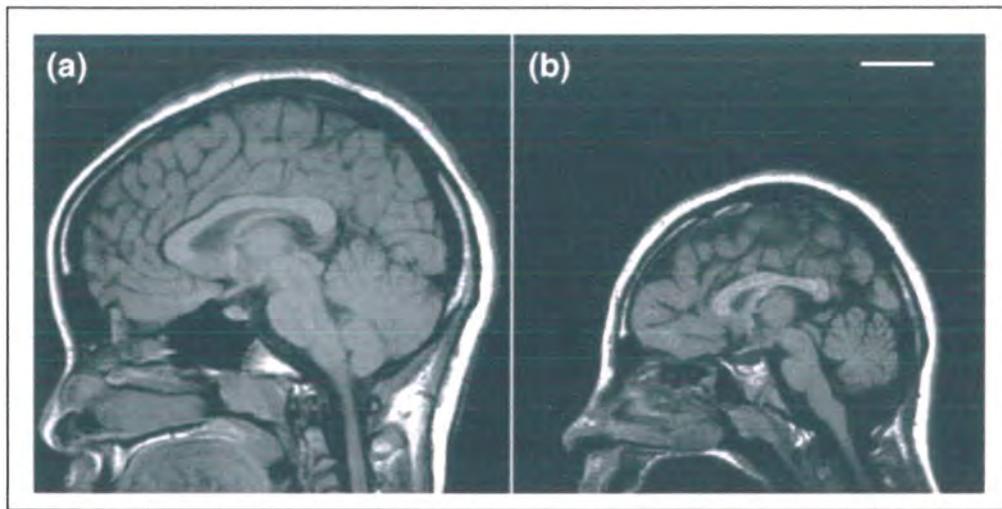


Figure 1.2: A comparison of magnetic resonance images from an individual with primary microcephaly and an unaffected individual of a similar age. (a) Sagittal T1-weighted image from an unaffected 11-year-old female control. (b) Sagittal T1-weighted image from a 13-year-old female with an MCPH5 mutation showing striking reduction in the size of the cerebral cortex, prominent sloping of the forehead and preserved midline structures. Figure reproduced from an original figure (Bond *et al.*, 2002).

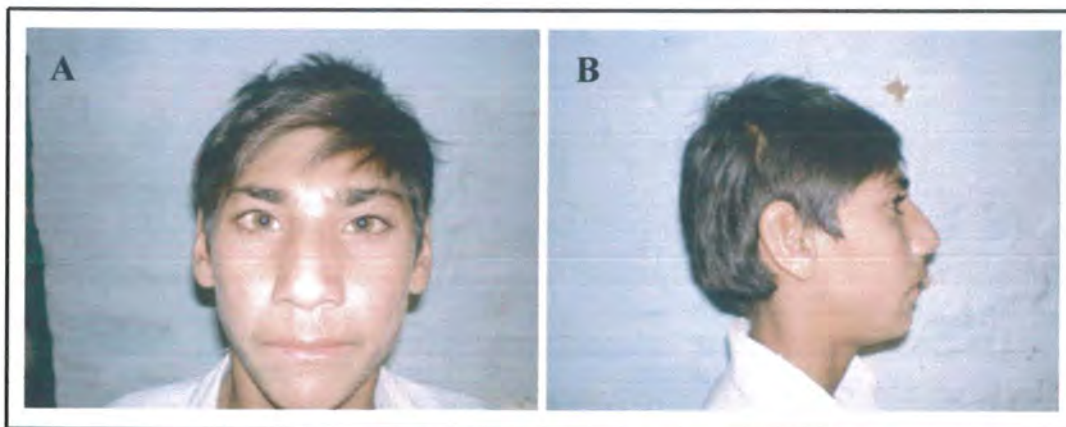


Figure 1.3: Phenotypic appearance of a typical MCPH patient. (A) frontal view. (B) Side view, prominent sloping forehead.

1.5 MCPH genes and their function

MCPH is genetically heterogeneous with seven loci (MCPH1-MCPH7) mapped by homozygosity mapping strategy using polymorphic markers in large consanguineous families with multiple number of affected individuals. Five genes identified so far are microcephalin (*MCPH1*), cyclin-dependent kinase 5 regulatory subunit associated protein 2 (*CDK5RAP2*), abnormal spindle like microcephaly associated (*ASPM*), centrosomal protein J (*CENPJ*) and STIL have been identified so far using positional cloning strategies (Table.1) (Bond *et al.*, 2002; Bond *et al.*, 2005; Jackson *et al.*, 2002). Clinically, patients with mutations at any of the loci are indistinguishable.

1.5.1 Microcephalin (*MCPH1*)

The first causative gene identified for primary microcephaly was Microcephalin (*MCPH1*). This gene was identified in two Pakistani families with primary microcephaly using positional cloning technique within an ancestral haplotype (Jackson *et al.*, 2002). Homozygous truncating mutation (S25X) was found in both families. Expression of gene was observed in fetal mouse brain during neurogenesis (Jackson *et al.*, 2002) with highest expression in lateral ventricles, the site of production of cerebral cortical neurons. Mutations in *MCPH1* are not so common as compared to other MCPH genes (Kumar *et al.*, 2002; Roberts *et al.*, 2002). However, *MCPH1* exhibits much broader phenotype like premature chromosomal condensation (PCC) syndrome (Neitzel *et al.*, 2002) is found to be allelic to *MCPH1* primary microcephaly (Trimborn *et al.*, 2004). Patients with PCC syndrome have microcephaly, short stature and abnormal cellular phenotype i.e. increased number of prophase like cells in peripheral blood smears with poor banding quality (Neitzel *et al.*, 2002). MRI scan shows periventricular neuronal heterotopias in PCC syndrome suggests that mutations in *MCPH1* may affect migration of neurons (Trimborn *et al.*, 2004). PCC syndrome was mapped to a large candidate region of 64 centimorgan (cM) on chromosome 8 using genomewide homozygosity mapping. A homozygous 1bp insertion mutation in exon 5 of the *MCPH1* (427insA) was identified in both of the affected individuals while their parents were carrier for this mutation. Increased number of prophase like cells is due to premature chromosomal condensation during early G2 phase and delayed decondensation in G1 phase of

the cell cycle. It has been found that using siRNA mediated depletion of *MCPHI* reproduce this phenotype explain the role of this protein in condensation process. This misregulated chromosomal condensation is mediated by condensin II (Trimborn *et al.*, 2006). A more recent work suggested centrosomal localization of *MCPHI* product, unlike previous reports of nuclear and chromatin associated distribution (Zhong *et al.*, 2005). Expression of microcephalin is reduced in many cancers including breast cancer cell lines and tumors of ovary and prostate in humans (Hagemann *et al.*, 2008). This reduction in microcephalin mRNA expression leads to increased chromosomal instability.

A 150-200 kb deletion encompassing the promoter and the first six exons of *MCPHI* in Iranian family with six mentally retarded children with mild microcephaly and high proportion of prophase like cells. Despite the severity of mutation affected individuals have only borderline microcephaly suggesting much wider phenotypic spectrum for *MCPHI* mutations, with autosomal recessive mental retardation being the only consistent finding (Garshasbi *et al.*, 2006). *MCPHI* encodes 835 amino acids polypeptide containing one N-terminal and two carboxyl terminal BRCT domains (Jackson *et al.*, 2002) which can bind to peptide and phosphopeptide

1.5.2 Abnormal spindle like microcephaly associated (*ASPM*)

Mutations in *ASPM* are the most common etiology for this defective neurogenesis (Bond *et al.*, 2003; Gul *et al.*, 2006b; Nicholas *et al.*, 2008). *ASPM* is orthologue of abnormal spindle (asp) in *Drosophila*. *ASPM* consists of 28 exons span over 63 kb of genomic DNA which contains an open reading frame of 10,434 bp (Bond *et al.*, 2002). A 3477 amino acid long *ASPM* protein is predicted to contain an N-terminal microtubule binding domain, two calponin homology domains which is similar to actin binding proteins, 81 IQ repeats motifs predicted to go through conformational changes upon binding to calmodulin and a C-terminal region of unrevealed job. It is identified that the N-terminal domain of *ASPM* known to be a member of novel family of ASH domains (*ASPM*, *SPD-2* and *Hydin*). These domains are known to be present in ciliary, flagellar, centrosomal and golgi associated proteins predict an alternative ciliary function of *ASPM* (Ponting, 2006). *ASPM* regulate movement of cerebrospinal fluid by its ciliary function which is required for neuronal migration during development. *ASPM* is highly expressed during

neurogenesis and appears to be involved in regulation of neurogenesis and is down regulated when neurogenesis is completed (Bond *et al.*, 2002; Kouprina *et al.*, 2005). Studies in mouse show that *ASPM* is extensively expressed in fetal and adult tissues and up regulated in many malignant conditions (Kouprina *et al.*, 2005). It localizes to spindle poles in the subventricular zone where it is suggested to regulate if the cell undergoes symmetrical or asymmetrical cell division, thereby decreasing the cell population for further cell division (Chenn and Walsh, 2003). Analyses of high-coverage expression profiling (HiCEP) confirmed that *ASPM* was down-regulated upon exposure to ionizing radiation in various human and murine cells. Additionally, *ASPM* was found down regulated in the irradiated fetal mouse brain, predominantly in the ventricular zones. A similar suppression was observed in the irradiated neurosphere cultures (Fujimori *et al.*, 2008). Until now 59 mutations have been reported in *ASPM* including one missense mutation (Table 4-1). Except for one missense mutation (Gul *et al.*, 2006b), all the other mutations identified so far incorporate premature stop codon leading to truncated protein products due to resistance of mRNA to nonsense mediated mRNA decay (NMD) (Kouprina *et al.*, 2005). *ASPM* truncation mutation has also been reported in patients with primary microcephaly and seizures (Shen *et al.*, 2005) thus broaden the clinical spectrum of *ASPM*.

1.5.3 Cyclin dependent kinase 5 regulatory associated protein (*CDK5RAP2*)

Cyclin dependent kinase 5 regulatory associated protein (*CDK5RAP2*) is a rare cause of MCPH. This gene consists of 34 exons (Bond *et al.*, 2005). Centrosomal localization of encoded protein product shows importance of centrosomes in development of central nervous system. *CDK5RAP2* is orthologue of centrosomin (*cnn*) gene of *Drosophila*. *Cnn* and *CDK5RAP2* are known to interact with γ -tubulin ring complexes in the centrosome. These complexes are responsible for production of microtubule for mitotic spindle (Fong *et al.*, 2008; Li and Kaufman, 1996; Terada *et al.*, 2003). Loss of *CDK5RAP2* function interferes with the ability of centrosome to function as a microtubule organizing centre (MTOC). This altered function may deregulate neurogenic cell divisions and hence the production of neurons.

So far, two mutations have been identified, c.243T>A (S81X) and IVS26-15A>G (E385fsX4) both lead to truncated protein product (Bond *et al.*, 2005). These mutants do not have centrosome-localizing properties (Fong *et al.*, 2008).

1.5.4 Centrosomal protein J (*CENPJ*)

Centrosomal protein J (*CENPJ*) also known as centrosomal P4.1 associated protein (*CPAP*) is also centrosomal associated protein and like *CDK5RAP2*, *CENPJ* was first identified in two Pakistani families with same single base deletion mutation, c.17_18delC (T6fsX3) in exon 2 (Bond *et al.*, 2005). A missense mutation, c.3704 A>T (E1235V) in exon 16 was identified in a family in which locus was mapped originally (Bond *et al.*, 2005). But this missense mutation yet not proved functionally (Hung *et al.*, 2004). A novel four base pair deletion c.3,243_3,246delTCAG mutation predicted to be protein truncating is also identified recently (Gul *et al.*, 2006a). *CENPJ* interact with γ -tubulin ring complexes (Bond *et al.*, 2005). *In vitro* assay identified a 112-amino acid domain (residues 311 to 422) able to destabilize microtubules. This domain could both depolymerise microtubule and inhibit microtubule nucleation (Hung *et al.*, 2004). Therefore, like *CDK5RAP2* may also have a role in microtubule production during neurogenesis (Bond *et al.*, 2005). *RNAi* based knockdown of *CENPJ* arrest all cells during mitosis and many of them have multipolar spindles (Cho *et al.*, 2006). However, affected individuals with *CENPJ* mutation do not have general growth deficiency.

1.5.5 *STIL* (SCL/TAL1 interrupting locus)

STIL (also known as *Sil* in mouse) encodes cytoplasmic protein involved in regulation of mitotic spindle organization in zebrafish and human cells and localizes to the mitotic spindle poles during metaphase only (Pfaff *et al.*, 2007). *STIL* localizes to the pericentriolar region in HeLa cells. Spindle poles during anaphase stage of cell cycle lacked *STIL* localization (Pfaff *et al.*, 2007). *STIL* expression has been identified in human fetal tissues including the fetal brain of spontaneously aborted fetus at 16 weeks of gestation using reverse transcriptase-polymerase chain reaction (Kumar *et al.*, 2009). *Sil*^{-/-} (null) mouse die with midline and left-right

asymmetry defects after embryonic day 10.5, whereas heterozygous mice (*Stil*^{+/-}) were normal (Izraeli *et al.*, 1999). The null mice showed defects in midline separation and arrest of neural tube closure defect showed that this gene has a role in fetal brain development (Izraeli *et al.*, 1999).

STIL consist of 18 exons and codes for 1288 amino acids long protein. Three mutations have been described in *STIL*. A homozygous nonsense mutation in exon 18 (c.3715C>T, p.Gln1239X), a single base pair deletion mutation (c.3655delG) in exon 18 leading to premature terminate protein of 1818 amino acids and a homozygous splice site mutation (c.IVS16+1G>A) (Kumar *et al.*, 2009).

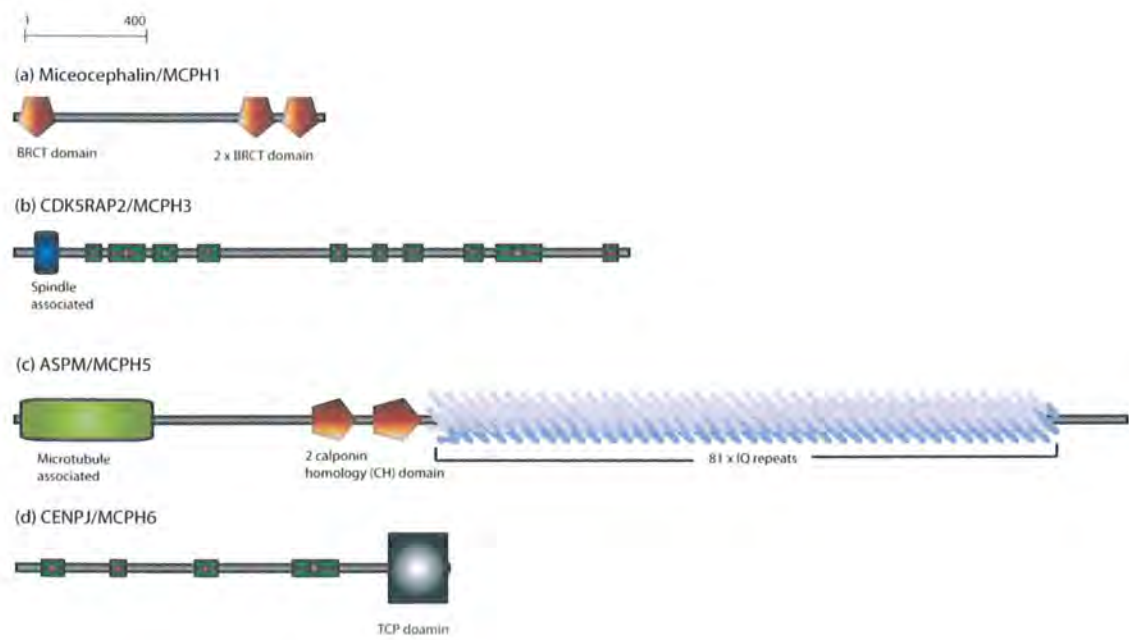


Figure 1.4: MCPH proteins and probable functional domains. (a) The *MCPH1* protein microcephalin contains three BRCT C-terminal domains, (b) *ASPM* contains an N-terminal microtubule-associated domain (green). The N-terminal region also contains two putative calponin-homology (CH) domains. The 81 IQ repeats are Ise-Gln calmodulin-binding domains. (c) The *MCPH3* gene, *CDK5RAP2*, encodes a spindle associated domain in the N-terminus. There are also several coiled-coil domains (d) *CENPJ*, similar to *CDK5RAP2*, also consists of numerous coiled-coil regions. At the C-terminus is the TCP10 C-terminus domain.

1.6 Objectives of study

Research has revealed that in cases of genetic disorders, understanding of molecular aetiology is fundamental to achieve the ultimate goal of gene therapy and to help alleviate the sufferings of individuals/families with inherited disorders. This study will therefore be helpful for genetic counsellors, molecular geneticists and medical geneticists for patient management and future research. The evolutionary lineage leading to humans is marked by a dramatic increase in brain size. It has been hypothesized that genes involved in regulation of brain size during development may also have tendency to be involved in brain enlargement during evolution (Gilbert *et al.*, 2005). This hypothesis was partly explained by recent research showing that microcephalin, *ASPM*, *CDK5RAP2* and *CENPJ*, four genes implicated in primary microcephaly (Bond *et al.*, 2002; Jackson, 2002 #230; Bond, 2005 #53), bear signatures of positive selection in the lineage leading to humans (Evans *et al.*, 2006; Kouprina *et al.*, 2004; Wang and Su, 2004; Zhang, 2003). Primary microcephaly is characterized by severe reduction in brain size, especially the cerebral cortex, but without having any other abnormality within or outside the nervous system lead to the conclusion that genes responsible for primary microcephaly are highly specific regulators of brain size during fetal life. As mentioned earlier, seven loci and five genes have been described for primary microcephaly till now. It is evident that more genes are involved for this disorder, as 18/56 northern Pakistani families and 5/9 Indian families showed no evidence of linkage to the known loci (Bond *et al.*, 2003; Kumar *et al.*, 2004).

The main objectives of the study are:

- To determine the phenotypic and genetic variability in primary microcephaly families from Pakistan
- To identify the loci/genes involved in primary microcephaly in Pakistani population
- To identify the mutations in families affected with primary microcephaly
- To correlate the clinical phenotype with the MCPH genes mutations
- Identification of new genes for this disorder may help to understand evolutionary mechanism of brain development.

2 MATERIALS AND METHODS

2.1 Families studied

Prior approval for this study was obtained from local ethical committee of National Institute for Biotechnology and Genetic Engineering (NIBGE), School of Biotechnology, Quaid-i-Azam University, Islamabad, Pakistan and regional ethical committee in Denmark.

In this study, 11 consanguineous families with primary microcephaly were ascertained from different regions of Pakistan. The families were identified by gathering information from different local sources. Informed consent was taken from all the families under study after explaining the purpose and benefits of this research project. All the families were visited at their homes and relevant clinical information was collected carefully. All family members (affected and normal) were clinically examined including head circumference. There was no evidence of environmental causes of MCPH. Clinical history was recorded for both affected and unaffected members of each family. The degree of mental retardation was assessed by standardized questionnaires for both affected and normal members of the family.

Pedigree information was collected from the family members and crosschecked by interviewing multiple family members. All the families showed autosomal recessive mode of inheritance. Family MCP3 belong to Bahawalpur district of Punjab while MCP6 and MCP7 from Muzaffargarh. MCP9 family was identified in district Multan, MCP11 and MCP15 from Sarghodha, while MCP18 belong to Kabirwala Tehsil in District Khanewal. MCP21 and MCP22 belong to district Toba Tek Singh in Punjab province. Two families MCP17 and MCP35 belong to North Western Frontier Province (NWFP) from Abbotabad and Karak districts respectively.

Photographs of all the affected members were taken for record purpose and for further molecular analysis blood samples were taken from the normal and affected family members to extract genomic DNA.

This thesis also includes molecular analysis of a patient (MCP36) with craniosynostosis and microcephaly born from consanguineous parents in Denmark (Tommerup *et al.*, 1993).

2.1.1 MCP3

MCP3 family originated from Bahawalpur district in Southern part of Punjab province. This family has total of 4 affected individuals born from consanguineous marriages. Pedigree analysis suggest autosomal recessive mode of inheritance. Pedigree of family is shown in figure 2.1. Individual IV-2 had head circumference (HC) >9 SD, while individuals V-2, V-3 and V-4 have HC 7, 8 and 9 SD below age and sex related mean in the population. The HC of the parents of affected individuals were normal. Individuals IV-2, V-2 had moderate mental retardation while V-3 and V-4 were retarded mildly. Apart from mild to moderate mental retardation and reduced HC, affected individuals had no other clinical malformations or symptoms.

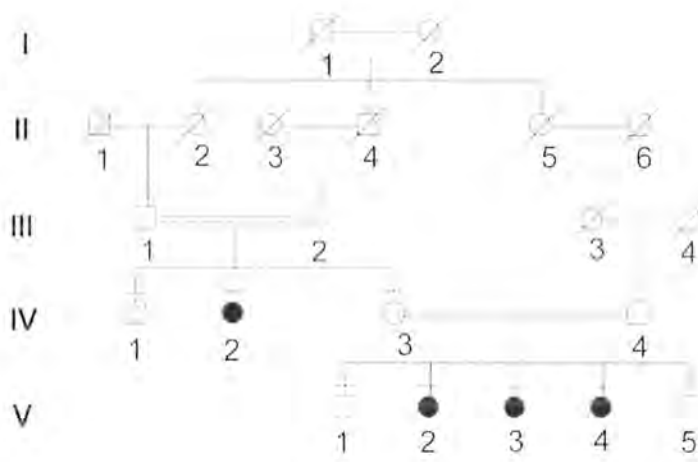


Figure 2.1: Pedigree of family MCP3 with autosomal recessive primary microcephaly. Solid symbols represent affected subjects, while the open symbols represent normal individuals. Horizontal bars above symbols denote individuals who were physically examined and their blood was sampled for molecular study.

2.1.2 MCP6

Family MCP6 originated from Muzaffargarh district in Punjab province. This family has total of seven affected individuals (3 males and 4 females) in two loops. Parents of both the loops have blood relation and are phenotypically normal, having normal HC and cognitive skills. Mode of inheritance in this family was suggested to be autosomal recessive. HC among affected individual was -7 to -9 SD below population mean. The degree of mental retardation was moderate to severe in all the affected members with poor cognitive skills. There were no symptoms of seizures or epilepsy.

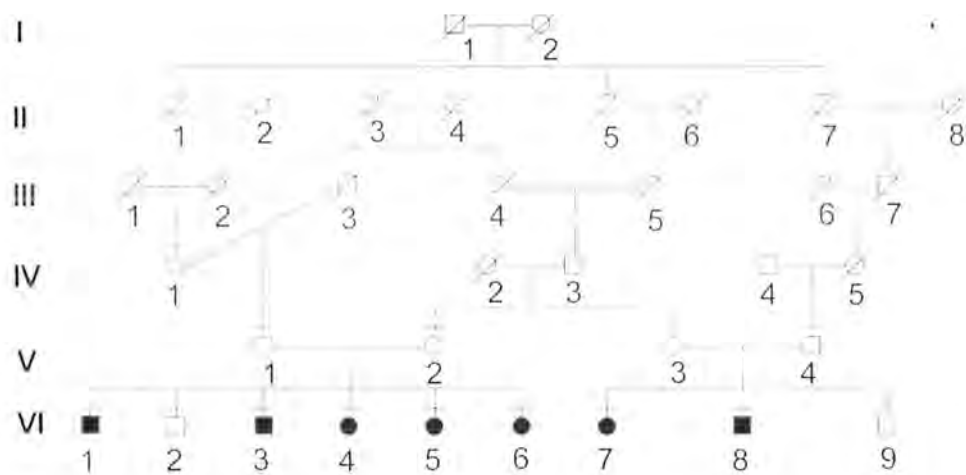


Figure 2.2: Pedigree of family MCP6 with autosomal recessive primary microcephaly. Solid symbols represent affected subjects, while the open symbols represent normal individuals. Horizontal bars above symbols denote individuals who were physically examined and their blood was sampled for molecular study.

2.1.3 MCP7

Family MCP7 originated from Khangarh town, Muzaffargarh district in Punjab province. This family has total of seven affected individuals (5 males and 2 females) in two loops. Mode of inheritance in this family was suggested to be autosomal recessive. HC among affected individual was -7 to -9 SD below the population mean. Parents of both the loops have blood relation and are phenotypically normal, having normal HC and cognitive skills. The degree of mental retardation was moderate to severe in all the affected members with poor cognitive skills. There were no symptoms of seizures or epilepsy.

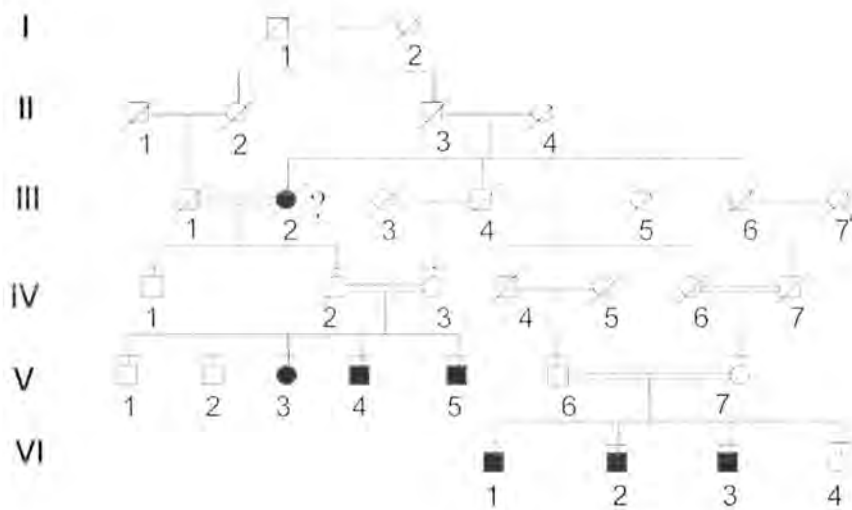


Figure 2.3: Pedigree of family MCP7 with autosomal recessive primary microcephaly. Solid symbols represent affected subjects, while the open symbols represent normal individuals. Horizontal bars above symbols denote individuals who were physically examined and their blood was sampled for molecular study.

2.1.4 MCP9

Family MCP9 originated from Multan city in Southern part of Punjab province. This family has only two affected children (one male and one female). Parents of affected children were first degree cousins. Parents were normal upon clinical examination with normal IQ, head circumference and had no signs of mental retardation. Both of the affected individuals (IV-1 and IV-2) aged 24 and 21 years respectively, have HC of -10SD with sharp sloping forehead. Individual IV-1 has severe degree of mental retardation with very poor cognitive skills with inability to feed himself. While individual IV-2 has moderate degree of mental retardation. No other neurological findings were observed during examination.

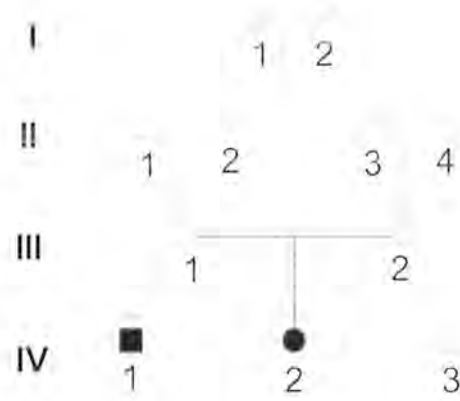


Figure 2.4: Pedigree of family MCP9 with autosomal recessive primary microcephaly. Solid symbols represent affected subjects, while the open symbols represent normal individuals. Horizontal bars above symbols denote individuals who were physically examined and their blood was sampled for molecular study.

2.1.5 MCP11

Family MCP11 belongs to a small village in district Sargodha, Punjab province. Pedigree of the family is shown (Figure 2.5). This family has a strong tradition of consanguineous marriages. Five generations pedigree has four affected individuals (3 males and one female) with primary microcephaly born to first cousin marriages. All the affected have moderate to severe mental retardation, reduced head circumference which was calculated to be $>8SD$ and sloping forehead. All the affected have very poor learning and self caring skills. There was no history of seizures or epilepsy. No other abnormality was associated with disease condition. Blood samples of four affected individuals, two parents and one phenotypically normal sibling was collected for DNA extraction to carry out molecular analysis.

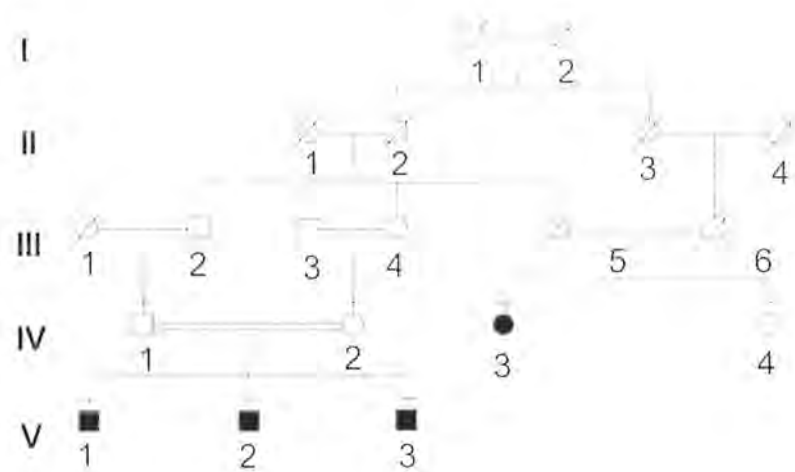


Figure 2.5: Pedigree of family MCP11 with autosomal recessive primary microcephaly. Solid symbols represent affected subjects, while the open symbols represent normal individuals. Horizontal bars above symbols denote individuals who were physically examined and their blood was sampled for molecular study.

2.1.6 MCP15

MCP15 originated from Sargodha city in Punjab province. This four generation pedigree has only two affected individuals (IV-1, IV-2) born to first cousin marriage. Both the affected individuals have reduced head circumference, IV-1 (-7 SD) and IV-2 has -8 SD and were mildly mentally retarded. In addition, they have seizures from childhood for which they were medically treated. There was no other clinical evidence explaining general growth deficiency.

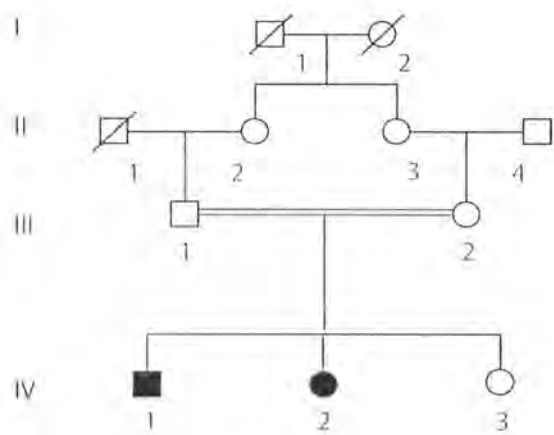


Figure 2.6: Pedigree of family MCP15 with autosomal recessive primary microcephaly. Solid symbols represent affected subjects, while the open symbols represent normal individuals. Horizontal bars above symbols denote individuals who were physically examined and their blood was sampled for molecular study.

2.1.7 MCP17

MCP17 originated from Hasanabdal (District Attock), Punjab province. This four generation pedigree (Figure 2.7) has four affected individuals (IV-1, IV-4, IV-5 & IV-6) born to first cousin marriage. Individuals IV-4, IV-5 & IV-6 in the right loop of pedigree were aged 35, 10 and 15 years and have HC of -10, -8 and -9 SD respectively. While individual IV-1 in the left loop has HC of -10 SD. All the affected individuals were severely mentally retarded. They showed well pronounced sloping forehead. There was no other clinically describable phenotypic abnormality.

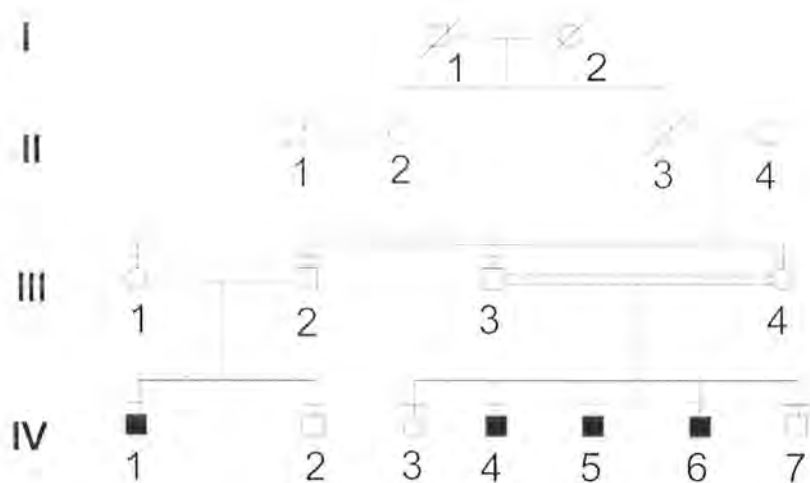


Figure 2.7: Pedigree of family MCP17 with autosomal recessive primary microcephaly. Solid symbols represent affected subjects, while the open symbols represent normal individuals. Horizontal bars above symbols denote individuals who were physically examined and their blood was sampled for molecular study.

2.1.8 MCP18

MCP18 was ascertained from District Khanewal. This family consists of eight affected individuals (five males and three females). The parents of affected individuals were first cousins. Pedigree and HCs of affected and normal individuals are shown in Figure 2.8. Pedigree information shows that all the affected individuals share same rare mutation via common ancestors. The degree of mental retardation was variable from mild to moderate and even severe represent no correlation of mutation and mental retardation, however all the affected were retarded mentally. Individual V-13 is represented as normal in the pedigree has HC of -2.5 SD. However, he has normal IQ level without any sign of mental retardation. No other morphological or nervous findings were observed in any of affected or normal individuals including parents.

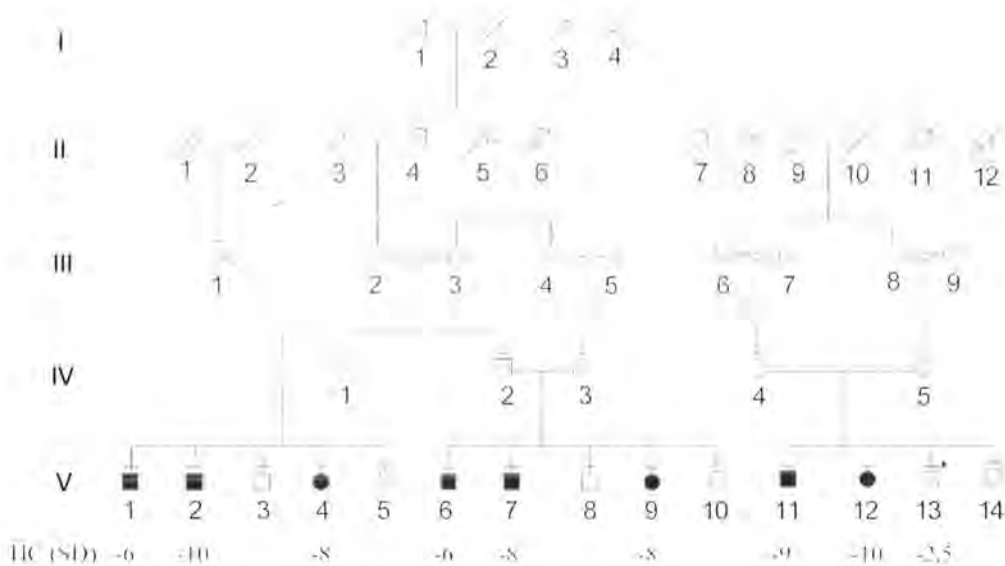


Figure 2.8: Pedigree of family MCP18 with autosomal recessive primary microcephaly. Solid symbols represent affected subjects, while the open symbols represent normal individuals. Horizontal bars above symbols denote individuals who were physically examined and their blood was sampled for molecular study.

2.1.9 MCP21

MCP21 family was identified and sampled from Toba Tek Singh district. This pedigree consists of five affected children but two of them IV-3 and IV-4 had died in first few years of their lives. Individuals V-3, V-4 and V-5 were 7, 9 and 18 years of age at the time of examination. HC of V-4 was calculated to be 42cm (-6 SD), while both V-3 and V-5 have <-9 SD as compared to normal values of age and sex. Environmental and maternal causes of microcephaly were excluded in each affected birth. Blood samples of seven individuals including three affected subjects were taken for investigation of etiology at molecular level.

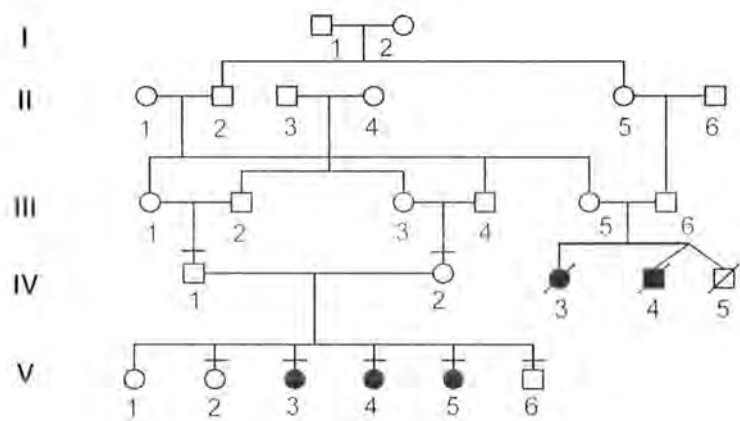


Figure 2.9: Pedigree of family MCP21 with autosomal recessive primary microcephaly. Solid symbols represent affected subjects, while the open symbols represent normal individuals. Horizontal bars above symbols denote individuals who were physically examined and their blood was sampled for molecular study.

2.1.10 MCP22

MCP22 family was identified and sampled from Toba Tek Singh district. This pedigree consists of three affected children IV-2, IV-3 and IV-4 (two sisters and one brother) born to first cousin parents. IV-2, IV-3 and IV-4 aged 20, 22 and 23 years and HC <-9, <-9 and <-8 SD respectively. IV-2 and IV-4 were severely mentally retarded but have no other neurological symptoms or physical abnormality except for pronounced sloping forehead. IV-3 has moderate mental retardation only. Both the parents and two normal brothers and a sister showed normal IQ upon examination. Blood samples of three affected and two normal siblings along with their parents were collected for molecular analysis.

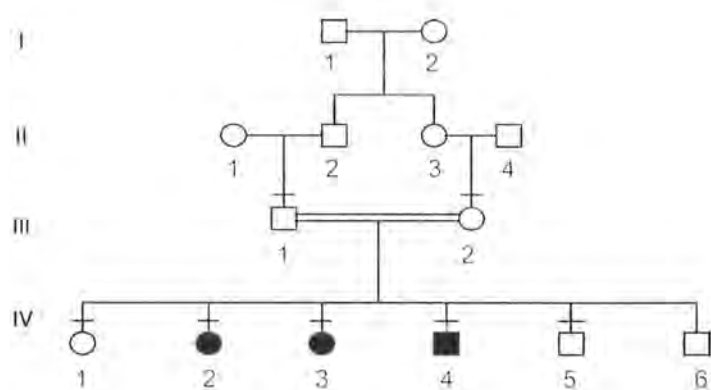


Figure 2.10: Pedigree of family MCP17 with autosomal recessive primary microcephaly. Solid symbols represent affected subjects, while the open symbols represent normal individuals. Horizontal bars above symbols denote individuals who were physically examined and their blood was sampled for molecular study.

2.1.11 MCP35

MCP35 family was sampled from Karak city in NWFP. This pedigree consists of two loops with three affected individuals in each loop (Figure 2.11). One affected individual III-5 died in early childhood. The parents of affected individuals in both the loops are not consanguineous. Individual III-1 and III-2 aged 19 and 15 years have HC of -9 and -6 standard deviation respectively compared to population age and sex mean. Both III-1 and III-2 were moderately mentally retarded, aggressive in behaviour, self injurious and according to their parents this aggression is progressing with age. Both these individuals have seizures from early age. Individual III-6, III-7 and III-8 in right loop were severely mentally retarded and have head circumference of -8 SD. No other detectable abnormality was observed in these patients. These patients did not exhibit seizures.

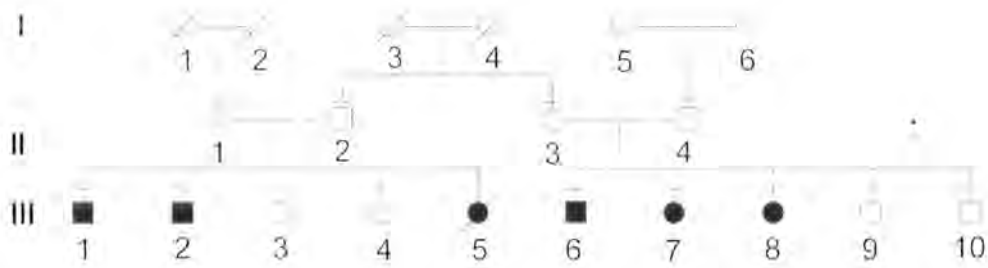


Figure 2.11: Pedigree of family MCP35 with autosomal recessive primary microcephaly. Solid symbols represent affected subjects, while the open symbols represent normal individuals. Horizontal bars above symbols denote individuals who were physically examined and their blood was sampled for molecular study.

2.1.12 MCP36

The patient was first clinically described by Tommerup *et al.*, (1993). The patient was the only child of a 33 years old mother and her 34 year old cousin. At birth, body weight of patient was 2255 g, and body length was 47 cm. the pregnancy period was normal without any complications. The birth was two weeks behind schedule as told by mother. The patient sat alone at age of seven months and walked upright with support at eight and half months. At the age of 10 months X-ray revealed a small cranium (HC; 37 cm) and craniosynostosis with almost complete closure of all the cranial sutures. There was no evidence of increased intracranial pressure. Her body and cranial growth was below the third percentile in all the subsequent measurements. At the age of 16 years, her body weight was 37 kg, her length 141 cm, and head circumference 44.5 cm (Tommerup *et al.*, 1993). A high frequency of spontaneous chromosomal breakage, endomitosis, endoreduplication and hypersensitivity toward alkylating agent (Trenimon) and the radiometric drug bleomycin was observed by the authors. The authors had also observed abnormal chromosomal spiralization and abnormal cellular division. They proposed that mutation may involve a gene important for DNA repair and/or regulation the cell cycle.

2.2 Clinical data

MCPH segregated as an autosomal recessive trait in all eleven families. Consanguinity was evident in all families except MCP35. All patients displayed reduced head circumference ($5 < Z < 12$ SD below normal) and sloping forehead whereas their parents were normal. Apparently there was no evidence of abnormal height or weight and general body growth in the affected individuals. The degree of mental retardation varied from mild to moderate even severe and it varies among affected individuals within the families. Some of the affected individuals have little native language skills and can perform little tasks. Others more severely affected cannot speak and have no feeding and self caring skills. In all families except MCP35 and MCP15, there were no other clinical neurological symptoms and no additional obvious dysmorphic features observed. Individuals III-1 and III-2 in family MCP35 displayed more aggressive behavior and according to family information the aggression increased with age. These two individuals were

mildly mentally retarded and could perform some learning and counting tasks. In addition, they occasionally had seizures from early childhood. These two individuals were routinely treated for seizures. In the same family, individual III-6 and III-7 were moderately mentally retarded and also displayed unfriendly social behavior. In MCP15 two affected sibs born by first cousin marriage have sloping forehead, mild mental retardation and HC is comparable to that of MCPH patients in addition they also exhibit seizures.

As these families were identified and sampled during field sampling trips so MRI scans for brain are not available to find out the gross pathological changes in brain as whole and cerebral cortex in particular.

Table 2.1: Standard solutions and kits used for experiments...

Sloutios and reagents	Concentration/manufacturer
Solution-A	0.32 M Sucrose, 10 mM Tris-HCl, 5 mM MgCl2, 1 % v/v Triton X-100, pH 7.4-7.6
Solution-B	10 mM Tris-HCl, 400 mM NaCl, 2 mM EDTA, pH 7.4-7.6
Solution-C	Phenol equilibrated with Tris-HCl containing Hydroxyquinoline and mercaptoethanol (pH 7.6-8.0).
Solution-D	Chloroform:Isoamyl alcohol (24:1)
TBE buffer	0.1 M Tris, 0.1 M boric acid, 2 mM EDTA
70 % Ethanol	Merck
3 M Sodium Acetate	pH 6
Proteinase K	(50 µg / ml)
Taq DNA polymerase	Fermentas, Qiagen,
Restriction enzymes	New England Biolabs
Exonuclease I	NEB
Shrimp Alkaline phosphatase	Fermentas
T4 PN Kinase	Promega
QIA quick PCR purification kit	Qiagen
BigDye Terminator v3.1 Cycle Sequencing Kit	Applied Biosystems
Size standard	Size standard Liz-600 (Applied Biosystems)
DNA ladder	50-bp, 100-bp (Fermentas)
Bromophenol blue gel loading dye	Sucrose 40 g, bromophenolblue 0.25 g, H2O till 100 ml
dNTPs	Fermentas
APS 10 %	10 % w/v APS in water, aliquoted and stored at 4 °C
Ethidium bromide	10 mg/ml EtBr in bidest H2O
TE buffer	10 mM Tris-HCl pH 7,5; 1 mM EDTA

2.3 Blood Sampling

Blood samples were drawn in 5 ml EDTA vacutainer tubes using 5 ml sterile syringes. Blood samples were transferred immediately to Human Molecular Genetics laboratory, NIBGE. Till the start of DNA extraction, blood samples were stored at 4 °C.

2.4 DNA extraction

DNA was extracted from peripheral blood samples using a standard protocol (Phenol: Chloroform). Briefly, 0.75 ml of blood was taken in 1.5 ml microcentrifuge tube and 0.75 ml of solution A (containing 0.32 M Sucrose, 10 mM Tris-HCl, 5 mM MgCl₂ and 1 % v/v Triton X-100 at pH 7.4-7.6) was added to it. After thorough mixing by inversion, the tubes were kept at room temperature for 10 min and then centrifuged for 1 min at 13,000 rpm and supernatant was discarded to separated white blood cells in the pellet. Pellet was resuspended in 400 µl of solution A and centrifuged for 1 min at 13,000 rpm. Supernatant was discarded and the pellet was resuspended in 400 µl of solution B (10 mM Tris-HCl, 400 mM NaCl and 2 mM EDTA, pH 7.4-7.6), then 25 µl of 10 % SDS and 8µl of Proteinase K (20 mg/ml) were added. The tubes were incubated at 37 °C overnight or 65 °C in water bath for 3 hrs. After incubation 0.5ml of freshly prepared equal volume of solution C (Phenol equilibrated with Tris-HCl containing Hydroxyquinoline and mercaptoethanol (pH 7.6-8.0) and solution D (Chloroform:Isoamyl alcohol (24:1) was added in each tube and was mixed properly. The solution was centrifuged for 10 min at 13,000 rpm to get rid of proteins. The upper aqueous phase was collected in a new 1.5ml tube and equal quantity of Solution D was added. After gentle mixing, centrifuged for 10 min at 13,000 rpm and again the upper aqueous phase was collected in a new 1.5 ml eppendorf tube. To the collected aqueous phase, 55 µl of 3M Na-acetate (pH 6) was added. DNA was precipitated by adding equal volume of Isopropanol (500 µl, stored at -20 °C). Precipitated DNA was pelleted by centrifuging at 13,000 rpm for 10 min. Clear supernatant was discarded without disturbing DNA pellet. Pelleted DNA was washed by 350 µl of 70% ethanol (stored at -20 °C) to get rid of excessive salts. To get rid of residual ethanol, DNA pellet was dried in vacuum dryer. After drying DNA was dissolved in 200 µl of double distilled deionized water and stored at 4 °C. Genomic DNA was quantified using NanoDrop™ 1000 Spectrophotometer at 260 nm wavelength. Each DNA was diluted to 50 ng/µl final concentration for amplification of genomic

fragment using polymerase chain reaction (PCR). The quality of extracted DNA was evaluated in 1 % agarose gel electrophoresis using ethidium bromide (0.5 µg/ml).

2.5 Polymerase chain reaction (PCR)

Polymerase chain reactions (PCR) were performed using a standard protocol in order to amplify genomic fragments for linkage analysis using microsatellite markers, sequencing and other downstream applications containing 10-20 pmol of each primer, 200 µM of each dGTP, dCTP, and dTTP and dATP, 1 U of Taq DNA polymerase, 1 X PCR buffer and 50 ng of template DNA in 25 µl reaction volume with 1.5 mM MgCl₂.

Thermal cycling conditions were as follows:

Table 2.2: PCR profile for amplification of genomic fragments.

Step	Temperature °C	Duration	No. Of cycles
Denaturation	95	5 min	1
Denaturation	95	30 s	40
Annealing	52-66	30 s	
Extension	72	30 s	
Final extension	72	7 min	1

For amplification of highly GC rich genomic segments samples were denatured at 98 °C.

2.6 Agarose gel electrophoresis

After PCR amplification, the amplified PCR product were separated and visualized by agarose gel electrophoresis. 1-2 % agarose gel prepared in 1 X TBE buffer was used. 0.5 µg/ml of ethidium bromide was added for visualization under U.V light. At least 0.25 volumes of bromophenol blue gel loading dye (Table 2.1) was added to the PCR product before loading into the wells. 1 X TBE buffer was used to perform electrophoresis at 100 volts for 30-40 min.

2.7 Genotyping using fluorescently labeled primers

Genotyping was performed by amplifying microsatellite repeats. Microsatellite markers were selected from Marshfield genetic map Marshfield Comprehensive Human Genetic Maps: (<http://research.marshfieldclinic.org/genetics/geneticresearch/compmaps.asp>) and genome database (<http://www.gdb.org/>). Markers physical positions were collected in UCSC genome browser (<http://genome.ucsc.edu/>). For amplification of microsatellite markers an 18-bp extension sequence was added to the 5' end of each forward primer to allow amplification by third primer which was FAM labelled at 5' end for allele detection in ABI3130xl genetic analyzer. All samples were amplified for the selected markers using a standard protocol containing 2.4 pmol of forwad primer, 6pmol of reverse primer, and 10pmol of FAM labelled primer, 200 μ M of each dGTP, dCTP, dTTP and dATP, 1.2 U of Taq DNA polymerase, 1X PCR buffer and 50 ng of template DNA in 12 μ l reaction volume.

Table 2.3: PCR thermal cycling conditions for fluorescently labeled microsatellite markers.

Step	Temperature °C	Duration	No. of cycles
Denaturation	95	10 min	1
Denaturation	95	30 s	30
Annealing	52-66	30 s	
Extension	72	30 s	
Denaturation	95	30 s	8
Annealing	50	1 min	
Extension	72	1 min	
Final extension	72	10 min	1

2.8 Preparation of samples for ABI 3130x/ genetic analyzer

Fragments were size separated in ABI 3130x/ genetic analyzer. Before the preparation of samples for genetic analyzer, agarose gel electrophoresis was performed to detect the quality of PCR amplification of genomic fragment. All the PCR amplified samples were prepared by thorough mixing 0.5 μ l of size standard LIZ-600 (Applied Biosystems), 0.5-1 μ l of fluorescently labelled PCR product (depending upon quality of PCR amplification) and 10 μ l of Hi-Di formamide in 96 well loading plates. This mixture was denatured at 95 °C for 1 min followed by quick chilling on ice and then loaded into the genetic analyzer for electrophoresis. Data was analyzed using GeneMapper Software v3.7 (Applied Biosystems).

2.9 Linkage analysis

The first step in gene identification is to genotype the affected families and search for the segregation of disease gene locus, by studying the familial transmission of marker alleles at consecutive polymorphic loci. This necessitates statistical methods to interpret genome-wide data. The explanatory unit for the strength of linkage is the *logarithm of odds* i.e. LOD score value, which is based on an equation developed by Newton E. Morton (Morton, 1955). The LOD score is the 10th base logarithm for the likelihood ratio or odds ratio for the likelihood of linkage at a given recombination fraction (q) between affection status and a marker locus to the likelihood of no linkage (Ott, 1985). In practice, this ratio is calculated for several values of recombination fraction. The frequency of one recombination event in 100 meioses equals a map distance of one centi Morgan (1 cM = 0.01 q) (Ott, 1991). This is 1 Mb on average in physical distance, but it varies between males and females and depends on chromosomal location. The estimate for linkage is the sum of LOD scores at a given recombination fraction in single families. The LOD score calculation is dependent on both the penetrance of the disease phenotype and mode of inheritance. The estimation of linkage for a single genomic locus depends only on the last meiosis and gives a reliable, but usually also relatively gross localization for the affection locus, the most likely distance between the loci studied being the recombination fraction at which the LOD score is highest. In theory, the probability of two recombinations in a region of 1 Mb is, on average, one in 10,000, but depends on the true

recombination frequency in a given region (Haldane, 1919). This figure holds true for one meiosis, but a linkage study utilizes information collected from siblings and several affected families. LOD scores >3 are considered significant since they indicate 1:1000 odds that the linkage did not occur by chance. LOD scores < -2 are generally considered as significant evidence against linkage (Morton, 1955; Ott, 1991).

Two point linkage analysis was carried out using Program LIPED Version for IBM PC/XT (Ott, 1985). Multipoint linkage analysis was performed using easyLINKAGE (Hoffmann and Lindner, 2005). For the analysis of autosomal recessive mode of inheritance with complete penetrance and a disease allele frequency of 0.001 were taken. Markers order and their maps distances were based upon Marshfield genetic map (<http://www.marshfield.org/genetics/>) (Broman *et al.*, 1998) and DeCode genetic map (Kong *et al.*, 2002).

2.10 Mutation screening

After linkage analysis, families established linkages to particular loci were subjected to direct sequencing of the candidate genes to identify the pathogenic mutations. Oligonucleotide primers were designed using web based software in primer3 website (<http://frodo.wi.mit.edu/>) to amplify the coding exons and exon-intron boundaries. Maximum melting temperatures for forward and reverse primers were kept between 57-60°C with a maximum melting difference of 1°C between the forward and reverse primers. Same primers were used for both PCR amplification and sequencing.

2.10.1 DNA sequencing

Sequencing of the entire candidate regions were performed using POP-7 polymer and an array length of 36 cm in an ABI 3130xl genetic analyzer (Applied Biosystem). Sequencing was performed using the following protocol. BigDye Terminator v.1.1 Cycle Sequencing Kit (Applied Biosystems) was used for sequencing PCR reaction.

2.10.2 Purification of PCR product from agarose gel

QIAquick Gel Extraction Kit (Qiagen) was used to purify PCR amplified DNA from agarose gel electrophoresis according to manufacturer’s protocol.

2.10.3 Purification of PCR product

Prior to sequencing PCR, all the amplified PCR products were purified using the following procedure.

- Added 1-2µl of PCR product to 0.25 µl (0.75 U) of exonuclease I (ExoI), 0.25 µl (0.75 U) of shrimp alkaline phosphatase (SAP) and 2.5-3.5 µl double distilled deionized water to make final volume 5 µl.
- After thorough mixing samples were incubated at 37 °C for 30 minutes followed by 80 °C for 20 min.

After incubation samples were immediately used as template for sequencing PCR.

2.10.4 Sequencing PCR reactions

BigDye Terminator v.1.1 Cycle Sequencing Kit (Applied Biosystems) was used for sequencing PCR reaction. Sequencing PCR was performed as follows.

Tables 2.4: Sequencing PCR mastermix mix.

Reagents	Volume (µl)
Template Exo-SAP treated	5
Primer (10 pmol)	0.25
Deionized distilled water	2.25
5X sequencing Buffer	1.5
BigDye reaction mix	1.0
Total volume	10

Table 2.5: Sequencing PCR profile.

Step	Temperature °C	Time	No. of cycles
Denaturation	95	1 min	1
Denaturation	95	10 s	} 30
Annealing	52-60	10 s	
Extension	60	4 min	

2.10.5 Precipitation of sequencing PCR products

Sequencing PCR reactions were purified in ABI 96 wells sample loading plates by adding 1 µl of 3M sodium acetate and 1 µl of 125 mM EDTA to the PCR product. 25 µl of 96 % ethanol (stored at -20 °C) was added to each reaction and mixed by gentle vortex. Plates were centrifuged for 30 min. at 4700 rpm at 4 °C after incubation at room temperature for 15 min. Supernatant was discarded by carefully inverting the plates onto 3-4 folds of paper towel. Inverted Plates were placed on new paper towel and centrifuged at 170 rpm for 1 min. PCR pellets were washed by adding 60µl of 70 % ethanol and centrifuged immediately at 4700 rpm for 10 min at 4 °C. Supernatant was discarded carefully by inverting the plates onto 3-4 folds of paper towel. Inverted Plates were placed on new paper towel and centrifuged at 170 rpm for 1 min. Samples were dried by incubating at 65 °C for 10-15 min. To the purified sequencing PCR products 10 µl of Hi-Di formamide (Applied Biosystems) were added and mixed thoroughly, followed by short centrifugation to collect all the sample volume to the bottom of the sample plates.

2.10.6 Sequencing data analysis

Sequences were analyzed using Chromaspro version 1.34 software by aligning them with control sequences obtained from www.ncbi.nlm.nih.gov. The obtained sequences were inspected in silico for mutations.

2.11 Restriction analysis

Restriction analysis was performed using appropriate restriction enzymes selected by using online web based software NEB cutter V2.0 (<http://tools.neb.com/NEBcutter2/index.php>). Each restriction digestion reaction was carried out using appropriate buffer according to manufacturer's instructions. Restriction fragments were analyzed by horizontal gel electrophoresis using 2-3% agarose gel.

Table 2.6: List of microsatellite markers used for Genotyping of Primary microcephaly families

Locus name	Position	Gene	Chromosomal position (bp)	STS Markers	Physical (bp)	Marshfield (cM)
MCPH1	8p23.1	Microcephalin	<u>6251529-6493434</u>	D8S1798	5087773	6.7
				D8S277	6504084	8.3
				D8S1819	6737322	10.0
				D8S1825	8962119	15.4
MCPH2	19q13.1-13.2	Unknown		D19S226	14494400	42.3
				D19S416	38760452	58.7
				D19S245	38789928	58.7
				D19S425	40185717	59.4
				D19S896	42170437	
				D19S224	41219845	61.5
				D19S570	42419494	62.0
				D19S897	43451100	
				D19S881	44039966	63.1
				D19S47	45006014	
				D19S223	46086645	
				D19S400	46219295	64.7
				D19S198	46844923	
				D19S420	48500600	66.3
MCPH3	9q34	CDK5RAP2	<u>122190969-122382258</u>	D9S1872	120829316	129.7
				D9S1682	124033005	132.1
				D9S1881	126019246	135.9
				D9S1821	128369347	137.4
MCPH4	15q15-q21	Unknown		D15S222	43232922	
				D15S659	44161167	43.5
				D15S962	54362316	47.9
				D15S98	54362316	59.1
MCPH5	1q31	ASPM	<u>195319997-195382287</u>	D1S2757	193004350	209.2
				D1S2816	194917156	211.1
				D1S1660	196877902	212.4
				D1S2622	198381006	214.1
				D1S373	198521089	214.1
				D1S1723	199657442	215.2
				D1S2655	200831887	216.8
				D1S1678	201798329	218.5
MCPH6	13q12.2	CENPJ	<u>24354412-24395085</u>	D13S787	23278722	8.9
				D13S221	25474761	12.9
				D13S1304	26268019	13.5

Table 2.7: Primers used for PCR amplification and subsequent sequencing of ASPM gene

Exon	Forward (5'→3')	Reverse (5'→3')	Product size (bp)
1	ccaagagccaccacagtta	actcccacgacctctacagc	579
2	tcccaaagactcctctgcaa	aattaagcagatagggtaggagaaa	471
3a	cgtacagagagtggcaagca	ggaaatgcagaagagcagaaa	460
3b	aattctagtctcattattagctccatga	caagcttgtagaaaacttggtca	425
3c	ctctggtacaggtggccttc	cccaactgttcttcaact	625
3d	gctctgaggggagaaaaatgg	tcctaaattttctgcagttcagg	419
3e	cagcaaaagcagaagaaaaatca	gcttcagttgctcggaaaag	386
4	ttcttcaggtctgtta	agtgcgtggagtacag	674
5	catttaggctaataaacagggaaat	cccaaaatgcttcagctct	434
6	caccacacatacacacaagaagg	gagctaacaggttgcgatga	633
7	tgtcattacgtgcaacacca	gctgccaaaaatcccacata	526
8	gggtggagggaaggagagta	tcctgagctttgtcttttgc	508
9	ggactcaccagacaggcatt	tcccatagagataattgggagga	475
10	cattgatgtaccacttccctga	aagttggaaaatattgatgaagttgc	502
11	cgctattttccaaagcaacc	tacttgcgactatggagca	479
12	tcacagttactggggcaaaa	gattccggcaataagtcgtc	404
13	tcatttgagggaaggtttgct	gtttgcctttggggaaaaa	557
14	gcaggtattccaccaaggtc	tgtgccatgctctcacataa	599
15	atccaaaagccttgcacaaa	cgcaaaactggttcagtggta	473
16	acctcccaacccaaaatac	gaccttgggtggaatacctgct	461
17	agccttctgctgaacaccat	cgacatgcctggaattatca	535
18a	gcttgaaagcaccgaaatct	ttggatggatttctgaattgg	631
18b	aaaatcgaactctgtctgtctca	tgc aaagagcttttagagaatgg	392
18c	gcagctgctcttaaatgcaaa	gctgcagccattcaattaca	500
18d	ttcttctctgattgacctgtg	gatgcaagccaggaaaatg	456
18e	gcagcttgatgttccctct	accttgtccgaaagcagatg	478
18f	ttttgaatcagaagagcagctt	gatggtacagggcgtaacaaga	439
18g	cacgtgcatatttacctga	caaaggcaacataaatgtgcta	580
18h	gcagttttcttgagagagaggaa	gaagacataattcaacatgcaca	538
18i	taagggttcagaggaatgc	gcaaagatactgggcaatgaa	581
18j	gccactgaagcttttggtga	ccaagcaaatagagctgcaa	633
18k	gcctctaaaagcagcctgaa	gacaatggcattctgctgtg	667
18l	tgatagcagctcttttctgctg	cagggccaaagttgattatga	488
18m	tggaaagataaatggtcacctca	tggtcacaagaaaactggaaa	468
19	gaaaatatcaacaaaaccaacca	caccactgttctcagaagactca	486
20	ttgactgaatatagatgtgtgtgaaa	cttctttcgtgtgcgtgtgt	451
21	tgacagtcagtgtcttctgcac	accttggcttacaccttca	583
22	ggtgaaaaggctaaatgtgtacg	tgctttctacactctgagttatgagtt	488
23	tgagttattctaccggctaatagc	aatgcctctgtggaaagctg	453
24	actctggggccatgttctcac	tggtcgataaatgctgtcca	573
25	tttcacctaagactcttgcaca	cctttctgccattcttgagg	435
26	gcaaaaagcaggttgaaca	aaagtctttgcacllgctg	447
27	accaaacattccattcttatca	gcgacagagcaagagagacc	451
28	tgataaaaaatgaagaatgtaataaaca	tgaagttctcccacctcttg	400

Table 2.8: Primer pairs used for PCR amplification and subsequent sequencing of *CENPJ* exons

Exon	Forward (5'→3')	Reverse (5'→3')	Product size (bp)
1	cgcctacgtcgaccactg	gaacgaagccactgaactgc	476
2	gccaattgctttgctagtt	tttcagagtgaaggggaaaaa	758
3	ttttagattttcgggtggctga	gcagctccttctgttccag	458
4	tggttttgttaaacaccatttcc	aacacggcaacactccatct	563
5	ccggcctcaagtgtcttaat	ggcagcttgacatatctctc	495
6,7	agggtgtggagagggattgtg	ccgctggagttgctgtctat	588
7b	aacaaccatttttaaacgaggag	tccttttcttttctcgttcc	598
7c	aagagccccataaggagagac	tgtgggctatcctctctgct	584
7d	gcactgactctgaggaacagc	ttgagcaataaggaaagtag-gattt	687
8	aaattcccactgatttctca	ttgactaccctgggtcatttt	500
9	gtaggcaccaatgaatgct	ttgctgaatgaatgaataatg-ga	471
10	tcgtcttaaatgtcgtctgttga	ttcacagtcactccccactg	495
11	cttgtttgctttggcctgtt	ggcgggaataagatgatgcac	398
12,13	cctgtgtcggagaactacaaa	tctgaacgagaaatggcaac	689
14,15,16	cgagtttgctactctcacg	aatatgggtgtcacatatcat-cag	761
17a	gcagaaacactgtagaaagttacaa	aaaaatgaagatgccacagg	500
17b	tgtacatttactgtggattctgttta	ccatgattactacctgttgtgtg	500

Table 2.9: Primer pairs used to PCR amplify and subsequent sequencing of *MAG* exons.

Exon	Forward (5'→3')	Reverse (5'→3')	Product size (bp)
1	gacccctccaggaaagagc	agccccaagccacacact	391
2	gagggagttgttgccagaga	tctttgctgcatgtcctgtc	399
3	gcaatgaaacaagacctgtc	ggcaagcaggagagctga	384
4	acaggtgctggggacctaa	caaatcagcacctcccagat	643
5	cagcaatggaggtggacaag	ccaggactgcctggttcc	572
6	tgtcactaacctcgctgtg	tgtctaccttggcctcgact	423
7	ctgaaccggtgtgctaggtt	gaggacaggcaaagccaata	484
8	aaaaaggaggggaaattgga	aaccggaaagggagaatttg	570
9	tgccaatcagtcagtcaa	caggaaccctctctcctctg	393
10-11	gaggctggtggttctgaaag	acatcaccagagaccaccttg	846
12	cggtccttgagaaaggaggt	cgcagctaccagctcagagt	846

Table 2.10: Primer pairs used to PCR amplify and subsequent sequencing of *SNX26* exons.

Exon	Forward (5'→3')	Reverse (5'→3')	Product size (bp)
1	ggagtggacgaaaggtaggg	gagggaccacggctgaag	576
2-3	gaagcagtctctgtcctcagc	ggctcctgcaacttttgcta	584
4-5	gtcaggggaccaggacatcac	tcagattggttgggacttgg	585
6	cccagcctgcttattcatc	tccttaaagccgaacacctg	481
7-8	tctgagtgcaggggctctt	atccatccatggcacttacc	579
9-10	acagaggatcggagctggt	caagatcgcagccaaacac	586
11-12	cccagggtatctcgtctctg	agccttgatcctgccactc	582
13-14	gaagaggggtccatccacct	atgctggtgttggcactgt	565
15	atctcaggaggccatgtcag	gaacatgagtcgccaggagga	467
16	aggcgtgatcagtttgaggt	caagaggtgggaatcctgag	482
17	gcctctctcatcagctcgtc	ctggcttcgctgcttct	476
18-19	tgctgacgctggaggaag	ggcccccaaatgtgaagtat	580
20	tggtgatgagctggacttca	gtggcagtggtgactccata	565
21a	tcggtgagtcctcagcctac	cctgtgaggggacagaacat	575
21b	acccccaccctacttaccaa	gctgagtagccaaggtggtc	567
21c	gacaggctcaatgcctccta	agtgaggggtgaagggaagga	572
21d	cagaaatggagggcaaagag	gcctccccaaaaggaaatag	582

Table 2.11: Primer pairs used to PCR amplify and subsequent sequencing of *CHST8* exons.

Exon	Forward (5'→3')	Reverse (5'→3')	Product size (bp)
1	gcagcgactctttctgagagc	ccttcctggcgtctctgc	646
2a	gctctggggatttcaggac	gaagctgctgttgggagag	551
2b	gcgacgagcagatgagttc	gaaggattcctccatttc	577
3	ggtgtgaaaggatggaaagg	gggtcttggcacagacttg	486
4	aagctgcccttcctagagc	tagcacctgcaaagaagc	378
5a	agtcagcctgtctccctcac	gcacctgcagtagagcac	548
5b	aagcgggtgatgcaggag	tgtctcgaactgcctacg	583
5c	cccgagttcgtccagtacc	gccaaaggaatgaggaaacag	570
5d	ggctctgaggacgtgagg	aggaagctgctctgaactg	490

Table 2.12: Primer pairs used to PCR amplify and subsequent sequencing of *ZNF302* exons.

Exon	Forward (5'→3')	Reverse (5'→3')	Product size (bp)
1	gctacttacaaagccgtgacc	ctcacaacagtgccaaagagg	498
2	gcgagtgtattaccagtgtgc	cccttaaattggacttgattaggtg	284
3	ttcccagtcattgtcacagc	cgggagcatggtacagaaat	356
4	tgcctaaagcttatctttccatt	gacagtatccctaaaatgcttcc	300
5a	tgtgttttctgggtgcttca	gtggcgactgaggattgact	593
5b	gccttcaaccagagcaaadc	ccttgagacatttgttgcatlc	586
5c	gtggaaaggccttcattcat	tttgatgggcagtaagattcg	549
5d	gcaataggaatctcctgcaaa	tgctagtctcccgctaaagg	569

Table 2.13: Primer pairs used to PCR amplify and subsequent sequencing of *ZNF599* exons.

Exon	Forward (5'→3')	Reverse (5'→3')	Product size (bp)
1	ccggattccgtcaaactaca	gccgtattacagcggatgg	581
2	gctcagtgggtcaggggtctc	gaaacccagcaagaggaggt	385
3	ttctgggggttcattgcag	tccaacctgaataaaggcaaa	384
4a	tgcagtaggcacagagacac	ccgtgcatgtgaagggtta	481
4b	gggttttacaggaacgagtca	ctcctgtgtgggtcacattg	594
4c	gctcctcattgctcaacata	caaaattgcaggttgggta	600
4d	gacaaaaaccctggagtgc	cctgccataaaaagattcaca	523
4e	tggtgacataccttccttttg	tcacaaagacacactccctca	587
4f	agtccagagccaggagagtt	ctgtacagttgctgtgttattgt	544

Table 2.14: Primer pairs used to PCR amplify and subsequent sequencing of *SIRT2* exons.

Exon	Forward (5'→3')	Reverse (5'→3')	Product size (bp)
1	tgcatcctgaccaatcagag	gaatcccactccccgaag	498
2	cggcatcactttgcatgtag	agaatctgcctttccccaga	399
3	tagccccagtgagctcttc	ctctggcactggtacccaac	336
4	gttgggtaccagtgccagag	acaaagtgaagcacctgga	485
5-6-7	ccccgtctagatgattggaa	acacgaggaaccaggacttg	765
8	tctggggatagcagtgtct	atgcagcaaggaggcagtag	372
9	taaacctgccacttgcttc	acaggaaatcaggcagttgg	489
10	tgagcagagtggacacctca	atttccccaggatggatct	359
11-12-13	agatccatcctggggagaat	ggttctgagctgaggaatgc	740
14-15	cctgggcaacaagagtgaa	aaggctctccagctccttct	579
16a	gatggaaggtaggagctga	gtgggggcagttagagatga	574
16b	ctccctccccaaaactgg	ccctcttgttaccctcactc	596

Table 2.14: Primer pairs used to PCR amplify and subsequent sequencing of *MCPH1* exons.

Exon	Forward (5'→3')	Reverse (5'→3')	Product size (bp)
1	tcccaggagaagagaaaaacc	gggagagagcaggagcag	462
2	tctcaaaccctgacttcgt	ccacaggcattgagttctga	457
3	gcgttatgcattcctttgag	aggatttcaaattactaggtgaggt	400
4	gagatgattttgggaagtttga	tcatcaatagcatatttaagacaactc	397
5	gccagttcacatacagtgcaa	tattatggctcccagccaag	442
6	gtggagggtggtggaggtaga	aacaaagccagccatgaaat	441
7	caggcaagttgactttaagatcc	aatttcagggggaaatttagaag	379
8a	cccttaagtggaaatgagaagaac	tttctctcggaggtgaatg	592
8b	tcttcaacaaaaggccacct	gaagagcagggctcctcaatg	595
8c	ttcgagttgcgtgacttctg	cctataagaaggaaaagtcttggaga	593
9	tgaattgcttgggatatgtga	gaatgcaaacaacgctttca	477
10	tgagtttctatctcttggcctgt	cgctcacatttggtagatgttt	397
11	tctgaagtttatttcccaggt	ttcccagctcacaggaaagt	483
12	tctgaagggactttgtgtctg	cgcgataaattgataaaagggtg	387
13	tcatcatcttctctggattctca	cgtctgctaacagcaaggag	596
14	ctggccagtgtagtgagaa	catggcgaaaccctgtct	695

Table 2.16: Primer sequences and restriction enzymes used for the confirmation of identified mutations.

Mutation	Forward (5'→3')	Reverse (5'→3')	Restriction enzyme
c.3477-3481delCGCTA	gcaggtattccaccaaggtc	tgtgccatgctctcacataa	<i>HgaI</i>
c.6730delA	ccctaaaaatagcctgaatgtatgt (mismatch primer)	gaagacataattcaacacatgcaca	<i>MaeIII</i>
c.9697C>T	actctgggccatgttctcac	aaaaatgattgtacaaaaattaaagctaca (mismatch primer)	<i>NlaIII</i>
c.9730C>T	actctgggccatgttctcac	tggtcgataaatgctgtcca	<i>TaqI</i>
c.9557C>G	tgagttattctaccggctaatagc	aatgcctctgtggaaagctg	<i>Fat I</i>
c.9492T>G	atgctcaatctttt gatgctaag (mismatch primer)	aatgcctctgtggaaagctg	<i>AhlI</i>
c.3978G>A	agccttctgctgaacaccat	cgacatgcctggaattatca	<i>AhdI</i>
c.9319C>T	ggtgaaaggctaaatgttgtagc	tgctttctacactctgagttatgagtt	<i>TaqI</i>
c.3055C>T	cgctatittccaaagcaacc	tacttgccgactatggagca	<i>BssSI</i>
c.7894C>T	gcctctaaaagcagcagcctgaa	gacaatggcattctgctgtg	<i>HpyI88I</i>

3 RESULTS

3.1 Linkage studies

Possible linkage to known MCPH loci was performed using highly polymorphic microsatellite markers. Microsatellite markers used for genotyping were: D8S1798, D8S277, D8S1819, and D8S1825 for the MCPH1 locus; D19S226, D19S416, D19S245, D19S425, D19S224, D19S570, D19S881, D19S400, D19S420, and D19S418 for the MCPH2 locus; D9S1872, D9S1682, D9S1881, and D9S1821 for the MCPH3 locus; D15S222, D15S659, D15S962, and D15S98 for the MCPH4 locus; D1S2757, D1S2816, D1S1660, D1S2622, D1S373, D1S1723, D1S2655, and D1S1678 for the MCPH5 locus; and D13S787, D13S1304, and D13S221 for the MCPH6 locus. Oligoneucleotide sequences to amplify microsatellite markers can be obtained from The Genome Database (<http://www.gdb.org>). Haplotypes were constructed (not shown) and analyzed for linkage or exclusion to known loci.

Initially, all the families were tested for homozygosity in all affected individuals with microsatellite repeats markers flanking *ASPM* (Table 2-6). Out of the eleven Pakistani families, six (MCP3, MCP6, MCP7, MCP9, MCP11 and MCP17) were potentially linked. For families MCP3, MCP6 and MCP7 a two point LOD score of 3.02, 4.2 and 4.3 ($\theta=0.0$) was calculated. Linkage was excluded for *ASPM* by heterozygosity in three families (MCP15, MCP21 and MCP22). Testing homozygosity in remaining known loci using microsatellite markers in these three families proved MCP15 linkage to MCPH2 locus whereas, MCP21 and MCP22 linked to MCPH6 locus (*CENPJ*). MCP18 and MCP35 did not prove linkage to any of the known loci. The haplotypes were re-analyzed in families MCP18 and MCP35 to identify families or part of families with possible compound heterozygous mutations. By careful analysis of haplotypes for all the loci in MCP18 and MCP35 it was hypothesized that both families may have compound heterozygous mutations in *ASPM*.

In Danish family MCP36, linkage analysis using polymorphic microsatellite markers revealed that the only patient in the family was homozygous at MCPH1 locus (8p23.1), whereas her consanguineous parents were heterozygous. As mutation in microcephalin gene (*MCPH1*) at MCPH1 locus is responsible for MCPH1 primary microcephaly, I supposed that patient may carry homozygous mutation in *MCPH1*.

3.2 Mutation analysis

3.2.1 Sequencing of *ASPM* in MCPH5 linked families

All 28 coding exons of *ASPM* gene including exon-intron boundaries were PCR amplified using previously published primers (Bond *et al.*, 2002). Two affected members from each family were initially sequenced bi-directionally using fluorescent dye chain termination technique on an ABI prism 3130xl sequencer. Sequences were analyzed by using chromaspro software version (ChromasPro 1.34) and were compared to reference sequences (<http://www.ncbi.nlm.nih.gov/>, <http://genome.ucsc.edu/>). By sequencing of *ASPM* gene in the six linked families (MCP3, MCP6, MCP7, MCP9, MCP11 and MCP17) to MCPH5 locus I found six homozygous mutations. In MCP3 I identified a 5bp deletion mutation leading to frameshift in exon 14 (c.3477_3481delCGCTA (A1160fsI181X) predicted to give rise to a truncated product of 1181 amino acids that include 21 novel amino acids residues. In MCP6 a single base deletion [c.6732delA (Y2245fs2258X)] was detected in exon 18. This frameshift mutation leads to premature stop codon 14 amino acids downstream in the same exon. In family MCP7 a C to T transition in exon 24 of gene at nucleotide position 9697 [c.9697C>T (R3233X)] producing a truncated product of 3233 amino acids was identified. Another T to G variation was found in family MCP17 in exon 23 [c.9492T>G (Y3164X)] leading to a truncated protein of 3163 amino acids. In the remaining two families I identified already published homozygous mutations: c.9557C>G (S3186X) in exon and c.9730C>T (R3244X) in exon 24 of the gene in families MCP11 and MCP9 respectively. All identified mutations were loss of function mutations suggesting a homogenous pathomechanism for the condition.

All identified mutations were tested in all members of the family in question and presence of mutation was confirmed in each case by restriction enzyme digest of PCR amplified fragments (Table 2.9).

3.2.2 Compound heterozygous *ASPM* mutations

3.2.2.1 Family MCP18

Sequencing of *ASPM* in the two apparently unlinked families (MCP18 and MCP35) resulted in identification of compound heterozygous mutations. In MCP18, a total of 8 individuals were affected in generation 5 of pedigree. It was found that individuals V-1, V-2, V-4, V-6, V-7 and V-9 have heterozygous C to T variation [c.3055C>T (R1019X)] in exon 11, whereas the second heterozygous mutation [c.7894C>T (Q2632X)] was located in exon 18. Both mutations predicted to produce truncated protein products. Whereas, the individuals V-11 and V-12 are homozygous for c.3055C>T (R1019X) in exon 11 of *ASPM*.

3.2.2.2 Family MCP35

MCP35 pedigree consists of two loops with three affected individuals in each loop (Figure. 2-11). One affected individual III-5 died in early childhood. The parents of affected individuals in both the loops are not consanguineous also the linkage analysis by homozygosity mapping did not confirm linkage to any of the known loci. Haplotype analysis in both the loops suggested possible compound heterozygous alleles in loop2 which was confirmed upon sequencing the affected individuals from both the loops. Affected individuals in loop B of this family were homozygous for G to A variation [c.3978G>A (W1326X)] in exon 17 of *ASPM* leading to a premature termination of protein by incorporating stop codon at site of mutation, whereas the affected individuals in loop1 of this family were heterozygous for the same mutation [c.3978G>A (W1326X)] which was inherited from their father. However, these individuals prove to be compound heterozygous for this mutation and a novel truncating disease variant in exon 22 [c.9319C>T (R3107X)] which was inherited from their mother.

3.2.3 Sequencing of *CENPJ*

In the initial experiments MCP21 and MCP22 suggested linkage to MCPH6 locus (*CENPJ*) by using homozygosity mapping using microsatellite markers. Both the families were sequenced for *CENPJ* by PCR amplifying all the 17 exons including exon-intron boundaries and sequenced directly in both directions in an ABI 3130xl genetic analyzer. Primers sequences and amplified product sizes are given (Table 2.8). A single base deletion mutation c.17_18delC (T6fsX3) was indentified in both the families leading to frameshift and premature stop codon incorporation of 3 novel amino acids (Figure 3-11). This mutation was already reported in two Pakistani families when *CENPJ* gene was first reported to be a cause of primary microcephaly (Bond *et al.*, 2005).

3.2.4 Mutation screening in control population

A total of 280 normal chromosomes from ethnically matched population were screened to determine the carrier frequency of the identified disease variants in *ASPM* and *CENPJ* in Pakistani population. By direct sequencing of respective exons only one heterozygote carrier (0.35 %) for c.9492T>G variant out of 280 normal chromosomes was identified. However, the frequency may be higher if entire coding regions of all the four known MCPH genes (*MCPH1*, *CDK5RAP2*, *ASPM* and *CENPJ*) were sequenced.

3.2.5 Family MCP15

MCP15 was excluded for *ASPM* involvement by linkage analysis using microsatellite markers. However, keeping in view the compound heterozygous mutations in *ASPM* in two of our unlinked families does not exclude the possibility of having *ASPM* mutation. Sequencing of all the coding regions of *ASPM* did not identify any disease mutation except for some known polymorphisms.

After exclusion of *ASPM* involvement, the family was tested for linkage to remaining five known loci using markers given in the table 2-6. Haplotype analysis for the MCPH2 locus using markers D19S416, D19S425, D19S224, D19S897, D19S47, D19S200, D19S198, and D19S420

describe possible linkage to this region (Figure 3.12). The minimum homozygous region shared by affected individuals lies between D19S416 (58.7 cM) to D19S47 (63.1 cM) is about 4.4 cM region. Physical position of minimum linked region is Ch19:38760452- 45383643 which is about 6.6 Mb (Figure 3.13).

3.2.6 Sequencing of candidate genes in MCPH2 region

A number of genes in the linkage region have been sequenced to find out the mutation in causative gene. Each candidate gene was selected based upon their expression in the brain during development, their role in cell cycle progression and process of cell division.

Six selected candidate genes *SIRT2*, *MAG*, *ZNF302*, *ZNF599*, *CHST8* and *SNX26* were selected for mutation screening by direct sequencing of entire coding regions including exon-intron boundaries and 5' and 3' UTR region.

SIRT2 is homolog to the yeast Sir2 protein characterized by sirtuin core domain. Human sirtuins may function as intracellular regulatory proteins with mono-ADP-ribosyltransferase activity. Hyperphosphorylated forms of *SIRT2* were confined to the M phase of the cell cycle and maintained throughout the M phase. Over expression of *SIRT2* resulted in increased NAD-dependent deacetylation and delayed cell cycle progression concluded that *SIRT2* is a regulator of mitotic progression (Dryden *et al.*, 2003). *SIRT2* comprises of 16 exons. All the exons were sequenced by designing appropriate primers including exon-intron boundaries. Sequencing of both affected and one normal did not reveal any disease causing mutation.

MAG (NM_080600) is a type I membrane protein and member of immunoglobulin super family. *MAG* is known to be involved in myelination of nerve fibers. It consists of 11 exons including 9 coding exons codes for 626 amino acids long protein. Sequencing of all the 11 exons did not show any mutation.

ZNF302 is highly expressed in foetal brain. It belongs to zinc finger family of genes which are involved in regulation of transcription. This comprises of 5 exons and sequencing of all the exons including intronic boundaries did not reveal any mutation.

ZNF599 belongs to family of transcription factors with zinc finger domain. This gene may be involved in transcriptional regulation. *ZNF599* has 4 exons and encodes 588 amino acids protein product. Sequencing of all the four exons using flanking primers did not show any mutation.

CHST8 express in the foetal brain during development. This gene consists of 5 exons. Sequencing of all the five exons and exon-intron boundaries did not reveal any mutation.

SNX26 belongs to sorting nexin family of gene. It contains a phox domain, a phosphoinositide binding domain involved in intracellular trafficking. This gene is highly expressed in fetal brain, during development. *SNX26* comprises of 21 exons which encodes 1126 amino acids protein. Sequencing of all the 21 exons using flanking primers did not show any mutation.

3.2.7 Sequencing of *MCPHI*

All the 14 coding exons including exon-intron boundaries were PCR amplified and subsequently sequenced in affected patient (MCP36) using appropriate primers (Table 2.15). Sequence analysis revealed a novel single nucleotide substitution (c. 302C>G) in exon 4 of *MCPHI* which incorporate premature stop codon leading to truncated protein product of 100 amino acids (p.S101X) when compared to reference sequences (<http://www.ncbi.nlm.nih.gov/>, <http://genome.ucsc.edu/>). Both the parents of patient were found heterozygous for the mutation. Domain prediction using SMART analysis (<http://smart.embl-heidelberg.de/>) shows that truncated protein product lack both of the C-terminal BRCT domains (Figure3.15). The same mutation was not found in 100 ethnically control samples.

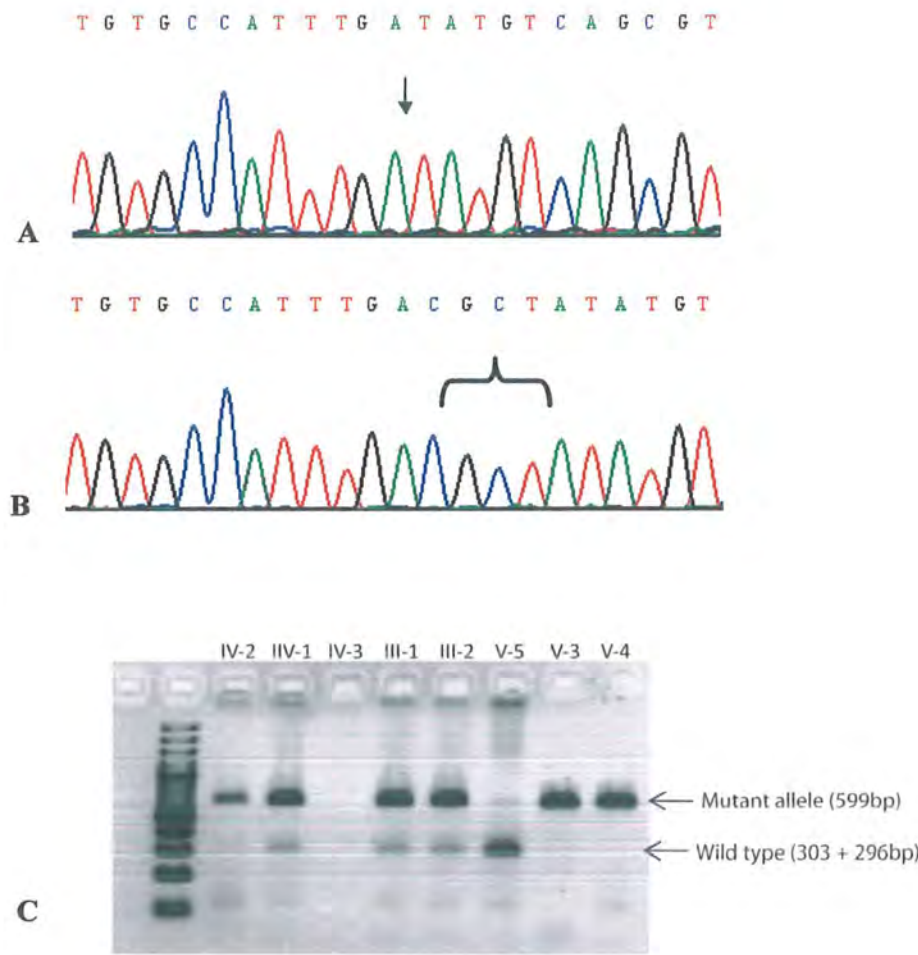


Figure 3.1: Representative Chromatogram of (A) homozygous affected individual and (B) a homozygous normal individual of family MCP3. Arrow shows site of mutation c.3477_3481delCGCTA in exon 14 of *ASPM*. (C) *HgaI* restriction analysis of all sampled members of family MCP3; mutant allele (599bp) and wild type allele (303,296bp).

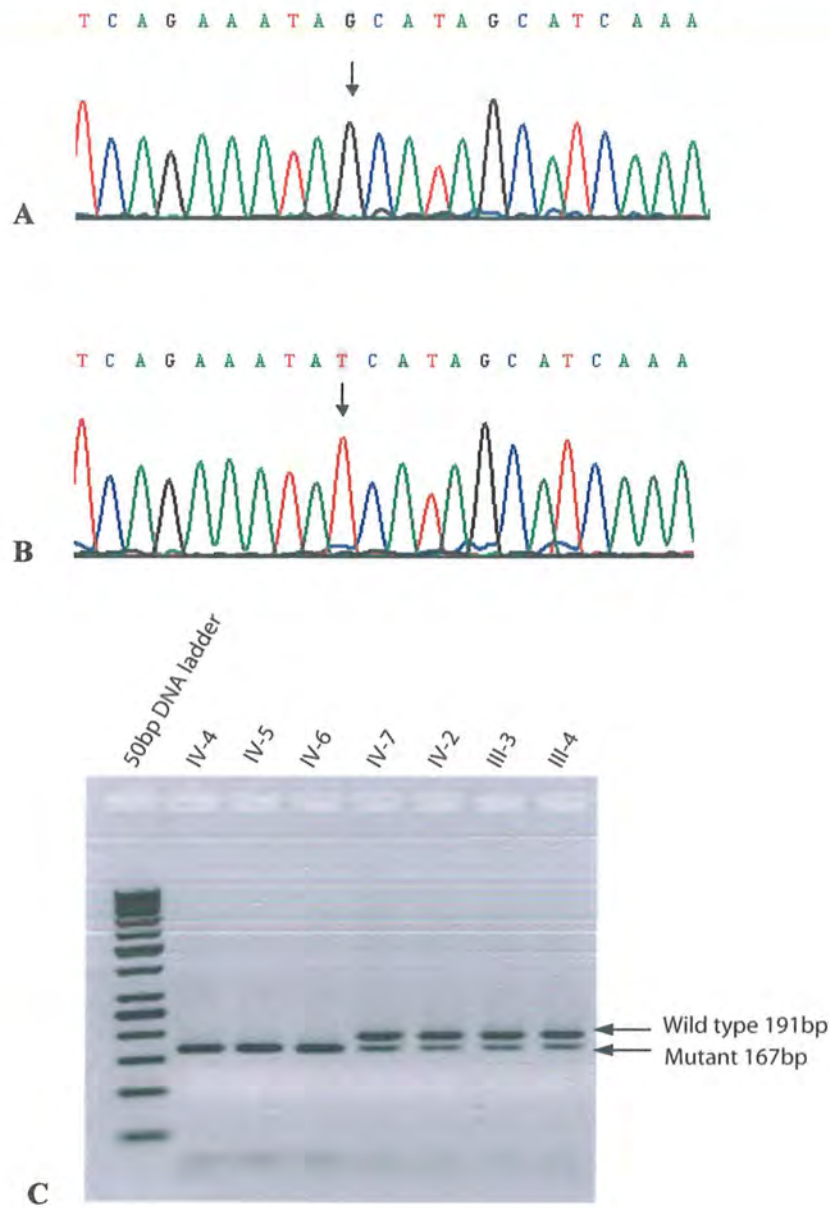


Figure 3.2: Representative Chromatogram of (A) homozygous affected individual, (B) homozygous normal individual of family MCP17. Arrow shows site of mutation c.9492T>G in exon 23 of *ASPM*. (C) *AluI* restriction analysis of all sampled members of family MCP3; mutant allele (167bp) and wild type allele (191bp).

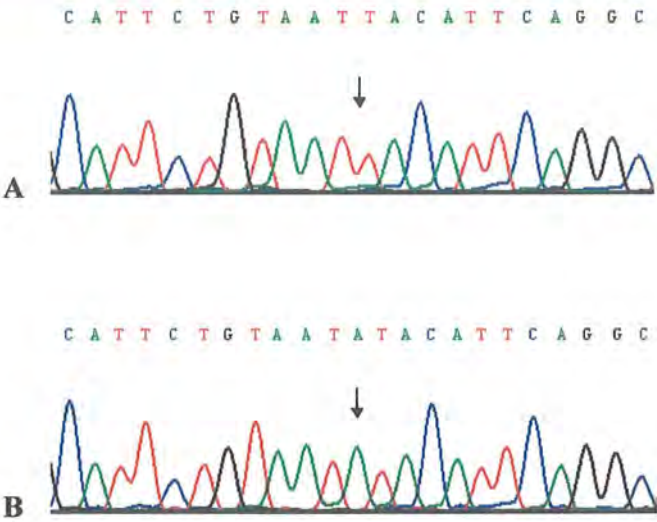


Figure 3.3: Chromatogram of representative homozygous affected individual (A) and homozygous normal individual (B) of family MCP6. Arrow shows site of mutation c.6732delA in exon 18 of *ASPM*.

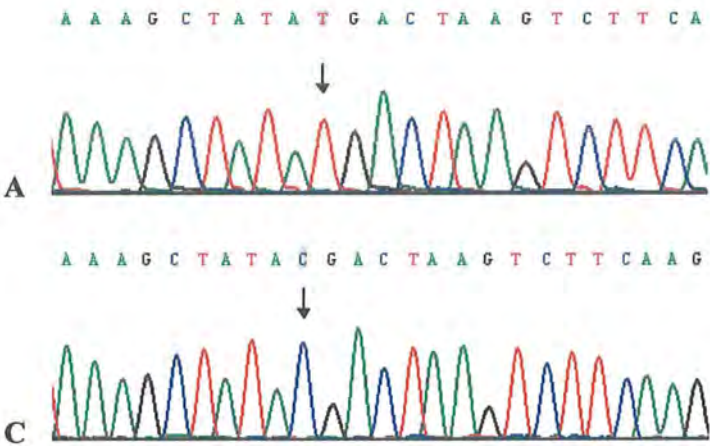


Figure 3.4: Chromatogram of representative homozygous affected individual (A) and homozygous normal individual (B) of family MCP7. Arrow shows site of mutation c.9697C>T in exon 24 of *ASPM*.

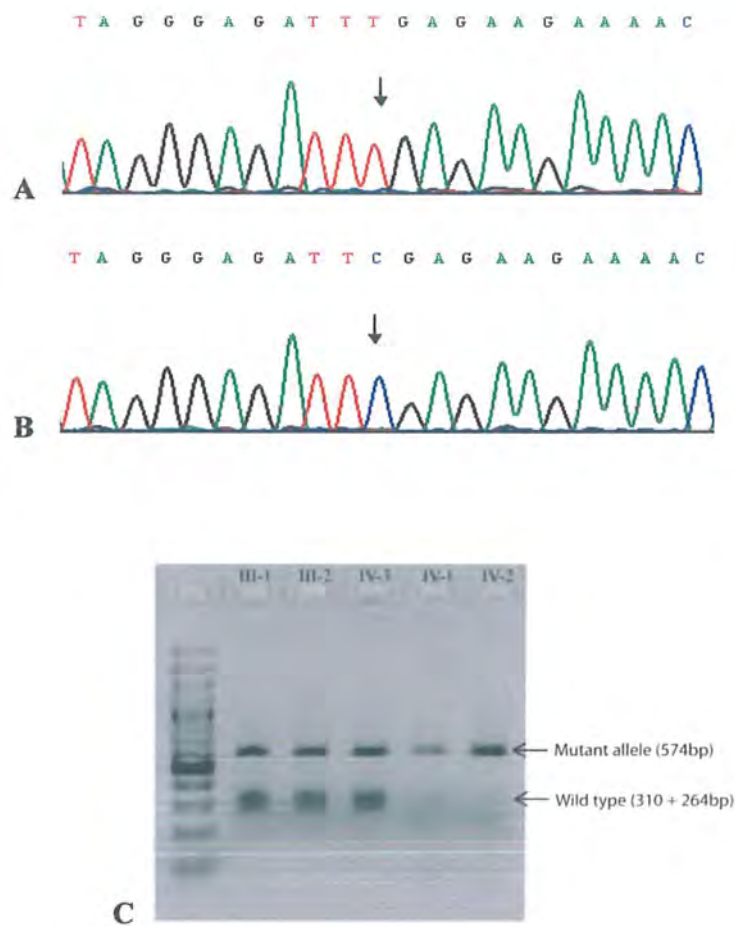


Figure 3.5: Chromatogram of representative homozygous affected individual (A) and homozygous normal individual (B) of family MCP9. Arrow shows site of mutation c.9730C>T in exon 24 of *ASPM*. *TaqI* restriction analysis of all sampled members (C) of family MCP9; mutant allele (574bp), wild type (310 + 264bp).

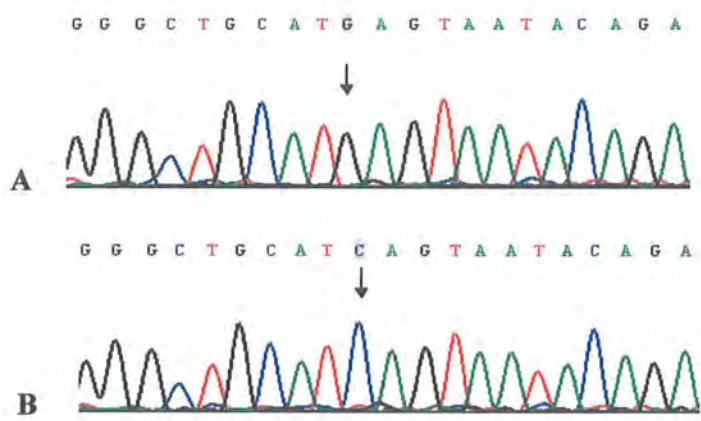


Figure 3.6: Chromatogram of representative homozygous affected individual (A) and homozygous normal individual (B) of family MCP11. Arrow shows site of mutation c.9557C>G in exon 23 of *ASPM*.

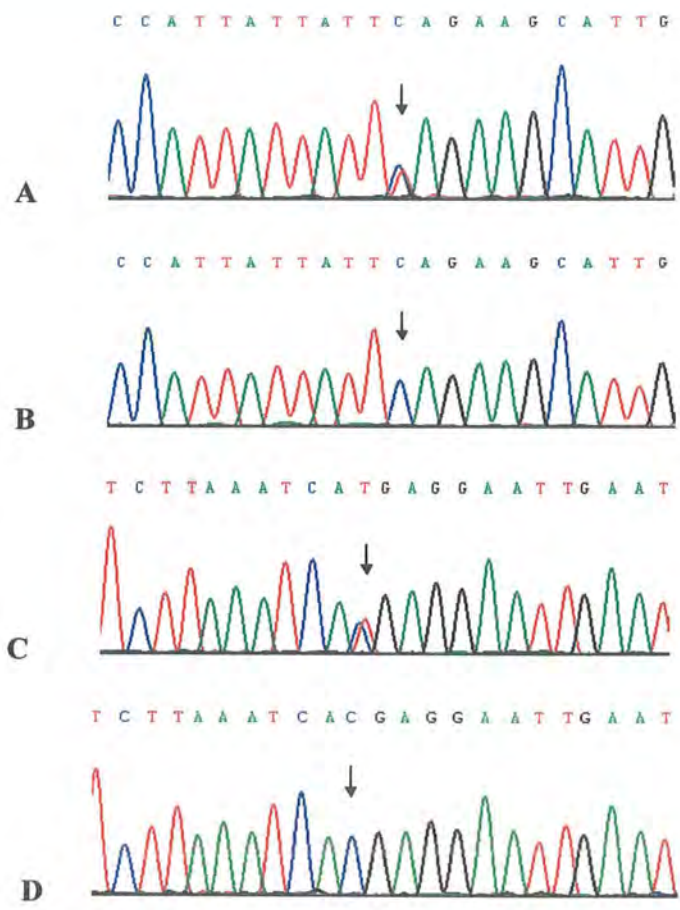


Figure 3.7: Chromatogram of (A) representative heterozygous affected individual with c.7894C>T mutation, (B) homozygous normal individual (C) heterozygous affected individual with c.3055C>T mutation and (D) homozygous normal for c.3055C>T mutation.

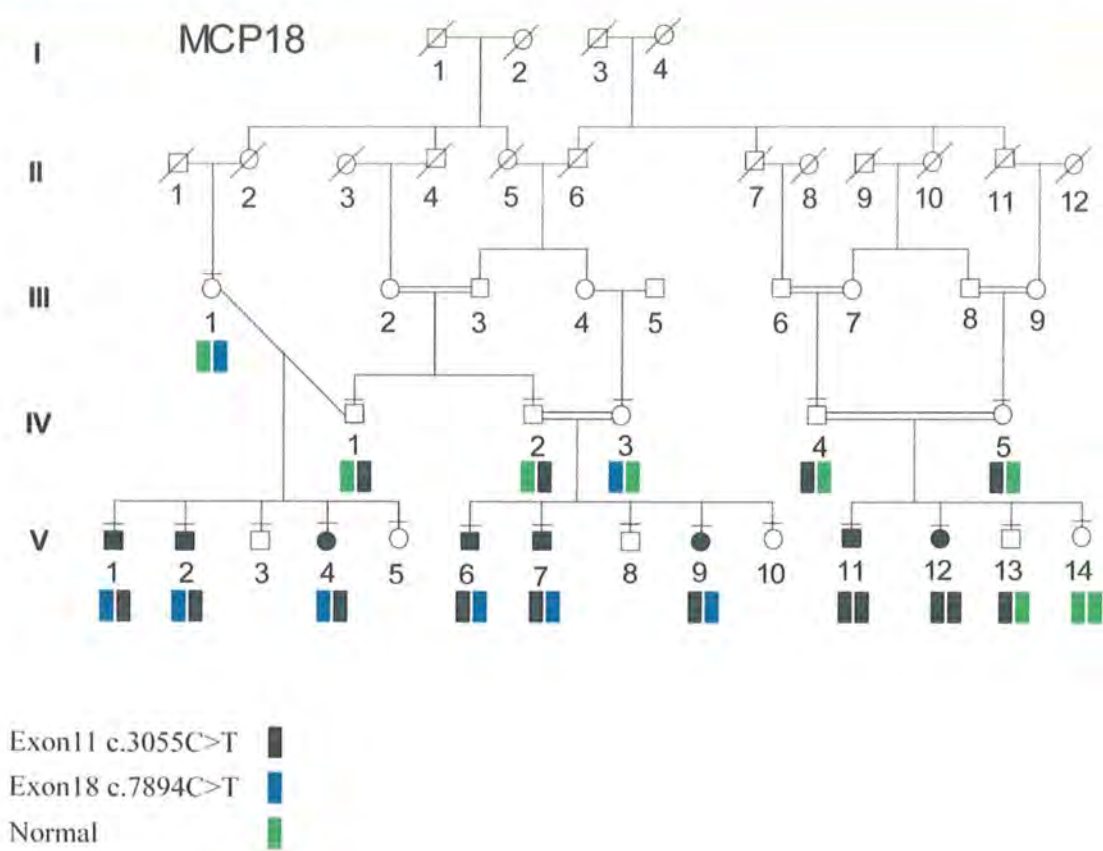


Figure 3.8: Segregation of compound heterozygous mutations (c.3055C>T and c.7894C>T) in MCP18 family. Affected individuals in right loop are homozygous for c.3055C>T. Whereas, affected subjects in middle and left loop are compound heterozygous.

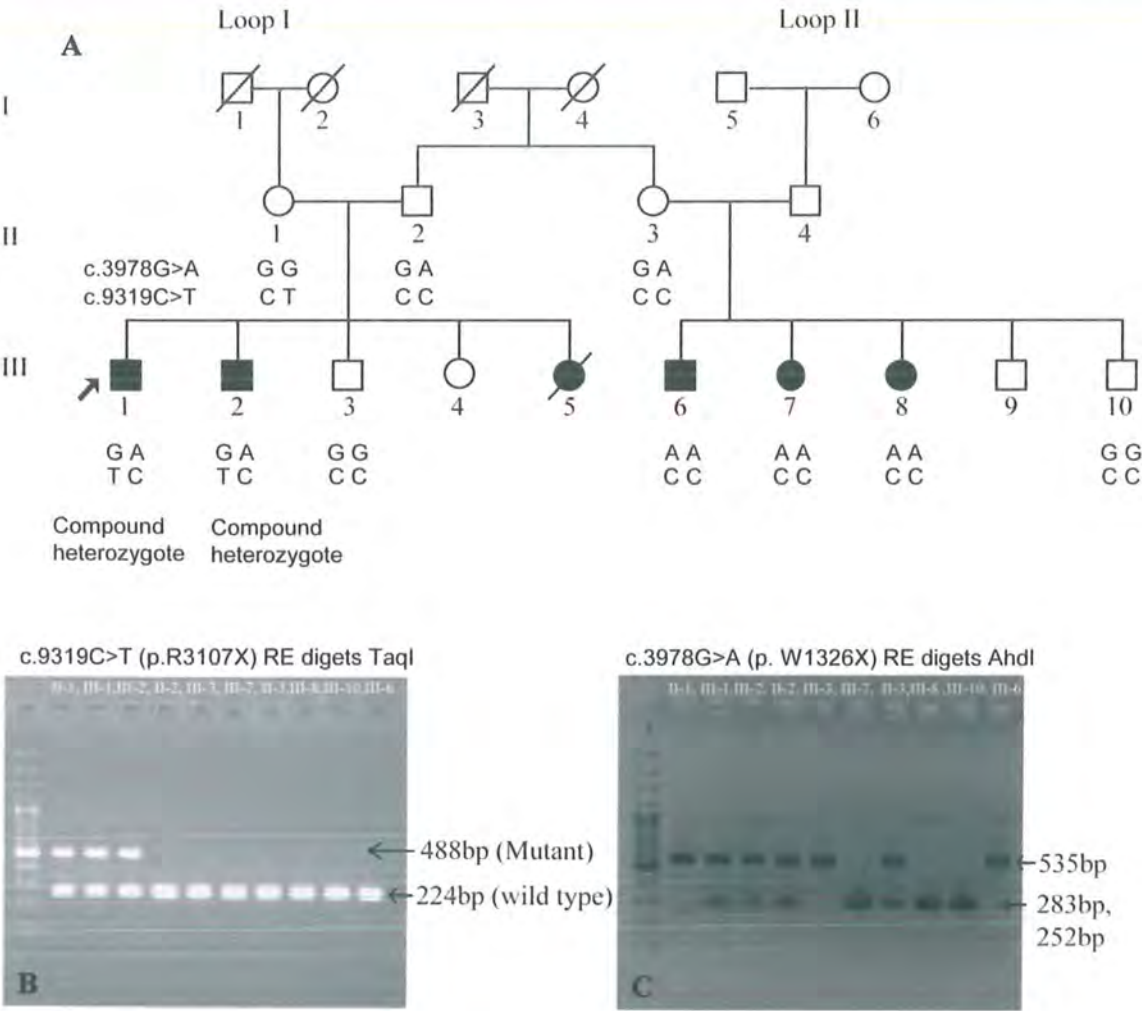


Figure 3.10: (A) Segregation of compound heterozygous mutations (c.3978G>A and c.9319C>T) in MCP35 family. Affected individuals in right loop (loop II) are homozygous for c.3978G>A, affected individuals in the left loop (loop I) are compound heterozygous. (B) Restriction digests using *TaqI* enzyme for ‘c.9319C>T’ mutation, (C) restriction digest using *AhdI* enzyme for ‘c.3978G>A’ mutation.

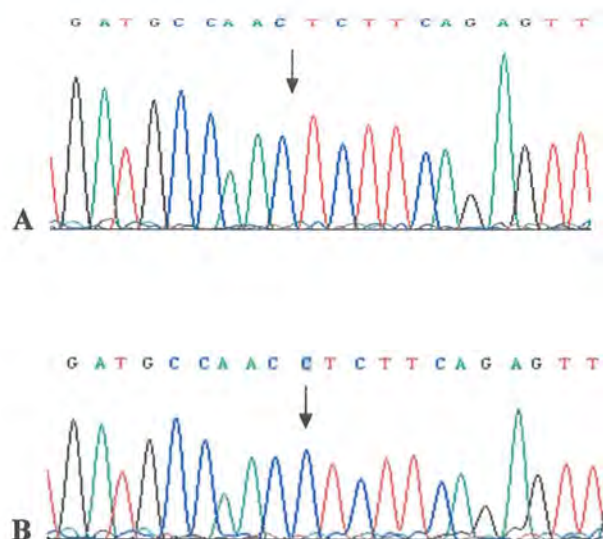


Figure 3.11: Chromatogram of representative homozygous affected individual in exon 2 of *CENPJ* in families MCP21 and MCP22 demonstrating single bp deletion (c.17_18delC). Site of deletion is indicated by arrow, (A) mutant, (B) wild type.

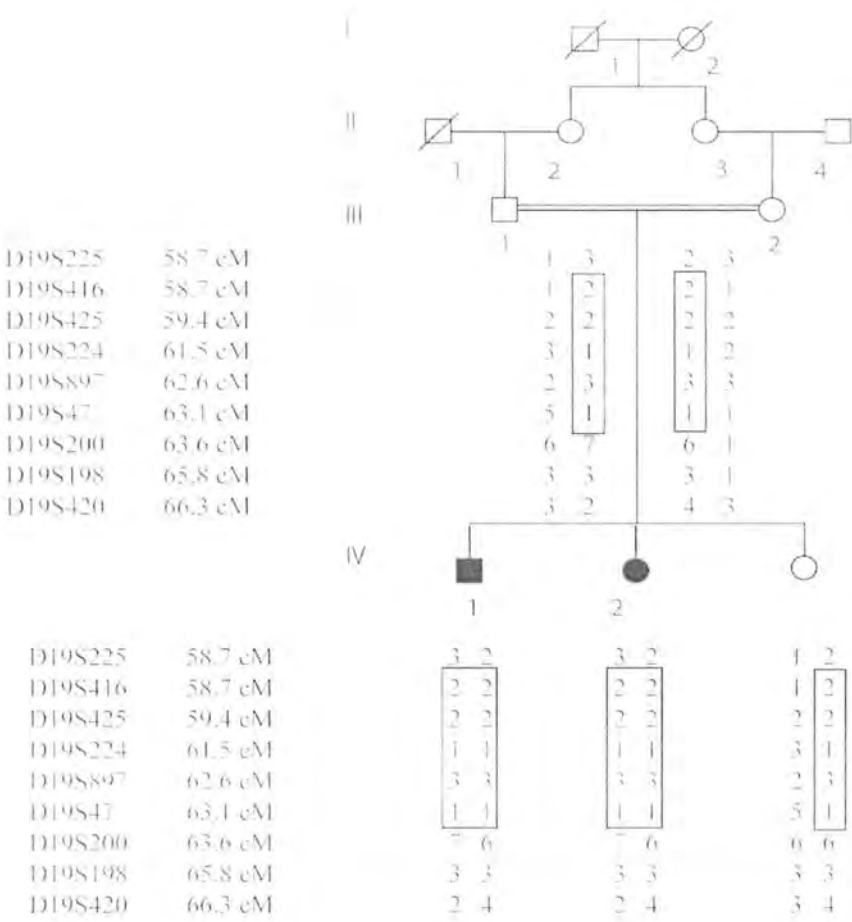


Figure 3.12: Haplotypes of the individuals in family MCP15 for nine microsatellite markers from chromosome 19 at MCPH2 locus. The homozygous region in affected subjects segregating with phenotype is shown in box.

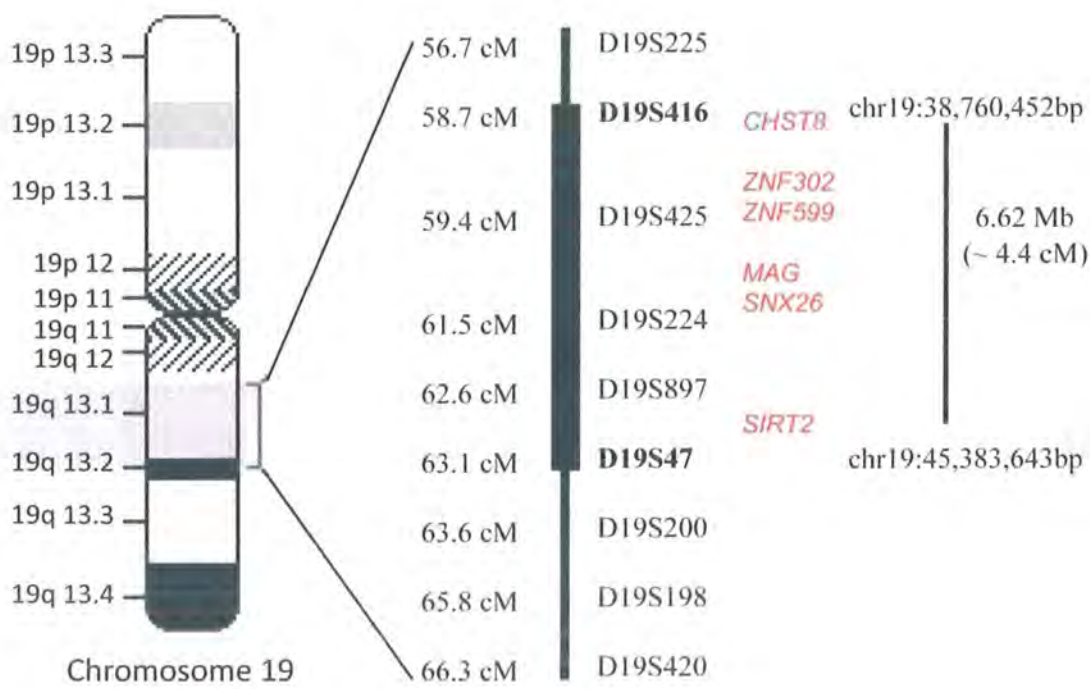


Figure 3.13: Genetic map of chromosome 19 markers. Distances are shown in centimorgan. The blackened bar indicates the minimum homozygous region shared by both affected individuals in family MCP15 at MCPH2 locus. Candidate genes sequenced in both affected individuals are written in red.

Table 3.1: Two point LOD score in family MCP15 at chromosome 19.

Marker	cM	Recombination fraction (θ)						
		0.00	0.01	0.05	0.1	0.2	0.3	0.4
D19S225	56.7	-2.27	-0.66	-0.08	0.09	0.14	0.08	0.03
D19S416	58.7	1.37	1.33	1.19	1.01	0.67	0.36	0.13
D19S425	59.4	0.40	0.38	0.33	0.26	0.15	0.06	0.01
D19S224	61.5	1.40	1.36	1.22	1.04	0.70	0.39	0.15
D19S897	62.6	0.99	0.96	0.86	0.74	0.50	0.29	0.12
D19S47	63.1	0.99	0.96	0.86	0.74	0.50	0.29	0.12
D19S200	63.6	-2.27	-0.66	-0.09	0.07	0.1	0.05	0.01
D19S198	65.8	0.69	0.67	0.59	0.50	0.33	0.18	0.08
D19S420	66.3	-2.14	-0.69	-0.12	0.03	0.05	-0.01	-0.04

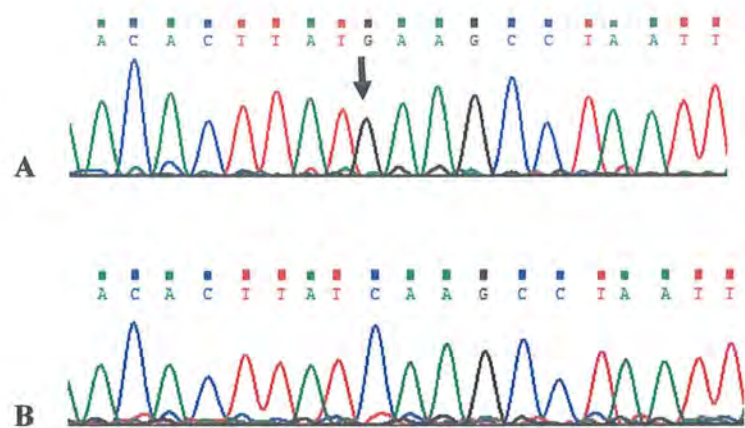


Figure 3.14: Chromatogram of representative homozygous affected individual in exon 4 of *MCPH1* in MCP36 demonstrating C>G substitution (c.302C>G). Site of mutation is indicated by arrow, (A) mutant, (B) wild type.

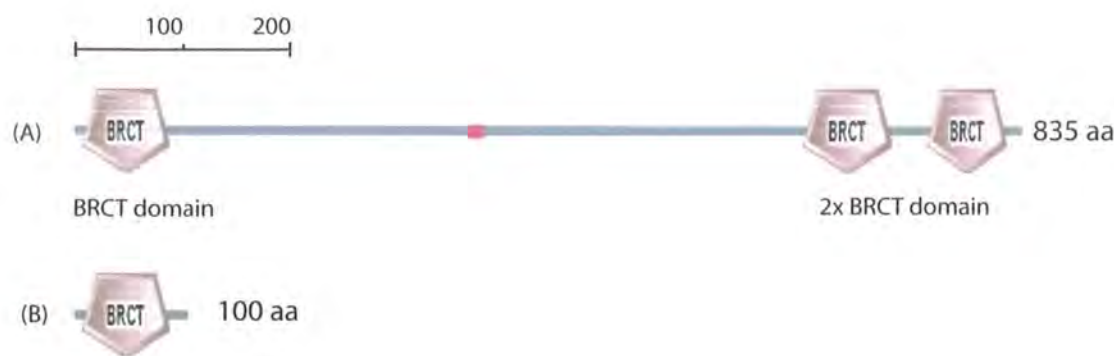


Figure 3.15: Domains of full length (A) and truncated protein (B) predicted by SMART (<http://smart.embl-heidelberg.de/>). Mutant protein lacks both C-terminal BRCT domains.

4 DISCUSSION

Primary microcephaly is an autosomal recessive neurogenic disorder. Reduced size of head is due to abnormal development of cerebral cortex during foetal life is accompanied with variable degree of mental retardation. The affected individuals are deficient in intellectual capabilities and high cognitive skills like language (Woods *et al.*, 2005). The incidence of MCPH is higher in Pakistani population as compared to rest of the world. The main reasons for higher incidence rate includes higher degree of consanguinity, large family size, little knowledge about the genetic basis of the disease, unreliability in prenatal diagnosis using conventional methods (Ultrasonography, informative only in last trimester of pregnancy) and unavailability of genetic testing facilities during prenatal life. Except for studies in northern Pakistani population, the disease is not yet characterized fully on molecular basis in most of the Pakistani population. Keeping in view the higher incidence of this lifelong disorder there is an urgent need to characterize the disease on molecular basis. This will help to devise a strategy to control the disease in this part of the world.

Homozygosity mapping is a powerful approach to localize and identify the genes underlying autosomal recessive genetic disorders (Lander and Botstein, 1987). The prerequisite for this strategy is availability of large consanguineous families with multiple affected individuals. These large families provide substantial information to deduce the inheritance pattern, phenotypic variability and finally identification of causative gene using homozygosity mapping. Moreover, large families could address the questions of genetic heterogeneity. Such large families are common in Pakistani population where consanguinity is estimated to be 70% and large family is generally desired.

Molecular genetic analysis of eleven consanguineous primary microcephaly families originating from different regions of Pakistani population was performed in the framework of this study. Out of eleven families analyzed, eight demonstrate mutations in *ASPM* (72.7%), two in *CENPJ* (18.2%) and one family linked to MCPH2 locus (9%). *ASPM* mutations identified in eight out of eleven MCPH families also support previous studies in which mutations in *ASPM* on chromosome 1q31.3 were reported as the major cause of MCPH in Pakistani and other populations (Bond *et al.*, 2002; Gul *et al.*, 2006b; Kumar *et al.*, 2004; Nicholas *et al.*, 2008). To

date 59 *ASPM* mutations have been published. Seven novel mutations identified in this study increase the total number of *ASPM* mutation to 66 (Table 4.1). Almost all of the identified mutations lead to premature terminated *ASPM* product except one missense mutation (Gul *et al.*, 2006b) which is yet to be proved functionally.

Compound heterozygous mutations in 2 apparently *ASPM* unlinked families have been identified in this study. Homozygosity mapping in these families did not establish linkage due to the segregation of two different disease alleles in these families. In MCP18, R1019X and Q2632X variants were found. Both mutations produce truncated protein products. Mutation R1019X falls in calponin homology domain (Actin binding domain) whereas Q2632X in IQ domain (calmodulin binding domain) of *ASPM*. MCP35, unlike the definition of MCPH individuals III-1 and III-2 (compound heterozygous, W1326X & R3107X) also has additional clinical symptoms of seizures from childhood that were medically treated. However, their homozygous cousins in other loop never had seizures partly explain a coincidental finding. Mutation W1326X was previously reported in homozygous form in MCPH (Kumar *et al.*, 2004) whereas it is possible that compound heterozygous mutations found in affected individuals may have some correlation with seizures like symptom. Mutation R3107X has not been described previously. Here, it is described only in compound heterozygous form in affected individuals. R3107X in homozygous form may also be associated with seizures as previously homozygous nonsense *ASPM* mutation is identified in patients with primary microcephaly and seizures (Shen *et al.*, 2005). A similar kind of report has been published recently in which MCPH patients with microcephaly exhibit seizures (Nicholas *et al.*, 2008). Therefore, it is possible that seizures may also be included in the clinical spectrum of MCPH although it is not present in most of the cases. Affected members of the two compound heterozygous families displayed a milder phenotype (HC-6SD) than all the other patients studied. However, the fact that patients with comparable homozygous mutations can have HCs of -5SD suggests that this difference is coincidental (Bond *et al.*, 2003).

Previously, a number of families have been reported to be unlinked to any known loci (Bond *et al.*, 2002; Gul *et al.*, 2006b; Kumar *et al.*, 2004). Excluded families may have mutations in *STIL* (seventh locus for MCPH on 1p32.3-p33) (Kumar *et al.*, 2009). Another possibility is occurrence of compound heterozygous mutations in apparently unlinked consanguineous families may partly explain why a considerable number of reported families were not linked to any known MCPH

locus using homozygosity mapping. High incidence of *ASPM* mutations in Pakistani population explains the existence of families with compound heterozygous mutations. Homozygosity mapping in families having compound heterozygous mutations for linkage analysis seems to be less efficient method as shown by two unlinked families. It is therefore suggested that possibility of compound heterozygous mutations in *ASPM* may also be considered while testing MCPH patients. Mutations in *ASPM* being the most common cause of MCPH, sequencing of *ASPM* in non linked families, isolated MCPH patients and non-consanguineous MCPH families may be adopted as the first line strategy in order to provide genetic counselling (Bond *et al.*, 2003; Nicholas *et al.*, 2008).

Homozygous mutations (A1160fs, I2244fs, Y3163X, S3186X, R3233X, and R3244X) were found in six linked families. A1160fs 1181X, Y2245fs 2258X, Y3164X and R3233X are novel disease variants whereas R3186X and R3244X have previously been published (Bond *et al.*, 2003; Gul *et al.*, 2006b). There was no correlation between the phenotype and site of truncation which has also been reported previously (Nicholas *et al.*, 2008). In total, we identified seven novel and three known mutations. All these mutations are nonsense producing a premature stop codon resulting into a truncated protein unable to perform normal function during neurogenesis in foetal life.

Two heterozygous mutation carriers had small heads (HC-2 to -3.5); MCP7 IV-3 and MCP18-13. However, like other heterozygous mutation carriers they were mentally normal which seems to be a rare finding.

Two families linked to MCPH6 locus (MCP21, MCP22) demonstrate 1bp deletion mutation c.17_18delC (T6fsX3) in exon 2 of *CENPJ* leading to premature termination of protein. This mutation was previously reported in two families from Northern Pakistan (Bond *et al.*, 2005). MCP21 and MCP22 originate from a geographically distinct region of Pakistan as compared to previously studied Northern Pakistani families. It may explain a common genetic mechanism for mutation occurrence.

Family MCP15 established linkage to MCPH2 locus on chromosome 19q (19q13.1-q13.2) whose causative gene is not yet identified. The affected individuals have primary microcephaly and also exhibit seizures clinically. The minimal critical region for MCPH2 locus was defined by

D19S416 and D19S420 which was about 7.6 cM in two consanguineous families from Northern Pakistan (Roberts *et al.*, 1999). The minimum homozygous region shared by two affected subjects in MCP15 is defined by D19S416 and D19S47. This substantially decreases the minimum critical interval from 7.6 cM to about 4.4 cM containing 162 genes. Direct sequencing of exons including exon intron boundaries and 5' and 3' UTRs of selected candidate genes i.e. *SIRT2*, *MAG*, *ZNF302*, *ZNF599*, *CHST8* and *SNX26* was performed. The candidate genes were selected on the basis of their expression profile in foetal brain during development. Unfortunately, no disease causing mutation was identified in any of the six selected candidate genes when compared to reference sequences (<http://www.ncbi.nlm.nih.gov/>). However, the possibility of a mutation in the regulatory or intronic regions cannot be excluded. Identification of MCPH gene at MCPH2 locus will help to understand the possible mechanism of cortical development and ultimately the evolution of human brain. Analysis of additional MCPH2 linked families will facilitate to further narrow down the linkage interval and explore the causative gene.

Affected patient in family MCP36 found homozygous for *MCPH1* region demonstrated a novel nonsense mutation (c. 302C>G) leading to truncated protein of 100 amino acid residues. Microcephalin acts as a regulator of chromosomal condensation in G2 and G1 phases of cell cycle (Trimborn *et al.*, 2004). Mutations in microcephalin have been demonstrated in MCPH1 primary microcephaly and PCC syndrome (Trimborn *et al.*, 2004; Trimborn *et al.*, 2005). Both condition showed cellular phenotype of premature chromosomal condensation. Chromosomal condensation is a well organized process which is required for entry of cell into mitosis and faithful segregation of the genome. Microcephalin acts as a negative regulator of condensin II by preventing premature chromosomal condensation before the start of prophase and allows well-timed decondensation post mitosis (Trimborn *et al.*, 2005). The mutant protein lacks both of the C-terminal BRCT domains. BRCT domain containing proteins are involved in DNA repair mechanism. Patient in MCP36 represent high degree of spontaneous chromosomal breakage, endomitosis and endoreduplication and sensitivity towards alkylating and radiomimetic drugs represent impaired DNA damage response. This impaired DNA repair mechanism in patient is explained by identification of mutation in microcephalin leading truncated protein product. Microcephalin associates with chromatin and co-localizes with mediator of DNA damage check point1 (MDC1) and H2A histone family, member X (H2AFX) at DNA –repair foci upon damage

induced by ionizing radiation (IR) (Cox *et al.*, 2006). The clinical findings in MCP36 patients demonstrated by Tommerup *et al.*, (1993) include spontaneous chromosomal breakage, endomitosis and endoreduplication upon exposure to Trenimon and radiomimetic drug bleomycin in phytohemagglutinin stimulated peripheral lymphocytes confirms that *MCPH1*/microcephalin is an important component of DNA damage repair mechanism and cell cycle regulation. In addition, almost complete craniosynostosis is demonstrated in patient at 10 months of age is not described earlier in patients with *MCPH1* mutations. This may be due limited clinical information in those patients or low degree of intracranial pressure due to reduced brain growth. This newly identified mutation in MCP36 strengthens the role of microcephalin in DNA damage response/repair mechanism, and cell cycle control leading to microcephaly with variable moderate mental retardation.

Identification of mutations in 10 Pakistani families analyzed in this study will help to design improved strategies of genetic counselling for Pakistani families with MCPH keeping in view the strong local tradition of cousin marriages in this part of world. Carrier screening and prenatal diagnosis using molecular biology techniques will also provide a rapid and reliable method in carrier couples at risk of having affected births. Ultrasonography and other methods of clinical diagnosis could not be used to diagnose MCPH until the third trimester of pregnancy and efficacy of these conventional methods is still questionable in case of MCPH. The mutation based carrier screening and prenatal diagnosis will provide highly reliable and early diagnosis to control this disease.

Table 4.1: Reported MCPH mutations in *ASPM*.

No.	Nucleotide position	Mutation type	Ethnicity	References
1	c.74delG	p.Arg25fs	Caucasian	(Nicholas <i>et al.</i> , 2008)
2	c.297+1460_3391-242del21844	Loss of microtubular binding domain	Caucasian	(Nicholas <i>et al.</i> , 2008)
3	c.349C>T	p.R117X	Pakistani/ Indian	(Bond <i>et al.</i> , 2003, Kumar <i>et al.</i> , 2004)
4	c.440delA	p.Lys147fs	Caucasian	(Nicholas <i>et al.</i> , 2008)
5	c.577C>T	p.Gln193X	Caucasian	(Nicholas <i>et al.</i> , 2008)
6	c.719delCT	p.S240fs	Pakistani	(Bond <i>et al.</i> , 2002)
7	c.1152_1153delAG	p.Ser384fs	Caucasian	(Nicholas <i>et al.</i> , 2008)
8	c.1179delT	p.Pro393fs	Caucasian	(Nicholas <i>et al.</i> , 2008)
9	c.1258delTCTCAAG	p.S420fs	Pakistani	(Bond <i>et al.</i> , 2002)
10	c.1260delTCAAGTC	p.S420fs	Pakistani	(Gul <i>et al.</i> , 2006c)
11	c.1366G>T	p.E456X	Turkish	(Bond <i>et al.</i> , 2003)
12	c.1406_1413delATCCTAAA	p.Asn469fs	Caucasian	(Nicholas <i>et al.</i> , 2008)
13	c.1590delA	p.Lys530fs	Caucasian	(Nicholas <i>et al.</i> , 2008)
14	c.1727delAG	p.K576fs	Yemni	(Bond <i>et al.</i> , 2003)
15	c.1959delCAAA	p.N653fs	Saudi Arabia	(Bond <i>et al.</i> , 2003)
16	c.1990C>T	p.Q664X	Pakistani	(Bond <i>et al.</i> , 2003)
17	c.2761-25A>G	Creates 'AG' motif between branch site and splice-acceptor site, exon 10 skipped, exon 11 frameshift with 30 novel amino acids then stop	Caucasian	(Nicholas <i>et al.</i> , 2008)
18	c.2967G>A	p.Trp989X	Caucasian	(Nicholas <i>et al.</i> , 2008)
19	c.3188T>G	p.Leu1063X	Pakistani	(Nicholas <i>et al.</i> , 2008)
20	c.3527C>G	p.S1176X	Jordanian	(Bond <i>et al.</i> , 2003)
21	c.3663delG	p.R1221fs	Pakistani	(Bond <i>et al.</i> , 2003)
22	c.3710C>G	p.Ser1237X	Caucasian	(Nicholas <i>et al.</i> , 2008)
23	c.3741+1G>A	Removes splice-donor site, additional 9 novel aa then stop	Caucasian	(Nicholas <i>et al.</i> , 2008)
24	c.3796G>T	p.Glu1266X	African	(Nicholas <i>et al.</i> , 2008)
25	c.3811C>T	p.R1271X	Dutch	(Bond <i>et al.</i> , 2003)
26	c.3978G>A	p.W1326X	Indian/ Pakistani	(Gul <i>et al.</i> , 2006c; Kumar <i>et al.</i> , 2004)
27	c.4195_4196insA	p.Thr1399fs	Moroccan	(Desir <i>et al.</i> , 2008)

No.	Nucleotide position	Mutation type	Ethnicity	References
28	c.4581delA	p.G1527fs	Pakistani	(Bond <i>et al.</i> , 2003)
29	c.4795C>T	p.R1599X	Pakistani	(Bond <i>et al.</i> , 2003)
30	c.5136C>A	p.Y1712X	Pakistani	(Gul <i>et al.</i> , 2007)
31	c.5149delA	p.I1717X	Pakistani	(Gul <i>et al.</i> , 2007)
32	c.6189T>G	p.Y2063X	Saudi Arabia	(Shen <i>et al.</i> , 2005)
33	c.6335_6336delAT	p.His2112fs	Pakistani	(Nicholas <i>et al.</i> , 2008)
34	c.7489_7493delTATAT	p.Tyr2497fs	caucasian	(Nicholas <i>et al.</i> , 2008)
35	c.7761T>G	p.Y2587X	Pakistani	(Bond <i>et al.</i> , 2002)
36	c.7782_7783delGA	p.Gln2594fs	Caucasian, Pakistani	(Nicholas <i>et al.</i> , 2008)
37	c.7859_7860delAG	p.Gln2620fs	Arab	(Nicholas <i>et al.</i> , 2008)
38	c.7895delAG	p.Q2632fs	Pakistani	(Bond <i>et al.</i> , 2003)
39	c.8130_8131delAA	p.Thr2710fs	Caucasian	(Nicholas <i>et al.</i> , 2008)
40	c.8378delT	p.Met2793fs	Pakistani	(Nicholas <i>et al.</i> , 2008)
41	c.8508delGA	p.Q2836fs	Pakistani	(Bond <i>et al.</i> , 2003)
42	c.8844delC	p.Ala2948fs	Caucasian	(Nicholas <i>et al.</i> , 2008)
43	c.9118insCATT	p.Y3040fs	Pakistani	(Gul <i>et al.</i> , 2006c)
44	c.9159delA	p.K3053fs	Pakistani	(Bond <i>et al.</i> , 2002)
45	c.9178C>T	p.Y3060X	Indian	(Kumar <i>et al.</i> , 2004)
46	c.9190C>T	p.R3064X	Pakistani	(Bond <i>et al.</i> , 2003)
47	c.9238A>T	p.K3080X	Pakistani	(Gul <i>et al.</i> , 2006c)
48	c.9539A>C	p.Q3180P	Pakistani	(Gul <i>et al.</i> , 2006c)
49	c.9557C>G	p.S3186X	Pakistani	(Bond <i>et al.</i> , 2003)
50	c.9681delA	p.Thr3227fs	Pakistani	(Nicholas <i>et al.</i> , 2008)
51	c.9730C>T	p.R3244X	Pakistani	(Gul <i>et al.</i> , 2007)
52	c.9745_9746delCT	p.Leu3249fs	Pakistani	(Nicholas <i>et al.</i> , 2008)
53	c.9754delA	p.R3252fs	Yemni	(Bond <i>et al.</i> , 2003)
54	c.9789T>A	p.Tyr3263X	Pakistani	(Nicholas <i>et al.</i> , 2008)
55	c.10059C>A	p.Y3353X	Pakistani	(Gul <i>et al.</i> , 2007)
56	IVS9+5G>T (2936+5G>T)	Remove splice donor site additional 2 amino acids then stop	Pakistani	(Bond <i>et al.</i> , 2003)

No.	Nucleotide position	Mutation type	Ethnicity	References
57	3082G>A	Remove splice donor site additional 3 amino acids then stop	Pakistani	(Bond <i>et al.</i> , 2003)
58	IVS25+1G>T (9984+1G>T)	Remove splice donor site additional 29 amino acids then stop	Pakistani	(Bond <i>et al.</i> , 2003)
59	Translocation t(1;4)(q31;p15.3)		European	(Pichon <i>et al.</i> , 2004)
60	c.3477_3481delCGCTA	p.A1160fs	Pakistani	Present Study
61	c.3055C>T	p.R1019X	Pakistani	Present Study
62	c.6732delA	p.I2245fs	Pakistani	Present Study *
63	c.7894C>T	p.Q2632X	Pakistani	Present Study
64	c.9319C>T	p.R3107X	Pakistani	Present Study
65	c.9492T>G	p.Y3164X	Pakistani	Present Study
66	c.9697C>T	p.R3233X	Pakistani	Present Study

Part 2

Inherited limb disorders

5 INTRODUCTION

Inherited limb malformations are genetically heterogeneous disorders which display a wide spectrum of phenotypic manifestations and may occur as an isolated deformity and as part of a syndrome. Isolated limb malformations are rare in general, but they are of clinical importance due to their overall frequency and severity. After the accomplishment of human genome project our understanding about the molecular basis of congenital limb malformations has greatly enhanced in the recent years. In addition, increasing knowledge of the molecular basis of embryonic development has significantly enhanced our understanding of embryonic limb development and various kinds of limb anomalies.

Inherited limb malformations can be distinguished into two main types: (1) isolated limb malformation without involvement of any other organ or tissue (Non-syndromic), (2) in combination with other abnormalities (Syndromic).

Isolated or non-syndromic hands malformations can be categorize into polydactyly, syndactyly, brachydactyly and split hand and foot malformations.

5.1 Polydactyly

Polydactyly is the most frequent human congenital limb deformity and has attracted attention since biblical times where it is described in Samuel II (Nicolai and Schoch, 1986). Polydactyly refers to the occurrence of supernumerary digits or part of them, ranging from complete duplication of a limb or a part of a limb to duplications of single digits (Schwabe and Mundlos, 2004). Polydactyly can be found as a genetically distinct isolated anomaly or in combination with other anomalies. Biesecker (2002) piled up 119 distinct disorders with polydactyly as a consistent feature. Author catalogued these disorders by phenotype and genotype and described numerous overlapping phenotypes, genetic heterogeneity of phenotypes (Biesecker, 2002). Isolated polydactyly is commonly found as preaxial polydactyly and postaxial polydactyly while polydactyly of central rays is not so common.

5.2 Types of polydactyly

5.2.1 Preaxial polydactyly (PPD)

Preaxial polydactyly (PPD) is most frequently observed and includes duplicated thumbs or great toes as well as various forms of triphalangeal thumbs and index finger duplication. PPD is a genetically heterogeneous group and is mostly inherited as an autosomal dominant trait. Sporadic cases of isolated PPD are most frequently found. It is further classified into four types as follows.

5.2.1.1 Thumb polydactyly (PPD1, OMIM: 174400)

PPD1 or thumb polydactyly involves duplication of one or more of the skeletal components of a biphalaengeal thumb. Severity varies from mere broadening of the distal phalanx with slight bifurcation at the tip to full duplication of the thumb including the metacarpals. PPD1 was described 3 to 4 times more frequent in Caucasians or Blacks. More females than males were affected. In PPD1 hands are most commonly affected and always unilateral (Bingle and Niswander, 1975).

5.2.1.2 Polydactyly of triphalangeal thumb (PPD2/TPT; OMIM: 174500)

The thumb in this malformation is usually opposable and possesses a normal metacarpal. This form of polydactyly consists of duplication of the distal phalanx, giving a 'duck-bill' appearance. TPT was first mapped at chromosome 7q36 using highly polymorphic markers (Tsukurov *et al.*, 1994). Point mutations in the sonic hedgehog (*SHH*) regulatory element has been identified on chromosome 7q36-associated preaxial polydactyly II (Lettice *et al.*, 2003). *SHH* normally expressed in the zone of polarizing activity (ZPA) posteriorly in the limb bud. Point mutations in *SHH* regulatory element leads to ectopic expression at the anterior margin in mouse models of PPD. An enhancer or regulatory element that drives normal *SHH* expression in the ZPA, the regulator, designated ZPA regulatory sequence (ZRS), lies within intron 5 of the *LMBR1* gene, which is about 1 Mb from *SHH*. Number of point mutations in ZRS has been identified that segregated with PPD2 as well as in the Hx mouse mutant (Dobbs *et al.*, 2000; Gurnett *et al.*, 2007; Lettice *et al.*, 2003). A duplicated region of 588 Kb comprising the ZRS was identified by

quantitative real-time polymerase chain reaction in a large pedigree with variable TPT-PS (Klopocki *et al.*, 2008). Heterozygous duplications involving the ZRS, ranging from 131 Kb to 398 kb have been identified in 5 Chinese families with triphalangeal thumb-polysyndactyly syndrome (TPT-PS) and syndactyly type IV (Sun *et al.*, 2008).

5.2.1.3 Index finger polydactyly (polydactyly, Preaxial III, OMIM: 174600)

In this form of polydactyly the thumb is replaced by one or two triphalangeal digits, which may or may not be opposable (Swanson and Brown, 1962). The feet, in some cases, show preaxial polydactyly of the 1st or 2nd toes (James and Lamb, 1963; Manoilloff, 1931). A constant radiological finding is distal epiphysis for the metacarpal of the accessory digits. A historically famous example is the Scipion family in which the malformation was inherited for over two thousand years (Manoilloff, 1931).

5.2.1.4 Preaxial polydactyly type IV (PPD IV, OMIM: 174700)

Preaxial polydactyly type IV is inherited as an autosomal dominant disorder. Although both preaxial polydactyly and syndactyly are cardinal features of this malformation, it is classified as a form of polydactyly because syndactyly does not occur in the absence of polydactyly (McClintic, 1935). The thumb shows only the mildest degree of duplication in PPD-IV, and syndactyly of various degrees affects fingers 3 and 4. Although the polydactyly is classically describe as preaxial, the more common presentation is postaxial polydactyly of hands and preaxial polydactyly of feet. The foot malformation is more constant and consists of duplication of part or all of the first or second toes and syndactyly affects all of the toes, especially the second and third. It is possible that this is the same disorder as that of cross polydactyly type I (CP1) (Ishikiriya *et al.*, 1991). The digital changes in PPD-IV are identical to those of Greig syndrome (GCPS; OMIM: 175700), but the facial features of Greig syndrome can be so mild and indistinguishable from the normal. Therefore, explanation of type IV preaxial polydactyly as distinct clinical entity is questionable by some researchers (Baraitser *et al.*, 1983). A single

nucleotide frameshift insertion mutation in *GLI3* resulting in a truncated protein of 1,245 amino acids in a family with preaxial polydactyly type IV was described (Radhakrishna *et al.*, 1999).

5.2.2 Postaxial polydactyly (PAP)

Postaxial polydactyly is characterized by supernumerary digits on the ulnar or fibular side of the hands or feet. It may be autosomal dominant or recessive trait. The incidence of postaxial polydactyly is 1 in 630 to 1 in 3300 in Caucasians and 1 in 100 to 300 in Blacks.

From the study of various pedigrees of postaxial polydactyly, it is suggested that 2 phenotypically and possibly genetically different varieties exist.

5.2.2.1 Postaxial polydactyly type A (PAPA)

Postaxial polydactyly type A is inherited as an autosomal dominant trait with marked penetrance and is characterized by a well developed digit articulating with fifth or an extra metacarpal. Four different genetic loci have been mapped for PAPA at chromosome 7p13.6 (PAPA1: OMIM 174200) in family with PAPA/B (Radhakrishna *et al.*, 1997a), 13q21-q32 (PAPA2: OMIM 602085) in family with PAPA (Akarsu *et al.*, 1997), 19p13.1-13.2 (PAPA3: OMIM 607324) in family with PAPA/B (Zhao *et al.*, 2002) and 7q21-q34 (PAPA4: OMIM 608562) in family with PAPA/B with partial Cutaneous syndactyly (Galjaard *et al.*, 2003). Heterozygous mutations including frameshift, missense and nonsense have been identified in the *GLI3* (Radhakrishna *et al.*, 1999; Radhakrishna *et al.*, 1997b).

5.2.2.2 Postaxial polydactyly type B (PAPB, OMIM: 174200)

Postaxial polydactyly type B represent more complicated genetic etiology. Rudimentary extra digit is not well formed and frequently represented by an extra skin tag (Pedunculated postminimus). In postaxial polydactyly A/B, both PAPA and PAPB are present in the affected individuals. Mutations in *GLI3* have been described in families with PAPA/B (Radhakrishna *et al.*, 1999).

5.3 Brachydactyly

The term brachydactyly refers to shortening of digits due to abnormal development of phalanges, metacarpals or both. Brachydactyly is genetically heterogeneous, it can occur as an isolated entity or as part of a complex malformation syndrome. Isolated brachydactyly usually occurs as autosomal dominant traits with high degree of phenotypic variability. In many cases brachydactyly may be present along with limb malformations like syndactyly, polydactyly, reduction defects and symphalangism. The prevalence of various forms of isolated brachydactyly is rare; except for type A3 and D whose prevalence is around 2% (Temtamy and McKusick, 1978). Bell (1951) classified isolated brachydactyly for the first time on anatomic basis, which is the most commonly used. He analyzed 124 families with autosomal dominant inheritance and categorized them into five major types; A to E. More comprehensive classification was done by Temtamy and McKusick (1978) in their research on the genetics of hand malformations. In latest classification of genetic skeletal diseases, brachydactyly is classified as a member of dysostoses group that include abnormalities of patterning of hands and feet and disorders of growth and differentiation. Dysostoses are usually static and arise during blastogenesis stage (first eight weeks of embryonic life) and thus can be differentiated from osteochondrodysplasias that usually arise at later stage of development. Dysostoses refers to abnormalities of individual bones alone or in combination with other bones and can be differentiated from osteochondrodysplasias where there is generalized skeletal involvement and continue to develop as a result of active gene involvement throughout life (Hall, 2002).

Later on brachydactyly was classified by Kornak and Mundlos (2003) using developmental approach as a member of disorders of early differentiation. They classified the skeletal disorders, which is based upon a combination of molecular pathology and embryology, taking into account the importance of development for the understanding of bone diseases. They have classified skeletal disorders into four major groups: disorders of skeletal patterning, disorders of early differentiation, disorders of growth and disorders of skeletal homeostasis.

5.3.1 Brachydactyly type A

Brachydactyly type A is characterized by hypoplasia or aplasia of middle phalanges. According to involvement of digits brachydactyly type A is further subdivided into A1-A5.

5.3.1.1 Brachydactyly type A1 (BDA1; OMIM: 112500)

In early 1900, Farabee and Drinkwater described this type of brachydactyly. In BDA1 all the middle phalanges are affected and variably shortened or fused with terminal phalanges. The proximal phalanges of thumbs and big toes are short. Depending upon severity of malformation it is divided into two forms as severe and minor brachydactyly. Brachydactyly type A1 is the first human trait which is interpreted in Mendelian terms (Farabee WC, 1903).

Type A1 brachydactyly is genetically heterogeneous and caused by mutations in the amino-terminal domain of the Indian hedgehog (*IHH*) located on chromosome 2q35-36 (Gao *et al.*, 2001). Second locus for BDA1 phenotype is mapped to chromosome 5p13.3-p13.2 (Armour *et al.*, 2002).

5.3.1.2 Brachydactyly type A2 (BDA2; OMIM: 112600)

BDA2 is characterized by a triangular shaped 2nd middle phalanx of the index finger and sometimes little finger. In the severe cases, the index finger is curved radially. Deformity of the 2nd toe is a more consistent finding than deformity of the index finger. It was first described by Mohr and Wriedt (1919). BDA2 families demonstrated autosomal dominant inheritance and can be caused by mutations in the human bone morphogenetic receptor 1B gene (*BMPR1B*) on chromosome 4q, that affect cartilage formation in a dominant-negative manner (Lehmann *et al.*, 2003). Kjaer *et al.* (2006) demonstrated that sparing of the 4th finger distinguishes the Mohr-Wriedt type BDA2 from BDA2 caused by mutations in *BMPR1B* and concluded that the growth and differentiation factor 5 gene (*GDF5*) on chromosome 20q11 is a novel BDA2 causing gene (Kjaer *et al.*, 2006). Mutations in *GDF5* alter the receptor binding affinities and can also cause symphalangism (Seemann *et al.*, 2005).

5.3.1.3 Brachydactyly type A3 (BDA3; OMIM: 112700)

BDA3 is characterized by shortening of the middle phalanx of the little finger. Slanting of the distal articular surface of the middle phalanx leads to radial deflection of the distal phalanx. It is inherited as an autosomal dominant fashion with reduced penetrance. It is not always associated with clinodactyly. A single flexion crease of the little finger indicates a short or absent middle phalanx. This type should be differentiated from other types, Kirner deformity and camptodactyly, in the former there is radial bowing of the terminal phalanx due to curving of its shaft. Camptodactyly is a flexure contracture deformity of the interphalangeal joints. Type A3 brachydactyly is very common. The frequency of BDA3 varied in different populations between 3.4% and 21%. No gene or locus has been identified for BDA3 type brachydactyly.

5.3.1.4 Brachydactyly type A4 (BDA4; OMIM: 112800)

This rare type of brachydactyly was first described by Temtamy and McKusick (1978) in four generations with an unusual type of brachydactyly. They described brachymesophalangy of 2nd and 5th digits. Sometime 4th digit may be affected with abnormal shaped middle phalanx leading to radial deviation of the distal phalanx. The feet also showed absence of the middle phalanges of the lateral four toes. Mutations in the homeobox containing gene (*HOXD13*) can give rise to limb malformations with variable expressivity and a wide spectrum of clinical manifestations including synpolydactyly and brachydacty types D and E. Zhao *et al.* (2007) found a link between *HOXD13* and two additional limb phenotypes, syndactyly type V and brachydactyly type A4, and suggested the term '*HOXD13* limb morphopathies' for the spectrum of limb disorders caused by *HOXD13* mutations.

5.3.1.5 Brachydactyly type A5 (BDA5; OMIM: 112900)

BDA5 type was reported by Bass, and Cuevas-Sosa and Garcia-Segur (1971). Absence of middle phalanges and nail dysplasia with duplicated distal phalanx of the thumb was described as clinical findings. No gene or locus has been identified so far.

5.3.2 Brachydactyly type B (BDB; OMIM: 113000)

Brachydactyly type B (BDB) is an autosomal dominant disorder characterized by shortening or hypoplasia of distal phalanges, nail dysplasia, hypoplasia of the middle phalanges and variable degree of distal and proximal symphalangism. The thumbs are always intact but frequently show flattening or duplication of the distal phalanges. Digits towards the radial side are more severely affected as compared to those on the ulnar side. It is an autosomal dominant disorder with variable degree of expression. BDB is caused by mutations in the receptor kinase-like orphan receptor 2 gene (*ROR2*) on 9q22. Patients with distal mutations have more severe phenotype than those with proximal mutations (Schwabe *et al.*, 2000). Autosomal recessive Robinow syndrome is also caused by mutations in *ROR2*. Six different heterozygous mutations in *NOG* gene in patients with BDB2 had been described (Lehmann *et al.*, 2007). The newly identified BDB mutations did not indicate a major loss of function in contrast to previously described loss-of-function mutations in *NOG*, which are associated with abnormal joint formation but without BDB. Mutations associated with BDB are disturbing the intricate balance of *BMP* signaling. The authors argued for a functional connection between *BMP* and *ROR2* signaling and supported previous findings of a modulating effect of *ROR2* on the *BMP* receptor pathway through the formation of a heteromeric complex of the receptors at the cell surface.

5.3.3 Brachydactyly type C (BDC; OMIM: 113100)

The hand deformity is characterized by brachymesophalangy of the second, third and fifth fingers with hyperphalangy of the index and middle finger and shortening of the 1st metacarpal. The fourth finger is not affected and it is therefore the longest digit in BDC. Accompanying skeletal or non-skeletal features such as short stature, talipes valgus, hip hypoplasia and spine deformities have also been described. Heterozygous mutations in the cartilage derived morphogenetic protein-1 (*CDMP1*) also known as *GDF5* resulting in loss of function has been reported for dominant form of BDC (Polinkovsky *et al.*, 1997). A recessive form BDC is known to be caused by homozygous missense mutation located within the *CDMP1* prodomain indicating an important function of the prodomain for the folding, secretion and availability of biologically active *CDMP1* (Schwabe *et al.*, 2004). It was suggested that factors other than locus

heterogeneity, such as genetic modifiers and/or environmental factors must play a role in phenotypic variability (Galjaard *et al.*, 2001). Non penetrance in mutation carriers was also described in families with BDC (Everman *et al.*, 2002).

5.3.4 Brachydactyly type D (BDD; OMIM: 113200)

In brachydactyly type D (BDD) the distal phalanx of the thumb alone is shortened to variable degrees. It may be either unilateral or bilateral. It has been noted that the base of the distal phalanx is broader than the surface of the proximal phalanx to which it articulates. It is inherited as an autosomal dominant trait with reduced penetrance. This kind of brachydactyly is quite common particularly high prevalence was reported in Israeli Arabs and in the Japanese population (Temtam and McKusick, 1978). A mutation in *HOXD13* has been described in an individual with BDD (Johnson *et al.*, 2003).

5.3.5 Brachydactyly type E (BDE; OMIM: 113300)

Brachydactyly type E (BDE) is inherited as a dominant trait and is characterized by variable shortening of the metacarpals with more or less normal length of phalanges. Occasionally, the metatarsals are also short. This results from hypoplastic and partially fused metacarpal epiphyses, visible on radiographs. First BDE family was reported with 17 affected members in three generations confirming autosomal dominant inheritance and variable expressivity (Temtam and McKusick, 1978).

BDE is classified into at least three subtypes: E1, in which shortening is limited to fourth metacarpal or metatarsal only (Hortling *et al.*, 1960); E2, in which variable combination of metacarpals are involved, with shortening of the first and third distal and second and third middle phalanges (McKusick and Milch, 1964) and E3, which may have a variable combination of short metacarpals without phalangeal involvement.

Missense mutations in the homeodomain of *HOXD13* in two cases with distinct limb phenotype exhibiting overlap with BDD and BDE have been described (Johnson *et al.*, 2003).

5.3.6 Brachymetatarsus IV (OMIM: 113475)

Ray and Haldane (1965) described shortening of fourth metatarsi resulting in unilateral or bilateral short fourth toes in 206 persons in Northeastern India with no instance of short metacarpals which distinguishes it from BDE. It is inherited as an autosomal dominant trait with approximately 27% penetrance. No locus or gene has been identified for this form of brachydactyly.

5.3.7 Sugarman brachydactyly (OMIM: 272150)

A new form of brachydactyly was described by Sugarman *et al.* (1974) of which conspicuous feature was a non-articulating great toe which was set dorsal and proximal to the usual position. The fingers were very short and had no motion at the proximal interphalangeal joints (sympalangism). The consanguinity in the family and the presence of 7 other affected persons among the patient's relatives made autosomal recessive inheritance likely. This form of brachydactyly is extremely rare. Only one affected family reported twice by both Sugarman *et al.* (1974) and Fujimoto *et al.* (1982).

5.3.8 Kirner deformity (OMIM: 128000)

The tip of the fifth finger points toward the thenar eminence due to bowing of the distal phalanx. X-ray shows angulation of the metaphysis of the phalanx. The lesion is probably not manifested before the fifth year of age. This malformation of little finger was first described by Kirner (1927). Pedigree studies favored dominant inheritance with incomplete penetrance. Its estimated incidence was 1 in 410, with a higher prevalence in females than males (David and Burwood, 1972). No gene or locus for Kirner deformity has yet been identified.

5.3.9 Brachydactyly as a part of syndrome

The number of syndromes with brachydactyly is extensive but it will be out of scope of this thesis to discuss all those conditions.

5.4 Syndactyly

Non-syndromic syndactyly is a quite common, heterogeneous hereditary malformation involving webbing of fingers and/or toes. The webbing may be partial or complete and the fusion of digits range from cutaneous to bony. The condition can be unilateral or bilateral. Interfamilial and intra-familial variability is quite common. Phenotypic variability is also common within individuals in different limbs. The majority of syndactylies show autosomal dominant mode of inheritance, with variability in expression and penetrance. There are only two forms of autosomal recessive forms of syndactyly i.e Cenani-Lenz syndactyly and Malik-Percin type (Cenani and Lenz, 1967; Malik *et al.*, 2004). The frequency of different forms of syndactyly varies in different populations and in a Latin-American study its prevalence of 3. per 10,000 births has been suggested (Castilla *et al.*, 1980).

5.4.1 Classification of syndactylies

Syndactylies were classified into syndromic and non-syndromic forms (Robolt, 1906). Julia Bell (1953) classified nonsyndromic syndactylies more significantly by reviewing 63 families with autosomal dominant inheritance. She classified different forms according to the involvement of hands and/or feet. Temtamy and McKusick (Temtamy and McKusick, 1978) described a new classification method based on clinical features and inheritance pattern. They classified syndactyly into five distinct types (I-V) which was based on the anatomic location of the web. All the five distinct types were reported to exhibit autosomal dominant inheritance with variable expression and incomplete penetrance. Autosomal recessive syndactylies were not part of this classification. Goldstein *et al.* (1994) extended the Temtamy and McKusick classification to eight types. They added an autosomal recessive entity, the Cenani-Lenz syndactyly as type VII (Cenani and Lenz, 1967). Nine types of non syndromic syndactylies have been described in the literature.

A more recent classification system was presented in 2005 to classify nine types of non-syndromic syndactyly. This system regrouped the syndactylies according to similarities in phenotypes and inheritance into three groups. Group 1 includes syndactylies with autosomal dominant inheritance with involvement of phalanges only. Group 2 includes autosomal dominant

syndactylies with phalanges as well as metacarpals or metatarsal involvement. Whereas, group 3 includes all the recessively inherited syndactylies with involvement of all bony element in hands or feet and radial or ulnar fusion as well as syndactyly with missing fingers (Malik *et al.*, 2005a). In this thesis, different isolated syndactyly types are reviewed according to the classification made by Temtamy and McKusick (1978) and Goldstein (1994).

5.4.1.1 Syndactyly Type I (SD1; MIM 185900)

Syndactyly type I also called 'Zygodactyly' is characterized by complete or partial webbing between the 3rd and 4th fingers and invariably 2nd and 3rd toes. Fusion of the distal phalanges is also common in some cases. Zygodactyly is the most common type which accounts for the majority of isolated syndactylies (Castilla *et al.*, 1980). It is mostly segregates as an autosomal dominant trait. The gene for type I syndactyly has been localized in a large German family to chromosome 2q34-q36 (Bosse *et al.*, 2000). An Iranian family linked to the same locus on chromosome 2q34-q36 was also described (Ghadami *et al.*, 2001). Syndactyly type I is genetically heterogeneous. Second locus was identified in a large Pakistani family with zygodactyly that was mapped to a new locus on 3p21.31 by genome wide linkage analysis (Malik *et al.*, 2005b). In an unrelated German family, zygodactyly was not linked to 2q31-q36 or 3p21.31.

5.4.1.2 Syndactyly Type II, Synpolydactyly (SPD; MIM 186000)

Syndactyly Type II or Synpolydactyly is second most frequent type of syndactyly characterized by a cutaneous or bony fusion between the 3rd and 4th fingers associated with complete or partial duplication of the 4th finger in the web. In the feet duplication of last toe is common (Temtamy and McKusick, 1978). Synpolydactyly shows an autosomal dominant mode of inheritance with variable degree of expression. It shows incomplete penetrance and high degree of phenotypic variability (Malik *et al.*, 2006). The penetrance of synpolydactyly is known to be 96% (Sayli *et al.*, 1995). The more severe phenotype shows complete soft tissue syndactyly which involves both hands and feet. In the hands there is polydactyly of the preaxial, mesoaxial,

and postaxial digits, loss of the normal shape of the carpal, metacarpal, and phalangeal bones (Akarsu *et al.*, 1995). First locus for synpolydactyly designated as SPD1 was reported to chromosome 2q31 in a large Turkish family (Sarfarazi *et al.*, 1995). Polyalanine tract expansion mutations in the homeobox containing gene (*HOXD13*) have been described for SPD (Muragaki *et al.*, 1996). Later studies showed that there is a correlation between the size of expansion in the polyalanine tract and the severity of SPD (Goodman *et al.*, 1997). More recent studies represent that *HOXD13* polyalanine repeat is polymorphic, and the expansion of ≤ 6 alanine residues in the *HOXD13* polyalanine repeat is not associated with the SPD1 phenotype (Malik *et al.*, 2007). Second synpolydactyly locus was identified in a patient with complex synpolydactyly with chromosomal translocation t(12;22), disrupting the fibulin-1 gene (*FBLN1*) on chromosome 22q13.3 (Debeer *et al.*, 2002). Third locus for synpolydactyly was mapped in Pakistani family with classical SPD phenotype at chromosome 14q11.2-q12 (Malik *et al.*, 2006).

5.4.1.3 Syndactyly Type III (MIM 186100)

This form of syndactyly has bilateral complete syndactyly between the 4th and 5th fingers. Usually it is soft tissue syndactyly but occasionally the distal phalanges are fused. The 5th finger is usually short with an absent or rudimentary middle phalanx. The feet are usually normal. Type III syndactyly has been reported as a part of oculodentodigital dysplasia (ODD; MIM 16420). The family reported by Johnston and Kirby (Johnston and Kirby, 1955) was one of the largest fully described pedigrees with seven affected males and seven affected females in five generations, with an autosomal dominant inheritance. Bony fusion was observed at the terminal phalanx of the fused phalanges. A family was described with type III syndactyly and a facial phenotype resembling that of oculodentodigital dysplasia (ODD) but without any of the other characteristic ocular and dental features (Brueton *et al.*, 1990). ODD was mapped on chromosome 6q22-q24 (Gladwin *et al.*, 1997). Isolated type III syndactyly may be encoded by the same gene as ODD syndrome. Mutation in *GJAI* was found which encodes for the gap junction protein alpha 1 protein (Paznekas *et al.*, 2003).

5.4.1.4 Syndactyly Type IV, Haas Type Syndactyly (MIM 186200)

Syndactyly type IV is characterized by complete fusion, affecting the fingers of both hands (Haas *et al.*, 1940). Flexion of the fingers gives the hands a cup-shaped form (Gillesen-Kaesbach and Majewski, 1991). Polydactyly, with 6 metacarpals and 6 digits is usually common. Partial cutaneous syndactyly of 2nd and 3rd toe is common. Haas type syndactyly is a rare phenotype. Mode of inheritance is autosomal dominant with variable expressivity. 235-kb duplication in intron 5 of the *LMBR1* involving the ZPA regulatory sequence (ZRS) is identified in Chinese families with type IV syndactyly (Sun *et al.*, 2008).

5.4.1.5 Syndactyly Type V (MIM 186300)

Syndactyly type V is a rare type of syndactyly. The characteristic finding in this type of syndactyly is the presence of an associated metacarpal and metatarsal fusion. The metacarpals and metatarsals most commonly fused are the 4th and 5th or the 3rd and 4th. Soft tissue syndactyly usually affects the 3rd and 4th fingers and the 2nd and 3rd toes. This disorder was first described in 5 generations of the family from the island of Seeland (Kemp and Ravn, 1932). Later, syndactyly type V was reported in a mother and 3 of her 4 children. All had fusion of metacarpals 4 and 5. None had metatarsal fusion although other anomalies of the feet were present (Robinow *et al.*, 1982). It is a rare autosomal dominant type with only few reports published so far (Kemp and Ravn, 1932; Robinow *et al.*, 1982; Temtamy and McKusick, 1978). Kjaer *et al.* (2005) described a polyalanine expansion in the *HOXD13* in the family reported by Kemp and Ravn (1932). A missense mutation in *HOXD13* has been reported in family with syndactyly type V (Zhao *et al.*, 2007)

5.4.1.6 Syndactyly Type VI, Mitten syndactyly

Mitten syndactyly is characterized by a webbing of last four digits in both hands and feet. Only one family has been described in the literature. The inheritance was autosomal dominant with variable expression and incomplete penetrance (Temtamy and McKusick, 1978). No MIM number has yet been assigned to Syndactyly Type VI.

5.4.1.7 Syndactyly Type VII, Cenani-Lenz Syndactyly (MIM 212780)

Cenani-Lenz syndactyly is characterized by complete syndactyly of hands and feet, abnormal phalanges, carpal and metacarpal fusion, giving the hand a spoon-like appearance. Occasional mesomelic shortening of arm, radio-ulnar and metacarpal synostosis, as well as disorganized phalanges have been observed. Feet are only mildly affected (Cenani and Lenz, 1967). Cenani-Lenz is known to be segregating as an autosomal recessive trait.

5.4.1.8 Syndactyly Type VIII

Syndactyly type VIII shows unilateral or bilateral fusion of metacarpal 4th and 5th. The 5th metacarpal is usually hypoplastic and the 5th ray is consequently short. For the isolated form, two possible hereditary mechanisms have been proposed: autosomal dominant and X-linked recessive (Lonardo *et al.*, 2004). No MIM number has yet been allocated to this phenotype.

5.4.1.9 Syndactyly Type IX, Malik-Percin type syndactyly

It was first described in a consanguineous Pakistani family with nonsyndromic, autosomal recessive syndactyly with mesoaxial reduction of the fingers, synostoses of the third and fourth metacarpals with associated single phalanges, fifth finger cleinodactyly, and preaxial webbing of the first 3 toes with a hypoplastic terminal phalanx in all toes (Malik *et al.*, 2004). The authors noted the similarities between the phenotype in this family and that of the severely affected individuals of the Turkish kindred described previously (Percin *et al.*, 1998).

5.5 Syndromic hand anomalies

5.5.1 Greig cephalopolysyndactyly syndrome

Greig cephalopolysyndactyly syndrome (GCPS; OMIM: 175700) is an autosomal dominant disorder which affects limb and craniofacial development. Prominent features of GCPS in hands include postaxial polydactyly (pedunculated postminimus), syndactyly of third and fourth finger,

broad and some time duplicated thumbs. Feet phenotype include preaxial polydactyly, syndactyly particularly of the first to third toes, broad toes and occasionally postaxial polydactyly. Craniofacial abnormalities are highly variable include macrocephaly, frontal bossing, hypertelorism, broad nose bridge, occasionally associated with late closure of cranial sutures and mild degree mental retardation. GCPS was mapped to chromosome 7p13. Large number of mutations including deletions, truncations or point mutations has been described in *GLI3* for GCPS.

There are many other non syndromic limb anomalies described in the literature. Long lists of syndromic conditions have also been recognized with associated hand anomalies including different types of syndactylies, brachydactylies and polydactylies but it will be beyond the scope of this study to review all those conditions in this thesis.

5.6 Limb development

The limb bud first appears as a small protrusion from the flank of the embryo with the establishment of a special group of cells termed the “limb field”. The limb bud of embryo formed at the lateral flank by proliferation of cells from the lateral plate. Soon after, cells from the lateral edges of adjacent somites invade the limb bud to form limb muscles, nerves and blood vessels. The limb bud grows in size and individual skeletal elements are laid down in proximo-distal fashion. The growth and patterning of limb in three dimensions is controlled by different signaling centers. The growth of limb along proximo-distal axis is controlled by signal from the overlying ectodermal layer at the distal tip of limb bud known as apical ectodermal ridge (AER). Fibroblast growth factors (*Fgfs*) express in AER play vital role in outgrowth of limb. Anterioposterior patterning is controlled by zone of polarizing activity located at the posterior margin of limb bud. Morphogenetic properties of ZPA are mediated by sonic hedgehog (SHH). *SHH* act as target molecule that maintains posteriorizing signal through bone morphogenetic proteins (BMPs) and *Fgf4* (Niswander *et al.*, 1993). *SHH* positively regulates *HOXD* (5'*HOX*) gene and Gremlin (*Gre*) expression in distal mesenchyme. *Wnt7a* and *Lmx1* genes control dorsal identity of limb and ventral identity is controlled by *En1* (Parr and McMahon, 1995). Homeobox genes clusters, A and D express in developing limb bud are involved in shape and identity and patterning of skeletal elements. The specification of fore and hind limb identity is controlled by certain T-box (*Tbx*) genes (Agarwal *et al.*, 2003).

6 MATERIALS AND METHODS

6.1 Methods

Methods for blood sampling, DNA extraction protocol, PCR amplification of genomic fragments for linkage analysis using microsatellite markers, DNA sequencing and restriction analysis procedure have been described in detail under section 2.

6.1.1 Nuclear extract preparation

Caco-2 cell were used for preparation of nuclear extract (Ausubel *et al.*, 2002). Two weeks after seeding differentiated Caco-2 cells were harvested and washed with PBS and followed by centrifugation (10 min at 1500 $\times g$). The cell pellet was resuspended in a hypotonic buffer [10 M HEPES, pH 7.9; 1.5 mM $MgCl_2$; 10 mM KCl; 0.5 mM DTT; 1 μ l/ml protease inhibitor cocktail (sigma)] in a volume five times the volume of the cell pellet and centrifuged immediately for 5 min at 1500 $\times g$ to remove salt from the PBS. The cell pellet was resuspended in hypotonic buffer to a final volume of three times the volume of cell pellet and allowed to swell on ice for 10 min. The cells were then homogenized in a glass Dounce homogenizer with ten up-and-down strokes. The nuclei were pelleted by centrifugation for 15 min at 3300 $\times g$. Nuclear extract was prepared by resuspension of the nuclei pellet in half volume of low-salt buffer. High-salt buffer [20 M HEPES, pH 7.9; 0.8 M KCl; 1.5 mM $MgCl_2$; 0.2 mM EDTA; 25 % glycerol; 0.5 mM DTT; 1 ml/ml protease inhibitor cocktail (Sigma)] equal to half the volume of the nuclei pellet were added in drop wise fashion under continuous mixing. The nuclei were extracted for 30 min with continuous gentle mixing. The extracted nuclei were removed by centrifugation (30 min at 20,000 $\times g$) and the resulting supernatant (the nuclear extract) was placed in dialysis tubing and dialysed against 50 volumes of dialysis buffer (20 M HEPES, pH 7.9; 20 % glycerol; 1.5 mM $MgCl_2$; 100 mM KCl; 0.2 mM EDTA; 0.5 mM DTT) for 5 hrs. After dialysis precipitates in the extract were removed by centrifugation (20 min at 20,000 $\times g$). The nuclear extracts were aliquoted in 1.5 ml eppendorf tubes and stored at -80 °C.

6.1.2 Annealing of probes for EMSA

Annealing of probes was made using 250 pmol of each oligonucleotide, 0.1 M NaCl in 100 μ l final volume in 0.5 ml PCR tube. The contents were mixed and incubated at 95 °C for 1 min in thermal cycler and then thermal cycler was turned off to let it cool slowly to room temperature.

6.1.3 Radioactive labelling of double stranded EMSA probes

Labelling of double stranded EMSA probes (dsEMSA probe) was performed using γ -³²P ATP using 1 μ l (2.5 pmol) of annealed oligonucleotides, 1 μ l of 10X kinase buffer (forward), 6 μ l of gamma (γ -³²P) ATP, 0.5 μ l T4 polynucleotide kinase in 10 μ l final volume. The contents were mixed and incubated at 37 °C for 30 min. After incubation 20 μ l of TE buffer was added to reaction mixture and labeled probes were purified using G25 column (GE health care) according to instructions provided.

6.1.4 Electrophoretical mobility shift assay (EMSA) procedure

Approximately 5 μ g of Caco-2 nuclear extract was added to 10 ml gel-shift buffer (25 mM Tris, pH 7.8; 5 mM MgCl₂; 6 mM KCl; 0.5 mM EDTA; 1 mM DTT; 0.5 mM PMSF; 5 % Ficoll; 2.5 % glycerol). Nonspecific binding to DNA was prevented by adding 1 mg dl-dC (Boehringer Mannheim) and 2.5 pmol of a 24-mer double stranded oligonucleotide with a random sequence due to high nonnspecific binding to oligonucleotides in Caco-2 nuclear extract. After the incubation on ice for 10 min, 25 fmol of γ -³²P -labelled oligonucleotides was added and incubated for 20 min on ice. Unlabelled specific double stranded oligonucleotides were added prior to probe in some EMSAs reaction in order to analyze for the specificity of the formed DNA/protein complexes. DNA/protein complexes and unbound DNA were separated by electrophoresis on a 5% non-denaturing polyacrylamide gel in 0.5 X TBE buffer at 220 V for 2 hrs at 4 °C. Gels were dried after electrophoresis and exposed in a phosphorImager (Amersham Biosciences).

6.1.5 Genome wide linkage analysis

Families excluded from all the respective known loci, a genome wide high density SNP genotyping using Affymetrix 10K-Chip Array Version 2 (Kennedy *et al.*, 2003) was performed according to manufacturer's protocol in order to define the homozygous region harboring the underlying disease gene. This oligonucleotide microarray allows genotyping of 10,204 SNPs in a single experiment. Total genomic DNA of 250 ng was digested with restriction enzyme *Xba*I and ligated to adapters that recognize the cohesive four bp overhangs. A general primer that recognizes the adapter sequence was used to amplify the ligated fragments. PCR conditions have been optimized to preferentially amplify fragments of 250-1,000 bp range. Amplified PCR product was then fragmented, labeled and hybridized to 10K array chip. For each SNP, 40 different 25 bp oligos are tiled on the chip to increase specificity. Perfectly matching oligos are specific for each allele and mismatch oligos have one mismatch in the centre of perfect match sequence. In an optimal hybridizing conditions only perfectly matched oligos hybridize to their respective alleles. The SNP data was analyzed by the Allegro version 1.2c and easyLINKAGE plus v5.08 to find homozygous regions consistent with disease phenotype. The boundaries of homozygous regions were further specified with highly polymorphic microsatellite markers.

6.1.6 Candidate gene search

The search for candidate genes in the region was performed in the NCBI database (Homo sapiens Gene Map, Build 36) after careful consideration of the biological characteristics of genes in the critical region. Each gene in the region was reviewed in Mouse Genome Informatics (<http://www.informatics.jax.org/>) for the phenotypic spectrum of mutant/Knock out mouse model if available. For mutation detection the exons and exon-intron boundaries of the genes were PCR amplified. The PCR products were subsequently cycle sequenced using the Big Dye Terminator Ready Reaction Mix (Applied Biosystems). By Blast search at NCBI the sequencing results were compared to reference sequences at NCBI.

6.1.7 Copy number variation detection

Affymetrix Genome Wide Human SNP Array 6.0 (SNP6) was used which contains 1.8 million genetic markers which include more than 906,600 single nucleotide polymorphisms (SNPs) and more than 946,000 probes for the detection of copy number variations (CNVs). It includes 202,000 probes targeting 5,677 CNV regions from Toronto Database of genomic variants and 744,000 probes evenly spaced along the genome. It can detect ten times more copy number changes than other SNP/CN platforms.

6.2 Families studied

A total of 10 families (nine Pakistani and one from Denmark) with various limb deformities were ascertained. All the families were visited at their places and informed written consents were taken. This study was approved by local ethical committee of National Institute for Biotechnology and Genetic Engineering (NIBGE), School of Biotechnology, Quaid-I-Azam University, Pakistan and regional ethical committee in Denmark.

6.2.1 Family PD1

Family PD1 originated from Southern Punjab region of Pakistan with preaxial polydactyly and triphalangeal thumb was ascertained. Analysis of three generation pedigree (Figure 6.1) with altogether 12 phenotypically affected subjects (9 males and 3 females) suggested autosomal dominant mode of inheritance. Most of the affected individuals have preaxial triphalangeal duplication. Individual III-6 has bilateral preaxial duplication (Figure 6.2). The duplicated first digit is triphalangeal in both hands and syndactylous in right hand. There is slight flexion crease of proximal inter-phalangeal (PIP) joint in left small finger. Individuals III-3, III-5, III-11 and III-12 have unilateral preaxial duplication which is triphalangeal. Individual II-7 was affected bilaterally but in the left hand instead of duplication the thumb was flat and wide. Unfortunately X-ray was not available to find out the abnormality. Feet in all the affected individuals were normal upon examination. No other signs of dysmorphology were noticed. All the affected individuals were mentally healthy having average IQ level. Radiographic examination of three affected members demonstrated duplicated thumbs with three phalanges. Metacarpals were normal in shape and number (Figure 6.2).

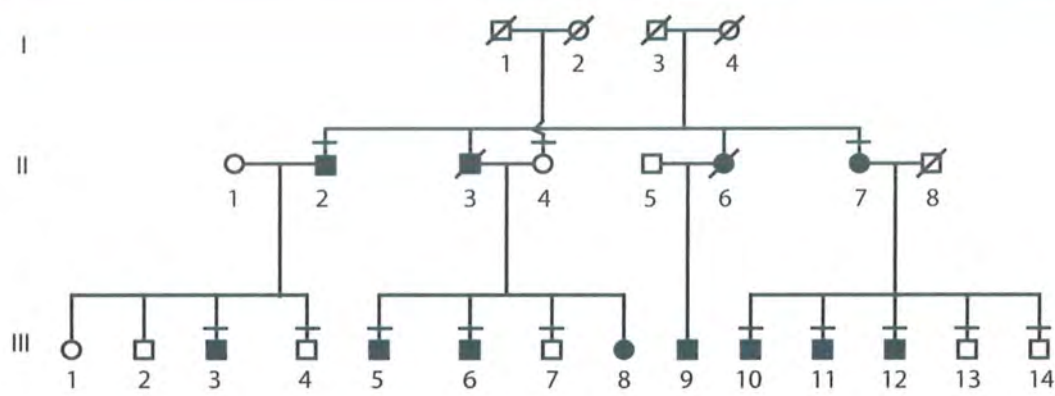


Figure 6.1: Pedigree of family PD1 with preaxial polydactyly with triphalangial thumb phenotype. Phenotypically affected individuals are shown by black filled in symbols. Clinically examined individuals are shown by straight line over the symbol.



Figure 6.2: Phenotypic appearance of affected subjects in family PD1 with preaxial polydactyly triphalangial thumb. (A & B) hands and feet of III-12; (C) clinical appearance of hands of male subject III-6; (D) radiograph of III-6 demonstrate duplicated thumbs with three phalanges.

6.2.2 Family PD2

Family PD2 exhibits digital phenotype of preaxial polydactyly type IV (PPD-IV) originated from small village of Southern Punjab province in Pakistan. A total of 12 members were affected in this family. Pedigree analysis predicted autosomal dominant mode of inheritance. Most of the affected individuals show postaxial polydactyly of hands along with partial or complete syndactyly of different digital elements. In feet almost all the affected subjects present preaxial polydactyly with variable syndactyly of 1st-4th toes. Detailed clinical phenotype of individual family members is described (Table 6.1). All the members were examined carefully for facial dismorphism which are normally present in GCPS. GCPS exhibit similar digital findings along with additional facial deformities which include macrocephaly, hypertelorism and frontal bossing.

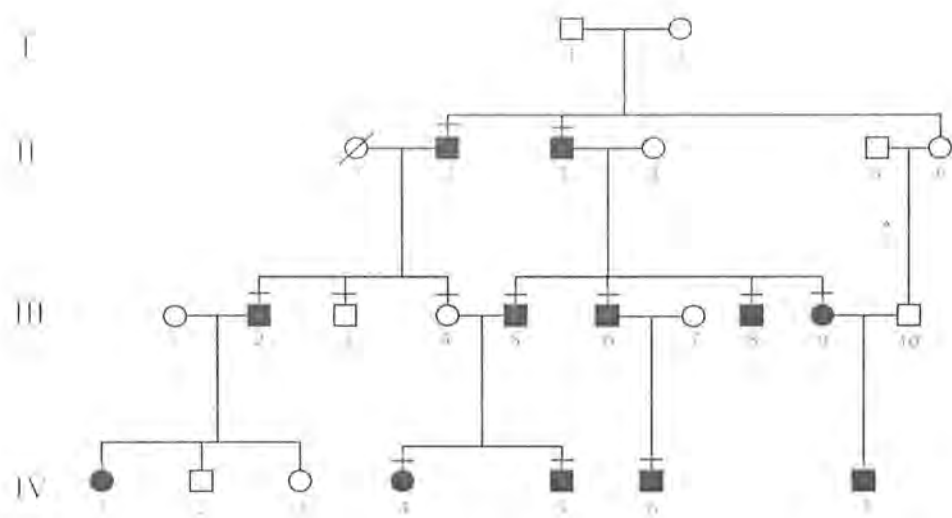


Figure 6.3: Pedigree of Family PD2. Phenotypically affected individuals are shown by black filled in symbols. Clinically examined individuals are shown by straight line over the symbol.

Table 6.1: Clinical description of family PD2.

Individual ID	Right hand	Left hand	Right foot	Left foot	Additional phenotype
II-2	Little finger valgus of distal phalanx.	Fourth distal phalanx turned anticlockwise. Little finger slightly increased length.	The hallux short and broad. 1st two toes slightly syndactyl.	The hallux was broad with a valgus of the distal phalanx. A preaxial interstitial polydactyly between the 1st and 2nd toe. Toes 1, 2 and 3 were extensively syndactyl.	HC. 54.5 cm (Normal).
III-6	Postaxial postminimus. Distal phalanx of thumb slightly hypoplastic.	Postaxial postminimus.	The hallux was broad with a valgus of the distal phalanx. A preaxial interstitial polydactyly between the 1st and 2nd toe. Toes 1,2,3 and 4 complete syndactyly.	The hallux was broad. A preaxial interstitial polydactyly between the 1st and 2nd toe. Toes 1,2,3 and 4 complete syndactyly.	HC. 53.5 cm (Normal). No facial deformity.
II-3	2nd, 3rd and 4th finger extra DIP flexion crease. Complete syndactyly of 3rd and 4th finger. 2nd and 3rd finger partially syndactyl. Little finger increased in length. Postaxial postminimus.	3rd and 4th finger extra DIP flexion crease. Complete syndactyly of 3rd and 4th finger. 50% webbing between thumb and index finger. Little finger increased in length. Postaxial postminimus.	A preaxial interstitial polydactyly between the 1st and 2nd toe. Valgus of the distal phalanx of the hallux. Complete syndactyly of first four toes.	A preaxial interstitial polydactyly between the 1st and 2nd toe. Valgus of the distal phalanx of the hallux. Complete syndactyly of first four toes	HC. 53.5 cm (Normal). No facial deformities observed
III-5	2nd and 3rd finger slightly syndactyl. Little finger extra PIP flexion crease.	3rd, 4th and 5th fingers are completely syndactyl. Distal phalanges fused. Postaxial postminimus.	The hallux was broad. 1st and 2nd toe syndactyl.	1st, 2nd and 3rd toe syndactyl.	HC normal.
IV-5	3rd and 4th digit complete syndactyly. Little finger slightly increased length. Postaxial postminimus removed surgically.	3rd, 4th and 5th digit complete syndactyly. Little finger increased length. Postaxial postminimus removed surgically.	Hallux broad and short. 1st, 2nd and 3rd toes syndactyl.	Hallux broad and short. 1st and 2nd toes syndactyl.	HC normal. No facial deformity.



Figure 6.4: Phenotypic appearance of affected subjects in Family PD2. (A, B & C) Photographs of face, hands and feet of subject III-6. Mild hypertelorism, bilateral postaxial postminimus, short distal phalanx of left thumb and syndactyly of first four toes with preaxial duplication; (D, E & F) face, left foot and hands of subject II-3. Postaxial postminimus, complete bilateral syndactyly of third and fourth digit, and partial syndactyly between thumb and index finger. In foot, syndactyly of first four toes with preaxial duplication; (G, H & I) face, hands and feet of subject II-2. Only feet are involved, duplicated great toe with syndactyly of 1st 2nd and 3rd toe in right foot.



Figure 6.5: Photographs and radiographs of hands and feet of IV-5. (A) present complete syndactyly of last three digits in right hand and 3rd and 4th digit in left hand, (B) radiographs of hands of IV-5 indicated synostosis of distal phalanges of 4th and 5th finger and middle phalanx of 4th digit, (C& D) shows bilateral incomplete syndactyly of 1st and 2nd toe. Duplicated rudimentary distal phalanx of 1st toe is indicated by arrows, (E) photograph of face of individual IV-5.

6.2.3 Family PD316

Family PD316 originated from Denmark has total of 20 subjects including 6 affected individuals. Phenotypes of affected subjects are described (Table 6.2). Unfortunately, photographs and radiographs of affected individuals are not available for presentation.

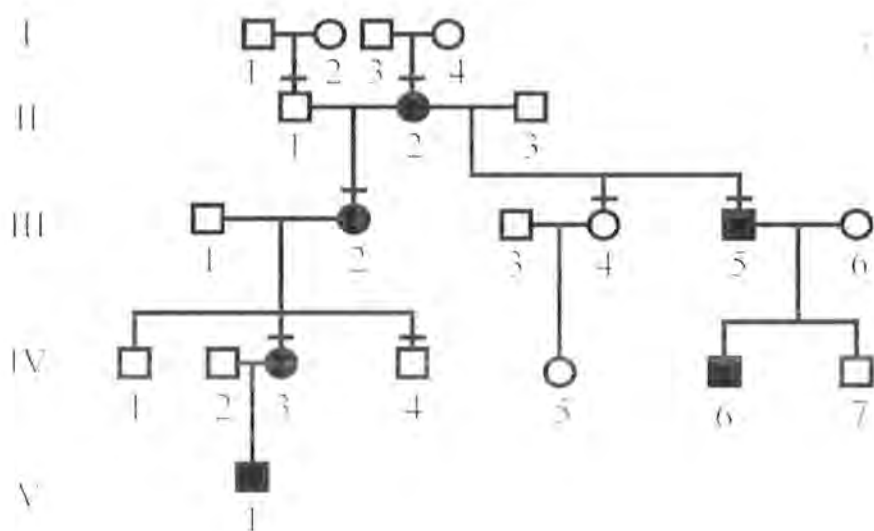


Figure 6.6: Pedigree of family PD316. Phenotypically affected individuals are shown by black filled in symbols. Clinically examined individuals are shown by straight line over the symbol.

Table 6.2: Clinical description of family PD316

Individual ID	Right hand	Left hand	Right foot	Left foot	Additional phenotype
II-2	Four finger flexion crease Thumb short, broad with radial deviation of the distal phalanx	Mild generalized brachydactyly of 3rd finger preaxial duplication with the first finger appearing short and broad with a mild radial deviation of the distal phalanx A postaxial postminimus 5th PIP joint camptodactyly	Preaxial interstitial polydactyly between toes 1 and 2 syndactyl web occurred involving toes 1, 2 and 3	Preaxial interstitial polydactyly between toes 1 and 2 The hallux appeared broad Toes 2, 3 and 4 were syndactyl	None
III-2	First finger appeared slightly broad with normal length 5th PIP joint camptodactyly	First finger appeared slightly broad with normal length. Fingers 2 to 5 were shorter than normal	Preaxial interstitial polydactyly between the 1st and 2nd toe Hallux slightly hypoplastic.	Preaxial interstitial polydactyly between the 1st and 2nd toe The hallux appeared hypoplastic with a hypoplastic 1st metatarsal.	None
III-5	First finger short and broad with a radial deviation of the distal phalanx Fingers 2 to 5 appeared short Index finger extra PIP flexion crease Fingers 3, 4 and 5 were syndactyl (25%) 5th finger flexion crease was lacking Postaxial postminimus had been removed earlier	First finger was short and broad with a radial deviation of the distal phalanx A preaxial interstitial Y-shaped duplication Index finger PIP flexion crease Fingers 2 and 3, 3 and 4, and 4 and 5 were syndactyl On the 5th finger only one proximal flexion crease was seen Postaxial postminimus had been removed.	The hallux appeared broad with a valgus of the distal phalanx. A preaxial interstitial duplication had been removed between the 1st and 2nd toe. Toes 2 and 3, 3 and 4, and 4 and 5 were syndactyl (90, 50 and 10%, respectively)	The hallux was broad with a preaxial interstitial polydactyly between the 1st and 2nd toe. Toes 2 and 3 were extensively syndactyl. Toes 4 and 5 were syndactyl too (50%).	None
III-4 Normal	Normal	Normal	Normal	Normal	Normal

6.2.4 Family PD7

Family PD7 presented Greig cephalopolysyndactyly syndrome (GCPS; MIM175700) originated from a small village in central region of Punjab province. The phenotype presented autosomal dominant mode of inheritance. Four affected members were examined clinically. Photographs and radiographs were taken to record the phenotype. The proband IV-6 has PAPA of left hand and right hand has PAPB while feet have bilateral duplication of 4th toe with well formed metatarsals. The last toes are disproportionally longer. In addition, he also has soft tissue syndactyly of 2nd and 3rd toe of right foot. Proband IV-6 presented facial dismorphism with macrocephaly and mild hypertelorism. Head circumference (HC) of proband was 57.5 cm at 5 years of age which approximately ≥ 4 SD as compared to population age and sex mean. There was a considerable phenotypic variability observed among the affected family members. Brother IV-5 of proband has PAPB of left hand and left foot only. He has a normal HC. Father of proband has bilateral PAPA of hands and feet. He has HC of 59.5 cm, approximately ≥ 2.5 SD. All the affected members have normal IQ level. The phenotypes of affected subjects are shown (Figure 6.8).

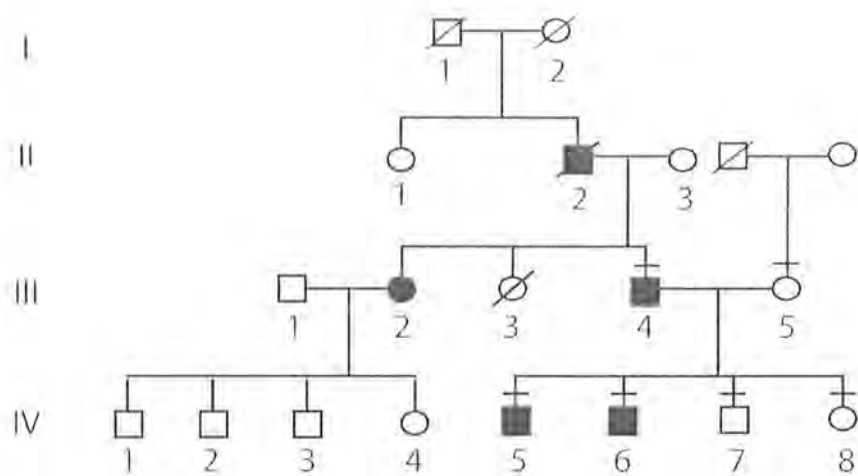


Figure 6.7: Pedigree of Family PD7 with Greig cephalopolysyndactyly syndrome. Phenotypically affected individuals are shown by black filled in symbols. Clinically examined individuals are shown by straight line over the symbol.



Figure 6.8: Phenotypic appearance of affected subjects in family PD7. (A, B, C, D & E) present face feet and hands of proband IV-6, facial dismorphism and bilateral PAPA/B, (F, G, H & I) present hands and feet of III-4 with bilateral PAPA.

6.2.5 Family PD16

PD16 family was identified in a district in Southern region of Punjab province. In this pedigree all the affected members have bilateral PAP-B of hands (Figure 6.10). Feet of all affected members were normal. The mode of inheritance was autosomal dominant. No other clinical abnormality was observed in this family. Blood samples from three affected and two normal subjects were available for molecular investigations.

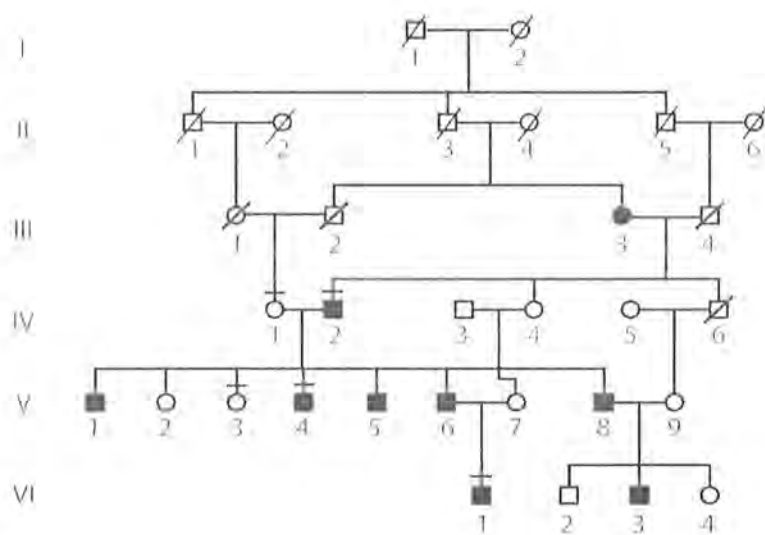


Figure 6.9: Pedigree of family PD16 with PAPB. Phenotypically affected individuals are shown by black filled in symbols. Clinically examined individuals are shown by straight line over the symbol.



Figure 6.10: Phenotypic appearance of affected subject in family PD16 with PAPB. (A) Hands of subject IV-2, and (B) hand of individual V-4, site of PAPB (removed surgically) is indicated by arrow.

6.2.7 Family BD1

Family BD1 originated from Multan region in Southern Punjab exhibit brachydactyly type E phenotype. The pedigree was constructed to infer the mode of inheritance after careful clinical examination of family members (Figure 6.11). An autosomal recessive inheritance is most likely. Pedigree includes nine affected individuals of which eight (V-3, VI-2, VI-4, VI-5, VI-6, VI-7, VI-8, VI-9) were examined physically. Seven phenotypically normal individuals were also examined and their blood was collected for further molecular analysis. Photographs of all the affected and normal individuals were obtained while X-rays of two affected and three normal subjects including two normal parents (V-5, V-6, and VI-3) were obtained for detailed clinical analysis.

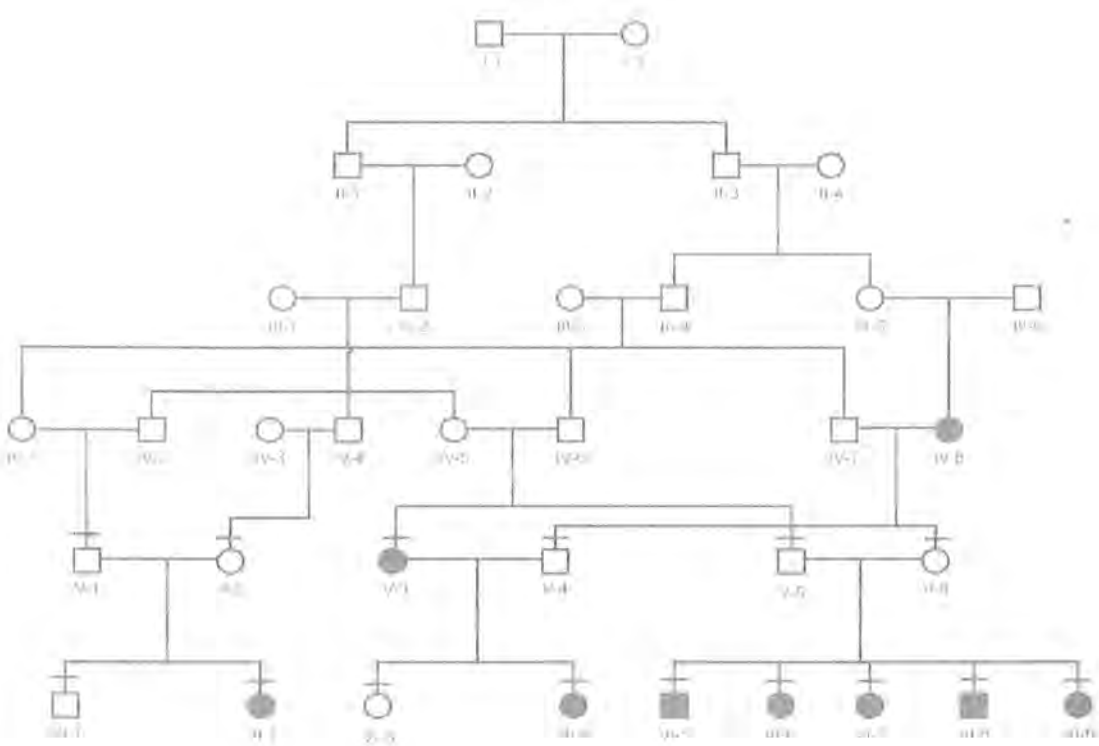


Figure 6.11: Pedigree of family BD1 with brachydactyly type E with autosomal recessive mode of inheritance. Solid symbols represent affected subjects, while the open symbols represent normal individuals. Clinically examined individuals are shown by horizontal bar over the symbol.

6.2.7.1 Clinical description

The proband IV-9 aged 25 at the time of examination has shortening of 3rd and 4th digit in both hands while in feet 3rd and 4th toes are markedly short bilaterally. X-rays examination of both hands and feet revealed bilateral shortening of 3rd and 4th metacarpal and metatarsal. Middle phalanx of 3rd and 4th toe is also hypoplastic. The distal heads of shortened metacarpals are relatively hypertrophic than normal. The proximal heads of 3rd and 4th proximal phalanges show mild hypertrophy. Rest of the phalanges in both hands and feet are normal in shape and length (Figure 6.12). Radiographic examination of both parents of proband demonstrated altogether normal hands and feet with no obvious reduction of metacarpals or metatarsal except for father (V-5) who displayed mild shortening of right 4th metacarpal bone. Father (V-5) of proband displayed a milder phenotype. X-rays examination showed a mild shortening of 3rd and 4th metatarsal of right foot.

Brother (IV-5) of proband showed feet involvement only whereas both of the hands were normal upon examination. Radiographic examination of feet demonstrates bilateral shortening of 4th metatarsal (Figure 6.12). Individual IV-6 is affected bilaterally and both hands and feet are involved. Shortening of 4th metacarpal and metatarsal of both hands and feet are evident. However, 3rd metacarpals and metatarsals were normal in contrast to proband. Second sister (VI-6) of proband is affected bilaterally. Only 3rd metacarpal of both hands was reduced in length. The feet phenotype is not identical to other affected subjects. There was shortening of 3rd metatarsal in right foot and in left foot 4th metatarsal was short.

Affected subject IV-2 was born from normal parents with no obvious signs of brachydactyly. She displayed short 4th metatarsal bilaterally. Hands of IV-2 were normal. In individual IV-4 only feet are involved with brachydactyly of 4th metatarsals. Subject IV-4 born from consanguineous parents and mother showed mild shortening of 3rd metatarsal of left foot.

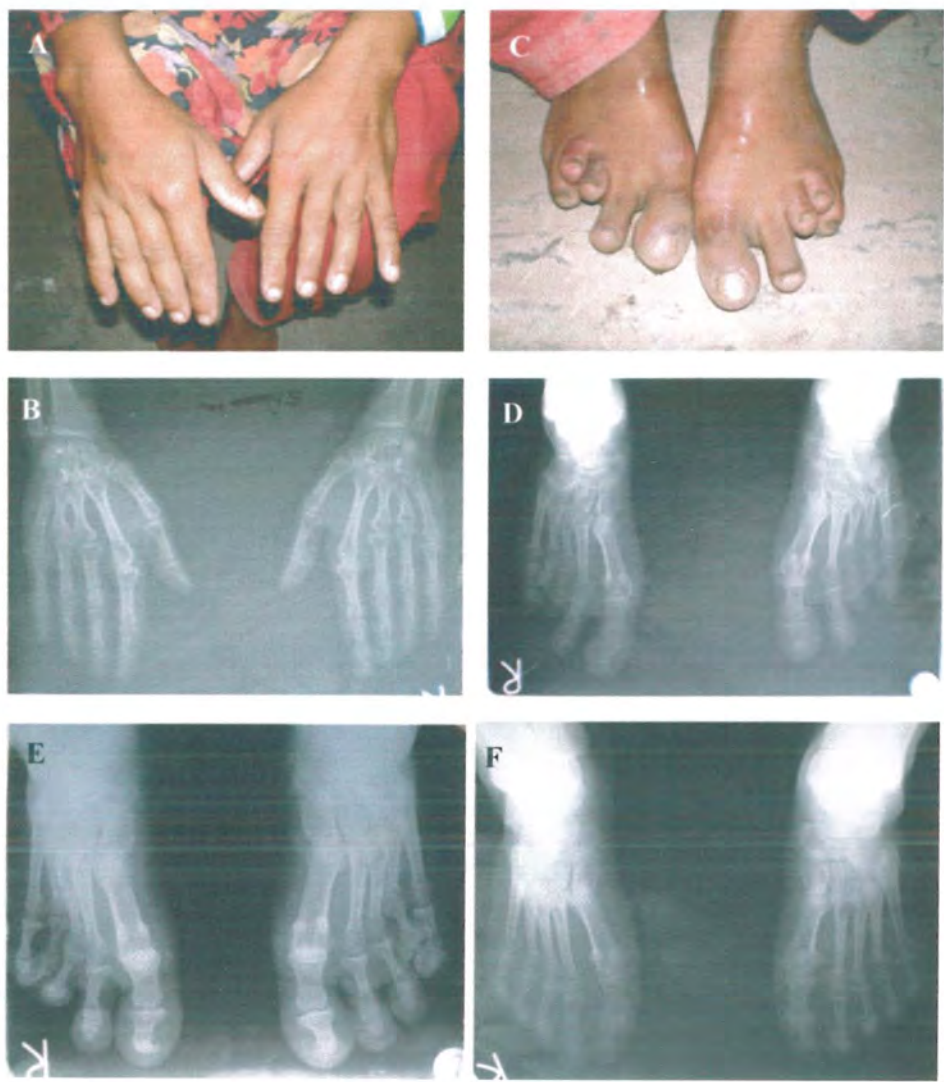


Figure 6.12: Clinical appearance of the proband in BD1 family with brachydactyly type E. (A & B) Hands of proband showing shortening of 3rd and 4th metacarpals in both hands. (C and D) Feet represent bilateral shortening of 3rd and 4th metatarsal. (E) Feet of IV-5 bilateral shortening of 4th metatarsal. (F) Feet of V-5 with mild hypoplasia of right 3rd and 4th metatarsal.

6.2.8 Syndactyly families

In this study we ascertained five families with non syndromic syndactyly from different regions in Punjab province in Pakistan. Families were indentified and approached during field sampling trips. All the families were visited at their homes and informed consent was obtained from each family before start of study. Detailed family information was collected to construct the pedigrees in each case to assemble information about normal and affected individuals and to find out the possible mode of inheritance. One family was presenting autosomal recessive mode of inheritance while rest of the families showed autosomal dominant inheritance pattern. In this thesis molecular analysis of a single family with recessive inheritance is presented. To exclude chances of error in pedigrees, information was crosschecked by interviewing different members in each family. Photographs and radiographs of affected as well normal individuals were also obtained for clinical investigations. Detailed clinical information was collected to find out phenotypic variability among affected subjects including involvement of different limbs and severity of the condition. For extraction of genomic DNA extraction blood samples from normal and affected subjects were taken in EDTA vessels for further analysis to find out the molecular basis of malformations.

6.2.8.1 Family PD14A

Family PD14A originated from Multan region in Southern Punjab. Three affected subjects (two females and one male) born from phenotypically normal parents. Presence of consanguinity and normal parents suggested an autosomal recessive pattern of inheritance. Proband V-4 of aged 22 presented bilateral complete soft tissue syndactyly of 3rd and 4th digits of upper limb. In the right hand partial webbing of 4th and 5th finger is evident. Small finger of both hands slightly reduced in length. Both feet presented normal phenotype except for slight reduction of 4th ray. No other dysmorphic features were noticed during examination (Figure 6.14, A, B).

Bother V-3 of proband has complete soft tissue syndactyly of 3rd and 4th finger in left hand, whereas in right hand webbing cover only 1/3 of interdigital space. Distal phalanx of last finger is curved medially in both hands (Figure 6.14, C). Both feet are normal.

Sister V-1 of proband has complete syndactyly of 3rd and 4th digit in left hand only (Figure 6.14, E). Little finger is also curved medially. Feet are normal.

Seven normal subjects (III-1, III-2, IV-1, IV-2, IV-3, V-2, and V-5) were examined carefully for any kind of malformation of hands or feet and found to be phenotypically normal. Blood samples from three affected and seven normal subjects were collected for further analysis.

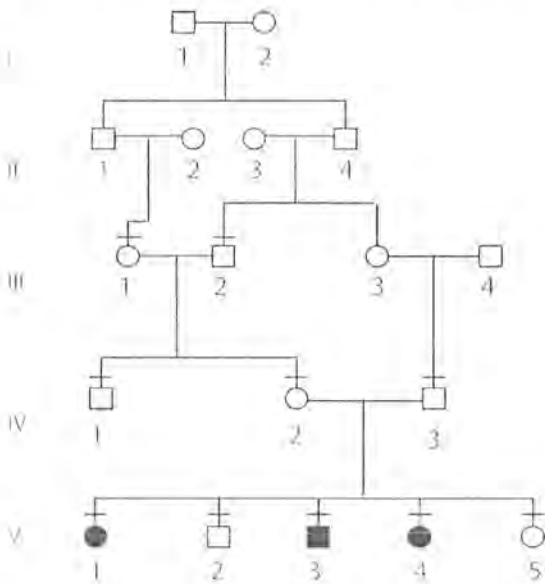


Figure 6.13: Pedigree of family PD14A with autosomal recessive syndactyly of 3rd and 4th finger.



Figure 6.14: Phenotype appearance of affected subjects in family PD14A. (A, B) hands and feet of proband V-4, (C, D) hands and feet of subject V-3, (E) left hands of V-1.

Table 6.3: List of microsatellite markers used for linkage studies.

Candidate Gene	Phenotype	Locus	Markers	Position cM
<i>LMBR1</i>	PPD2	7q36	D7S550 D7S559 D7S2423	178.41 181.97 181.97
<i>GLI3</i>	PAPA1,PAPB, GCPS, PPD-IV	7p13	D7S2548 D7S671 D7S691 D7S2428	61.53 62.87 63.67 65.55
<i>HOXD13</i>	SPD1, BDE	2q31	D2S1238 D2S2307 D2S2314 D2S1244	177.53 180.79 182.24 182.56
<i>FBLN1</i>	SPD2	22q13.31	D22S1141 D22S444 D22S1170	52.61 51.54 55.26
<i>Unknown</i>	SPD3	14q11.2-q12	D14S990 D14S581 D14S264 D14S1431 D14S608 D14S262 D14S54 D14S1040 D14S1034 D14S121	14.60 21.51 22.66 27.01 28.01 28.01 31.75 31.75 31.75 34.43
<i>GJA1</i>	Syndactyly typ III, ODD syndrome	6q22.31	D6S1037 D6S1712	122.51 122.51
<i>Unkown</i>	SD1	2q34-q36	D2S143 D2S2382 D2S301 D2S1371 D2S2249 D2S173 D2S163 D2S344	210.43 213.49 214.71 215.25 215.78 215.78 218.45 219.52
<i>Unkown</i>	ZD1	3p21.31	D3S2409 D3S3629 D3S2456	70.61 70.61 70.61

Table 6.4: Primer pairs used to PCR amplify and subsequent sequencing of *GLI3* exons.

Exon	Forward (5'→3')	Reverse (5'→3')	Product size (bp)
1	cttttcacccccgtgagtag	tgacagccatttcactcca	664
2	cctgtggagaagtgtcatcc	aggttgagtgccaaaatagaga	496
3	ccagccctgtagctctcaaa	aaaaagaatgggaaagaagtaggg	579
4	gccttctcaggtaggtgcag	cttcagtgaacccacgaaca	483
5	cgatgctctgcctgcattat	accactgccaatgaggtgtt	575
6	tggaagtaagagcacaatttgagt	gggtctcaggatgtccaat	498
7	aagcccttgaagacaaaata	taatctggggcccaataact	586
8	aggtctgcgtgtatgtgtgc	cacgtccacaaaaactgaag	596
9	gccgcatgaacgtattttct	ttagtcactccatatctagccttttg	485
10	tgcacagatatgattttattgtttga	cgtaggctccgagttttctt	456
11	aagcatgcatacacagttagcaa	accgaggcatttatcaccag	498
12	catctgaatcccaataaatgcag	agtcccacctaggaagctcaa	496
13	gaggtatctgaacacctcaaagc	ctgagctgatcgacttcacg	600
14	ccagcttcattcaccagaa	gtttttaaaatatggacaatcccaaa	653
15a	gcctgggacaccagaaatagt	ctcctcggggcatgaact	624
15b	cctcaaggccaagtacgc	ctcgtaccctgcttggttct	544
15c	gagaacgtcaccttgagtc	ggctgcctgttgagacagtt	575
15d	gagcacttgatgtccacaa	ttgtgtcactgagctgtcctg	559
15e	tcaagcttggcagttgtcag	gctagggaggtcagcaaaga	587
15f	cctgagcccaagtatcattca	tggtcacaagcacaccaact	588

Table 6.5: Primer pairs used to PCR amplify and subsequent sequencing of *HOXD13* exons.

Exon	Forward (5'→3')	Reverse (5'→3')	Product size (bp)	Annealing Temp (°C)
1a	atgagccgcgccgggagctgggac	cgaggcgtgcggcgatgacttgagcgc	474	63
1b	ggctactacagctgccgtatgtcgacg	tgtcgggcccttttccatcgcccc	411	63
2	taggtgctccgaatatccc	gtggccaacctggaccac	323	63

Table 6.6: Primer pairs used to PCR amplify and subsequent sequencing of *TFAP2A* exons.

Exon	Forward (5'→3')	Reverse (5'→3')	Product size (bp)
1a	ctggagctgatggcaagatt	gcccgttttctctgtcttc	477
1b	cggcagatttgtgtactgg	cctctctctgcagcttctcc	599
1c	ccttctccctccctcttt	gcgtgttccttaatccgtgt	561
1d	tcgatttccaggcattcttc	gatgcaaatggagagggtgt	649
2	tttctgaaaagaacttagagctga	aggggagctccagaaaccatt	805
3	gggtgtgcagtgaaacctct	gcattgctgttctgtgccta	393
4	cgaggaagggaagtagcaga	ccacttggtctacgctctt	556
5	tccctctttaaatgtcttgg	aattccattcacatctggctat	398
6	tgcattccaccagatcctaca	cccaagaatcccacctgtatt	497
7a	ctgaaagggtggctggatctc	gcagcagcagcagtagca	587
7b	gcagtgacaaagaggagaagc	ttgtcatcatcttttggtttt	552
7c	tcaacaacagcaacaacaaca	caaaatctttccagggtcca	686
7d	ggtgacaaacagctggacaa	ttcagctgcttattgcaagg	600
7e	catagtcctttgttggccaga	cctctgagacaaattccaaagc	586

Table 6.7: Primer pairs used to PCR amplify and subsequent sequencing of *JARID2* exons.

Exon	Forward (5'→3')	Reverse (5'→3')	Product size (bp)
3	cattcaaaagggatgtgtgc	tcaagagattgggtgaatgg	392
4	aggaagagtttgcttgaaatagg	gaaaaatgaacatggcagagag	397
5	ggcagtagagatcagttgctttg	gaacgagctttgccttcac	399
6	gttcctcgcctaacacatgg	tcacctcctgcttcttgagc	475
7a	actacaggctgctggctctg	gtgtgcctcttcagctcc	562
7b	ggftgaacccaaagtcatgc	tcacgttgagcttgacac	577
7c	gacgagatccccgcctc	gaagcggaaactggagcttc	396
8a	ctgtcagagtcctggctcatag	ccacctccttgagcttg	500
8b	aaggccacacagagaacgac	acccaggggaatcagagaac	346
9	gaatacaaggtggcccacag	aacacagaggacgaactcagc	357
10,11	tctgttctgaggggtgtgtg	ccggcagtgcttagaagg	493
12	ctggctttgagtcctcttc	aggcctgaacacagagaagc	371
13	gagcagagcctctcgtgtg	ttttgctgtgtccctatgc	325
14	tcactcttgaccagtgacg	ttcaaagacatattccaaagggaac	499
15a	aattcaagatttagaaattcagacagc	ccagcagaggggacacac	383
16	agcaggcctcacttctgac	agagcggcctccctcttc	399
17	atttcagcatttcagtc	ctgcagagccctgactacc	399
18a	tgttggttggtgtggtgaag	tcagccatggggcaatac	585
18b	caagctgtctttgcactagctc	tcgtcgtctttctcttcttc	599
18c	gaaggcggacgttgttc	caccgagaaaaaggctcaag	596
18d	atgcatttgcgttcatttg	acagcaaggccatagaaacc	557
18e	actgccaggaacgtcctatg	ggccacatggaaaccattag	491

Table 6.8: Primer pairs used to PCR amplify and subsequent sequencing of *DTNBPI* exons.

Exon	Forward (5'→3')	Reverse (5'→3')	Product size (bp)
1	aaaacgagaaggcctggtg	acaggacggaccctggac	479
2	aggattgaggctgcagtgag	cagatgcactcaacaaatctaagg	299
3	atctctggggcaaaatgatg	aaataattccaatcactgcattaag	390
4	tttacatcaccatggactcagg	ggtgctttattcagggagtttc	483
5	attggaggtttctgcactg	tcattttctgtggaatcctcaac	499
6	gcaaaacaatctcaacaatgtg	tgttgaaacctttgtctttatcag	350
7	ttggtttaggctcattgtactg	ccacctgtgattaagcaaac	356
8	ccagcccagtctgtaaacg	aacagaacggaacttctgagg	395
9a	ttgaaggaagcttaggaaatgc	tctcaactcacaaagttaccg	500
9b	aacccacggttccacac	ctacagatggctgaggtgctg	500
9c	agcaaafatgggctgaggtg	aatagaggcccaaaggcaag	524
10	cctggaacaaaaaccacacc	ggacatgtgtattfagaagccttg	583

Table 6.9: Primer pairs used to PCR amplify and subsequent sequencing of *GMPR* exons.

Exon	Forward (5'→3')	Reverse (5'→3')	Product size (bp)
1	gtacacctgagggggaagg	cgccccagtcctcaaacac	495
2	gagaatccagggacctttgtc	aatgacccaaagcagctcac	363
3	gtttggttttggtgcttagg	caatggcacagggctagag	372
4	cctctgctgttgcattgtgc	agcggctacctatcctttcc	495
5	tggctccagggtatgaaattctg	ccccgagaagctcaattatg	392
6	cacagagggtcacctggtc	agcagggcctctgtttctg	377
7	ttctgaccacagaggaagc	acctccaggagaccagaac	395
8	aggtccagcctttctcttgac	caccaaacactgctgctctg	500
9a	gaggggtggggctctggttttc	gaagcctccaggcagcag	460
9b	agctaaccctggggacaaag	gccccctctaaggtagcttg	497

Table 6.10: Primer pairs used to PCR amplify and subsequent sequencing of *MYLIP* exons.

Exon	Forward (5'→3')	Reverse (5'→3')	Product size (bp)
1	gcc gctattggctgatcg	cttcttcgggaaagtgtg	743
2	ccgtggaactttgttttcc	atggaactccgcatcaaac	455
3	tgtgacttttaaaattgccttcc	gtgcctcgaacatcagagag	431
4	ttcgctaaatacatgaaacatcag	cattcctaagagctgactgtcg	457
5	gaagcgtctgatttttctgc	attctgtactagactcattgacacaac	391
6a	ccagacgtaaaactggaaggac	cttccttcagcttgcgtagc	471
6b	acaaccagagcccttcacac	ggcaatgccttttaggtcac	381
7a	aacctgtgagacggcaaag	tttgctatgttgccacttc	571
7b	aactccagtcatgggaccag	ggcctgtggggtagggatag	494
7c	atgattggaaggcaaacagg	aaccaaacccttcgaaac	559
7d	tgggtgtgctttgcttgaac	tcccgaatataaaagacagagtcc	563
7e	tgtttcttgcacagacattttg	agaagtttctctgaattgtagagcac	349

Table 6.11: Primer pairs used to PCR amplify and subsequent sequencing of *ATXN1* exons.

Exon	Forward (5'→3')	Reverse (5'→3')	Product size (bp)
4	gcagtgagatggcttcatcc	acgettgaagaagaagttctgg	369
5	cttgctgtgtgcatgtg	acacccccaccactatcttg	334
6	cagccaaataatcacgcac	ggaccacgtgatgaggagag	395
7	gggaaaagagcaagaacattg	tgctaataccccttcaacacc	395
8a	tgatgtcctttccctccttc	gagtagtcagccctgtgg	496
8b	acacaaggctgagcagcag	gttgggcaggaccatcac	586
8c	gaggagaaggccctacc	tggaaatgtggacgtactgg	676
8d	tcaccgtacgagtcag	aggcactgcagcaactg	499
8e	agcaagcaatcacctacgc	cttgccaggagatgatgatg	580
9a	ccattcagcctgtgtgtgc	cgaccacctctcttctctc	532
9b	gctctctgagaatggcgaaac	cgggacttttctctgacac	586
9c	ttccacgagtgctgtcagtg	cacaacacctggtgacatc	594
9d	cagatggcagatttggaag	ccaagatgcttgtaataaagtg	598
9e	ttcagattccagtgtagcatgag	tcagtcccccaaaccttcc	559
9f	agaaccttgcgatttgac	cactttaagatgcattcaaaacc	500
9g	tcaaatcgagatttaattgttgg	ataattgcaagtgccctgag	559
9h	gtgggctcattcttcagtc	ctccctctggctccttc	568
9i	tgtcccatttcattctcttc	aagagaaagctgccacaagg	596
9j	gggggtctgttccttgagac	gtgtggcccagacaaactg	593
9k	gaaattagtcagggcgaaaag	tccacaagatgcaggaaatc	588
9l	gactctgcggaacctttcac	tcacctggtgcaaatgaag	584
9m	tatgggtgaggaagcagagc	tttcttcagcttctcaaatcagg	588
9n	actccaaacaacttgacaccc	tgaagaaaaagaagttgcaatgg	599
9o	gaggggaactcggattctg	catggggacatgaaaaactg	593
9p	agcacccccacttacaattc	aaaggatttaccctactctg	567
9q	ctcaagctgtgtcttcagagc	aaagttctctgtcacataaaagc	564
9r	tgacatggccagtacagagg	ctccctacctccgacctacc	574

Table 6.12: Primer pairs used to PCR amplify and subsequent sequencing of *FREMI* exons.

Exon	Forward (5'→3')	Reverse (5'→3')	Product size (bp)
1	ggaccaaccagcagaag	tcttcagatgcttgcatt	548
2a	gctgaactcataggctggttg	gggtgatgctgatgaaggtg	469
2b	tccaggaggaagcacagaag	ttgcaagtcaccatttcaa	466
3	atgggggtagggtagaggtg	aggcctccagttctgttga	400
4	gagaggctgggagtagagca	ctgacactgttcagccagcta	580
5	gttctctgaggcagtgaagg	cagttttaccccaaaagca	429
6	ccccaggtgattccaatatg	tgaggcaatgaatgtacaaagg	573
7	gagatgtgggaactgcagaa	aacaacaaaagctactatgtgatgc	398
8	ctgcaaagggcataaactc	tgggcccaagagatgcta	347
9	ggctgcacactttccttagc	gcacaaccttgacagatca	660
10	aatgcagattccttgggtaca	ttttgttaatcgattgttttcaa	400
11	gctcctgaatcatttgacagaa	cctgaccaatggagcaagtaa	451
12	agagcaccaatttcttctca	gatgccacacacttaattggaaa	366
13	tgggtggcatttacagtgttca	ctccctctccttgcctttt	448
14	tcttgaaaaattagtttgcattgga	ttcaactgacctgttgagtg	472
15	tgctgggtttttgtgtgtg	tagacttcccagcctccaga	371
16	ggctgttgtttcatgtgtctg	gctgcttctgttttaattggaa	500
17	tgggttttacatttatattccaca	aacagatttgggtttccaca	497
18	tttctgctggctttctgttctc	tcataaatataaggaagggagtc	500
19	tgttgatgggttgctgttgt	acatagccttcccactcct	493
20	gcaatttcttttaggactcatcc	ccctcagcctctagtaaccatc	500
21	tgcactgataaatgaactcttgc	tgcactaaagggttctcatgc	424
22	gagcctgtttcattctctca	tgttgaatttaccatgttga	496
23	aaaatcaggtaaagtggcaaaaa	aaggaaagaaggaggaggaaa	448
24	cgtattaattttgattttgcacag	tgcaccagagctgaaaaatg	587
25	tgcaagatctgcccttgatt	tgaagtgaagcaagatcacg	698
26	gaatccaaaacgtgggacag	ggctcagcttcaaaccctct	480
27	agctcgtgcatttgagttt	tccatgagcttgtgaaatgg	452
28	ccatcactggtgtaggttgat	caaggaggtttgtgcttaga	400
29	aaaatgcatgttgcttgat	ggatggctccctgaggagt	379
30	cccttgcatactgcagctta	ggaggaaaaccacatgaagc	580
31	tgggtgggaaaaccatccat	gcataactgtgcaaggaacca	500
32	tgggcgtgggaaatctta	ctctgaacaccaagcctct	323
33	caaatcctcttattcttttgccttg	ggaagcatttgtgtgggtaa	400
34	cacaaatgcttcccaacaaa	ttttcctcttgcccttcaa	373
35	ggctgactccctttgtggta	actccctcagggctcctaaa	388
36	ccccaccctgcagatactt	tggctagatctattggtgccta	396
37	ttagaacctgggcccacac	tcattagaggtaacgggaccaa	681

Table 6.13: Primer pairs used to PCR amplify and subsequent sequencing of putative regulatory regions.

Physical position (bp) on chromosome 6	Forward (5'→3')	Reverse (5'→3')	Product size (bp)
16095610-16096143	tcacacaagctgctggttc	cgtgtttgatggggcttc	534
16100045-16100638	tcacaccagcttgattgg	gctcctttctaaagagctccag	594
16192811-16193271	gactatttggacattttgctttc	cagtgactggccagagtaattc	461
16188059-16188649	tgctctttaaggctggcatag	aaagtggagtccaaaactcaaac	591
16188516-16188984	tcaggtgcctgtatactgctg	tttgctgggcaaattaaaag	469
16215139-16215648	gccgtaagccagcttttc	attgtacagcaggtaaatgatacac	510
16232250-16232786	tccaagtattctgcaatgaacag	actgggtctgatctggatgg	537
16115566-16116180	tgcatcaacatgcaaaagatg	aaatgacagcagattcagaggag	615
16166935-16167457	acctgtgttccttccaatcg	aacattttccagctcacgttg	523
16149031-16149515	cctgaagagggtccgagagg	tgcttattgagtgcgaggaac	485

Table 6.14: Primer pairs used to PCR amplify and sequencing of sonic hedgehog (*SHH*) regulatory element (ZRS) in intron5 of *LMBR1*.

Physical position	Forward (5'→3')	Reverse (5'→3')	Product size
Chr7:156276898-156277541	cctctggccagtggttaaatg	gggggaaaaagtcacatctggt	644bp
Chr7:156276475-156277103	ggtggaagcgaagagttctg	caattgggggattgtagagg	629bp

Wild type: TCAGGCCTCCATCTTAAAGAGACACAGAG
 ATAGTCCGGAGGTAGAATTTCTCTGTGTG

Mutant: TCAGGCCTCCATCGTAAAGAGACACAGAG
 ATAGTCCGGAGGTAGCATTTCTCTGTGTG

Figure 6.15: Sequences of double stranded oligonucleotide probes used for EMSAs.

7 RESULTS AND DISCUSSION

7.1 Family PD1

7.1.1 Linkage analysis and Mutation detection

Linkage to candidate region at 7q36 associated with preaxial polydactyly and triphalangeal thumb (PPD2) was performed using highly polymorphic microsatellite markers (Table 6.3). LOD score calculated at marker D7S550, D7S559 and D7S2423 was 1.73, 0.54 and 1.06 at recombination fraction zero ($\theta=0.00$) respectively. Maximum multipoint LOD score of 1.93 was obtained at recombination frequency 0.01. This region spans *SHH* and its cis-acting regulatory element (ZRS), which is well conserved among various species lying in intron 5 of *LMBR1*. Direct sequencing of ZRS identified a novel point mutation (T>G) at base position 4976 in intron 5 of *LMBR1*. Mutation was confirmed by restriction analysis (Figure 7.2) in all the sampled family members using *MseI* restriction enzyme and standard protocol described in Section 2. The mutation 4976T>G was present in all the phenotypically affected individuals, while two phenotypically normal individuals were carrier for the mutation. Unfortunately, X-rays of phenotypically normal carrier were not available to record minor changes. Screening of 280 unrelated normal chromosomes from ethnically matched population did not reveal any mutation carrier. Analysis of control population reveals that this is not a rare polymorphism.

7.1.2 Electrophoretic mobility shift assay

To check for the possible specific transcription factor binding site associated with mutation EMSA was performed using 29-mer wild type (T) and mutant (G) γ - ^{32}P -labelled synthetic oligonucleotide probes (Figure 6.15) and Caco-2 cells nuclear extract. EMSA result shows that there is a specific DNA/protein binding in mutant probes whereas no such binding occurs in wild type probes. Competitive DNA/protein binding was detected using unlabelled mutant probes whereas such competition was not detected with unlabelled wild type probe (Figure 7.3).

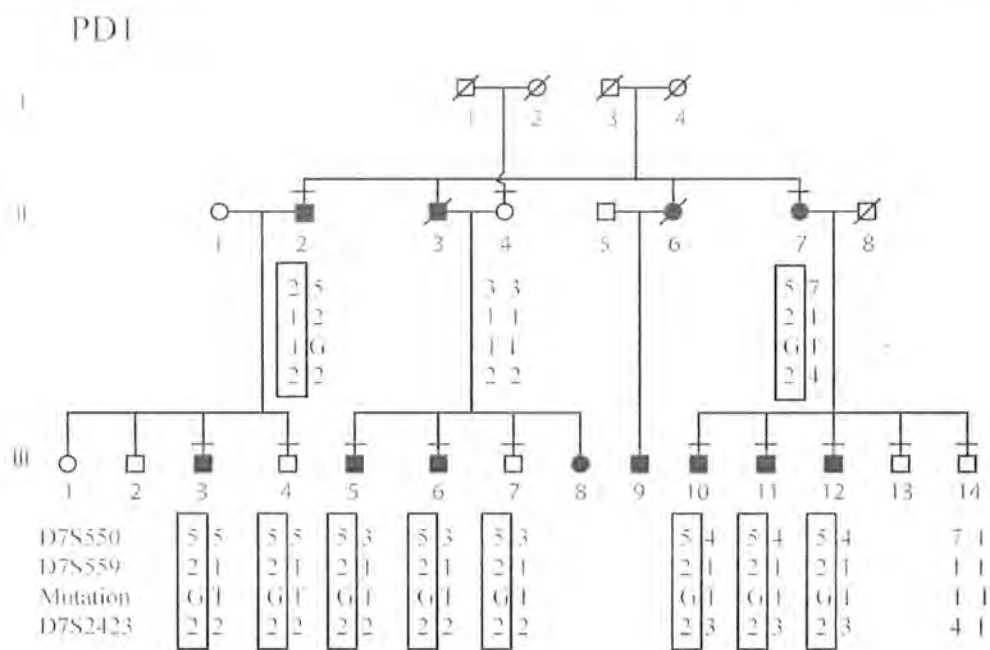


Figure 7.1: Pedigree of family PD1 and haplotypes of the individuals at 7q36 using microsatellite markers. The region in affected subjects segregating with phenotype is shown in box.

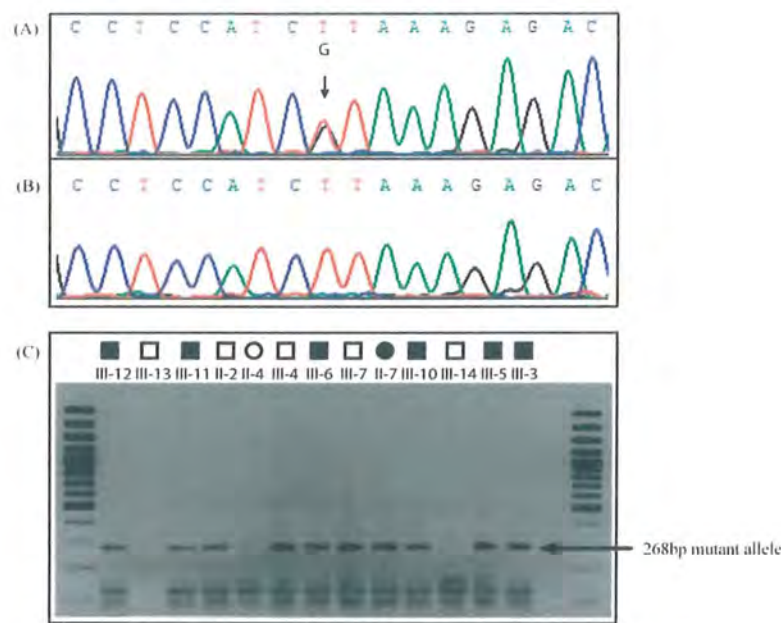


Figure 7.2: Representative chromatogram of mutation (4976 T>G) in ZRF (*SHH* regulatory element) in the intron 5 of *LMBR1* identified in family PD1. (A) Mutant, (B) Wild type, and (C) Restriction analysis using *MseI* restriction enzyme in all the sampled family members (normal and affected), 268bp mutant allele is indicated by arrow.

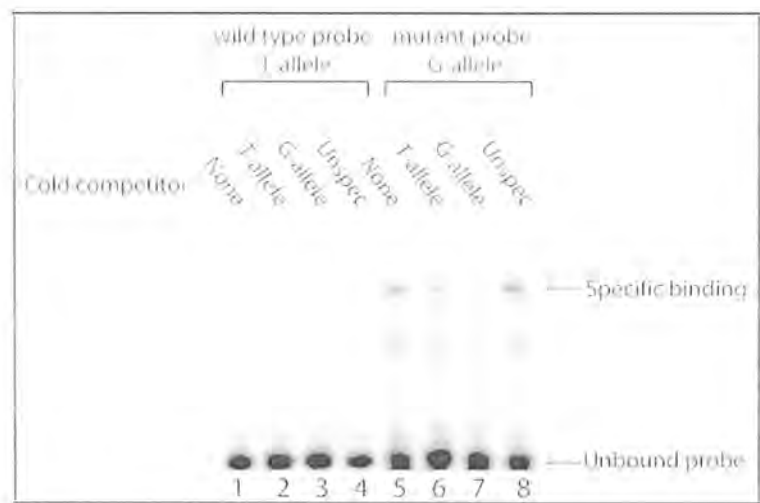


Figure 7.3: Electrophoretic mobility shift assay of the conserved element demonstrating binding of Caco-2 cell line nuclear extract to both wild type (T-allele) and mutant allele (G-allele). Unlabelled probes were added to demonstrate specific binding to both alleles. Specific binding is indicated by arrow.

Table 7.1: Spectrum of ZRS mutations identified in different species.

Specie	Mutation	Ethnicity	Reference
Human			
	4220C>T	Chinese	(Wang et al., 2007)
	4618C>G	Dutch	(Lettice et al., 2003)
	4818A>T	Belgian 1	(Lettice et al., 2003)
	4842T>C	Belgian 2	(Lettice et al., 2003)
	4917G>A	Cuban	(Lettice et al., 2003)
	4976 T>G	Pakistan	Present study
	5134C>G	N. American(caucasian)	(Gurnett et al., 2007)
	5252A>G	N. American(caucasian)	(Gurnett et al., 2007)
	4808T>C	UK	(Furniss et al., 2008)
Mouse			
	4919A>G	Mouse	(Lettice et al., 2008)
	5067T>C	Hx Neb, mouse	
	5068G>A	Hx, mouse	(Lettice et al., 2003)
Cat			
	4765G>C	Cat, UK	(Lettice et al., 2008)
	4988A>G	Cat, USA	(Lettice et al., 2008)
	4990A>T	Cat, UK	(Lettice et al., 2008)

7.1.3 Discussion

Preaxial polydactyly is one of the most frequently happening human limb congenital malformations. The phenotype is rather variable in affected families with whole digit duplication to simple addition of 3rd phalanx leading to triphalangial thumb. Single nucleotide substitutions in cis-acting regulatory element (ZRS) have been described in human, mouse and cat in recent years (Table 7.1). So far there are no reports for molecular basis of PPD2 families in Pakistani population. The regulatory element, ZRS is about 1 Mb upstream of target gene (*SHH*), located in the intron 5 of *LMBR1* and involved in regulation of expression of *SHH* in developing limb bud (Gurnett *et al.*, 2007; Lettice *et al.*, 2003). *SHH* is normally expressed in zone of polarizing activity (ZPA) posteriorly in the developing limb bud. Mouse model of PPD have shown that point mutations in ZRS element leads to ectopic expression of *SHH* at the anterior margin of limb bud (Lettice *et al.*, 2008). Heterozygous duplication including ZRS element has also been described in family with triphalangial thumb-polysyndactyly syndrome (Klopocki *et al.*, 2008; Sun *et al.*, 2008).

It has been found that long range promoter-enhancer interaction is specific to limb bud tissues (Amano *et al.*, 2009). The ZRS mutations responsible for preaxial polydactyly act via gain of function mechanism rather than inactivation of ZRS activity as homozygous deletion of ZRS element in mouse exhibit acheiropodia due to loss of *SHH* expression in the developing limb bud (Sagai *et al.*, 2004). Until now, 14 point mutations (Figure 7.4) have been reported distributed throughout the entire length of ZRS element suggested that entire element is important in regulation of *SHH* expression in ZPA of the limb (Furniss *et al.*, 2008; Gurnett *et al.*, 2007; Lettice *et al.*, 2003; Lettice *et al.*, 2008; Masuya *et al.*, 2007; Sagai *et al.*, 2004).

Sequence comparison around the reported mutation suggested that each mutation seems to affect individual transcription factor binding sites except for Hx and Cuban mutations, both result from G to A substitutions in a four nucleotide sequence ACTG (Loots *et al.*, 2002). Thus, each mutation acts by its own individual mechanism leading to ectopic expression of *SHH* (Lettice *et al.*, 2008). However, phenotypes produced by different point mutations in ZRS are almost identical. In family PD1 mutation 4976T>G lies in highly conserved region of ZRS among human, mouse, fugu and chicken. However, the disorder in family PD1 is not fully penetrant as two of the heterozygous mutation carriers are normal upon visual inspection. Low penetrance in

family PD1 shows that this mutation is not so much potent to disrupt the normal function of ZRS. A similar finding has previously been reported in which phenotypically normal mutation carriers were described (Furniss *et al.*, 2008; Gurnett *et al.*, 2007). EMSA results demonstrate specific binding of nuclear factor to mutant probes which suggests that T>G alteration at 4976 position is of functional importance leading to ectopic expression of *SHH* in limb bud upon binding of specific transcription factor. This hypothesis is supported by preferential binding of *HnRNP U* to mutated sequence in DZ mouse model (Zhao *et al.*, 2009). However, the sequence comparison around 463T>G mutation and DZ mouse mutation exclude the possibility of *HnRNP U* binding in this case. So, factors other than *HnRNP U* may involve in the pathogenesis of abnormal limb malformation in PD1 family. Another possibility is the production of tissue specific small RNAs upon binding of specific transcription factors to ZRS. Those small RNAs may influence *SHH* expression but it needs functional evidence. However, further experiments in transgenic mice are required to confirm pathogenic nature of the mutation.

Present data extend our knowledge about mutation spectrum in ZRS element and its phenotypic outcomes. The novel mutation identified in conserved non coding element in Pakistani family with PPD2 shows that whole of the ZRS element is essential for proper limb development. Functional study of the identified mutation will help to understand the signaling mechanisms in vertebrate limb development, regulatory mechanism of ZRS element and the genetic basis of the human limb development.

7.2 Family PD2

7.2.1 Linkage analysis and Mutation detection

An autosomal dominant inheritance inferred in family PD2 with GCPS. The variability in phenotype among the affected subjects has been described in section 6 (Table 6.1). *GLI3* is the most likely candidate; linkage analysis was performed using microsatellite markers (Table 6.3) at chromosome 7p13 (Figure 7.4). A significant LOD score (Z_{\max}) of 1.78 and 2.7 for marker D7S691 and for mutation at recombination fraction zero ($\theta = 0.0$) was obtained respectively. Positive LOD score (Table 7.2) shows evidence of linkage at 7p13 spanning a candidate gene *GLI3*.

Sequencing of all the exons including exon-intron boundaries revealed a novel A to T substitution (c.1702A>T) in exon 13 leading to an immediate stop codon at amino acid position 568 (Figure 7.5). The identified nonsense mutation p.R568X lies in the Zinc finger domain (ZFD) of *GLI3* leading to truncated protein product of 567 amino acids instead of 1580. This substitution leads to loss of restriction site for *BglII*. Restriction analysis of all the sampled family members confirmed segregation of mutant allele in all of the affected family members (Figure 7.5). Mutation was not found in any of the phenotypically normal individual, thus revealed 100% penetrance.

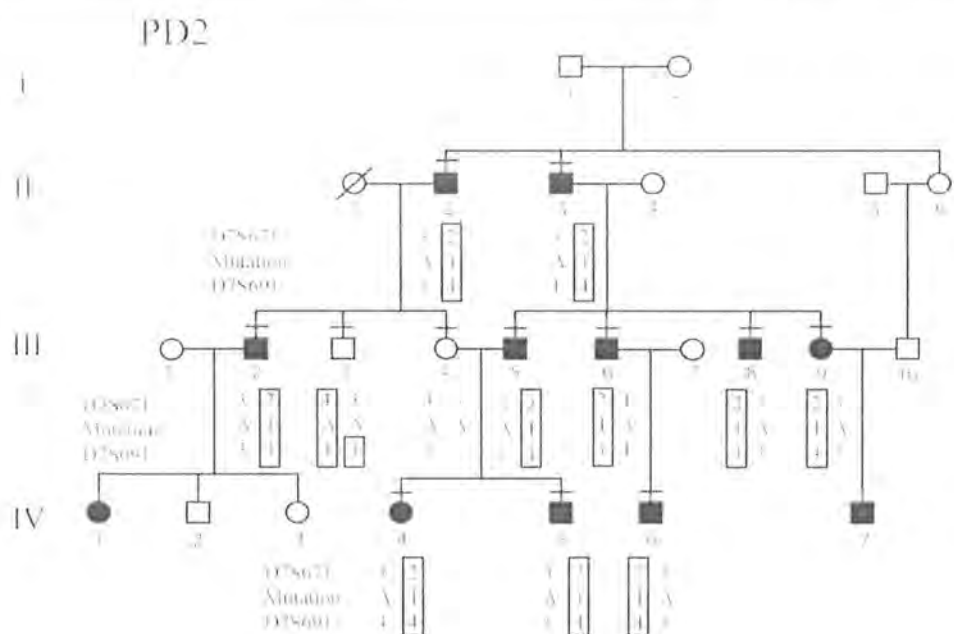


Figure 7.4: Linkage analysis using STRs flanking *GLI3* in family PD2.

Table 7.2: Two point LOD score for family PD2 on chromosome 7p13.

Position	Marker	Recombination fraction (θ)						
		0.00	0.01	0.05	0.1	0.2	0.3	0.4
Chr7:41,983,792	Mutation	2.70	2.65	2.46	2.20	1.66	1.07	0.45
63.67cM	D7S691	1.78	1.75	1.60	1.42	1.04	0.62	0.21

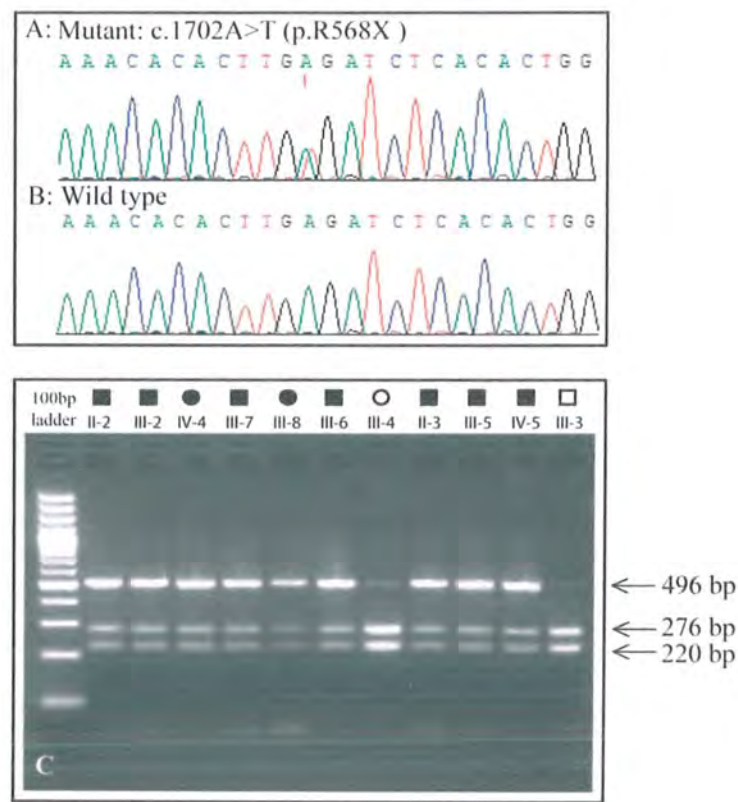


Figure 7.5: Chromatogram and restriction analysis of family PD2. (A) heterozygous mutant, (B) homozygous normal, (C) restriction analysis after PCR amplifying exon 13 of *GLI3* of whole PD2 family using *BglII* enzyme, mutant allele (496 bp), and wild type alleles (276 & 220 bp) are indicated by arrow.

7.3 Family PD316

Sequencing of *GLI3* in family PD316 identified a 2 bp deletion c.1853_1854delAC leading to frameshift (p.Y618fs). This novel frameshift mutation inserts premature stop codon after incorporating 55 novel amino acids starting from frame shift codon producing 673 amino acids long truncated protein. The mutant allele found consistent with all of the affected members while none of the normal carried this deletion. This mutation c.1853_1854delAC lies within the zinc finger domain (ZFD) of *GLI3*. Screening of 100 control samples from ethnically matched population did not reveal any carrier.

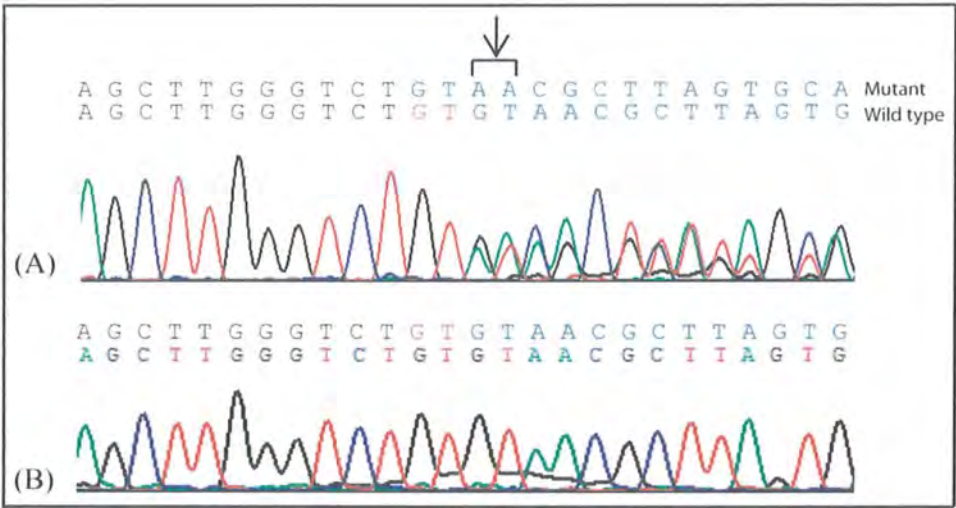


Figure 7.6: Chromatogram of mutation in family PD316. (A) Heterozygous mutant and (B) homozygous normal.

7.4 Family PD7

A single nucleotide substitution mutation c.4574C>T identified by sequencing of *GLI3* leading to missense substitution of Proline to Leucine at amino acid position 1525 (p.P1525L) in exon 15. Mutation lies in C-terminal after the domain 7 of *GLI3* which is highly conserved among the species (Figure 7.7). This substitution was not detected in any of the normal individual in the family. Screening of 400 ethnically matched normal chromosome did not identified any carrier predict that it may be a pathogenic variant rather than a rare polymorphism.

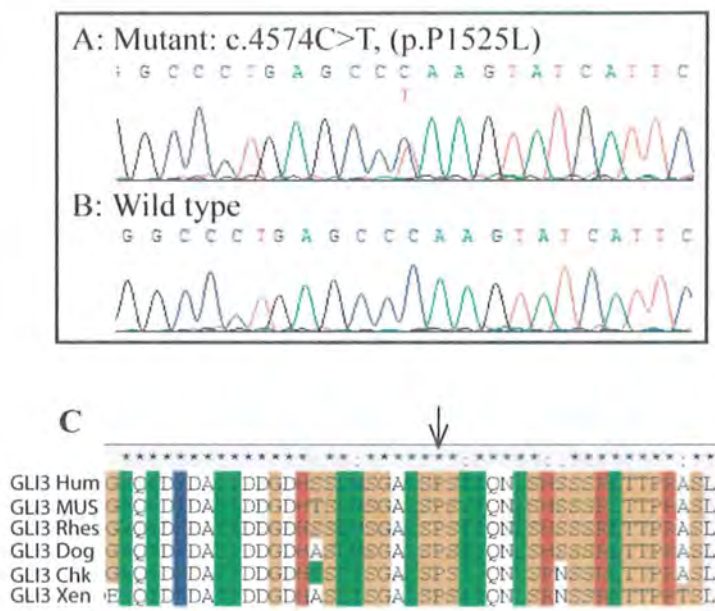


Figure 7.7: Chromatogram of mutation in family PD7. (A) Heterozygous mutant, (B) homozygous normal, and (C) amino acids sequence comparison of *GLI3* proteins from different species and site of missense mutation (P1525L) in family PD7 is indicated by arrow.

7.5 Family PD16

Family PD16 with PAPB a single nucleotide substitution of C to T at coding nucleotide position 3557 in all affected individuals in heterozygous form. This substitution (c.3557C>T) leads to missense codon, proline to leucine at amino acid position 1186 (p.P1186L) in exon 15 of *GLI3*. This substitution incorporate restriction site for *PstI* restriction enzyme which is used to confirm the mutation in all the family members (Figure 7.8). A non-synonymous SNP described earlier at coding nucleotide 4576 of *GLI3* (c. 4567C>G) leading to p.L1523V was also indentified to segregate with c.3557C>T (p.P1186L). Sequencing of 400 ethnically matched normal chromosome did not reveal any carrier.

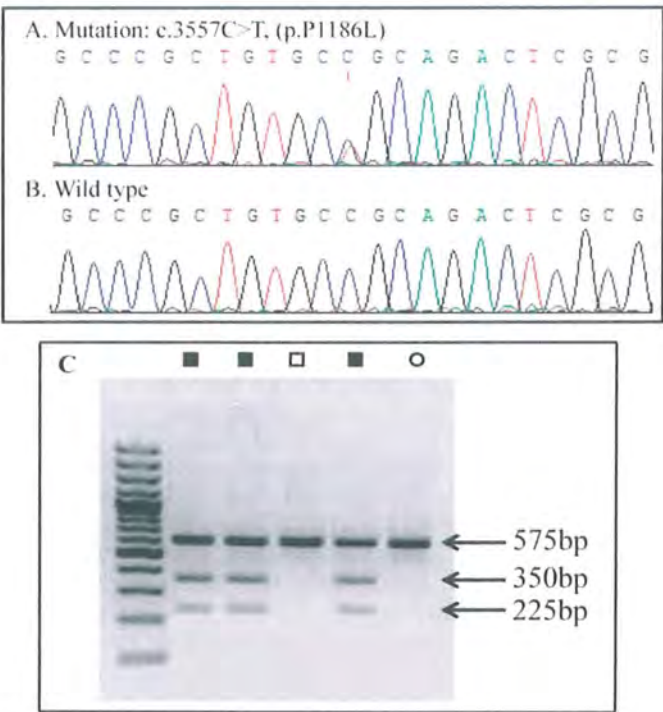


Figure 7.8: Chromatogram and restriction analysis of family PD16. (A) Heterozygous mutation carrier, (B) wild type, and (C) restriction analysis for the identified mutation in all the sampled family members.

7.6 Discussion

GLI3 (OMIM 165240) is a zinc finger transcription factor that regulates downstream genes by direct binding to the promoter regions of the target genes (Vortkamp *et al.*, 1995). *GLI3* is involved in sonic hedgehog pathway. *GLI3* is known to be a bifunctional transcription factor. Studies on cubitus interruptus (*ci*) which is *GLI* gene homolog in *Drosophila* is regulated by hedgehog (*hh*). It normally localizes to cytoplasm and in the presence of *hh*, *ci* protein (155 kDa) is translocated to nucleus where it activates the downstream genes. In the absence of *hh*, *ci* is processed to 75 kDa N-terminal protein with zinc finger domain (ZFD) that represses the downstream genes (Aza-Blanc *et al.*, 1997). Mutations in *GLI3* have been identified in various digital abnormalities termed as *GLI3* marphopathies (Radhakrishna *et al.*, 1999). Syndromic and non syndromic digital anomalies included in *GLI3* marphopathies are Geig cephalopolysyndactyly syndrome (GCPS) (Kalff-Suske *et al.*, 1999), Pallister- Hall syndrome (PHS) (Kang *et al.*, 1997), preaxial polydactyly type-IV (PPD-IV) (Radhakrishna *et al.*, 1999), acrocallosal syndrome (ACS; OMIM 200990) and postaxial polydactyly type A/B (PAP A/B) (Radhakrishna *et al.*, 1997b).

The digital phenotype in GCPS is extremely variable even within a single individual when contralateral limbs are compared (Biesecker, 2006). The most common limb finding in GCPS is postaxial polydactyly of upper limbs and preaxial polydactyly of the lower limbs. The cutaneous syndactyly of 3rd and 4th digit is very common in hands but it is highly variable among the affected individuals even in the same family. In feet, syndactyly of 2nd and 3rd toe is more commonly found. However, it may involve variably different toes. The facial findings in GCPS include hypertelorism, variable macrocephaly and wide nose bridge but these craniofacial findings are markedly inconsistent and sometimes may not be present. The digital phenotypes in PPD-IV are exactly similar as like in GCPS but have no craniofacial abnormalities. A single nucleotide frameshift insertion resulting in a truncated protein product of 1,245 amino acids have been described in a preaxial polydactyly type IV family (Radhakrishna *et al.*, 1999). In another report a nonsense mutation (R290X) has been claimed in a patient with PPD-IV phenotype (Fujioka *et al.*, 2005). However, craniofacial features of proband were not normal (Biesecker, 2006). A similar mutation was reported in four independent families with GCPS (Johnston *et al.*, 2005) concluded that patient had GCPS phenotype with mild craniofacial abnormalities. GCPS is

caused by variety of different mutations which includes nonsense, missense and splicing mutations, and deletions, insertion and different translocation mutations (Johnston *et al.*, 2005). Whereas, PHS is mainly caused only by nonsense, frameshift, and splicing mutations (Johnston *et al.*, 2005). A clear genotype phenotype correlation has been described among the frameshift and nonsense mutations in *GLI3*. Johnston *et al.* (2005) predicted that *GLI3* mutations in first third and last third of the gene produce GCPS phenotype whereas mutations in second third of the gene cause PHS. Authors also proposed relaxed GCPS diagnostic criteria of preaxial polydactyly and the presence of at least one additional feature (syndactyly, macrocephaly, hypertelorism, or postaxial polydactyly). In the present study families PD2, PD316 and PD7 are diagnosed as GCPS based upon diagnostic criteria proposed by Johnston *et al.* (2005).

In the present study four novel mutations in four distinct families have been identified. In family PD2, a single nucleotide substitution mutation [c.1702A>T (p.R568X)] leading immediate stop codon in exon 13 is identified. Two base pairs deletion mutation [c.1853_1854delAC (p.Y618fs)] leading to frameshift and premature terminated protein product of 673 amino acids is identified in family PD316 from Denmark. Both the mutations R568X and Y618fs lie in zinc finger domain in the first third of *GLI3* producing truncated protein product which may affect the DNA binding property of zinc finger domain leading to haploinsufficiency of *GLI3*. These mutations have not been reported before for any of the phenotype associated with *GLI3* mutation. In family PD7, a novel C to T substitution at coding nucleotide 4574 (p.P1525L) in exon 15 of *GLI3* is identified. The third mutation which is a missense mutation (c.4574C>T (p.P1525L) lies in the last third of *GLI3*. Missense mutation P1525L lies in the C terminal region of *GLI3* protein in the transactivation domain (TA) (Kalff-Suske *et al.*, 1999). Multiple sequence alignment using clustal analysis showed that amino acid proline at 1525 position is highly conserved among various species (Figure 7.7). This substitution was not identified in the control population. It is most likely that P1525L may lead to disruption of normal *GLI3* functioning. Johnston *et al.* (2005) proposed that *GLI3* mutations in first third and last third of the gene cause GCPS phenotype. Mutations identified in PD2, PD316 and PD7 support this genotype phenotype correlation. However, the affected individuals in family PD2 and PD316 have no obvious facial deformities which are commonly observed in GCPS. It is also observed that most of the clinically affected individuals in all the three families do not have facial abnormalities except for affected subjects in PD7. Similar findings have been reported previously that facial anomalies

are highly variable in affected families and can be so mild to be detected (Biesecker, 2006). In family PD16, at coding nucleotide position 3557, C to T substitution leading to missense incorporation of amino acid (p.P1186L) is identified. Screening of 400 control chromosomes predicts that it is not a rare polymorphism. This mutation 3557C>T is newly described; lie in the region of *GLI3* in which truncating mutations are associated with GCPS (Johnston *et al.*, 2005). Additional features of GCPS or PHS were not evident in any of the affected family members. Postaxial polydactyly type B in family PD16 may be a milder phenotype of GCPS. Previously, 1-bp deletion (c.2372delC, P791RfsX3) in exon 14 of *GLI3* has been reported in a family with bilateral postaxial polydactyly type B (Furniss *et al.*, 2007).

In conclusion four novel *GLI3* variants are reported in four families from different localities in Pakistan and Denmark. The variability in phenotype with respect to mutation in the affected family members may help to understand the phenotypic spectrum of *GLI3* mutation. The study also highlights the importance of intact *GLI3* gene for normal limb development. Two missense mutations identified in GCPS and PAPB family require further studies using experimental models and bioinformatics tools for protein modeling to find out the pathogenesis of disease and functional importance of variants.

7.3 Family BD1

The phenotype in BD1 family is typically identical to brachydactyly type E (BDE). BDE is reported to be inherited as an autosomal dominant disorder and is caused by missense mutations in *HOXD13* (Johnson *et al.*, 2003). However, autosomal recessive form of BDE has not been reported so far in the literature. BD1 family may be a novel type of isolated BDE with recessive inheritance pattern. The most consistent limbs phenotype in BD1 family is shortening of 3rd and 4th metacarpals and metatarsals. Phalanges are also involved with hypoplasia of middle phalanges of 3rd and 4th toe. In some affected subjects only 4th metatarsals is hypoplastic. Feet are affected in all the affected subjects. Most severe cases show involvement of both hands and feet with hypoplasia of middle phalanges of 3rd and 4th toe.

7.3.1 Exclusion of locus on 2q31 (HOXD13) for brachydactyly type E

Linkage to *HOXD13* region on chromosome 2q31 which is known to be responsible for autosomal dominant form brachydactyly type E (BDE) was performed (Johnson *et al.*, 2003). A number of highly polymorphic microsatellite markers flanking *HOXD13* were used (Table 6.3). Haplotypes constructed for the region do not show homozygosity in the affected subjects. Haplotypes were also examined for autosomal dominant mode of inheritance. After exclusion of *HOXD13* using microsatellite markers, direct sequencing of *HOXD13* gene was performed in two of the affected individuals to confirm the exclusion for *HOXD13* involvement. Sequencing of the coding regions does not reveal any mutation.

7.3.2 Genome-wide search using 10K SNP array and fine mapping

Genome wide search was performed using 10K SNP array in the selected family members of BD1. A single homozygous region with significant LOD score (Zmax) of 3.24 between SNP_A-1513140 (18.13 cM) and SNP_A-1511110_2 (33.91 cM) was identified on chromosome 6p24.1-p22.3 in individuals V-3 and VI-2 in left and middle branch by calculation of 10K SNP array data for recessive mode of inheritance and Caucasian allele frequencies after removing the uninformative SNPs. However, in right branch haplotypes were consistent though not

homozygous. This can probably be due to one disease allele is inherited from outside the loop indicating another disease allele or a distant founder event resulting in a degenerated disease haplotype. Additional microsatellite markers were used to fine map the homozygous region identified by 10K SNP array in the whole family. A small homozygous region found to be consistent with all the affected subjects between the marker D6S260 (29.9 cM) and D6S274 (32.6 cM) on chromosome 6p22.3 (Physical position: 15,512,454 bp -16,579,402 bp). Maximum two point LOD score (Z_{\max}) of 5.00 at recombination fraction ($\theta=0.0$) was calculated at marker locus D6S18xAG (Table 7.3).

7.3.3 Mutation screening

The boundary markers D6S260 and D6S274 span ~1 Mb region containing only seven genes. The genes include LOC441131, LOC644906, JARID2, LOC100131159, MRPL42P2, DTNBP1, MYLIP, GMPR, and ATXN1. Sequencing of coding regions and exon intron boundaries and 5' and 3' UTRs of *JARID2*, *MYLIP*, *DTNBP1*, *GMPR* and *ATXN1* gene was done in two affected subjects. The sequences were compared to reference sequences at NCBI (<http://www.ncbi.nlm.nih.gov/>). No sequence variant was identified in any of these genes in the affected individuals. However, possibility of mutation in intronic or promoters region cannot be ruled out.

The region was further fine mapped by analyzing more STS markers using simple repeats information taken from UCSC genome browser (<http://genome.ucsc.edu>). After fine mapping, the physical linkage interval lies between 15,837,143 to 16,579,402 bp on chromosome 6. The region further excluded *JARID2* and *DTNBP1* as possible candidates.

A search in the candidate region was done for conserved non coding regions with predicted transcription factor binding affinity using UCSC genome browser (<http://genome.ucsc.edu>). Sequencing of selected non coding regions did not reveal any variant (Primer sequences and amplified region given in Table 6.13).

7.3.4 Genome wide SNP array 6.0 analysis to detect copy number variation

To detect any copy number variation (homozygous deletions or duplication), SNP6 (Affymetrix) analysis was performed. SNP6 analysis results were analyzed for copy number variation using Affymetrix Genotyping Console software (version 3.0.2). Unfortunately, no copy number variation was detected in the region flanked by D6S260 (29.9 cM) and D6S274 (32.6 cM) on chromosome 6 (Physical position: 15,512,454 bp-16,579,402 bp). However, a number of CNVs were identified genome wide (Table 7.4a, 7.4b).

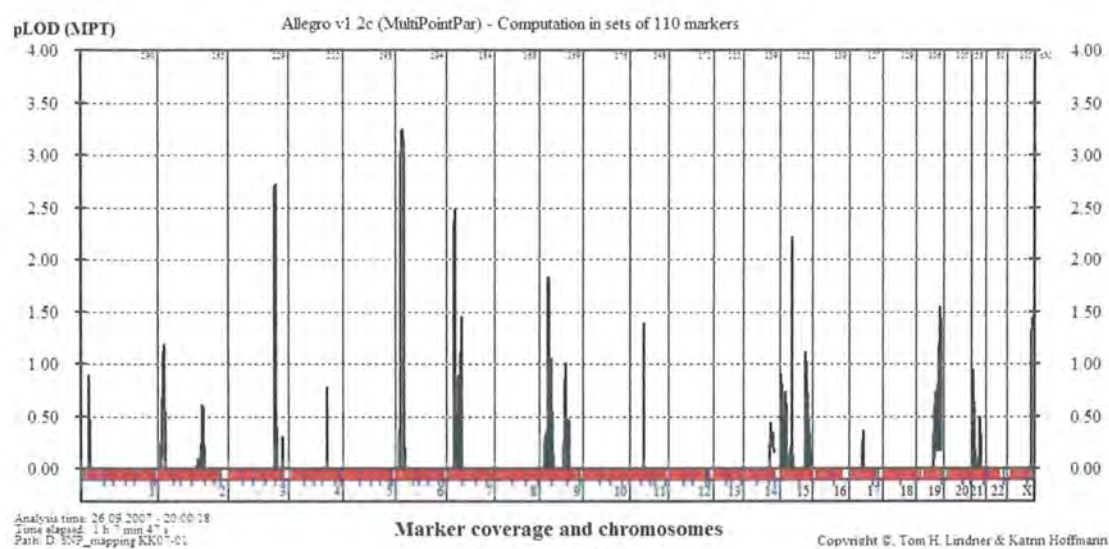


Figure 7.9: Whole genome parametric (Allegro) linkage result using easyLINKAGE plus v5.08 in family BD1. Maximum multipoint LOD score obtained on chromosome six.

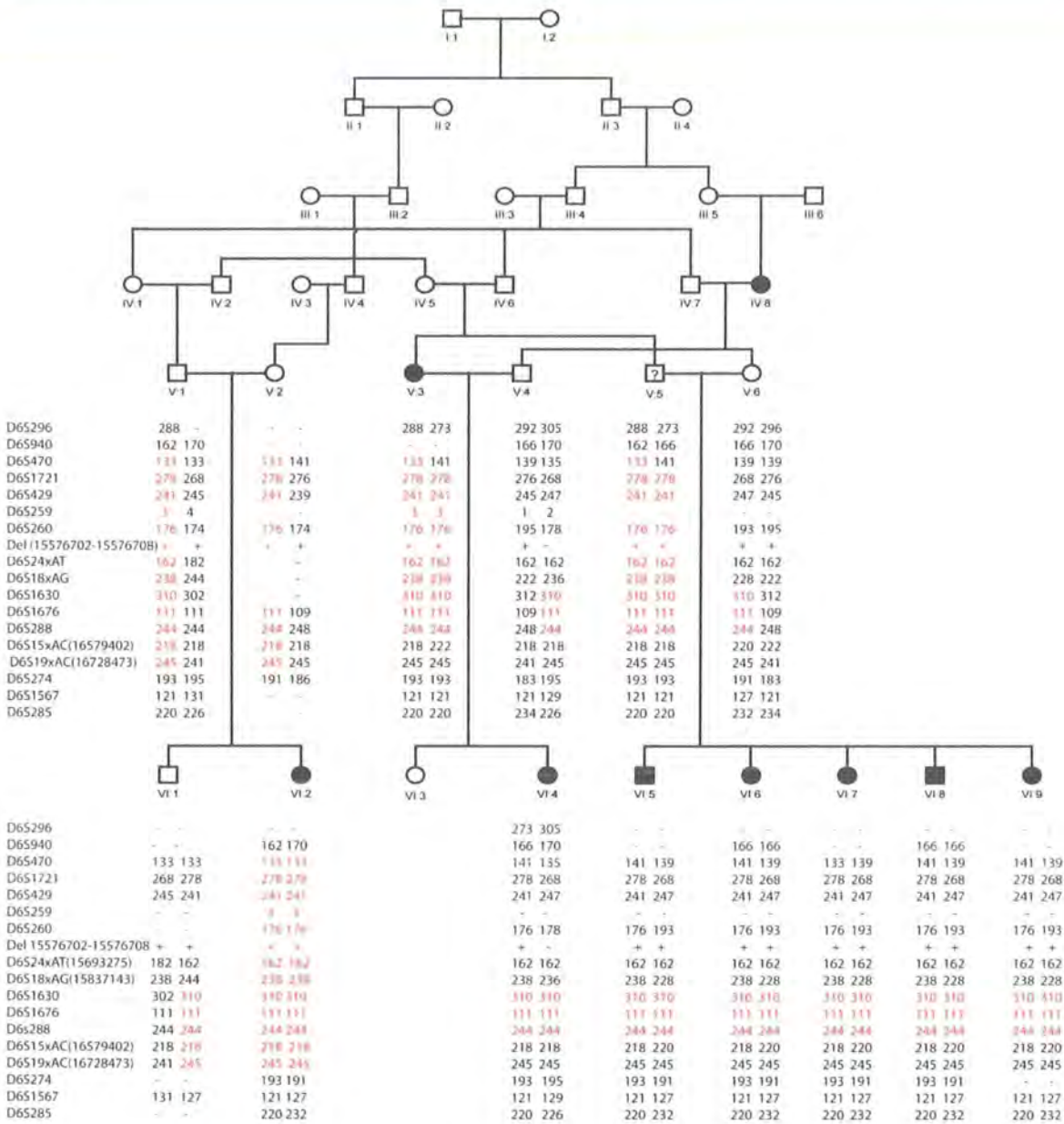


Figure 7.10: Family BD1 with autosomal recessive brachydactyly type E. Microsatellite markers used to narrow down the homozygous region identified by 10K SNP array. Minimum disease associated haplotype shared by all the affected individuals are shown in red.

Table 7.3: Two point LOD score for family BD1 on chromosome 6p24.1-p22.3.

Marker	cM/Physical position (bp)	Recombination fraction (θ)						
		0.00	0.01	0.05	0.1	0.2	0.3	0.4
D6S18xAG	15837143-15837179	5.00	4.80	4.40	3.80	2.60	1.40	0.40
D6S1630	29.9	4.80	4.70	4.20	3.60	2.4	1.2	0.3
D6S1676	29.9	3.55	3.48	3.21	2.81	1.93	1.02	0.22
D6S288	31.0	3.19	3.19	2.93	2.56	1.73	0.88	0.18
D6Sx15AC	16579402-16579432	-infinite	0.25	1.43	1.69	1.50	1.00	0.43

Disease allele frequency (p) = 0.1%

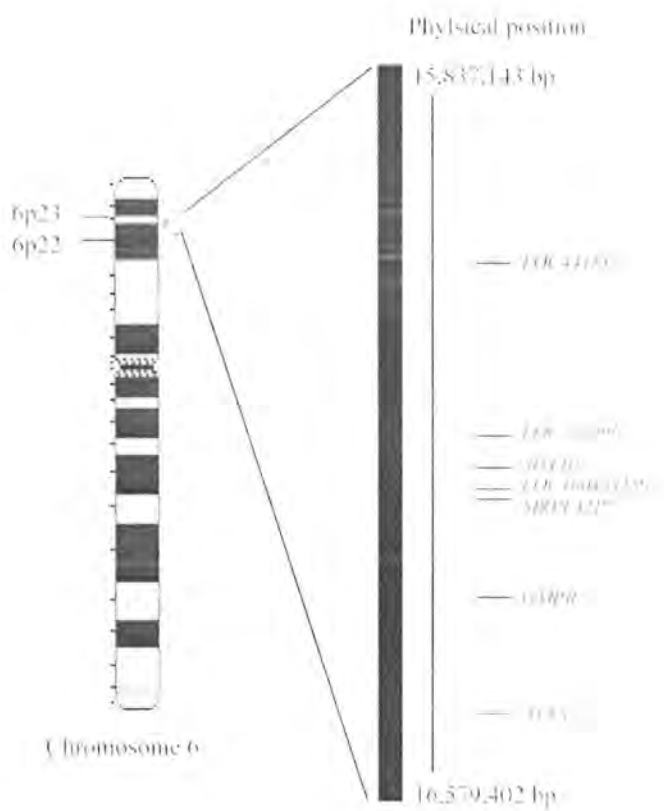


Figure 7.11: Genetic map of novel locus on chromosome 6 mapped in BD1 family.

Table 7.4a: Copy number variations (CNVs) identified by SNP6 analysis.

Loss/ Gain	Chromo- some	Cytoband start	Cytoband end	Size (kb)	Markers	Start	End	Start marker	End marker
Gain	X	q21.31	q21.31	32	17	88255043	88286883	CN_958646	CN_958659
Gain	X	q21.31	q21.31	123	34	90735643	90858856	SNP_A- 8583318	CN_972057
Gain	X	q26.3	q26.3	36	25	134585148	134620812	SNP_A- 8651860	CN_401208
Gain	X	q28	q28	57	76	153220607	153277758	CN_919270	CN_921417
Gain	Y	p11.31	p11.31	73	8	3076489	3149646	CN_945771	CN_945785
Gain	Y	p11.2	p11.2	45	8	3320443	3365294	CN_945820	CN_945832
Gain	Y	p11.2	p11.2	60	6	3471571	3531481	CN_945854	CN_945863
Gain	Y	p11.2	p11.2	34	5	4447653	4481798	CN_950260	CN_950265
Gain	Y	p11.2	p11.2	70	10	4540827	4610549	CN_950277	CN_950292
Gain	Y	p11.2	p11.2	27	5	4737743	4765177	CN_950324	CN_950332
Gain	Y	p11.2	p11.2	129	12	4876814	5006307	CN_950353	CN_952489
Gain	Y	p11.2	p11.2	49	11	5278803	5327831	CN_952547	CN_952559
Gain	Y	p11.2	p11.2	189	20	5667698	5856688	CN_954721	CN_954757
Gain	Y	p11.2	p11.2	49	7	6068013	6116733	CN_954809	CN_954821
Gain	Y	p11.2	q11.1	1642	9	10669230	12310916	CN_417111	CN_958808
Gain	Y	q11.222	q11.222	28	6	20661910	20690017	CN_950133	CN_950138
Gain	Y	q11.23	q11.23	27	5	26100286	26127296	CN_972627	CN_972629
Loss	1	q44	q44	97	42	246780602	246877269	CN_477703	SNP_A-4289125
Loss	2	q31.2	q31.2	53	26	178756631	178809296	SNP_A- 8457495	CN_820164
Loss	3	p24.2	p24.2	30	33	24302278	24332543	CN_1010129	SNP_A-2296546
Loss	3	p22.3	p22.3	46	19	33671452	33717767	CN_1028314	CN_1030406
Loss	4	p11	p11	68	10	48788531	48856503	CN_1049640	CN_1049650
Loss	4	q13.2	q13.2	55	32	70162229	70217321	CN_1113957	CN_278285
Loss	4	q13.2	q13.2	56	30	70237060	70292908	CN_1113992	CN_1116073
Loss	4	q34.1	q34.1	25	6	173664905	173690283	CN_1066301	SNP_A-4264629
Loss	6	q25.3	q25.3	25	22	158633764	158659170	CN_1177157	CN_1177173
Loss	7	q11.23	q11.23	49	17	71805575	71855066	CN_1258963	SNP_A-2297252
Loss	7	q11.23	q11.23	42	14	72971349	73013103	CN_1227575	CN_1227584
Loss	7	q11.23	q11.23	144	34	75994465	76138571	CN_1236608	SNP_A-8614764
Loss	7	q11.23	q11.23	128	52	76140871	76268861	CN_1238776	SNP_A-2045806
Loss	7	q11.23	q11.23	146	84	76288401	76434828	SNP_A- 8348429	CN_1241051
Loss	7	q21.3	q21.3	26	21	97010276	97036072	SNP_A- 8596545	SNP_A-8323607
Loss	7	q35	q35	136	28	143561999	143697868	CN_1201747	CN_1201782
Loss	8	p11.23	p11.23	116	45	39366256	39482091	CN_1283686	CN_1283732
Loss	8	q24.22	q24.22	54	31	132994639	133048184	CN_1280568	CN_1280586

Table 7.4b: Copy number variations (CNVs) identified by SNP6 analysis.

Loss/ Gain	Chromo- some	Cytoband start	Cytoband end	Size (kb)	Markers	Start	End	Start marker	End marker
Loss	9	p11.2	p11.2	538	33	44191212	44728821	CN_1322580	CN_1324742
Loss	9	p11.2	p11.2	86	6	45338598	45424853	CN_1327027	CN_1324820
Loss	9	q22.1	q22.1	31	7	89696625	89727712	CN_1331760	SNP_A-8573966
Loss	10	q11.22	q11.22	36	12	46338178	46374551	CN_558668	CN_558681
Loss	10	q21.3	q21.3	41	32	67969885	68010448	SNP_A-4235825	CN_539829
Loss	12	q13.11	q13.11	39	19	47043451	47082804	CN_615968	CN_615977
Loss	14	q22.1	q22.1	47	56	51133476	51180079	CN_673312	SNP_A-2216218
Loss	14	q32.2	q32.2	81	66	95464809	95546119	CN_684981	CN_685010
Loss	15	q11.2	q11.2	286	116	19803358	20089383	CN_680694	SNP_A-2133472
Loss	15	q13.3	q13.3	31	17	29706262	29737545	CN_691782	CN_691795
Loss	17	p11.2	p11.2	133	15	18254543	18387392	CN_749700	CN_751784
Loss	17	q11.2	q11.2	35	17	26430004	26464680	SNP_A-8673844	SNP_A-8319357
Loss	17	q21.31	q21.32	357	44	41750175	42107467	CN_146343	CN_739354
Loss	21	q22.11	q22.11	42	18	34012838	34054459	CN_876276	CN_876288
Loss	22	q11.23	q11.23	52	19	22674410	22726802	CN_915262	CN_915281

7.3.5 Discussion

Brachydactyly is a rare and genetically heterogeneous disorder. It can be an isolated condition or may be part of associated malformations. Different forms of isolated brachydactylies have been described (A-E) and most of them inherited in dominant fashion except for brachydactyly type C. Brachydactyly type E is inherited as an autosomal dominant entity characterized by variable shortening of the metacarpals or metatarsals. Temtamy and McKusick (1978) reported BDE for the first time in a family with multiple numbers of affected individuals in three generations confirming autosomal dominant inheritance and variable expressivity. Missense mutations in *HOXD13* were reported in two cases exhibiting overlap with BDD and BDE (Johnson *et al.*, 2003). So far there are no reports of recessive form of BDE. In the present study a novel locus in a large consanguineous family with recessive form of BDE is localized on chromosome 6p22.3 using homozygosity mapping. After fine mapping, the candidate interval is substantially reduced to 742 Kb. This region spans only seven genes including four pseudogenes. However, to date none of the gene in the region has been reported for limb disorders in human or mice. Sequencing of protein coding genes which include *MYLIP*, *GMPT* and *ATXN1* did not reveal any mutation. Therefore, in this rare form of BDE identification of causative gene is not so simple. Sequencing of some selected conserved non coding regions with putative transcription factor binding affinity did not reveal any variation. Analysis of SNP6 did not reveal any homozygous deletion or duplication in the region. However, the chances of deletions or duplication less than 30 kb cannot be excluded. There are four pseudogenes in the candidate linkage interval and sequencing of those genes may be useful to find out the underlying disease gene. Another approach may be to find more families linked to same locus with identical phenotypes. Recruitment of new families from different regions or ethnic background may be useful to find out the underlying gene as it is most likely that they may carry different mutation.

7.4 Family PD14A

7.4.1 Novel isolated autosomal recessive 2nd and 3rd digit syndactyly

Syndactyly was first classified into five phenotypically distinct types based upon anatomical involvement of different digital elements (Temtamy and McKusick, 1978). All those five distinct types segregated in autosomal dominant fashion. In syndactyly type I, which is also known as zygodactyly, 3rd and 4th fingers of hands are most commonly syndactylous with occasional fusion of distal phalanges. In feet there is usually a complete or partial webbing of 2nd and 3rd toes but mostly hands are only affected. A five generation family with 18 affected males and 29 females with autosomal dominant inheritance and variable degree of expressivity were described (Lueken, 1938). Type I syndactyly is grouped into four subtypes which are all autosomal dominantly inherited (Malik *et al.*, 2005a). Subtype 1 or zygodactyly is the most common form and involve soft tissue webbing of 2nd and 3rd toes without hand involvement. Subtype 2 is characterized by cutaneous and/or bony fusion of 3rd and 4th fingers and 2nd and 3rd toes. Subtype 2 is mapped to 2q34-q36 (Bosse *et al.*, 2000). The phenotype in family PD14A shows cutaneous syndactyly of 3rd and 4th digit characteristic of syndactyly type I. However, syndactyly type I is inherited as an autosomal dominant trait (Temtamy and McKusick, 1978). The phenotype in family PD14A does not fit to any of these two well described autosomal recessive types of syndactylies. The detailed clinical examination of the family revealed that it is a novel syndactyly type I with 3rd and 4th digit syndactyly and an autosomal recessive inheritance.

7.4.2 Exclusion studies and Genome wide linkage analysis

To find out possible linkage to known syndactyly loci, genotyping was performed using microsatellite markers (Table 6.3) on chromosome 2q34-q36 (syndactyly type I), 3p21.31 (zygodactyly), 2q31 (SPD1 locus, *HOXD13*), 6q22.31 (*GJA1*, syndactyly type III), 22q13.31 (SPD2), 14q11.2-q12 (SPD3) and 17p13.3 (syndactyly type IX). Haplotype analysis does not show linkage to any of these loci using homozygosity mapping.

After exclusion from all the known syndactyly loci a genome wide search was performed in the affected subjects using 10K Affymetrix chip to identify a novel homozygous region segregating

with the phenotype. Two autozygous regions on chromosome 2 and 9 were identified. Homozygous region on chromosome 2 lies between SNP_A-1507852 (149.80 cM) and SNP_A-1517555 (158.25 cM). However, linkage to chromosome 2 was excluded using microsatellite markers in all the sampled family members including parents and normal siblings. The only homozygous region left on chromosome 9 lies between SNP_A-1518820 (24.97 cM) and SNP_A-1514897 (46.08 cM). After fine mapping using microsatellite markers the region is flanked by markers, SNP_A-1518820 and D9S21AT (marker not available in Marshfield genetic map). The physical positions of flanking markers are 12018387 bp to 15340449 bp with maximum LOD score (Z_{\max}) of 2.35 for given locus ($\theta=0.00$).

7.4.3 Sequencing of candidate gene

The region spans only 22 genes. None of the gene was previously reported for isolated syndactyly in human. *FREMI* (Fras1 related extracellular matrix protein 1) encodes a member of novel family of extracellular matrix proteins characterized by 12 consecutive CSPG repeats and a varying number of Calx- β domains (Jadeja *et al.*, 2005; Kiyozumi *et al.*, 2005). Mutations in *Frem1* and *Frem2* give rise to the head blebs and myelencephalic blebs phenotype in mice respectively (Jadeja *et al.*, 2005; Smyth *et al.*, 2004; Timmer *et al.*, 2005). These mutant mice represent animal models of Fraser syndrome which is a rare autosomal recessive genetic disorder characterized by cryptophthalmos, syndactyly and renal defects (McGregor *et al.*, 2003; Slavotinek and Tiffit, 2002). Mutant mice phenotype includes cryptophthalmos, syndactyly and sub-epidermal blistering (Kiyozumi *et al.*, 2006). However, no mutation has so far been reported in *FREMI* in human. *FREMI* could be a possible candidate gene in the region for isolated syndactyly in PD14A family. *FREMI* comprises of 37 exons including 36 coding exons. All the 37 exons and exon intron boundaries including 5' and 3' UTR regions were sequenced directly in all the three affected members of PD14A family using appropriate primer pairs (Primers sequences given in table 6.12) and sequences were compared to reference sequences at NCBI (<http://www.ncbi.nlm.nih.gov/>). A novel single nucleotide G to A substitution at coding nucleotide position 1289 (c.1289G>A) in exon eight leading to missense incorporation of glutamine instead of arginine at amino acid position 430 of *FREMI* (p.R430Q) is identified (Figure 7.15). Arginine

at 430 amino acid position of *FREMI* is not only conserved among different vertebrate species (Human, rhesus, mouse, elephant, chicken, lizard, dog and x-tropicalis), it is also conserved among *FREM* family of genes (Figure 7.16, 7.17). Sequencing of all the family members including normal subjects confirmed segregation of homozygous mutation with disease phenotype. Sequencing of 290 control individuals (580 chromosomes) identified five heterozygote carriers, but none of normal control is homozygous for mutant allele (c.1289G>A). Frequency of mutant allele in control population is calculated to be 0.0086 according to the Hardy-Weinberg ($p + q = 1$).

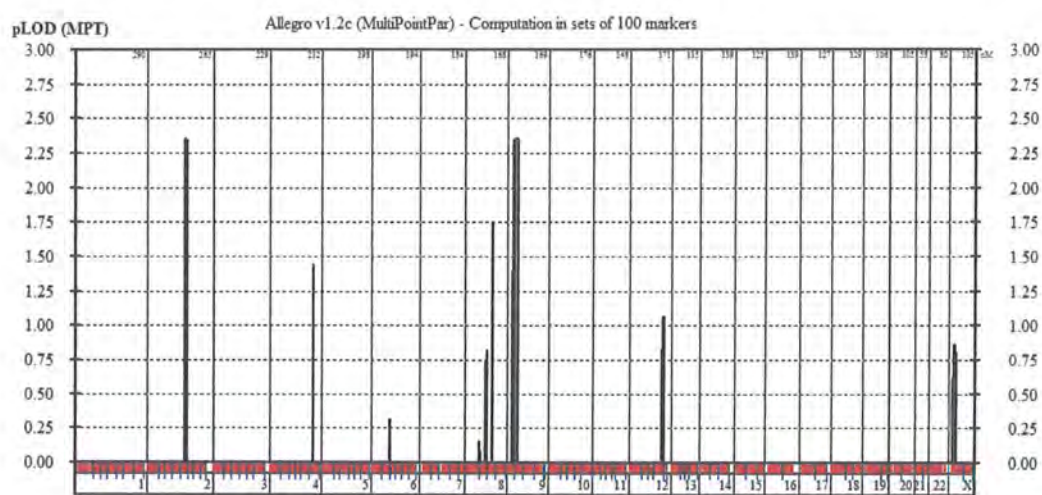


Figure 7.12: Whole genome parametric (Allegro) linkage result using easyLINKAGE plus v5.08 in family PD14A. Maximum multipoint LOD score obtained on chromosome 2 and 9.

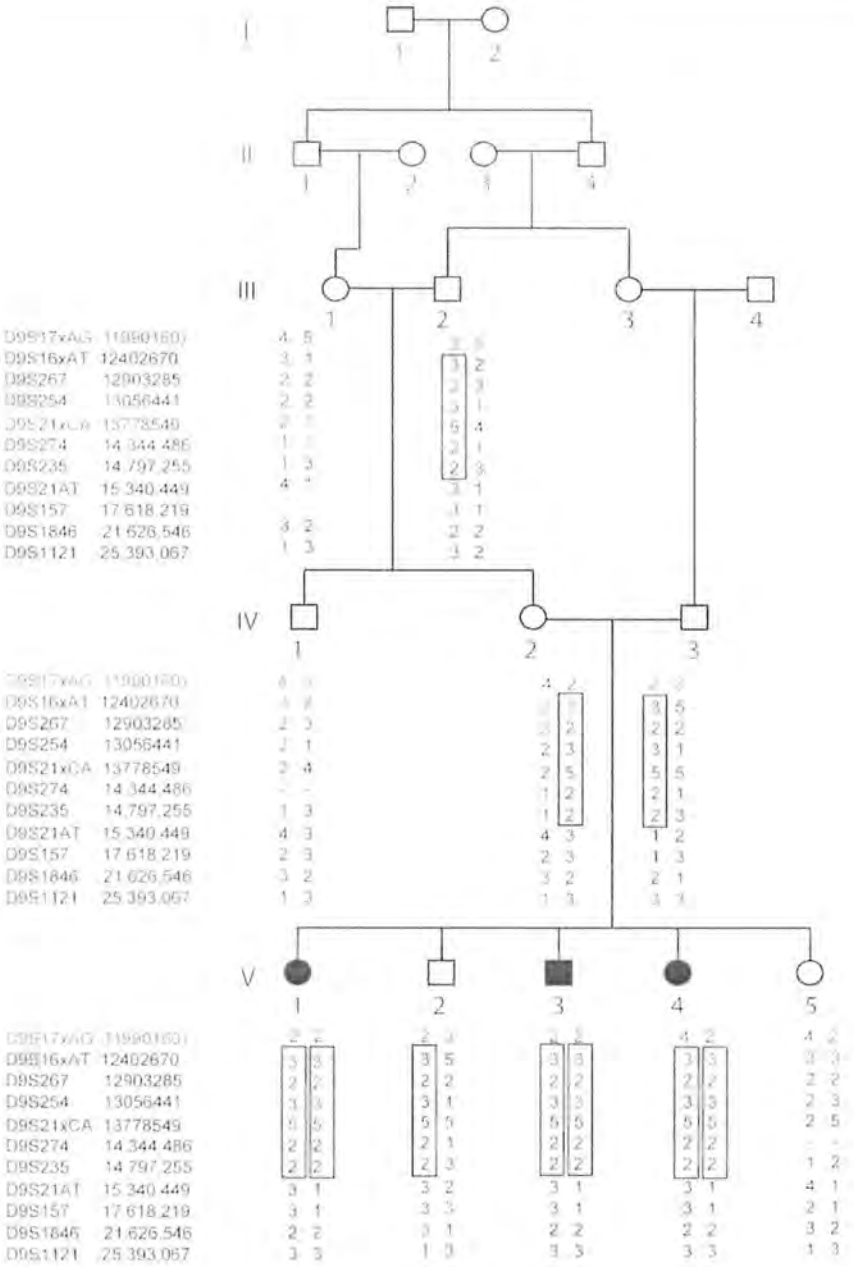


Figure 7.13: Family PD14A with autosomal recessive 3rd and 4th digit syndactyly. Microsatellite markers used to narrow down the homozygous region on chromosome 9 identified by 10K SNP array. Minimum disease associated haplotype shared by all the affected individuals are shown by box.

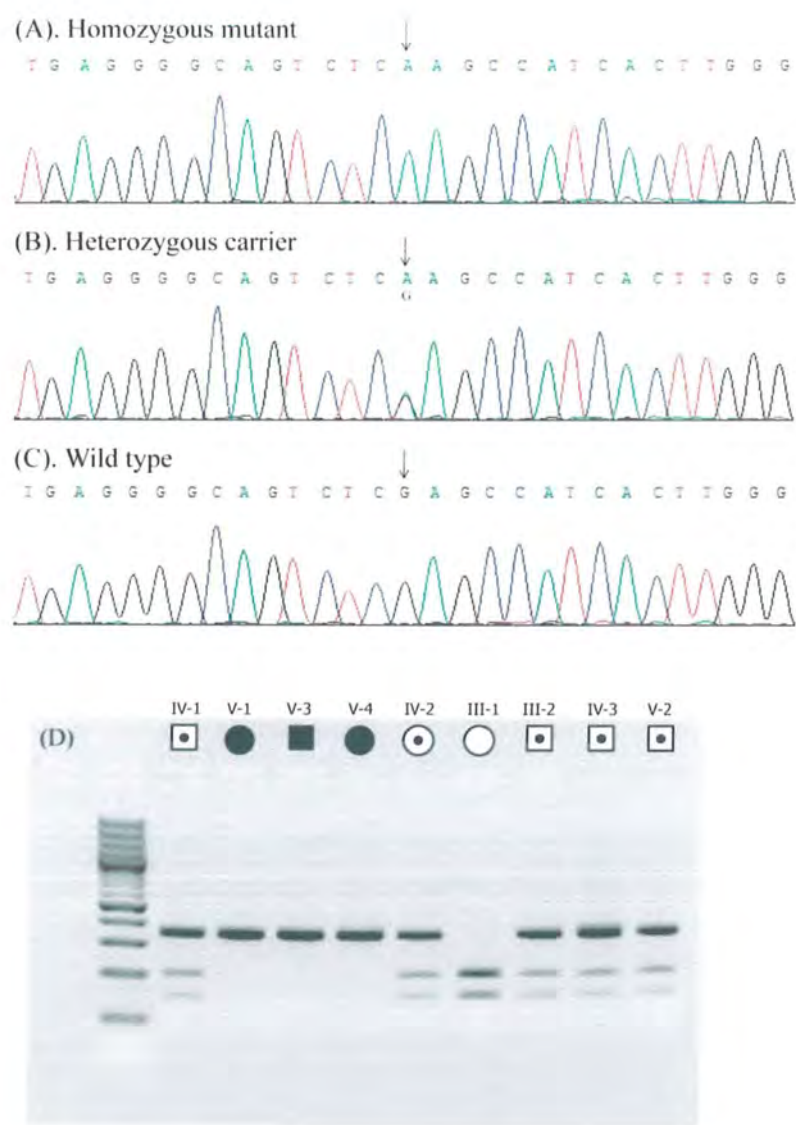


Figure 7.14: Chromatogram and restriction analysis of family PD14A. (A) Homozygous affected mutant, (B) heterozygous carrier, (C) homozygous normal, (D) restriction analysis after PCR amplification of exon 8 of *FREM1* for all the sampled members in PD14A family using *XhoI* enzyme, mutant allele (347 bp), wild type alleles (204 & 143 bp).



Figure 7.15: Amino acid sequence comparison of 2nd CSPG repeat in *FREM1*, *FREM2* and *FREM3* proteins. Site of substitution is indicated by arrow is highly conserved among all family members.



Figure 7.16: Conservation of *FREM1* among various vertebrate species. Six consecutive amino acids are highly conserved among all the species. Site of substitution (p.R430Q) indicated by arrow is highly conserved among all family members.

7.4.4 Discussion

Non-syndromic syndactyly is a quite common, heterogeneous hereditary malformation involving cutaneous or bony webbing of fingers and/or toes. The condition can be unilateral or bilateral. Interfamilial and intra-familial variability is commonly observed. The majority of reported cases of syndactylies show autosomal dominant mode of inheritance, with variability in expression and penetrance. The frequency of different forms of syndactyly varies in different populations and in a Latin-American study its prevalence of 3 per 10,000 births has been suggested (Castilla *et al.*, 1980). There are only two forms of autosomal recessive syndactyly i.e Cenani-Lenz type and Malik-Percin type (Cenani and Lenz, 1967; Malik *et al.*, 2004).

According to latest classification proposed by Malik *et al.* (2005), all kinds of autosomal recessive syndactylies are placed in group 3. It includes syndactyly type VII and type IX. In syndactyly type VII (Cenani-Lenz type) carpal and radio-ulnar fusion along with metacarpal/metatarsal fusion (Cenani and Lenz, 1967) is evident. Whereas, syndactyly type IX or Malik-Percin type syndactyly shows metatarsal and/or metacarpal synostosis along with missing fingers (Malik *et al.*, 2004; Percin *et al.*, 1998). The phenotype in family PD14A does not fit to any of these two well described autosomal recessive types of syndactylies. The detailed clinical examination of the family revealed that it is a novel type 3rd and 4th digit syndactyly with an autosomal recessive inheritance. Initially homozygosity mapping using 10K Affymetrix SNP array and finally fine mapping of the candidate loci using highly informative microsatellite markers led to the identification of a putative novel locus consistent with disease phenotype on chromosome 9p23-p22.3 with a maximum LOD score of 2.35. The candidate region spans 22 genes. Studies in mouse models showed that mutation in *Frem1* leads to the head blebs phenotype in mice (Jadeja *et al.*, 2005; Smyth *et al.*, 2004; Timmer *et al.*, 2005). The head bleb mouse represent animal model of Fraser syndrome, a rare autosomal recessive genetic disorder characterized by cryptophthalmos, syndactyly and renal defects (McGregor *et al.*, 2003; Slavotinek and Tiffi, 2002). Mutant mice phenotype includes cryptophthalmos, syndactyly and subepidermal blistering (Kiyozumi *et al.*, 2006). However, no mutation has so far been reported in *FREMI* in human. *FREMI* could be a possible candidate gene in the region for isolated syndactyly in PD14A family. Sequencing of *FREMI* revealed a missense mutation (p.R430Q) in the affected individuals. This missense incorporation of glutamine which is neutral polar instead

of a basic polar amino acid arginine, may disrupt the normal functioning of *FREMI*. *FRASI/FREM* gene family (*FREMI*, *FREM2*, and *FREM3*) encodes for structurally similar extracellular basement proteins (Jadeja *et al.*, 2005; McGregor *et al.*, 2003). *FRASI* and *FREM2* mutation have been identified in human in Fraser syndrome (van Haelst *et al.*, 2008). Syndactyly is a consistent feature in Fraser syndrome. *Frem1* protein has been detected in the basement membrane of apical ectodermal ridge (AER) at E. 10.5 of limb bud and it persists until E. 16.5 of differentiated limb. In addition, *Frem1* also localizes intracellularly in periderm cells which could reflect a novel function for *Frem1* apart from a basement membrane component (Chiotaki *et al.*, 2007). Expression of *Frem1* in the AER of developing and differentiated limb bud which plays a central role in signaling events during limb morphogenesis may predict its novel function in digit separation. However, possibility of missense mutation in *FREMI* could produce a defect in digit separation requires more families to study in addition to the functional studies in experimental models to prove the pathogenic nature of mutation.

REFERENCES

- Agarwal, P., Wylie, J. N., Galceran, J., Arkhitko, O., Li, C., Deng, C., Grosschedl, R., and Bruneau, B. G. (2003). Tbx5 is essential for forelimb bud initiation following patterning of the limb field in the mouse embryo. *Development* **130**(3), 623-33.
- Aicardi, J. (1998). Malformations of the central nervous system. In *Diseases of the nervous system in childhood* (Aicardi, J., ed.) 90-91.
- Akarsu, A. N., Akhan, O., Sayli, B. S., Sayli, U., Baskaya, G., and Sarfarazi, M. (1995). A large Turkish kindred with syndactyly type II (synpolydactyly), 2. Homozygous phenotype? *J Med Genet* **32**(6), 435-41.
- Akarsu, A. N., Ozbas, F., and Kostakoglu, N. (1997). Mapping of the second locus of postaxial polydactyly type A (PAP-A2) to chromosome 13q21-q32. (Abstract), *Am. J. Hum. Genet.* **61** (suppl.), A265.
- Amano, T., Sagai, T., Tanabe, H., Mizushina, Y., Nakazawa, H., and Shiroishi, T. (2009). Chromosomal dynamics at the Shh locus: limb bud-specific differential regulation of competence and active transcription. *Dev Cell* **16**(1), 47-57.
- Armour, C. M., McCready, M. E., Baig, A., Hunter, A. G., and Bulman, D. E. (2002). A novel locus for brachydactyly type A1 on chromosome 5p13.3-p13.2. *J Med Genet* **39**(3), 186-8.
- Ausubel, F. M., Brent, R., Kingston, R. E., Moore, D. D., Seidman, J. G., Smith, J. A., and Struhl, K., (2002). *Current Protocols in Molecular Biology*, Wiley, New York.
- Aza-Blanc, P., Ramirez-Weber, F. A., Laget, M. P., Schwartz, C., and Kornberg, T. B. (1997). Proteolysis that is inhibited by hedgehog targets Cubitus interruptus protein to the nucleus and converts it to a repressor. *Cell* **89**(7), 1043-53.
- Badano, J. L., Teslovich, T. M., and Katsanis, N. (2005). The centrosome in human genetic disease. *Nat Rev Genet* **6**(3), 194-205.
- Baraitser, M., Winter, R. M., and Brett, E. M. (1983). Greig cephalopolysyndactyly: report of 13 affected individuals in three families. *Clin Genet* **24**(4), 257-65.
- Biesecker, L. G. (2002). Polydactyly: how many disorders and how many genes? *Am J Med Genet* **112**(3), 279-83.
- Biesecker, L. G. (2006). What you can learn from one gene: GLI3. *J Med Genet* **43**(6), 465-9.

- Bingle, G. J., and Niswander, J. D. (1975). Polydactyly in the American Indian. *Am J Hum Genet* 27(1), 91-9.
- Bond, J., Roberts, E., Mochida, G. H., Hampshire, D. J., Scott, S., Askham, J. M., Springell, K., Mahadevan, M., Crow, Y. J., Markham, A. F., Walsh, C. A., and Woods, C. G. (2002). ASPM is a major determinant of cerebral cortical size. *Nat Genet* 32(2), 316-20.
- Bond, J., Roberts, E., Springell, K., Lizarraga, S. B., Scott, S., Higgins, J., Hampshire, D. J., Morrison, E. E., Leal, G. F., Silva, E. O., Costa, S. M., Baralle, D., Raponi, M., Karbani, G., Rashid, Y., Jafri, H., Bennett, C., Corry, P., Walsh, C. A., and Woods, C. G. (2005). A centrosomal mechanism involving CDK5RAP2 and CENPJ controls brain size. *Nat Genet* 37(4), 353-5.
- Bond, J., Scott, S., Hampshire, D. J., Springell, K., Corry, P., Abramowicz, M. J., Mochida, G. H., Hennekam, R. C., Maher, E. R., Fryns, J. P., Alswaid, A., Jafri, H., Rashid, Y., Mubaidin, A., Walsh, C. A., Roberts, E., and Woods, C. G. (2003). Protein-truncating mutations in ASPM cause variable reduction in brain size. *Am J Hum Genet* 73(5), 1170-7.
- Bosse, K., Betz, R. C., Lee, Y. A., Wienker, T. F., Reis, A., Kleen, H., Propping, P., Cichon, S., and Nothen, M. M. (2000). Localization of a gene for syndactyly type 1 to chromosome 2q34-q36. *Am J Hum Genet* 67(2), 492-7.
- Brand, S., and Rakic, P. (1979). Genesis of the primate neostriatum: [3H]thymidine autoradiographic analysis of the time of neuron origin in the rhesus monkey. *Neuroscience* 4(6), 767-78.
- Broman, K. W., Murray, J. C., Sheffield, V. C., White, R. L., and Weber, J. L. (1998). Comprehensive human genetic maps: individual and sex-specific variation in recombination. *Am J Hum Genet* 63(3), 861-9.
- Brueton, L. A., Huson, S. M., Farren, B., and Winter, R. M. (1990). Oculodentodigital dysplasia and type III syndactyly: separate genetic entities or disease spectrum? *J Med Genet* 27(3), 169-75.
- Castilla, E. E., Paz, J. E., and Orioli-Parreiras, I. M. (1980). Syndactyly: frequency of specific types. *Am J Med Genet* 5(4), 357-64.
- Cenani, A., and Lenz, W. (1967). [Total syndactylia and total radioulnar synostosis in 2 brothers. A contribution on the genetics of syndactylia]. *Z Kinderheilkd* 101(3), 181-90.

- Chenn, A., and McConnell, S. K. (1995). Cleavage orientation and the asymmetric inheritance of Notch1 immunoreactivity in mammalian neurogenesis. *Cell* **82**(4), 631-41.
- Chenn, A., and Walsh, C. A. (2003). Increased neuronal production, enlarged forebrains and cytoarchitectural distortions in beta-catenin overexpressing transgenic mice. *Cereb Cortex* **13**(6), 599-606.
- Chiotaki, R., Petrou, P., Giakoumaki, E., Pavlakis, E., Sitaru, C., and Chalepakis, G. (2007). Spatiotemporal distribution of Frasl/Frem proteins during mouse embryonic development. *Gene Expr. Patterns* **7**, 381-388.
- Cho, J. H., Chang, C. J., Chen, C. Y., and Tang, T. K. (2006). Depletion of CPAP by RNAi disrupts centrosome integrity and induces multipolar spindles. *Biochem Biophys Res Commun* **339**(3), 742-7.
- Cox, J., Jackson, A. P., Bond, J., and Woods, C. G. (2006). What primary microcephaly can tell us about brain growth. *Trends Mol Med* **12**(8), 358-66.
- David, T. J., and Burwood, R. L. (1972). The nature and inheritance of Kirner's deformity. *J Med Genet* **9**(4), 430-3.
- Debeer, P., Schoenmakers, E. F., Twal, W. O., Argraves, W. S., De Smet, L., Fryns, J. P., and Van De Ven, W. J. (2002). The fibulin-1 gene (FBLN1) is disrupted in a t(12;22) associated with a complex type of synpolydactyly. *J Med Genet* **39**(2), 98-104.
- Desir, J., Cassart, M., David, P., Van Bogaert, P., and Abramowicz, M. (2008). Primary microcephaly with ASPM mutation shows simplified cortical gyration with antero-posterior gradient pre- and post-natally. *Am J Med Genet A* **146A**(11), 1439-43.
- Dobbs, M. B., Dietz, F. R., Gurnett, C. A., Morcuende, J. A., Steyers, C. M., and Murray, J. C. (2000). Localization of dominantly inherited isolated triphalangeal thumb to chromosomal region 7q36. *J Orthop Res* **18**(3), 340-4.
- Dobyns, W. B. (2002). Primary microcephaly: new approaches for an old disorder. *Am J Med Genet* **112**(4), 315-7.
- Dolk, H. (1991). The predictive value of microcephaly during the first year of life for mental retardation at seven years. *Dev Med Child Neurol* **33**(11), 974-83.
- Dryden, S. C., Nahhas, F. A., Nowak, J. E., Goustin, A. S., and Tainsky, M. A. (2003). Role for human SIRT2 NAD-dependent deacetylase activity in control of mitotic exit in the cell cycle. *Mol Cell Biol* **23**(9), 3173-85.

- Evans, P. D., Vallender, E. J., and Lahn, B. T. (2006). Molecular evolution of the brain size regulator genes CDK5RAP2 and CENPJ. *Gene* **375**, 75-9.
- Everman, D. B., Bartels, C. F., Yang, Y., Yanamandra, N., Goodman, F. R., Mendoza-Londono, J. R., Savarirayan, R., White, S. M., Graham, J. M., Jr., Gale, R. P., Svarch, E., Newman, W. G., Kleckers, A. R., Francomano, C. A., Govindaiah, V., Singh, L., Morrison, S., Thomas, J. T., and Warman, M. L. (2002). The mutational spectrum of brachydactyly type C. *Am J Med Genet* **112**(3), 291-6.
- Farabee WC (1903). Hereditary and sexual influence in meristic variation: a study of digital malformations in man. *In PhD thesis Harvard University*.
- Finlay, B. L., and Darlington, R. B. (1995). Linked regularities in the development and evolution of mammalian brains. *Science* **268**(5217), 1578-84.
- Fong, K. W., Choi, Y. K., Rattner, J. B., and Qi, R. Z. (2008). CDK5RAP2 is a pericentriolar protein that functions in centrosomal attachment of the gamma-tubulin ring complex. *Mol Biol Cell* **19**(1), 115-25.
- Fujimori, A., Yaoi, T., Ogi, H., Wang, B., Suetomi, K., Sekine, E., Yu, D., Kato, T., Takahashi, S., Okayasu, R., Itoh, K., and Fushiki, S. (2008). Ionizing radiation downregulates ASPM, a gene responsible for microcephaly in humans. *Biochem Biophys Res Commun* **369**(3), 953-7.
- Fujimoto, A., Smolensky, L. S., and Wilson, M. G. (1982). Brachydactyly with major involvement of proximal phalanges. *Clin Genet* **21**(2), 107-11.
- Fujioka, H., Ariga, T., Horiuchi, K., Otsu, M., Igawa, H., Kawashima, K., Yamamoto, Y., Sugihara, T., and Sakiyama, Y. (2005). Molecular analysis of non-syndromic preaxial polydactyly: preaxial polydactyly type-IV and preaxial polydactyly type-I. *Clin Genet* **67**(5), 429-33.
- Furniss, D., Critchley, P., Giele, H., and Wilkie, A. O. (2007). Nonsense-mediated decay and the molecular pathogenesis of mutations in SALL1 and GLI3. *Am J Med Genet A* **143A**(24), 3150-60.
- Furniss, D., Lettice, L. A., Taylor, I. B., Critchley, P. S., Giele, H., Hill, R. E., and Wilkie, A. O. (2008). A variant in the sonic hedgehog regulatory sequence (ZRS) is associated with triphalangeal thumb and deregulates expression in the developing limb. *Hum Mol Genet* **17**(16), 2417-23.

- Galjaard, R. J., Smits, A. P., Tuerlings, J. H., Bais, A. G., Bertoli Avella, A. M., Breedveld, G., de Graaff, E., Oostra, B. A., and Heutink, P. (2003). A new locus for postaxial polydactyly type A/B on chromosome 7q21-q34. *Eur J Hum Genet* **11**(5), 409-15.
- Galjaard, R. J., van der Ham, L. I., Posch, N. A., Dijkstra, P. F., Oostra, B. A., Hovius, S. E., Timmenga, E. J., Sonneveld, G. J., Hoogeboom, A. J., and Heutink, P. (2001). Differences in complexity of isolated brachydactyly type C cannot be attributed to locus heterogeneity alone. *Am J Med Genet* **98**(3), 256-62.
- Gao, B., Guo, J., She, C., Shu, A., Yang, M., Tan, Z., Yang, X., Guo, S., Feng, G., and He, L. (2001). Mutations in IHH, encoding Indian hedgehog, cause brachydactyly type A-I. *Nat Genet* **28**(4), 386-8.
- Garshasbi, M., Motazacker, M. M., Kahrizi, K., Behjati, F., Abedini, S. S., Nieh, S. E., Firouzabadi, S. G., Becker, C., Ruschendorf, F., Nurnberg, P., Tzschach, A., Vazifehmand, R., Erdogan, F., Ullmann, R., Lenzner, S., Kuss, A. W., Ropers, H. H., and Najmabadi, H. (2006). SNP array-based homozygosity mapping reveals MCPHI deletion in family with autosomal recessive mental retardation and mild microcephaly. *Hum Genet* **118**(6), 708-15.
- Ghadami, M., Majidzadeh, A. K., Haerian, B. S., Damavandi, E., Yamada, K., Pasallar, P., Najafi, M. T., Nishimura, G., Tomita, H. A., Yoshiura, K. I., and Niikawa, N. (2001). Confirmation of genetic homogeneity of syndactyly type I in an Iranian family. *Am J Med Genet* **104**(2), 147-51.
- Gilbert, S. L., Dobyns, W. B., and Lahn, B. T. (2005). Genetic links between brain development and brain evolution. *Nat Rev Genet* **6**(7), 581-90.
- Gillessen-Kaesbach, G., and Majewski, F. (1991). Bilateral complete polysyndactyly (type IV Haas). *Am J Med Genet* **38**(1), 29-31.
- Gladwin, A., Donnai, D., Metcalfe, K., Schrandt-Stumpel, C., Brueton, L., Verloes, A., Aylsworth, A., Toriello, H., Winter, R., and Dixon, M. (1997). Localization of a gene for oculodentodigital syndrome to human chromosome 6q22-q24. *Hum Mol Genet* **6**(1), 123-7.
- Goodman, F. R., Mundlos, S., Muragaki, Y., Donnai, D., Giovannucci-Uzielli, M. L., Lapi, E., Majewski, F., McGaughan, J., McKeown, C., Reardon, W., Upton, J., Winter, R. M.,

- Olsen, B. R., and Scambler, P. J. (1997). Synpolydactyly phenotypes correlate with size of expansions in HOXD13 polyalanine tract. *Proc Natl Acad Sci U S A* **94**(14), 7458-63.
- Gul, A., Hassan, M. J., Hussain, S., Raza, S. I., Chishti, M. S., and Ahmad, W. (2006a). A novel deletion mutation in CENPJ gene in a Pakistani family with autosomal recessive primary microcephaly. *J Hum Genet* **51**(9), 760-4.
- Gul, A., Hassan, M. J., Mahmood, S., Chen, W., Rahmani, S., Naseer, M. I., Dellefave, L., Muhammad, N., Rafiq, M. A., Ansar, M., Chishti, M. S., Ali, G., Siddique, T., and Ahmad, W. (2006b). Genetic studies of autosomal recessive primary microcephaly in 33 Pakistani families: Novel sequence variants in ASPM gene. *Neurogenetics* **7**(2), 105-10.
- Gul, A., Hassan, M. J., Mahmood, S., Chen, W., Rahmani, S., Naseer, M. I., Dellefave, L., Muhammad, N., Rafiq, M. A., Ansar, M., Chishti, M. S., Ali, G., Siddique, T., and Ahmad, W. (2006c). Genetic studies of autosomal recessive primary microcephaly in 33 Pakistani families: novel sequence variants in ASPM gene. *Neurogenetics*.
- Gul, A., Tariq, M., Khan, M. N., Hassan, M. J., Ali, G., and Ahmad, W. (2007). Novel protein-truncating mutations in the ASPM gene in families with autosomal recessive primary microcephaly. *J Neurogenet* **21**(3), 153-63.
- Gurnett, C. A., Bowcock, A. M., Dietz, F. R., Morcuende, J. A., Murray, J. C., and Dobbs, M. B. (2007). Two novel point mutations in the long-range SHH enhancer in three families with triphalangeal thumb and preaxial polydactyly. *Am J Med Genet A* **143**(1), 27-32.
- Hagemann, C., Anacker, J., Gerngras, S., Kuhnel, S., Said, H. M., Patel, R., Kammerer, U., Vordermark, D., Roosen, K., and Vince, G. H. (2008). Expression analysis of the autosomal recessive primary microcephaly genes MCPH1 (microcephalin) and MCPH5 (ASPM, abnormal spindle-like, microcephaly associated) in human malignant gliomas. *Oncol Rep* **20**(2), 301-8.
- Haldane, J. B. S. (1919). The mapping function. *J Genet* **8**, 299-309.
- Hall, C. M. (2002). International nosology and classification of constitutional disorders of bone (2001). *Am J Med Genet* **113**(1), 65-77.
- Haydar, T. F., Ang, E., Jr., and Rakic, P. (2003). Mitotic spindle rotation and mode of cell division in the developing telencephalon. *Proc Natl Acad Sci U S A* **100**(5), 2890-5.
- Hoffmann, K., and Lindner, T. H. (2005). easyLINKAGE-Plus--automated linkage analyses using large-scale SNP data. *Bioinformatics* **21**, 3565-3567.

- Hortling, H., Puupponen, E., and Koski, K. (1960). Short-metacarpal or metatarsal bones: pseudo-pseudohypoparathyroidism. *J Clin Endocrinol Metab* **20**, 466-72.
- Hung, L. Y., Chen, H. L., Chang, C. W., Li, B. R., and Tang, T. K. (2004). Identification of a novel microtubule-destabilizing motif in CPAP that binds to tubulin heterodimers and inhibits microtubule assembly. *Mol Biol Cell* **15**(6), 2697-706.
- Ishikiriyama, S., Sawada, H., Nambu, H., and Niikawa, N. (1991). Crossed polydactyly type I in a mother and son: an autosomal dominant trait? *Am J Med Genet* **40**(1), 41-3.
- Izraeli, S., Lowe, L. A., Bertness, V. L., Good, D. J., Dorward, D. W., Kirsch, I. R., and Kuehn, M. R. (1999). The SIL gene is required for mouse embryonic axial development and left-right specification. *Nature* **399**(6737), 691-4.
- Jackson, A. P., Eastwood, H., Bell, S. M., Adu, J., Toomes, C., Carr, I. M., Roberts, E., Hampshire, D. J., Crow, Y. J., Mighell, A. J., Karbani, G., Jafri, H., Rashid, Y., Mueller, R. F., Markham, A. F., and Woods, C. G. (2002). Identification of microcephalin, a protein implicated in determining the size of the human brain. *Am J Hum Genet* **71**, 136-42.
- Jackson, A. P., McHale, D. P., Campbell, D. A., Jafri, H., Rashid, Y., Mannan, J., Karbani, G., Corry, P., Levene, M. I., Mueller, R. F., Markham, A. F., Lench, N. J., and Woods, C. G. (1998). Primary autosomal recessive microcephaly (MCPH1) maps to chromosome 8p22-pter. *Am J Hum Genet* **63**(2), 541-6.
- Jadeja, S., Smyth, I., Pitera, J. E., Taylor, M. S., van Haelst, M., Bentley, E., McGregor, L., Hopkins, J., Chalepakis, G., Philip, N., Perez Aytes, A., Watt, F. M., Darling, S. M., Jackson, I., Woolf, A. S., and Scambler, P. J. (2005). Identification of a new gene mutated in Fraser syndrome and mouse myelencephalic blebs. *Nat Genet* **37**(5), 520-5.
- James, J. I., and Lamb, D. W. (1963). Congenital Abnormalities of the Limbs. *Practitioner* **191**, 159-72.
- Jamieson, C. R., Fryns, J. P., Jacobs, J., Matthijs, G., and Abramowicz, M. J. (2000). Primary autosomal recessive microcephaly: MCPH5 maps to 1q25-q32. *Am J Hum Genet* **67**(6), 1575-7.
- Jamieson, C. R., Govaerts, C., and Abramowicz, M. J. (1999). Primary autosomal recessive microcephaly: homozygosity mapping of MCPH4 to chromosome 15. *Am J Hum Genet* **65**(5), 1465-9.

- Johnson, D., Kan, S. H., Oldridge, M., Trembath, R. C., Roche, P., Esnouf, R. M., Giele, H., and Wilkie, A. O. (2003). Missense mutations in the homeodomain of HOXD13 are associated with brachydactyly types D and E. *Am J Hum Genet* 72(4), 984-97.
- Johnston, J. J., Olivos-Glander, I., Killoran, C., Elson, E., Turner, J. T., Peters, K. F., Abbott, M. H., Aughton, D. J., Aylsworth, A. S., Bamshad, M. J., Booth, C., Curry, C. J., David, A., Dinulos, M. B., Flannery, D. B., Fox, M. A., Graham, J. M., Grange, D. K., Guttmacher, A. E., Hannibal, M. C., Henn, W., Hennekam, R. C., Holmes, L. B., Hoyme, H. E., Leppig, K. A., Lin, A. E., Macleod, P., Manchester, D. K., Marcelis, C., Mazzanti, L., McCann, E., McDonald, M. T., Mendelsohn, N. J., Moeschler, J. B., Moghaddam, B., Neri, G., Newbury-Ecob, R., Pagon, R. A., Phillips, J. A., Sadler, L. S., Stoler, J. M., Tilstra, D., Walsh Vockley, C. M., Zackai, E. H., Zadeh, T. M., Brueton, L., Black, G. C., and Biesecker, L. G. (2005). Molecular and clinical analyses of Greig cephalopolysyndactyly and Pallister-Hall syndromes: robust phenotype prediction from the type and position of GLI3 mutations. *Am J Hum Genet* 76(4), 609-22.
- Johnston, O., and Kirby, V. V., Jr. (1955). Syndactyly of the ring and little finger. *Am J Hum Genet* 7(1), 80-2.
- Kalff-Suske, M., Wild, A., Topp, J., Wessling, M., Jacobsen, E. M., Bornholdt, D., Engel, H., Heuer, H., Aalfs, C. M., Ausems, M. G., Barone, R., Herzog, A., Heutink, P., Homfray, T., Gillessen-Kaesbach, G., Konig, R., Kunze, J., Meinecke, P., Muller, D., Rizzo, R., Streng, S., Superti-Furga, A., and Grzeschik, K. H. (1999). Point mutations throughout the GLI3 gene cause Greig cephalopolysyndactyly syndrome. *Hum Mol Genet* 8(9), 1769-77.
- Kang, S., Graham, J. M., Jr., Olney, A. H., and Biesecker, L. G. (1997). GLI3 frameshift mutations cause autosomal dominant Pallister-Hall syndrome. *Nat Genet* 15(3), 266-8.
- Kemp, T., and Ravn, J. (1932). Ueber erbliche Hand-und Fussdeformitaeten in einem 140-koepfigen Geschlecht, nebst einigen Bemerkungen ueber Poly-und Syndaktylie beim Menschen. *Acta Psychiat. Neurol. Scand.* 7, 275-296.
- Kirner, J. (1927). Doppelseitige Verkrummungen des Kleinfingerendgliedés als selbstandiges Krankheitsbild. *Fortschr Geb Roentgenstr Nuklearmed* 36, 804.
- Kiyozumi, D., Osada, A., Sugimoto, N., Weber, C. N., Ono, Y., Imai, T., Okada, A., and Sekiguchi, K. (2005). Identification of a novel cell-adhesive protein spatiotemporally

- expressed in the basement membrane of mouse developing hair follicle. *Exp Cell Res* **306**(1), 9-23.
- Kiyozumi, D., Sugimoto, N., and Sekiguchi, K. (2006). Breakdown of the reciprocal stabilization of QBRICK/Frem1, Fras1, and Frem2 at the basement membrane provokes Fraser syndrome-like defects. *Proc Natl Acad Sci U S A* **103**(32), 11981-6.
- Kjaer, K. W., Eiberg, H., Hansen, L., van der Hagen, C. B., Rosendahl, K., Tommerup, N., and Mundlos, S. (2006). A mutation in the receptor binding site of GDF5 causes Mohr-Wriedt brachydactyly type A2. *J Med Genet* **43**(3), 225-31.
- Kjaer, K. W., Hansen, L., Eiberg, H., Utkus, A., Skovgaard, L. T., Leicht, P., Opitz, J. M., and Tommerup, N. (2005). A 72-year-old Danish puzzle resolved--comparative analysis of phenotypes in families with different-sized HOXD13 polyalanine expansions. *Am J Med Genet A* **138**(4), 328-39.
- Klopocki, E., Ott, C. E., Benatar, N., Ullmann, R., Mundlos, S., and Lehmann, K. (2008). A microduplication of the long range SHH limb regulator (ZRS) is associated with triphalangeal thumb-polysyndactyly syndrome. *J Med Genet* **45**(6), 370-5.
- Komai, T., Kishimoto, K., and Ozaki, Y. (1955). Genetic study of microcephaly based on Japanese material. *Am J Hum Genet* **7**(1), 51-65.
- Kong, A., Gudbjartsson, D. F., Sainz, J., Jonsdottir, G. M., Gudjonsson, S. A., Richardsson, B., Sigurdardottir, S., Barnard, J., Hallbeck, B., Masson, G., Shlien, A., Palsson, S. T., Frigge, M. L., Thorgeirsson, T. E., Gulcher, J. R., and Stefansson, K. (2002). A high-resolution recombination map of the human genome. *Nat Genet* **31**(3), 241-7.
- Kouprina, N., Pavlicek, A., Collins, N. K., Nakano, M., Noskov, V. N., Ohzeki, J., Mochida, G. H., Risinger, J. I., Goldsmith, P., Gunsior, M., Solomon, G., Gersch, W., Kim, J. H., Barrett, J. C., Walsh, C. A., Jurka, J., Masumoto, H., and Larionov, V. (2005). The microcephaly ASPM gene is expressed in proliferating tissues and encodes for a mitotic spindle protein. *Hum Mol Genet* **14**(15), 2155-65.
- Kouprina, N., Pavlicek, A., Mochida, G. H., Solomon, G., Gersch, W., Yoon, Y. H., Collura, R., Ruvolo, M., Barrett, J. C., Woods, C. G., Walsh, C. A., Jurka, J., and Larionov, V. (2004). Accelerated evolution of the ASPM gene controlling brain size begins prior to human brain expansion. *PLoS Biol* **2**(5), E126.

- Kumar, A., Blanton, S. H., Babu, M., Markandaya, M., and Girimaji, S. C. (2004). Genetic analysis of primary microcephaly in Indian families: novel ASPM mutations. *Clin Genet* **66**(4), 341-8.
- Kumar, A., Girimaji, S. C., Duvvari, M. R., and Blanton, S. H. (2009). Mutations in STIL, encoding a pericentriolar and centrosomal protein, cause primary microcephaly. *Am J Hum Genet* **84**(2), 286-90.
- Kumar, A., Markandaya, M., and Girimaji, S. C. (2002). Primary microcephaly: microcephalin and ASPM determine the size of the human brain. *J Biosci* **27**(7), 629-32.
- Lander, E. S., and Botstein, D. (1987). Homozygosity mapping: a way to map human recessive traits with the DNA of inbred children. *Science* **236**(4808), 1567-1570.
- Leal, G. F., Roberts, E., Silva, E. O., Costa, S. M., Hampshire, D. J., and Woods, C. G. (2003). A novel locus for autosomal recessive primary microcephaly (MCPH6) maps to 13q12.2. *J Med Genet* **40**(7), 540-2.
- Lehmann, K., Seemann, P., Silan, F., Goecke, T. O., Irgang, S., Kjaer, K. W., Kjaergaard, S., Mahoney, M. J., Morlot, S., Reissner, C., Kerr, B., Wilkie, A. O., and Mundlos, S. (2007). A new subtype of brachydactyly type B caused by point mutations in the bone morphogenetic protein antagonist NOGGIN. *Am J Hum Genet* **81**(2), 388-96.
- Lehmann, K., Seemann, P., Stricker, S., Sammar, M., Meyer, B., Suring, K., Majewski, F., Tinschert, S., Grzeschik, K. H., Muller, D., Knaus, P., Nurnberg, P., and Mundlos, S. (2003). Mutations in bone morphogenetic protein receptor 1B cause brachydactyly type A2. *Proc Natl Acad Sci U S A* **100**(21), 12277-82.
- Lettice, L. A., Heaney, S. J., Purdie, L. A., Li, L., de Beer, P., Oostra, B. A., Goode, D., Elgar, G., Hill, R. E., and de Graaff, E. (2003). A long-range Shh enhancer regulates expression in the developing limb and fin and is associated with preaxial polydactyly. *Hum Mol Genet* **12**(14), 1725-35.
- Lettice, L. A., Hill, A. E., Devenney, P. S., and Hill, R. E. (2008). Point mutations in a distant sonic hedgehog cis-regulator generate a variable regulatory output responsible for preaxial polydactyly. *Hum Mol Genet* **17**(7), 978-85.
- Li, K., and Kaufman, T. C. (1996). The homeotic target gene centrosomin encodes an essential centrosomal component. *Cell* **85**(4), 585-96.

- Lonardo, F., Della Monica, M., Riccardi, G., Riccio, I., Riccio, V., and Scarano, G. (2004). A family with X-linked recessive fusion of metacarpals IV and V. *Am J Med Genet A* **124A**(4), 407-10.
- Loots, G. G., Ovcharenko, I., Pachter, L., Dubchak, I., and Rubin, E. M. (2002). rVista for comparative sequence-based discovery of functional transcription factor binding sites. *Genome Res* **12**(5), 832-9.
- Lueken, K. G. (1938). Ueber eine Familie mit Syndaktylie. *Z. Mensch. Vererb. Konstitutionsl* **22**, 152-159.
- Malik, S., Abbasi, A. A., Ansar, M., Ahmad, W., Koch, M. C., and Grzeschik, K. H. (2006). Genetic heterogeneity of synpolydactyly: a novel locus SPD3 maps to chromosome 14q11.2-q12. *Clin Genet* **69**(6), 518-24.
- Malik, S., Ahmad, W., Grzeschik, K. H., and Koch, M. C. (2005a). A simple method for characterising syndactyly in clinical practice. *Genet Couns* **16**(3), 229-38.
- Malik, S., Arshad, M., Amin-Ud-Din, M., Oeffner, F., Dempfle, A., Haque, S., Koch, M. C., Ahmad, W., and Grzeschik, K. H. (2004). A novel type of autosomal recessive syndactyly: clinical and molecular studies in a family of Pakistani origin. *Am J Med Genet A* **126A**(1), 61-7.
- Malik, S., Girisha, K. M., Wajid, M., Roy, A. K., Phadke, S. R., Haque, S., Ahmad, W., Koch, M. C., and Grzeschik, K. H. (2007). Synpolydactyly and HOXD13 polyalanine repeat: addition of 2 alanine residues is without clinical consequences. *BMC Med Genet* **8**, 78.
- Malik, S., Schott, J., Ali, S. W., Oeffner, F., Amin-ud-Din, M., Ahmad, W., Grzeschik, K. H., and Koch, M. C. (2005b). Evidence for clinical and genetic heterogeneity of syndactyly type I: the phenotype of second and third toe syndactyly maps to chromosome 3p21.31. *Eur J Hum Genet* **13**(12), 1268-74.
- Manoiloff, E. O. (1931). A rare case of hereditary hexadactylism. *Am. J. Phys. Anthropol.* **15**, 503-508.
- Masuya, H., Sezutsu, H., Sakuraba, Y., Sagai, T., Hosoya, M., Kaneda, H., Miura, I., Kobayashi, K., Sumiyama, K., Shimizu, A., Nagano, J., Yokoyama, H., Kaneko, S., Sakurai, N., Okagaki, Y., Noda, T., Wakana, S., Gondo, Y., and Shiroishi, T. (2007). A series of ENU-induced single-base substitutions in a long-range cis-element altering Sonic hedgehog expression in the developing mouse limb bud. *Genomics* **89**(2), 207-14.

- McClintic, B. S. (1935). Five generations of polydactylism. *J. Hered.* **26**, 141-144.
- McCreary, B. D., Rossiter, J. P., and Robertson, D. M. (1996). Recessive (true) microcephaly: a case report with neuropathological observations. *J Intellect Disabil Res* **40 (Pt 1)**, 66-70.
- McGregor, L., Makela, V., Darling, S. M., Vrontou, S., Chalepakis, G., Roberts, C., Smart, N., Rutland, P., Prescott, N., Hopkins, J., Bentley, E., Shaw, A., Roberts, E., Mueller, R., Jadeja, S., Philip, N., Nelson, J., Francannet, C., Perez-Aytes, A., Megarbane, A., Kerr, B., Wainwright, B., Woolf, A. S., Winter, R. M., and Scambler, P. J. (2003). Fraser syndrome and mouse blebbed phenotype caused by mutations in FRAS1/Fras1 encoding a putative extracellular matrix protein. *Nat Genet* **34**(2), 203-8.
- McKusick, V. A., and Milch, R. A. (1964). The clinical behavior of genetic disease: selected aspects. *Clin Orthop Relat Res* **33**, 22-39.
- Mochida, G. H., and Walsh, C. A. (2001). Molecular genetics of human microcephaly. *Curr Opin Neurol* **14**(2), 151-6.
- Morton, N. E. (1955). Sequential tests for the detection of linkage. *Am J Hum Genet* **7**(3), 277-318.
- Moynihan, L., Jackson, A. P., Roberts, E., Karbani, G., Lewis, I., Corry, P., Turner, G., Mueller, R. F., Lench, N. J., and Woods, C. G. (2000). A third novel locus for primary autosomal recessive microcephaly maps to chromosome 9q34. *Am J Hum Genet* **66**(2), 724-7.
- Muragaki, Y., Mundlos, S., Upton, J., and Olsen, B. R. (1996). Altered growth and branching patterns in synpolydactyly caused by mutations in HOXD13. *Science* **272**(5261), 548-51.
- Neitzel, H., Neumann, L. M., Schindler, D., Wirges, A., Tonnies, H., Trimborn, M., Krebsova, A., Richter, R., and Sperling, K. (2002). Premature chromosome condensation in humans associated with microcephaly and mental retardation: a novel autosomal recessive condition. *Am J Hum Genet* **70**(4), 1015-22.
- Nicholas, A., Woods, G., Swanson, E., Cox, J., Karbani, G., Malik, S., Springel, K., Hampshire, D., Ahmed, M., Bond, J., Di Benedetto, D., Fichera, M., Romano, C., and Dobyns, W. (2008). The molecular landscape of ASPM mutations in primary microcephaly. *J Med Genet.*
- Nicolai, J. P., and Schoch, S. L. (1986). Polydactyly in the Bible. *J Hand Surg [Am]* **11**(2), 293.

- Niswander, L., Tickle, C., Vogel, A., Booth, I., and Martin, G. R. (1993). FGF-4 replaces the apical ectodermal ridge and directs outgrowth and patterning of the limb. *Cell* **75**(3), 579-87.
- Ott, J. (1985). Analysis of human genetic linkage. *The Johns Hopkins University Press, Baltimore, Maryland.*
- Ott, J. (1991). Analysis of human genetic linkage, Rev. ed. *The Johns Hopkins University Press, Baltimore, Maryland.*
- Parr, B. A., and McMahon, A. P. (1995). Dorsalizing signal Wnt-7a required for normal polarity of D-V and A-P axes of mouse limb. *Nature* **374**(6520), 350-3.
- Pattison, L., Crow, Y. J., Deeble, V. J., Jackson, A. P., Jafri, H., Rashid, Y., Roberts, E., and Woods, C. G. (2000). A fifth locus for primary autosomal recessive microcephaly maps to chromosome 1q31. *Am J Hum Genet* **67**(6), 1578-80.
- Paznekas, W. A., Boyadjiev, S. A., Shapiro, R. E., Daniels, O., Wollnik, B., Keegan, C. E., Innis, J. W., Dinulos, M. B., Christian, C., Hannibal, M. C., and Jabs, E. W. (2003). Connexin 43 (GJA1) mutations cause the pleiotropic phenotype of oculodentodigital dysplasia. *Am J Hum Genet* **72**(2), 408-18.
- Percin, E. F., Percin, S., Egilmez, H., Sezgin, I., Ozbas, F., and Akarsu, A. N. (1998). Mesoaxial complete syndactyly and synostosis with hypoplastic thumbs: an unusual combination or homozygous expression of syndactyly type I? *J Med Genet* **35**(10), 868-74.
- Pfaff, K. L., Straub, C. T., Chiang, K., Bear, D. M., Zhou, Y., and Zon, L. I. (2007). The zebra fish cassiopeia mutant reveals that SIL is required for mitotic spindle organization. *Mol Cell Biol* **27**(16), 5887-97.
- Pichon, B., Vankercckhove, S., Bourrouillou, G., Duprez, L., and Abramowicz, M. J. (2004). A translocation breakpoint disrupts the ASPM gene in a patient with primary microcephaly. *Eur J Hum Genet* **12**(5), 419-21.
- Polinkovsky, A., Robin, N. H., Thomas, J. T., Irons, M., Lynn, A., Goodman, F. R., Reardon, W., Kant, S. G., Brunner, H. G., van der Burgt, I., Chitayat, D., McGaughan, J., Donnai, D., Luyten, F. P., and Warman, M. L. (1997). Mutations in CDMP1 cause autosomal dominant brachydactyly type C. *Nat Genet* **17**(1), 18-9.
- Ponting, C., and Jackson, A. P. (2005). Evolution of primary microcephaly genes and the enlargement of primate brains. *Curr Opin Genet Dev* **15**(3), 241-8.

- Ponting, C. P. (2006). A novel domain suggests a ciliary function for ASPM, a brain size determining gene. *Bioinformatics* **22**(9), 1031-5.
- Radhakrishna, U., Blouin, J. L., Mehenni, H., Patel, U. C., Patel, M. N., Solanki, J. V., and Antonarakis, S. E. (1997a). Mapping one form of autosomal dominant postaxial polydactyly type A to chromosome 7p15-q11.23 by linkage analysis. *Am J Hum Genet* **60**(3), 597-604.
- Radhakrishna, U., Bornholdt, D., Scott, H. S., Patel, U. C., Rossier, C., Engel, H., Bottani, A., Chandal, D., Blouin, J. L., Solanki, J. V., Grzeschik, K. H., and Antonarakis, S. E. (1999). The phenotypic spectrum of GLI3 morphopathies includes autosomal dominant preaxial polydactyly type-IV and postaxial polydactyly type-A/B; No phenotype prediction from the position of GLI3 mutations. *Am J Hum Genet* **65**(3), 645-55.
- Radhakrishna, U., Wild, A., Grzeschik, K. H., and Antonarakis, S. E. (1997b). Mutation in GLI3 in postaxial polydactyly type A. *Nat Genet* **17**(3), 269-71.
- Ray, A. K., and Haldane, J. B. (1965). The genetics of a common Indian digital abnormality. *Proc Natl Acad Sci U S A* **53**(5), 1050-3.
- Roberts, E., Hampshire, D. J., Pattison, L., Springell, K., Jafri, H., Corry, P., Mannon, J., Rashid, Y., Crow, Y., Bond, J., and Woods, C. G. (2002). Autosomal recessive primary microcephaly: an analysis of locus heterogeneity and phenotypic variation. *J Med Genet* **39**(10), 718-21.
- Roberts, E., Jackson, A. P., Carradice, A. C., Deeble, V. J., Mannan, J., Rashid, Y., Jafri, H., McHale, D. P., Markham, A. F., Lench, N. J., and Woods, C. G. (1999). The second locus for autosomal recessive primary microcephaly (MCPH2) maps to chromosome 19q13.1-13.2. *Eur J Hum Genet* **7**(7), 815-20.
- Robinow, M., Johnson, G. F., and Broock, G. J. (1982). Syndactyly type V. *Am J Med Genet* **11**(4), 475-82.
- Sagai, T., Masuya, H., Tamura, M., Shimizu, K., Yada, Y., Wakana, S., Gondo, Y., Noda, T., and Shiroishi, T. (2004). Phylogenetic conservation of a limb-specific, cis-acting regulator of Sonic hedgehog (Shh). *Mamm Genome* **15**(1), 23-34.
- Sarfarazi, M., Akarsu, A. N., and Sayli, B. S. (1995). Localization of the syndactyly type II (synpolydactyly) locus to 2q31 region and identification of tight linkage to HOXD8 intragenic marker. *Hum Mol Genet* **4**(8), 1453-8.

- Sayli, B. S., Akarsu, A. N., Sayli, U., Akhan, O., Ceylaner, S., and Sarfarazi, M. (1995). A large Turkish kindred with syndactyly type II (synpolydactyly). I. Field investigation, clinical and pedigree data. *J Med Genet* **32**(6), 421-34.
- Schwabe, G. C., and Mundlos, S. (2004). Genetics of congenital hand anomalies. *Handchir Mikrochir Plast Chir* **36**(2-3), 85-97.
- Schwabe, G. C., Tinschert, S., Buschow, C., Meinecke, P., Wolff, G., Gillesen-Kaesbach, G., Oldridge, M., Wilkie, A. O., Komec, R., and Mundlos, S. (2000). Distinct mutations in the receptor tyrosine kinase gene ROR2 cause brachydactyly type B. *Am J Hum Genet* **67**(4), 822-31.
- Schwabe, G. C., Turkmen, S., Leschik, G., Palanduz, S., Stover, B., Goecke, T. O., and Mundlos, S. (2004). Brachydactyly type C caused by a homozygous missense mutation in the prodomain of CDMP1. *Am J Med Genet A* **124A**(4), 356-63.
- Seemann, P., Schwappacher, R., Kjaer, K. W., Krakow, D., Lehmann, K., Dawson, K., Stricker, S., Pohl, J., Ploger, F., Staub, E., Nickel, J., Sebald, W., Knaus, P., and Mundlos, S. (2005). Activating and deactivating mutations in the receptor interaction site of GDF5 cause symphalangism or brachydactyly type A2. *J Clin Invest* **115**(9), 2373-81.
- Shen, J., Eyaid, W., Mochida, G. H., Al-Moayyad, F., Bodell, A., Woods, C. G., and Walsh, C. A. (2005). ASPM mutations identified in patients with primary microcephaly and seizures. *J Med Genet* **42**(9), 725-9.
- Slavotinek, A. M., and Tiffit, C. J. (2002). Fraser syndrome and cryptophthalmos: review of the diagnostic criteria and evidence for phenotypic modules in complex malformation syndromes. *J Med Genet* **39**(9), 623-33.
- Smyth, I., Du, X., Taylor, M. S., Justice, M. J., Beutler, B., and Jackson, I. J. (2004). The extracellular matrix gene *Frem1* is essential for the normal adhesion of the embryonic epidermis. *Proc Natl Acad Sci U S A* **101**(37), 13560-5.
- Sugarman, G. I., Hager, D., and Kulik, W. J. (1974). A new syndrome of brachydactyly of the hands and feet with duplication of the first toes. *Birth Defects Orig Artic Ser* **10**(5), 1-8.
- Sun, M., Ma, F., Zeng, X., Liu, Q., Zhao, X. L., Wu, F. X., Wu, G. P., Zhang, Z. F., Gu, B., Zhao, Y. F., Tian, S. H., Lin, B., Kong, X. Y., Zhang, X. L., Yang, W., Lo, W. H., and Zhang, X. (2008). Triphalangeal thumb-polysyndactyly syndrome and syndactyly type IV

- are caused by genomic duplications involving the long range, limb-specific SHH enhancer. *J Med Genet* **45**(9), 589-95.
- Swanson, A. B., and Brown, K. S. (1962). Hereditary triphalangeal thumb. *J. Hered.* **53**, 259-265.
- Takahashi, T., Nowakowski, R. S., and Caviness, V. S., Jr. (1995). The cell cycle of the pseudostratified ventricular epithelium of the embryonic murine cerebral wall. *J Neurosci* **15**(9), 6046-57.
- Temtamy, S. A., and McKusick, V. A. (1978). The genetics of hand malformations. *Birth Defects Orig Artic Ser* **14**(3), i-xviii, 1-619.
- Terada, Y., Uetake, Y., and Kuriyama, R. (2003). Interaction of Aurora-A and centrosomin at the microtubule-nucleating site in *Drosophila* and mammalian cells. *J Cell Biol* **162**(5), 757-63.
- Timmer, J. R., Mak, T. W., Manova, K., Anderson, K. V., and Niswander, L. (2005). Tissue morphogenesis and vascular stability require the Frem2 protein, product of the mouse myelencephalic blebs gene. *Proc Natl Acad Sci U S A* **102**(33), 11746-50.
- Tolmie, J. L., McNay, M., Stephenson, J. B., Doyle, D., and Connor, J. M. (1987). Microcephaly; genetic counselling and antenatal diagnosis after the birth of an affected child. *Am J Med Genet* **27**(3), 583-94.
- Tommerup, N., Mortensen, E., Nielsen, M. H., Wegner, R. D., Schindler, D., and Mikkelsen, M. (1993). Chromosomal breakage, endomitosis, endoreduplication, and hypersensitivity toward radiomimetic and alkylating agents: a possible new autosomal recessive mutation in a girl with craniosynostosis and microcephaly. *Hum Genet* **92**(4), 339-46.
- Trimborn, M., Bell, S. M., Felix, C., Rashid, Y., Jafri, H., Griffiths, P. D., Neumann, L. M., Krebs, A., Reis, A., Sperling, K., Neitzel, H., and Jackson, A. P. (2004). Mutations in microcephalin cause aberrant regulation of chromosome condensation. *Am J Hum Genet* **75**(2), 261-6.
- Trimborn, M., Richter, R., Sternberg, N., Gavvovidis, I., Schindler, D., Jackson, A. P., Prott, E. C., Sperling, K., Gillessen-Kaesbach, G., and Neitzel, H. (2005). The first missense alteration in the MCPHI gene causes autosomal recessive microcephaly with an extremely mild cellular and clinical phenotype. *Hum Mutat* **26**(5), 496.

- Trimborn, M., Schindler, D., Neitzel, H., and Hirano, T. (2006). Misregulated chromosome condensation in MCPH1 primary microcephaly is mediated by condensin II. *Cell Cycle* 5(3), 322-6.
- Tsukurov, O., Boehmer, A., Flynn, J., Nicolai, J. P., Hamel, B. C., Traill, S., Zaleske, D., Mankin, H. J., Yeon, H., Ho, C., and et al. (1994). A complex bilateral polysyndactyly disease locus maps to chromosome 7q36. *Nat Genet* 6(3), 282-6.
- Van Den Bosch, J. (1959). Microcephaly in the Netherlands: a clinical and genetical study. *Ann Hum Genet* 23(2), 91-116.
- van Haelst, M. M., Maiburg, M., Baujat, G., Jadeja, S., Monti, E., Bland, E., Pearce, K., Hennekam, R. C., and Scambler, P. J. (2008). Molecular study of 33 families with Fraser syndrome new data and mutation review. *Am J Med Genet A* 146A(17), 2252-7.
- Vortkamp, A., Gessler, M., and Grzeschik, K. H. (1995). Identification of optimized target sequences for the GLI3 zinc finger protein. *DNA Cell Biol* 14(7), 629-34.
- Wang, Y. Q., and Su, B. (2004). Molecular evolution of microcephalin, a gene determining human brain size. *Hum Mol Genet* 13(11), 1131-7.
- Wang, Z. Q., Tian, S. H., Shi, Y. Z., Zhou, P. T., Wang, Z. Y., Shu, R. Z., Hu, L., and Kong, X. (2007). A single C to T transition in intron 5 of LMBR1 gene is associated with triphalangeal thumb-polysyndactyly syndrome in a Chinese family. *Biochem Biophys Res Commun* 355(2), 312-7.
- Woods, C. G., Bond, J., and Enard, W. (2005). Autosomal recessive primary microcephaly (MCPH): a review of clinical, molecular, and evolutionary findings. *Am J Hum Genet* 76(5), 717-28.
- Zhang, J. (2003). Evolution of the human ASPM gene, a major determinant of brain size. *Genetics* 165(4), 2063-70.
- Zhao, H., Tian, Y., Breedveld, G., Huang, S., Zou, Y., Y, J., Chai, J., Li, H., Li, M., Oostra, B. A., Lo, W. H., and Heutink, P. (2002). Postaxial polydactyly type A/B (PAP-A/B) is linked to chromosome 19p13.1-13.2 in a Chinese kindred. *Eur J Hum Genet* 10(3), 162-6.
- Zhao, X., Sun, M., Zhao, J., Leyva, J. A., Zhu, H., Yang, W., Zeng, X., Ao, Y., Liu, Q., Liu, G., Lo, W. H., Jabs, E. W., Amzel, L. M., Shan, X., and Zhang, X. (2007). Mutations in

- HOXD13 underlie syndactyly type V and a novel brachydactyly-syndactyly syndrome. *Am J Hum Genet* **80**(2), 361-71.
- Zhao, J., Ding, J., Li, Y., Ren, K., Sha, J., Zhu, M., and Gao, X. (2009). HnRNP U mediates the long-range regulation of Shh expression during limb development. *Hum Mol Genet* **18**(16), 3090-7.
- Zhong, X., Liu, L., Zhao, A., Pfeifer, G. P., and Xu, X. (2005). The abnormal spindle-like, microcephaly-associated (ASPM) gene encodes a centrosomal protein. *Cell Cycle* **4**(9), 1227-9.

Appendix

Preaxial polydactyly/triphalangeal thumb is associated with changed transcription factor-binding affinity in a family with a novel point mutation in the long-range *cis*-regulatory element ZRS

Muhammad Farooq¹, Jesper T Troelsen², Mette Boyd², Hans Eiberg², Lars Hansen³, Muhammad Sajid Hussain¹, Shoaib ur Rehman¹, Aysha Azhar¹, Amjad Ali¹, Syeda Marriam Bakhtiar¹, Niels Tommerup³, Shahid Mahmood Baig^{*1} and Klaus W Kjaer³

A *cis*-regulatory sequence also known as zone of polarizing activity (ZPA) regulatory sequence (ZRS) located in intron 5 of *LMBR1* is essential for expression of sonic hedgehog (*SHH*) in the developing posterior limb bud mesenchyme. Even though many point mutations causing preaxial duplication defects have been reported in ZRS, the underlying regulatory mechanism is still unknown. In this study, we analyzed the effect on transcription factor binding of a novel ZRS point mutation (463T>G) in a Pakistani family with preaxial polydactyly and triphalangeal thumb. Electrophoretic mobility shift assay demonstrated a marked difference between wild-type and the mutant probe, which uniquely bound one or several transcription factors extracted from Caco-2 cells. This finding supports a model in which ectopic anterior *SHH* expression in the developing limb results from abnormal binding of one or more transcription factors to the mutant sequence.

European Journal of Human Genetics advance online publication, 13 January 2010; doi:10.1038/ejhg.2009.225

Keywords: preaxial polydactyly; triphalangeal thumb; point mutation; *SHH* regulatory sequence, regulatory element

INTRODUCTION

Regulatory elements are important for establishing correct expression domains in time and space. The increasing pace by which such elements are being reported leads to the natural question how these elements carry out their function. Initial identification of a balanced translocation,¹ and subsequent point mutations^{2,3} in families with preaxial polydactyly (PPD) and triphalangeal thumb lead to the discovery of a long-range sonic hedgehog regulatory element (ZRS), which was later also found to be duplicated in PPD patients.^{4,5} ZRS is located in intron 5 of *LMBR1*, 1 Mb 5' of the target gene. The ZRS is necessary for proper posterior expression in the limb.⁶ Mouse models with ZRS point mutations showed ectopic sonic hedgehog (*SHH*) expression anteriorly,^{2,7} but it is still unknown how the mutations impair the normal function of the regulatory element. We hypothesized that single-nucleotide mutations in this element change the binding affinity for various transcription factors and tested it for a novel mutation detected in a three-generation family of Pakistani origin by electrophoretic mobility shift assay (EMSA).

MATERIALS AND METHODS

Family PD1 was examined at home in the Southern Punjab region and informed written consent was obtained from all participating individuals. This study was approved by the local ethical committee of the National Institute for Biotechnology and Genetic Engineering (NIBGE), School of Biotechnology,

Quaid-i-Azam University, Pakistan. Peripheral blood samples were collected and DNA was extracted using a standard protocol (phenol:chloroform). Linkage to the known candidate region at 7q36 associated with PPD and triphalangeal thumb was performed using the highly polymorphic microsatellite markers D7S550, D7S559 and D7S2423. All samples were PCR amplified using radioactive-labeled forward primer (protocol available on request) and the alleles were size separated on 8% non-denaturing polyacrylamide gel. Direct sequencing of the 1-kb region containing ZRS was performed with the following oligonucleotide primers: forward1 5'-CCTCTGGCCAGTGTAAATG-3', reverse1 5'-GGGGGAAAAAGTCATCTG GT-3'; forward2 5'-GGTGAAGCGAAGAGTCTG-3', reverse2 5'-CAATTGGG GGATTGTAGAGG-3' (TAG Copenhagen, Copenhagen, Denmark), using the dideoxy chain-termination method (BigDye ver 1.1, Applied Biosystems, Foster city, CA, USA) on an ABI 3130xl sequencer. Sequencing results were analyzed using ChromasPro software (ChromasPro 2.1, Technelysium Pty Ltd, Tewantin QLD, Australia). The identified mutation and its segregation was confirmed by agarose gel electrophoresis of *MseI* (New England Biolabs, Ipswich, MA, USA) digested PCR fragments.

EMSA is a standard technique commonly used to detect the interaction between proteins and γ -32P-labeled nucleic acids. It is thus well suited to test our hypothesis that the transcription factor-binding potential of the mutant ZRS sequence differs from the wild type (wt). The Caco-2 cell line derives from a cancerous human epithelial colorectal adenocarcinoma. Caco-2 cells do express *SHH* mRNA in both differentiated and undifferentiated stages (<http://gastro.imbg.ku.dk/chipchip/>). The Caco2 cell line can be used to test whether the transcription factor-binding properties of the mutated sequence differs from that of the wild type.

¹Human Molecular Genetics Laboratory, Health Biotechnology Division, National Institute for Biotechnology & Genetic Engineering (NIBGE), Faisalabad, Pakistan; ²Department of Cellular and Molecular Medicine, University of Copenhagen, Copenhagen, Denmark; ³Department of Cellular and Molecular Medicine, Wilhelm Johannsen Centre for Functional Genome Research, University of Copenhagen, Copenhagen, Denmark

*Correspondence: Dr SM Baig, Human Molecular Genetics Laboratory, Health Biotechnology Division, National Institute for Biotechnology & Genetic Engineering, PO Box 577, Faisalabad 38000, Pakistan. Tel: +924 1255 1638; Fax: +924 1265 1472; E-mail: shahid_baig2002@yahoo.com

Received 17 June 2009; revised 13 November 2009; accepted 18 November 2009

Standard EMSA was performed using 29-mer wild-type (T) and mutant (G) γ -32P-labeled synthetic oligonucleotide probes (Figure 1) and Caco-2 cells nuclear extract as previously described.⁸ Labeled probes were purified using the G25-spin column (Amersham Biosciences, Sunnyvale, CA, USA). Probe/protein complexes and unbound probes were separated by electrophoresis on 5% non-denaturing polyacrylamide gel in 0.5 \times TBE buffer at 220 V for 2 h at 4°C. Gels were dried after electrophoresis and exposed in a phosphorImager (Amersham Biosciences).

RESULTS

Out of 13 examined members 8 had dominantly segregating PPD and triphalangeal thumb. Four additional members were said to be affected. Confirmative radiographic examination was performed in three affected members. The metacarpals were normal in shape and number (Figure 2B). The duplicated phalanx was triphalangeal in most cases and occurred unilaterally in III-3, III-5, III-11 and III-12. The feet were normal and no other signs of dysmorphology were noticed. All individuals appeared mentally normal.

Initial STS marker analysis supported possible linkage when assuming dominant inheritance with decreased penetrance (Figure 2A). Segregation analysis of the haplotypes confirmed that all affected individuals shared the same haplotype. Two clinically normal individuals also did. Direct sequencing of ZRS showed a novel point mutation 463T>G (named according to Furniss *et al.*⁹) in intron 5 of *LMBR1* (Figure 3) in all individuals sharing this haplotype. Restriction



Figure 1 Sequences of double-stranded oligonucleotide probes used for EMSA.



Figure 2 (A) Pedigree of family PD1 and haplotypes at 7q36 using microsatellite markers. The region in affected subjects segregating with the phenotype is boxed. Clinically examined individuals are shown by a horizontal line over the symbol. (B) Phenotypic appearance of affected subjects in the family PD1 with PPD triphalangeal thumb. (a and b) The hands and feet of III-12, (c) clinical appearance of hands of male subject III-6, (d) radiograph of III-6 demonstrating duplicated thumbs with three phalanges.

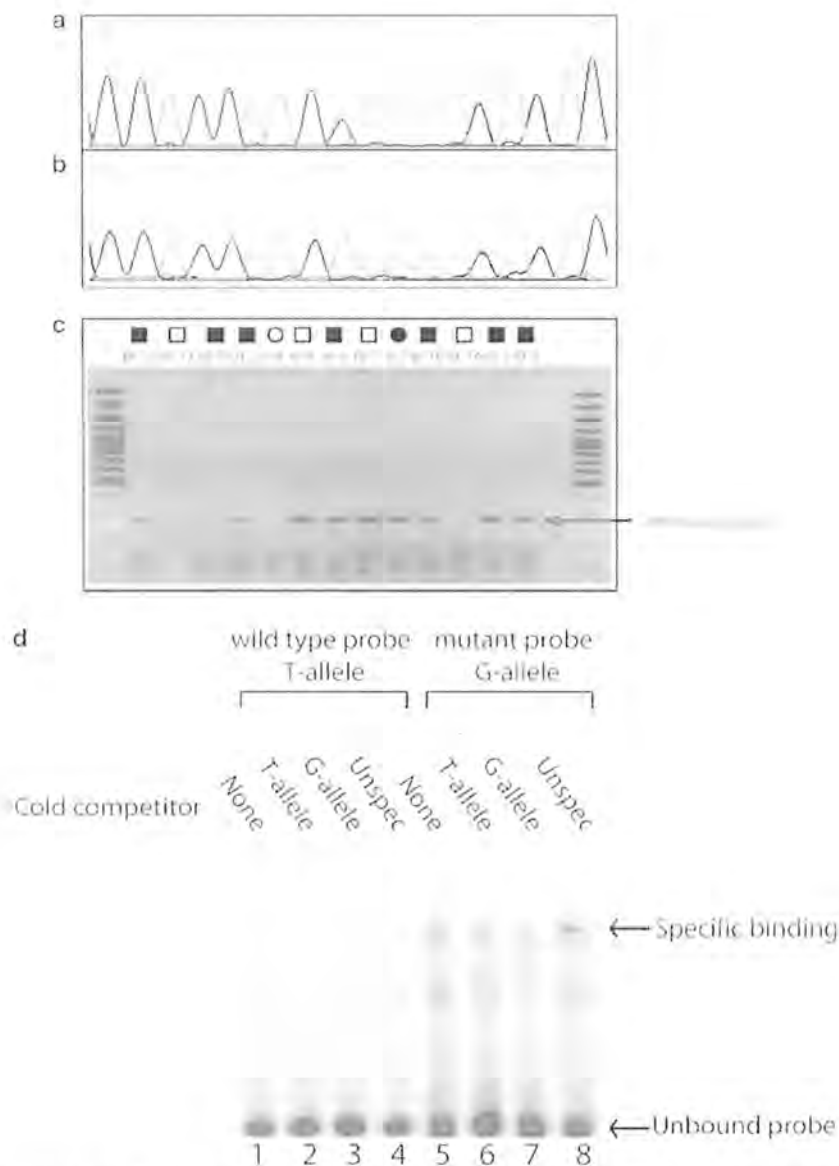


Figure 3 (a) Representative chromatogram of the heterozygous mutation (463 T>G) in ZRS. (b) Wild type. (c) Restriction analysis using *MseI* restriction enzyme in all the sampled family members (normal and affected); the 268-bp mutant allele is indicated by an arrow. (d) EMSA of the conserved element demonstrating binding of Caco-2 cell line nuclear extract to both wild-type (T-allele) and mutant allele (G-allele). Unlabeled probes were added to demonstrate specific binding to both alleles. Specific binding is indicated by arrow.

enzyme analysis confirmed the finding. The mutation was absent in 280 unrelated normal chromosomes from the same population. EMSA analysis using Caco-2 cells nuclear extract showed specific DNA/protein binding for the mutant probes and not the wild-type probes (Figure 3d). In addition, competitive DNA/protein binding was detected using unlabeled mutant probes, whereas such competition was not detected using wild-type probe.

DISCUSSION

PPD is one of the most frequently occurring human limb malformations. The phenotype is quite variable in affected families with a simple addition of the third phalanx leading to triphalangial thumb to whole digit duplication. Point mutations in the *cis*-acting regulatory

element (ZRS) have been described in many families in recent years. The ZRS lies 1 Mb upstream of its target gene (*SHH*) and is located in intron 5 of *LMBR1*.^{2,10} *SHH* is normally expressed in the zone of polarizing activity (ZPA) posteriorly in the developing limb bud. Mouse models of PPD have shown that point mutations in ZRS lead to ectopic expression of *SHH* at the anterior margin of limb bud.¹¹ Heterozygous duplications including ZRS have also been described in families with triphalangial thumb-polysyndactyly syndrome.^{4,5} It has been found that this long-range promoter-enhancer interaction is specific to limb bud tissues.⁶ It is still a matter of debate how duplications and point mutations can cause the same phenotypic defect. However, the frequency of very rare single point nucleotide changes among families and animal models with PPD clearly supports

that these changes are indeed pathogenic and not only rare variants. Homozygous deletion of the ZRS element in mouse results in a complete loss of *SHH* expression in the limb bud leading to acheiropodia.⁶ Until now, 14 point mutations have been reported scattered throughout the ZRS element, suggesting that all the elements are important in regulation of *SHH* expression in the developing limb.^{2,3,7,9–11} Phenotypes produced by different point mutation in ZRS are almost identical.

The nucleotide mutated in family PD1 is highly conserved between human, mouse, chicken and fugu. EMSA results for this mutation clearly demonstrate specific binding of nuclear factors to mutant probes, supporting that the pathogenic effect of the T>G alteration at position 463 acts by altering its affinity for transcription factors. Interestingly, this hypothesis was recently supported in a novel ZRS mutant mouse model (DZ), in which the authors found specific preferential binding of the transcription factor *HnRNP U* to the mutated sequence.¹² *HnRNP U* is indeed expressed in Caco2 cells (<http://gastro.sund.ku.dk/chipchip>); however, the sequence comparison around the DZ mouse mutation (which preferentially bound to *HnRNP U*) and 463T>G mutation predicts that factor(s) other than *HnRNP U* may have bound to 463T>G mutant.¹² A yeast hybrid screen using the mutant and wild-type DNA sequence as bait and based on a cDNA library derived from limb bud cells, followed by subsequent sequencing of positive clones, should be carried out to characterize the bound factor(s) in more detail.

CONFLICT OF INTEREST

The authors declare no conflict of interest.

ACKNOWLEDGEMENTS

The Higher Education Commission of Pakistan is kindly acknowledged for funding Muhammad Farooq. The Wilhelm Johannsen Centre for Functional Genome research was established by the Danish National Research Foundation.

- 1 Lettice LA, Horikoshi T, Heaney SJ *et al*: Disruption of a long-range cis-acting regulator for Shh causes preaxial polydactyly. *Proc Natl Acad Sci USA* 2002; **99**: 7548–7553.
- 2 Lettice LA, Heaney SJ, Purdie LA *et al*: A long-range Shh enhancer regulates expression in the developing limb and *lin* and is associated with preaxial polydactyly. *Hum Mol Genet* 2003; **12**: 1725–1735.
- 3 Sagai T, Masuya H, Tamura M *et al*: Phylogenetic conservation of a limb-specific, cis-acting regulator of sonic hedgehog (Shh). *Mamm Genome* 2004; **15**: 23–34.
- 4 Klopocki E, Ott CE, Benatar N, Ullmann R, Mundlos S, Lehmann K: A microduplication of the long range SHH limb regulator (ZRS) is associated with triphalangeal thumb-polysyndactyly syndrome. *J Med Genet* 2008; **45**: 370–375.
- 5 Sun M, Ma F, Zeng X *et al*: Triphalangeal thumb-polysyndactyly syndrome and syndactyly type IV are caused by genomic duplications involving the long range, limb-specific SHH enhancer. *J Med Genet* 2008; **45**: 589–595.
- 6 Sagai T, Hosoya M, Mizushima Y, Tamura M, Shiroishi T: Elimination of a long-range cis-regulatory module causes complete loss of limb-specific Shh expression and truncation of the mouse limb. *Development* 2005; **132**: 797–803.
- 7 Masuya H, Sezutsu H, Sakuraba Y *et al*: A series of ENU-induced single-base substitutions in a long-range cis-element altering sonic hedgehog expression in the developing mouse limb bud. *Genomics* 2007; **89**: 207–214.
- 8 Troelsen JT, Mitchelmore C, Olsen J: An enhancer activates the pig lactase phlorizin hydrolase promoter in intestinal cells. *Gene* 2003; **305**: 101–111.
- 9 Furniss D, Lettice LA, Taylor IB *et al*: A variant in the sonic hedgehog regulatory sequence (ZRS) is associated with triphalangeal thumb and deregulates expression in the developing limb. *Hum Mol Genet* 2008; **17**: 2417–2423.
- 10 Gurnett CA, Bowcock AM, Dietz FR, Morcuende JA, Murray JC, Dobbs MB: Two novel point mutations in the long-range SHH enhancer in three families with triphalangeal thumb and preaxial polydactyly. *Am J Med Genet A* 2007; **143**: 27–32.
- 11 Lettice LA, Hill AE, Deyvenney PS, Hill RE: Point mutations in a distant sonic hedgehog cis-regulator generate a variable regulatory output responsible for preaxial polydactyly. *Hum Mol Genet* 2008; **17**: 978–985.
- 12 Zhao J, Ding J, Li Y *et al*: HnRNP U mediates the long-range regulation of Shh expression during limb development. *Hum Mol Genet* 2009; **18**: 3090–3097.

Muhammad Farooq,^{1,2} Shahid Baig,² Niels Tommerup,¹ and Klaus W. Kjaer^{1*}

¹Department of Cellular and Molecular Medicine, Wilhelm Johannsen Center for Functional Genome Research, University of Copenhagen, Copenhagen, Denmark

²Health Biotechnology Division, National Institute for Biotechnology and Genetic Engineering, Faisalabad, Pakistan

Received 23 June 2009; Accepted 7 November 2009

Craniosynostosis-microcephaly with chromosomal breakage and other abnormalities (CMCB; OMIM 218455) [Tommerup et al., 1993] was initially described as a condition distinct from premature chromosome condensation syndrome (PCC; OMIM 606858) [Neitzel et al., 2002]. In contrast to peripheral lymphocytes from patients with PCC, those from patients with CMCB exhibited a high proportion of endomitoses and endoreduplications, a high spontaneous chromosomal-breakage rate, and an increased sensitivity towards both alkylating agents and X-rays. Furthermore, the structure of the condensed metaphases in CMCB cells was abnormal, showing spontaneous coiling and banding patterns, even in metaphase spreads where the nuclear membrane was absent. This was not the case in lymphoblast or fibroblast cell lines from patients with PCC. Another striking difference was the fact that prophase-like cells did not show labeling when 3H-thymidine was added 3 hr prior to harvesting. In addition, despite many attempts, it was not possible to establish EBV-transformed or fibroblast cell lines from the patient with CMCB. These differences lead Neitzel et al. to conclude that PCC was a novel microcephaly-mental retardation syndrome. Subsequent identification of *Microcephalin* (*MCPH1*) as the causative gene for PCC [Trimborn et al., 2004, 2005; Garshasbi et al., 2006] led us to re-evaluate this question in the original Danish CMCB patient with craniosynostosis, microcephaly, ptosis, "bird-like" facies, and moderate mental retardation.

Indeed, in contrast to her parents, the patient was homozygous for the *MCPH1* flanking polymorphic microsatellite markers (D8S1798, D8S277, D8S1819, and D8S1825; data not shown). Direct sequencing of all coding exons including flanking intronic regions of *MCPH1* was performed using BigDye Terminator v.1.1

Farooq M, Baig S, Tommerup N, Kjaer KW. 2010. Craniosynostosis-microcephaly with chromosomal breakage and other abnormalities is caused by a truncating *MCPH1* mutation and is allelic to premature chromosome condensation syndrome and primary autosomal recessive microcephaly type 1.

Am J Med Genet Part A 152A:495–497.

Cycle Sequencing Kit (Applied Biosystems Foster city, CA) in an ABI 3130xl genetic analyzer. This analysis showed a novel single nucleotide substitution (c. 302C > G; S101X) in exon 4 of *MCPH1* (Fig. 1), leading to a presumptive premature truncation of the protein after amino acid residue 100. Both parents were heterozygous for the mutation and were not known to be related by descent. The sequences were analyzed using ChromasPro software (ChromasPro 2.1, Technelysium Pty Ltd, Tewantin, Australia).

The first mutation in *MCPH1* (S25X) was found in two families with primary autosomal recessive microcephaly (OMIM 251200) [Jackson et al., 2002] that was shown in a later study of patient cell

*Correspondence to:

Klaus W. Kjaer, Wilhelm Johannsen Centre for Functional Genome Research-Medical Genetics, University of Copenhagen, Blegdamsvej 3B, Copenhagen N 2200, Denmark. E-mail: kwk@sund.ku.dk

Published online 22 January 2010 in Wiley InterScience

(www.interscience.wiley.com)

DOI 10.1002/ajmg.a.33234

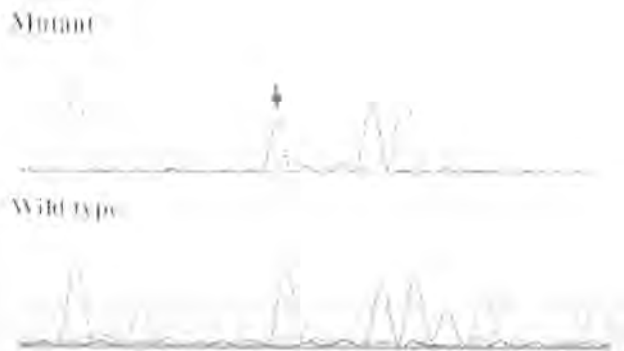


FIG. 1. Chromatogram showing homozygosity for c.302C > G in exon 4 of *MCPH1* in the patient (indicated by arrow). [Color figure can be viewed in the online issue, which is available at www.interscience.wiley.com.]

lines to share the cellular phenotype with PCC patients with a 427insA mutation [Alderton et al., 2006]. The fact that the cellular phenotype was milder than that observed in siRNA knock-down *MCPH1* cells led the authors to suggest that the alleles were hypomorphic.

MCPH1 encodes a polypeptide 835 amino acids in length that contains one N-terminal and two carboxy-terminal BRCT domains involved in protein–protein binding (Fig. 2). Whereas the 427insA mutation causes nonsense-mediated decay (even though residual mRNA was identified), residual truncated *MCPH1* protein was found in cells with the S25X mutation [Alderton et al., 2006]. Whether caused by mRNA decay or truncation, both PCC mutations cause loss of the N-terminal BRCT domain, which is presumably intact in CMCB cells. Mouse embryonic fibroblasts from a mouse *Mcp1* knock-out model recapitulate the PCC cellular phenotype. However, when a series of deletion mutants were used, only those with an intact N-terminal BRCT domain rescued this phenotype, even in the absence of the two C-terminal BRCT domains [Wood et al., 2008]. The significance of the N-terminal BRCT domain thus provides a possible molecular explanation for the substantial cellular differences between CMCB and PCC.

Interestingly, it was recently found that *MCPH1* links repair of DNA damage to chromatin remodeling by binding to the

ATP-dependent chromatin remodeling complex SWI-SNF, which in turn allows specific recruitment to and maintenance at DNA lesions. When knocked down, DNA damage is not repaired due to lack of SWI-SNF recruitment [Peng et al., 2009]. The fact that CMCB cells are significantly more prone to DNA damage than PCC cell lines might suggest that the N-terminal BRCT domain could have a specific function in this process.

Clinically, the description of the initial patient adds craniosynostosis, ptosis, and “bird-like” facies with micrognathia to the spectrum of *MCPH1*-related phenotypes, in addition to the microcephaly and moderate mental retardation that are well known [Tommerup et al., 1993].

In conclusion, our finding widens the spectrum of clinical and cellular phenotypes seen in families with *MCPH1*-associated microcephaly, and provides additional clues to the function of the first 100 amino acid residues of *MCPH1*. Finally, they strongly suggest that CMCB be considered part of the *MCPH1*-related disease spectrum.

ACKNOWLEDGMENTS

The Wilhelm Johannsen Centre for Functional Genome Research was established by the Danish National Research Foundation. The Higher Education Commission of Pakistan and the IMK Almene Fond are kindly acknowledged for funding Muhammad Farooq.

REFERENCES

- Alderton GK, Galbiati L, Griffith E, Sirinya KH, Neitzel H, Jackson AP, Jeggo PA, O'Driscoll M. 2006. Regulation of mitotic entry by microcephalin and its overlap with ATR signaling. *Nat Cell Biol* 8:725–733.
- Garshasbi M, Motazacker MM, Kahrizi K, Behjati F, Abedini SS, Nieh SE, Firouzabadi SG, Becker C, Ruschendorf F, Nurnberg P, Tzschach A, Vazifehmand R, Erdogan F, Ullmann R, Lenzner S, Kuss AW, Ropers HH, Najmabadi H. 2006. SNP array-based homozygosity mapping reveals *MCPH1* deletion in family with autosomal recessive mental retardation and mild microcephaly. *Hum Genet* 118:708–715.
- Jackson AP, Eastwood H, Bell SM, Adu J, Toomes C, Carr IM, Roberts E, Hampshire DJ, Crow YJ, Mighell AJ, Karbani G, Jafri H, Rashid Y, Mueller RF, Markham AF, Woods CG. 2002. Identification of microcephalin, a protein implicated in determining the size of the human brain. *Am J Hum Genet* 71:136–142.
- Neitzel H, Neumann LM, Schindler D, Wirges A, Tonnie H, Trimborn M, Krebsova A, Richter R, Sperling K. 2002. Premature chromosome condensation in humans associated with microcephaly and mental retardation: A novel autosomal recessive condition. *Am J Hum Genet* 70:1015–1022.
- Peng G, Yim EK, Dai H, Jackson AP, Burgt IV, Pan MR, Hu R, Li K, Lin SY. 2009. BRIT1/*MCPH1* links chromatin remodeling to DNA damage response. *Nat Cell Biol* 11:865–872.
- Tommerup N, Mortensen E, Nielsen MH, Wegner RD, Schindler D, Mikkelsen M. 1993. Chromosomal breakage, endomitosis, endoreduplication, and hypersensitivity toward radiomimetic and alkylating agents: A possible new autosomal recessive mutation in a girl with craniosynostosis and microcephaly. *Hum Genet* 92:339–346.
- Trimborn M, Bell SM, Felix C, Rashid Y, Jafri H, Griffiths PD, Neumann LM, Krebs A, Reis A, Sperling K, Neitzel H, Jackson AP. 2004. Mutations



FIG. 2. BRCT domains of full length (A) and truncated protein in CMCB cells (B) as predicted by SMART (<http://smart.embl-heidelberg.de/>). The N-terminal BRCT domain is intact whereas C-terminal BRCT domains are missing.

- in *microcephalin* cause aberrant regulation of chromosome condensation. *Am J Hum Genet* 75:261–266.
- Trimborn M, Richter R, Sternberg N, Gavvovidis I, Schindler D, Jackson AP, Prott EC, Sperling K, Gillessen-Kaesbach G, Neitzel H. 2005. The first missense alteration in the MCPH1 gene causes autosomal recessive microcephaly with an extremely mild cellular and clinical phenotype. *Hum Mutat* 26:496.
- Wood JL, Liang Y, Li K, Chen J. 2008. Microcephalin/MCPH1 associates with the Condensin II complex to function in homologous recombination repair. *J Biol Chem* 283:29586–29592.

Compound Heterozygous ASPM Mutations in
Pakistani MCPH Families

Farooq Muhammad,¹ Shahid Mahmood Baig,¹ Lars Hansen,² Muhammad Sajid Hussain,¹
Iram Anjum Inayat,¹ Muhammad Aslam,¹ Javed Anver Qureshi,¹ Muhammad Toilat,³ Elisabeth Kirst,³
Muhammad Wajid,¹ Peter Nürnberg,³ Hans Eiberg,⁴ Niels Tommerup,² and Klaus W. Kjaer^{2*}

¹Human Molecular Genetics Laboratory, Health Biotechnology Division, National Institute for Biotechnology & Genetic Engineering (NIBGE), Faisalabad, Pakistan

²Wilhelm Johannsen Centre for Functional Genome Research, Department of Cellular and Molecular Medicine, University of Copenhagen, Copenhagen, Denmark

³Institute for Genetics, University of Cologne, Cologne, Germany

⁴Department of Cellular and Molecular Medicine, University of Copenhagen, Copenhagen, Denmark

Received 7 July 2008; Accepted 23 December 2008

Autosomal recessive primary microcephaly (MCPH) is characterized by reduced head circumference (≤ 4 SD) and mental retardation without any other neurological manifestation. Of the four identified MCPH genes, homozygous truncating mutations in *ASPM* (MCPH5) account for >50% of all reported families. In spite of the high frequency of MCPH in Pakistan, only one case of compound heterozygosity for mutations in *ASPM* has been reported yet. In this larger MCPH study we examined 10 families including 39 persons (18 probands). Haplotype analysis of eight STR markers suggested linkage by homozygosity in 10 families, and coanalysis of atrophic skulls in the remaining families demonstrated possible compound heterozygosity in two families. Direct sequencing indeed confirmed compound heterozygosity in two and homozygous mutations in 10 families, respectively, showing that up to 10% of families with MCPH caused by *ASPM* are compound heterozygous. In total we identified 16 different nonsense or frameshift mutations of which 12 were novel thereby increasing the number of mutations in *ASPM* significantly from 33 to 45. We found no correlation between the severity of the condition and the site of truncation. We suggest that the high frequency of compound heterozygosity observed in this study is taken into consideration as part of future genetic testing and counseling for Pakistani MCPH families. © 2009 Wiley-Liss, Inc.

Key words: microcephaly; NIBGE; compound heterozygosity; *ASPM* variants

INTRODUCTION

Autosomal recessive primary microcephaly (MCPH; MIM251200) is characterized by reduced head circumference ($HC \leq 4$ SD) and variable degree of mental retardation without other clinical symptoms. In spite of the profound brain size reduction in MCPH

How to Cite this Article

Muhammad F, Mahmood Baig S, Hansen L, Sajid Hussain M, Anjum Inayat I, Aslam M, Anver Qureshi J, Toilat M, Kirst E, Wajid M, Nürnberg P, Eiberg H, Tommerup N, Kjaer KW. 2009. Compound heterozygous *ASPM* mutations in Pakistani MCPH families.

Am J Med Genet Part A 149A:926–930.

patients the normal brain architecture may be preserved [McCreary et al., 1996]. Six loci have been mapped (MCPH1–MCPH6) [Woods et al., 2005] and of the four genes identified so far (*Microcephalin*, *CDK5RAP2*, *CENPJ*, and *ASPM*) truncating mutations in *ASPM* account for >50% of reported families [Bond et al., 2002, 2003; Kumar et al., 2004]. In spite of a specially high incidence of MCPH in Pakistan due to consanguineous marriages [Woods et al., 2005; Gul et al., 2006] only one case of compound heterozygosity has been reported yet [Bond et al. 2003]. *ASPM* expression during neurogenesis is localized to ventricular zones which contain progenitor cells for different neural cell pools [Bond et al., 2003]. An animal model is still not reported.

Additional supporting information may be found in the online version of this article.

*Correspondence to:

Klaus W. Kjaer, Wilhelm Johannsen Centre for Functional Genome Research, Department of Cellular and Molecular Medicine, Panum Institute 24.4, Blegdamsvej 3, 2200 Copenhagen N, Denmark.

E-mail: kwk@imb.gu.dk

Published online 7 April 2009 in Wiley InterScience

(www.interscience.wiley.com)

DOI 10.1002/ajmg.a.32749

MATERIALS AND METHOD

In this study we ascertained 37 Pakistani MCPH families with two to 10 affected individuals from Central and Southern Punjab or the North Western Frontier province (Fig. 1a,b). Inclusion criteria were HC reduced by more then 4 SD, mental retardation, and absence of other symptoms and obvious dysmorphic features. In total 319 persons including 140 patients were personally examined in their home and studied molecularly. Informed consent was obtained from all individuals or their legal guardians. Pedigree data was given by family members, a clinical history was recorded for both affected and unaffected individuals, and the phenotype documented by photos. The mental function was assessed by standardized questionnaires in all family members.

DNA was extracted from peripheral blood samples using a standard protocol (Phenol: Chloroform). Initially, all families were tested for linkage to ASPM by homozygosity mapping using the highly polymorphic microsatellite markers D1S2757, D1S2816, D1S1660, D1S2622, D1S373, D1S1723, D1S2655, and D1S1678. Secondly, haplotypes were re-analyzed in each sib ship of families not linked by homozygosity to identify families, or part of families with possible compound heterozygous mutations. All samples were

PCR amplified using a standard protocol (available upon request). PCR fragments were size separated on an 8% nondenaturing polyacrylamide gel. Finally, 22 families were analyzed in depth for mutations in ASPM. All 28 coding exons including splice sites were PCR amplified using previously published primers [Bond et al., 2003]. Two affected members from each family were initially sequenced bi-directionally using fluorescent dye chain termination technique on an ABI prism 3130xl sequencer. Sequences were analyzed by using chromaspro software (ChromasPro 1.34). Each mutation was confirmed by restriction enzyme analysis of PCR amplified fragments (supporting information Table I may be found in the online version of this article), and all family members were tested. The frequency of all novel mutations was tested in 288 control chromosomes from healthy Pakistani individuals.

RESULTS AND DISCUSSION

Twenty families mapped to ASPM by homozygosity (MCP2, MCP3, MCP6, MCP7, MCP9, MCP11, MCP13, MCP16, MCP17, MCP19, MCP25, MCP26, MCP31, MCP32, MCP34, MCP38, MCP39, MCP40, MCP42, and MCP44), and two additional

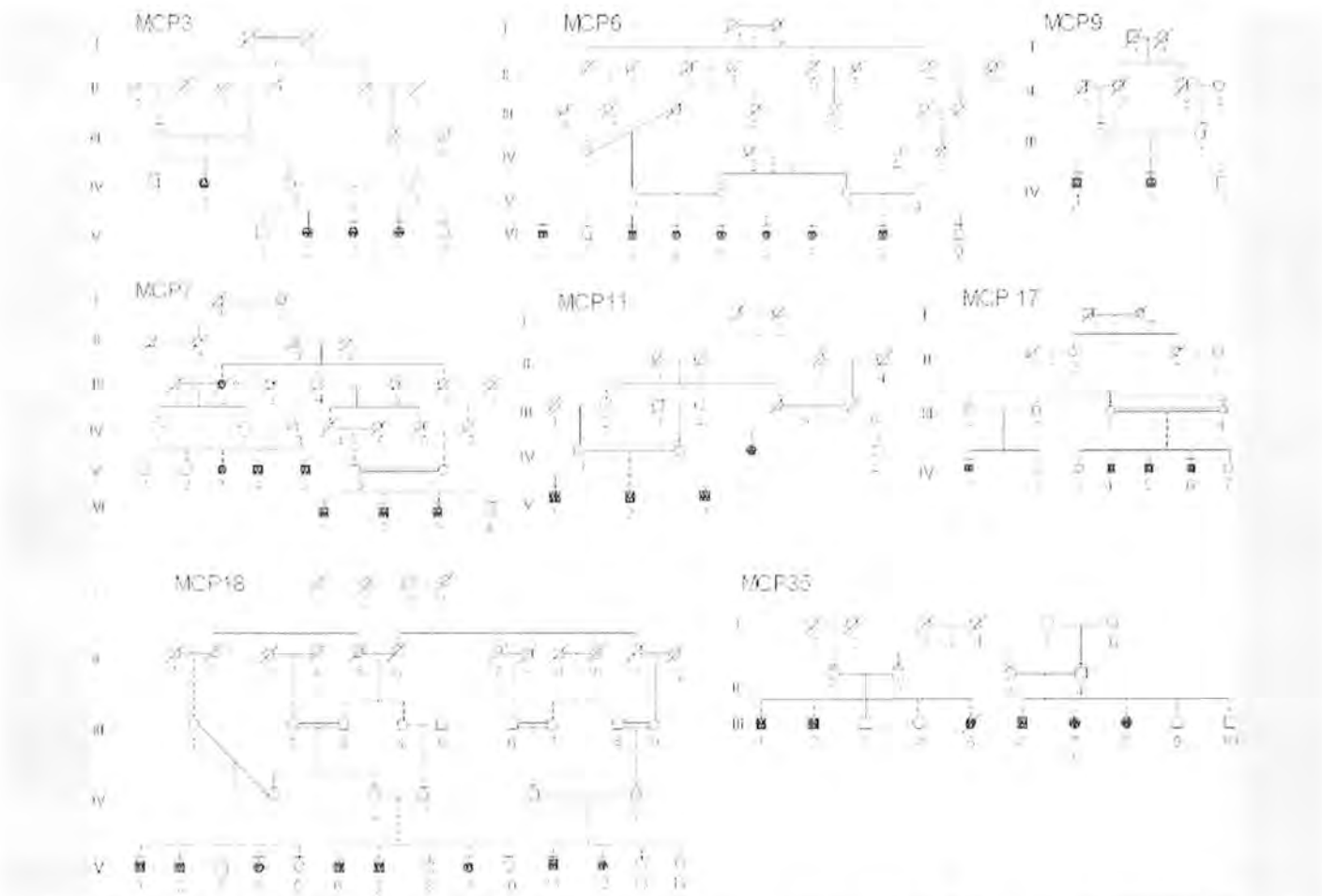


FIG. 1. a,b: Pedigrees of 22 families including 94 affected persons with MCPH caused by mutations in ASPM. The 215 examined individuals are marked with a horizontal line above the symbol.

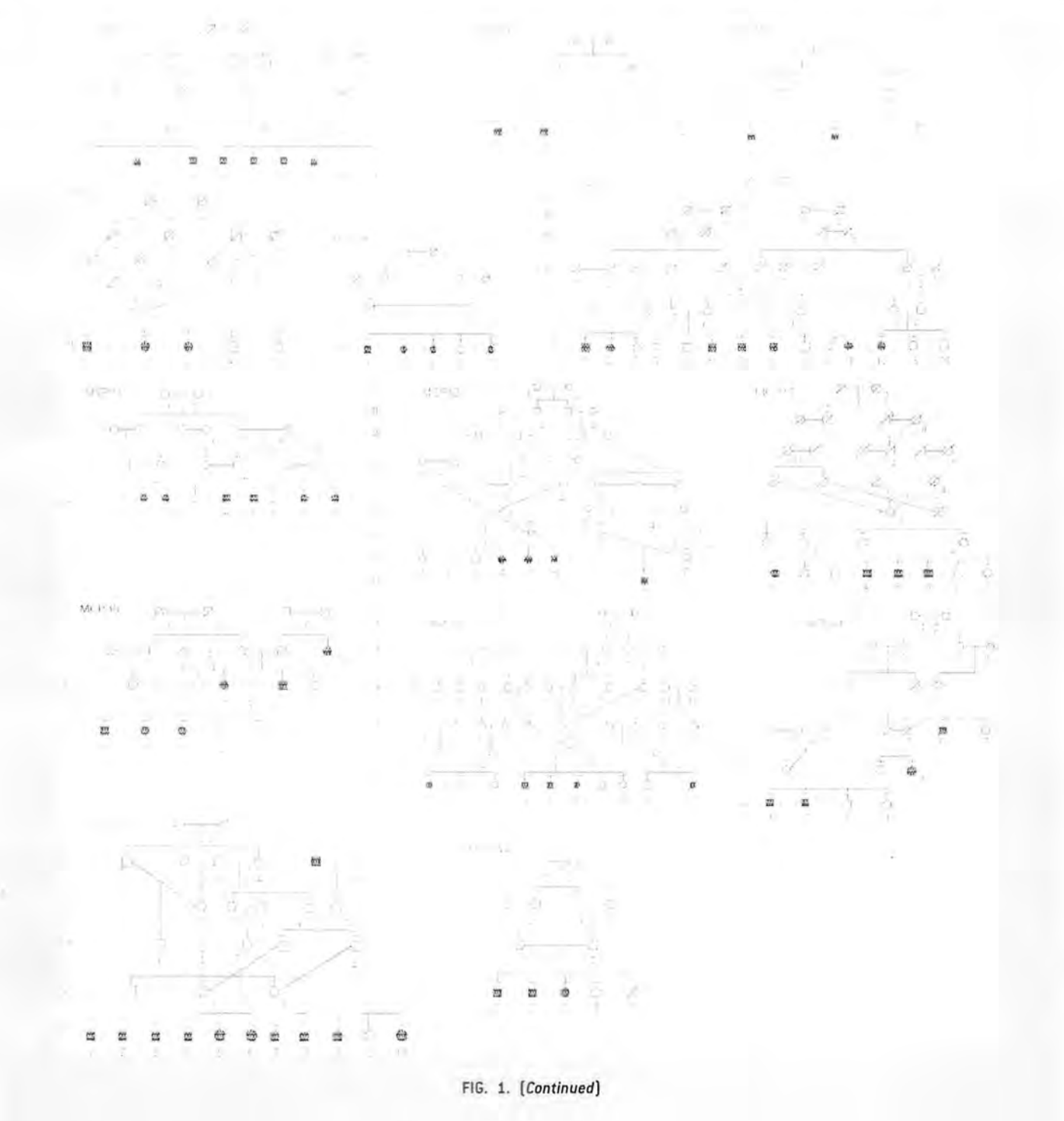


FIG. 1. [Continued]

families were suggestive of compound heterozygosity: MCP18 (left and middle loop), and MCP35 (left loop) (Fig. 1) (mapping data not shown). Direct sequencing of *ASPM* in these two families revealed compound heterozygosity for three novel and one known nonsense mutations: MCP18 (left and middle loop): c.3055C>T;R1019X/c.7894C>T;Q2632X, and in MCP35 (left loop): c.3978G>A;W1326X/c.9319C>T;R3107X). Sequencing of *ASPM* in the remaining twenty linked families showed homozygosity for 9 novel nonsense or frameshift mutations

(c.3477_3481delCGCTA;A1160fs (MCP3), c.6732delA;Y2245fs (MCP6), c.9697C>T;R3233X (MCP7), c.9492T>G;Y3164X (MCP13 and MCP17), c.2938C>T;R980X (MCP26), c.9677_9678insG;C3226fs (MCP25), c.9595A>T; K3199X (MCP39), c.1002delA;V335fs (MCP2), c.8668C>T;Q2890X (MCP16), c.3055C>T;R1019X (MCP19)), and four known mutations (c.9557C>G;S3186X (MCP11), c.9730C>T;R3244X (MCP9, MCP38 and MCP40), c.3978G>A;W1326X (MCP31, MCP32 and MCP34) and c.8508_8509delGA;K2837fs (MCP42)) (Fig. 2). None



FIG. 2. Chromatograms showing the mutated sequence in each family next to a wt sequence for the same region.

of the identified mutations were found in 288 control chromosomes except c.9492T>G that was identified in 1/288 chromosomes suggesting that the frequency of pathogenic *ASPM* mutations in the general population is very low. Still it is possible that higher frequencies are found in more isolated regions. All mutations are predicted to impair the normal function of *ASPM* by premature truncation, which is in accordance with previous data. So far only one missense mutation is reported in *ASPM* causing primary microcephaly [Gul et al., 2006]. The data increases the number of known mutations in *ASPM* significantly from 35 to 47 (supporting information Table II may be found in the online version of this article). Notably, affected members of the two compound heterozygous families displayed a milder phenotype (HC -6 SD) than all other studied patients. However, the fact that patients with comparable homozygous mutations can have HCs of -5 SD suggests that this difference may be coincidental [Bond et al., 2003]. Occurrence of compound heterozygosity in apparently unlinked families may partly explain why a considerable number of reported families were not linked by homozygosity to any known MCPH locus [Bond et al., 2002].

Seizures were reported in patients with a homozygous W2063X mutation [Shen et al., 2005]. Two compound heterozygous individuals from MCP35 (III-1/III-2; W1326X/R3107X) had had seizures from childhood that were medically treated. However, as their homozygous cousins (III-6, III-7, and III-8) in right loop never had seizures this may be a coincidental finding. The limited data on this association still precludes conclusiveness. Unfortunately, brain scans could not be performed in these rural areas.

Notably, two heterozygous mutation carriers had small heads (HC -2 to -3.5 SD): MCP7 IV-3 and MCP18 V-13. However, as all other heterozygous mutation carriers were mentally normal and had normal head size this is apparently a rare finding.

With a detection rate of *ASPM* mutations in 59.5% (22/37) of ascertained MCPH families our study is in accordance with previous data [Bond et al., 2003; Gul et al., 2006]. Our data demonstrate that MCPH linked to *ASPM* is almost invariably caused by truncating mutations. In line with previous observations we did not find any correlation between the phenotype and the site of truncation.

In conclusion, in this study of MCPH families we found compound heterozygosity in ~10% of families with MCPH caused by *ASPM*. As *ASPM* is consistently found to be the most common cause of MCPH our data strongly suggest that sequencing of the gene is the first step of any molecular analysis in MCPH patients, even in absence of homozygosity for the *ASPM* locus. Furthermore,

our data significantly increased the number of observed *ASPM* mutations from 35 to 47.

Wilhelm Johannsen Centre was established by the Danish National Research Foundation. Higher Education Commission of Pakistan is kindly acknowledged for funding F.M. and IMK Almene Fond for funding K.W.K.

Bond J, Roberts E, Mochida GH, Hampshire DJ, Scott S, Askham JM, Springell K, Mahadevan M, Crow YJ, Markham AF, Walsh CA, Woods CG. 2002. *ASPM* is a major determinant of cerebral cortical size. *Nat Genet* 32:316–320.

Bond J, Scott S, Hampshire DJ, Springell K, Corry P, Abramowicz MJ, Mochida GH, Hennekam RCM, Maher ER, Fryns JP, Alswaid A, Jafri H, Rashid Y, Mubaidin A, Walsh CA, Roberts E, Woods CG. 2003. Protein-truncating mutations in *ASPM* cause variable reduction in brain size. *Am J Hum Genet* 73:1170–1177.

Desir J, Cassart M, David P, Van Bogaert P, Abramowicz M. 2008. Primary microcephaly with *ASPM* mutation shows simplified cortical gyration with antero-posterior gradient pre- and post-natally. *Am J Med Genet Part A* 146A:1439–1443.

Gul A, Hassan MJ, Mahmood S, Chen W, Rahmani S, Naseer MI, Dellefave L, Muhammad N, Rafiq MA, Ansar M, Chisti MS, Ali G, Siddique T, Ahmad W. 2006. Genetic studies of autosomal recessive primary microcephaly in 33 Pakistani families: Novel sequence variants in *ASPM* gene. *Neurogenetics* 7:105–110.

Kumar A, Blanton SH, Babu M, Markandaya M, Girimaji SC. 2004. Genetic analysis of primary microcephaly in Indian families: Novel *ASPM* mutations. *Clin Genet* 66:341–348.

McCreary BD, Rossiter JP, Robertson DM. 1996. Recessive (true) microcephaly: A case report with neuropathological observations. *J Intellect Disabil Res* 40:66–70.

Pichon B, Vankerckhove S, Bourrouillou G, Duprez L, Abramowicz MJ. 2004. A translocation breakpoint disrupts the *ASPM* gene in a patient with primary microcephaly. *Eur J Hum Genet* 12:419–421.

Shen J, Eyaid W, Mochida GH, Al-moayyad F, Bodell A, Woods CG, Walsh CA. 2005. *ASPM* mutations identified in patients with primary microcephaly and seizures. *J Med Genet* 42:725–729.

Woods CG, Bond J, Enard W. 2005. Autosomal recessive primary microcephaly (MCPH): A review of clinical, molecular, and evolutionary findings. *Am J Hum Genet* 76:717–728.